

Supporting Information

Synthesis of Tellurium-Containing π -Extended Aromatics with Room-Temperature Phosphorescence

Mengjing Jiang,^{†,§} Jimin Guo,^{†,§} Bingxin Liu,[†] Qitao Tan,^{*,†} and Bin Xu^{*,†,‡}

[†]Department of Chemistry, Innovative Drug Research Center, Shanghai University, 99 Shangda Road, Shanghai 200444, China

[‡]State Key Laboratory of Organometallic Chemistry, Shanghai Institute of Organic Chemistry, Chinese Academy of Sciences, Shanghai 200032, China

CONTENTS:

1. General Information	S2
2. Synthesis and Characterization	S3
3. Mechanistic Studies	S18
4. X-ray Crystallographic Data	S21
5. Electrochemical Properties	S24
6. Studies of the Photophysical Properties	S26
7. Theoretic Calculations	S35
8. References	S44
9. Copies of NMR Spectra	S46

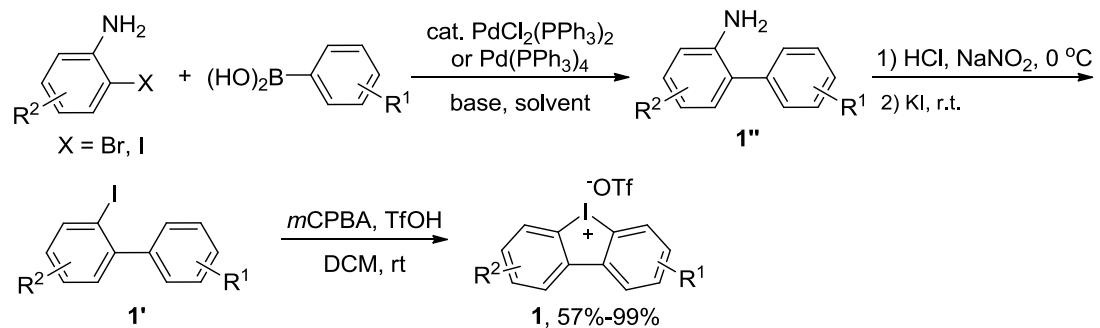
1. General Information

All reagents were obtained from commercial sources without further purification, and solvents were used as received except specifically mentioned. Silica gel plate GF254 were used for thin layer chromatography (TLC) and silica gel 300-400 mesh were used for flash column chromatography. All melting points were taken on a SGWX-4A digital melting point apparatus without correction. Infrared spectra were obtained using an AVATAR 370 FT-IR spectrometer. NMR spectra were recorded on Bruker AV-500 (500 MHz) and JEOL (400 MHz) spectrometers. Mass spectra and high resolution mass spectra were recorded with an Agilent 5975N using an electrospray ionization (ESI) techniques. DART Positive and MALDI-FT MS (solid-state analyte in TCNQ or DHB matrix) were carried out on a Thermo Scientific LTQ Orbitrap XL and FT Ultra spectrometer, respectively. Ultraviolet spectra were measured on a PEGeneral spectrometer. The steady fluorescence spectra were recorded on a Shimadzu RF5301 spectrometer. The lifetimes were measured using an Edinburgh Instruments FLS 1000 spectrophotometer. The crystal structure was recorded on a Bruker SMART APEX-II X-ray diffraction spectrometer with a graphite-monochromatized MoK_α ($\lambda=0.71073\text{ \AA}$) radiation. Powder XRD was recorded on a Haoyuan DX-2700 diffraction spectrometer. Cyclic voltammetry (CV) was performed on a CHI660B electrochemical analyzer at room temperature in inert atmosphere with a three-electrode configuration in CH₂Cl₂ solution containing the substrate and 0.1 M tetrabutylammonium perchlorate (*n*-Bu₄NClO₄) as the supporting electrolyte. A glassy carbon disc served as the working electrode, a platinum wire and a commercial Ag/Ag⁺ electrode (0.01 M AgNO₃ in CH₃CN) served as the counter and the reference electrodes, respectively. The scan rate was 0.1 V/s. The HOMO energy values were estimated from the onset potentials of the first oxidation. After calibration of the measurements against Fc/Fc⁺, the HOMO levels were calculated according to the following equations: $E_{\text{HOMO}}(\text{eV}) = -[E_{\text{ox}}(\text{onset}) - E_{1/2}(\text{Fc}/\text{Fc}^+) + 4.8]$, where $E_{1/2}(\text{Fc}/\text{Fc}^+)$ is the half-wave potential of the Fc/Fc⁺ couple (the oxidation potential of which is assumed at 4.8 eV) against the Ag/Ag⁺ electrode. Yields refer to chromatographically and spectroscopically pure compounds, unless otherwise indicated. Theoretical calculations were carried out using the Gaussian 09 program. DFT was used for ground state structure optimization and TD-DFT for excited-state computations at B3LYP/cc-pVTZ-(PP) level of theory.

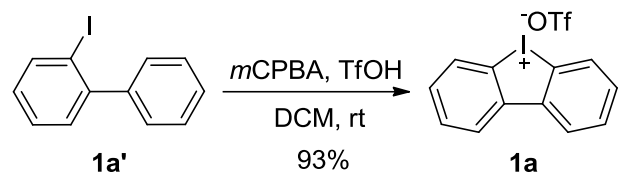
2. Synthesis and Characterization

2.1 Synthesis of Cyclic Diaryliodonium Salts

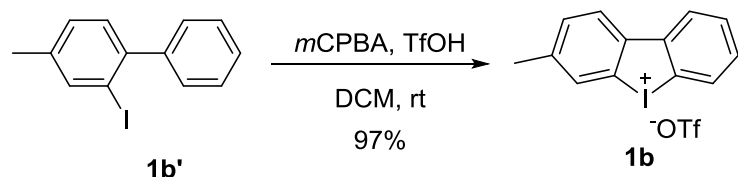
General synthetic route:



Cyclic diaryliodonium salts were readily prepared from the corresponding **1'**, which was prepared from 2-aminobiphenyls **1''**. 2-Aminobiphenyls were previously prepared in gram scale.^{S1} The iodonium salts were moisture stable and can be stored for long time without obvious change.

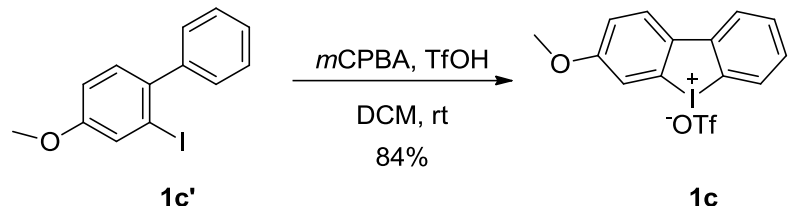


Diphenyliodonium trifluoromethanesulfonate (1a):^{S2} A solution of **1a'** (2.4 g, 8.5 mmol) was dissolved in CH₂Cl₂ (35 mL). To the solution was added *m*-CPBA (85%, 2.6 g, 12.75 mmol) in 30 mL CH₂Cl₂, followed by triflic acid (2.3 ml, 25.5 mmol) with stirring, during which a sticky black gum formed on the flask-wall. After stirred for 1 h, the solvent was decanted. Ether (20 mL) was added to the residue and a well-dispersed white solid precipitated, and stirred for 10 min. The solid was filtered and washed with ether (3×15 mL), affording **1a** as a white solid (3.35 g, 93%). M.p. 247-249 °C; IR (KBr, cm⁻¹): 3050, 1624, 1578, 1259, 1165, 1032, 642; ¹H NMR (500 MHz, DMSO-*d*₆): δ 8.50 (dd, *J* = 7.9, 1.3 Hz, 2H), 8.23 (dd, *J* = 8.3, 0.9 Hz, 2H), 7.91-7.83 (m, 2H), 7.75-7.68 (m, 2H); ¹³C NMR (125 MHz, DMSO-*d*₆): δ 141.7, 131.1, 130.7, 130.6, 127.0, 121.6, 120.7 (q, ¹J_{C-F} = 295 Hz); MS (ESI): m/z 279 [M-OTf]⁺.

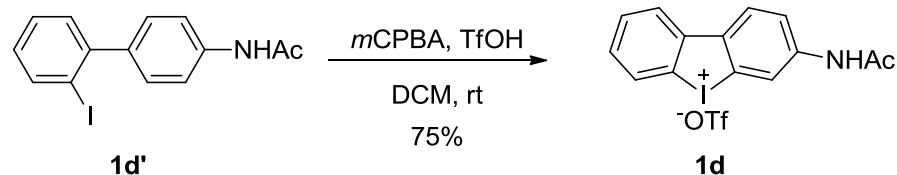


3-Methyldibenzo[*b,d*]iodol-5-ium trifluoromethanesulfonate (1b):^{S3} Following the procedure for **1a**, with **1b'** (1.0 g, 3.5 mmol), *m*-CPBA (85%, 1.1 g, 5.25 mmol) and

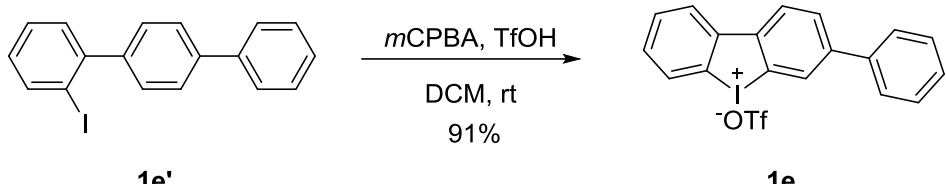
triflic acid (0.9 mL, 10.5 mmol), **1b** was obtained as a white solid (1.5 g, 97%). M.p. > 300 °C; IR (KBr, cm⁻¹): 3095, 2925, 1595, 1449, 1392, 1238, 1164, 1026, 823, 760, 636; ¹H NMR (500 MHz, DMSO-*d*₆): δ 8.34 (dd, *J* = 8.0, 1.2 Hz, 1H), 8.26 (d, *J* = 8.1 Hz, 1H), 8.15 (d, *J* = 8.3 Hz, 1H), 7.92 (s, 1H), 7.80 (t, *J* = 7.6 Hz, 1H), 7.65 (td, *J* = 8.4, 1.4 Hz, 1H), 7.60 (d, *J* = 8.7 Hz, 1H); ¹³C NMR (125 MHz, DMSO-*d*₆): δ 141.7, 141.5, 139.1, 131.6, 130.6, 130.6, 130.5, 130.2, 126.6, 126.5, 121.6, 121.2, 120.5 (q, ¹*J*_{C-F} = 257 Hz), 21.2; MS (ESI, m/z): 293 [M-OTf]⁺.



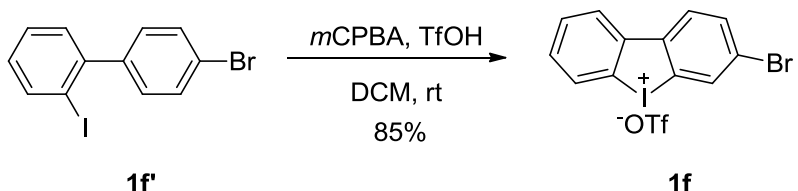
3-Methoxydibenzo[b,d]iodol-5-ium trifluoromethanesulfonate (1c):^{S2} Following the procedure for prepare **1a**, with **1c'** (620 mg, 2 mmol), *m*-CPBA (85%, 610 mg, 3 mmol) and triflic acid (0.6 mL, 6.8 mmol), **1c** was obtained as an orange solid (769 mg, 84%). M.p. 274-276 °C. IR (KBr, cm⁻¹): 3097, 2983, 2946, 1597, 1554, 1496, 1249, 1026, 829, 636; ¹H NMR (500 MHz, DMSO-*d*₆): δ 8.34 (d, *J* = 8.9 Hz, 1H), 8.33 (dd, *J* = 7.9, 1.4 Hz, 1H), 8.16 (dd, *J* = 8.3, 1.0 Hz, 1H), 7.80 (t, *J* = 7.6 Hz, 1H), 7.73 (d, *J* = 2.6 Hz, 1H), 7.67-7.57 (m, 1H), 7.42 (dd, *J* = 8.8, 2.6 Hz, 1H), 3.91 (s, 3H); ¹³C NMR (125 MHz, DMSO-*d*₆): δ 160.7, 141.5, 134.3, 130.7, 130.5, 129.8, 127.6, 126.3, 122.7, 120.9, 120.7 (q, ¹*J*_{C-F} = 321 Hz), 117.8, 114.7, 56.1; MS (ESI): m/z 309 [M-OTf]⁺.



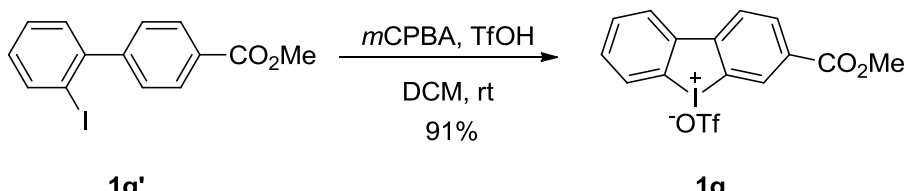
3-Acetamidodibenzo[b,d]iodol-5-ium trifluoromethanesulfonate (1d):^{S4} Following the procedure for **1a**, with **1d'** (337 mg, 1.0 mmol), *m*-CPBA (85%, 300 mg, 1.5 mmol) and triflic acid (0.4 mL, 4.5 mmol), **1d** was obtained as a white solid (362 mg, 75%). M.p. 254-256 °C. IR (KBr, cm⁻¹): 3321, 3092, 2362, 1645, 1591, 1451, 1383, 1264, 1175, 1029, 900, 641; ¹H NMR (500 MHz, DMSO-*d*₆): δ 10.51 (s, 1H), 8.83 (s, 1H), 8.33 (d, *J* = 8.7 Hz, 1H), 8.31 (dd, *J* = 8.0, 1.2 Hz, 2H), 8.17 (d, *J* = 8.2 Hz, 1H), 7.81 (t, *J* = 8.0 Hz, 1H), 7.69 (dd, *J* = 8.6, 2.0 Hz, 1H), 7.63 (t, *J* = 7.8 Hz, 1H), 2.15 (s, 3H); ¹³C NMR (125 MHz, DMSO-*d*₆): δ 169.0, 141.6, 141.2, 136.1, 130.6, 130.5, 130.1, 126.9, 126.2, 122.5, 121.5 (q, ¹*J*_{C-F} = 320 Hz), 121.0, 120.1, 119.4, 24.2; MS (ESI): m/z 336 [M-OTf]⁺.



3-Phenyldibenzo[*b,d*]iodol-5-ium trifluoromethanesulfonate (1e):^{S2} Following the procedure for **1a**, with **1e'** (855 mg, 2.4 mmol), *m*-CPBA (85%, 732 mg, 3.6 mmol), triflic acid (0.75 ml, 8.4 mmol), **1e** was obtained as a brown solid (1.10 g, 91%). M.p. 275-277 °C. IR (KBr, cm⁻¹): 3064, 1592, 1449, 1387, 1236, 1163, 833, 634; ¹H NMR (500 MHz, DMSO-*d*₆): δ 8.51 (d, *J* = 8.3 Hz, 1H), 8.48 (d, *J* = 7.7 Hz, 1H), 8.44 (d, *J* = 1.5 Hz, 1H), 8.21 (d, *J* = 8.2 Hz, 1H), 8.13 (dd, *J* = 9.7, 1.5 Hz, 1H), 7.85 (t, *J* = 7.5 Hz, 1H), 7.76 (d, *J* = 7.5 Hz, 2H), 7.71 (t, *J* = 7.8 Hz, 1H), 7.57 (t, *J* = 7.6 Hz, 2H), 7.48 (t, *J* = 7.4 Hz, 1H); ¹³C NMR (125 MHz, DMSO-*d*₆): δ 142.6, 141.3, 140.6, 138.0, 131.1, 130.8, 130.6, 129.4, 129.1, 128.7, 128.1, 127.2, 127.1, 126.8, 122.6, 121.8, 120.7 (q, ¹*J*_{C-F} = 320 Hz); MS (ESI): m/z 355 [M-OTf]⁺.

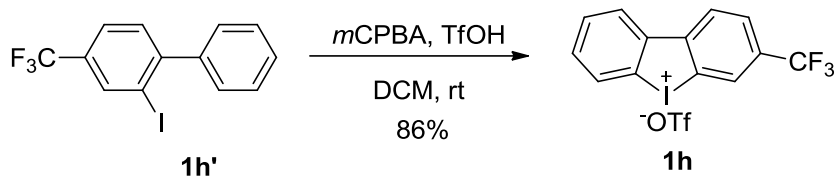


3-Bromodibenzo[*b,d*]iodol-5-ium trifluoromethanesulfonate (1f):^{S4} Following the procedure for **1a**, with **1f'** (2.7 g, 7.5 mmol), *m*-CPBA (85%, 2.28 g, 11.25 mmol) and triflic acid (2.5 mL, 28 mmol), **1f** was obtained as a cyan solid (3.24 g, 85%). M.p. 291-294 °C. IR (KBr, cm⁻¹): 3094, 2357, 1573, 1443, 1369, 1277, 1174, 1079, 1022, 817, 635; ¹H NMR (500 MHz, DMSO-*d*₆): δ 8.46 (d, *J* = 7.9 Hz, 1H), 8.38 (d, *J* = 8.5 Hz, 1H), 8.32 (d, *J* = 2.0 Hz, 1H), 8.19 (d, *J* = 8.2 Hz, 1H), 8.03 (dd, *J* = 8.5, 2.0 Hz, 1H), 7.85 (t, *J* = 8.0 Hz, 1H), 7.74 (t, *J* = 8.4 Hz, 1H); ¹³C NMR (125 MHz, DMSO-*d*₆): δ 141.0, 140.7, 133.8, 132.6, 131.5, 130.8, 130.5, 128.2, 127.2, 122.8, 122.5, 121.9, 120.7 (q, ¹*J*_{C-F} = 321 Hz); MS (ESI, m/z): 357, 359 [M-OTf]⁺.

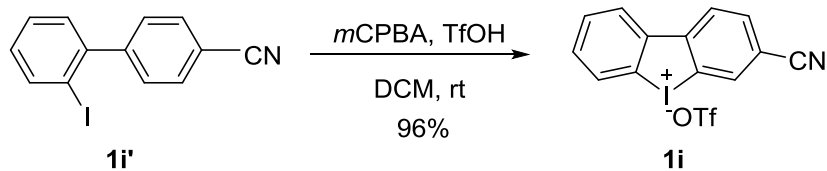


3-(Methoxycarbonyl)dibenzo[*b,d*]iodol-5-ium trifluoromethanesulfonate (1g):^{S3} Following the procedure for **1a**, with **1g'** (913 mg, 2.7 mmol), *m*-CPBA (85%, 822 mg, 4mmol) and triflic acid (0.85 ml, 9.6 mmol), **1g** was obtained as a white solid (1.2 g, 91%). M.p. 295-297 °C. IR (KBr, cm⁻¹): 3105, 2950, 2871, 1720, 1636, 1437, 1383, 1235, 1170, 1026, 759; ¹H NMR (500 MHz, DMSO-*d*₆): δ 8.76 (d, *J* = 1.6 Hz, 1H), 8.56 (d, *J* = 8.4 Hz, 1H), 8.53 (dd, *J* = 8.0, 1.3 Hz, 1H), 8.29 (dd, *J* = 8.3, 1.6 Hz, 1H), 8.23 (dd, *J* = 8.2, 0.9 Hz, 1H), 7.89 (td, *J* = 8.0, 0.9 Hz, 1H), 7.77 (td, *J* = 8.5, 1.4 Hz, 1H), 3.95 (s, 3H); ¹³C NMR (125 MHz, DMSO-*d*₆): δ 164.6, 145.8, 140.5, 132.1,

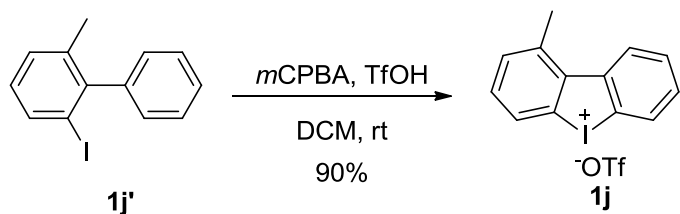
131.4, 131.1, 131.0, 130.9, 130.7, 127.9, 126.8, 122.8, 121.8, 120.7 (q, $^1J_{C-F} = 321$ Hz), 52.8; MS (ESI): m/z 337 [M-OTf]⁺.



3-(Trifluoromethyl)dibenzo[b,d]iodol-5-ium trifluoromethanesulfonate (1h):^{S2} Following the procedure for **1a**, with **1h'** (1.40 g, 4 mmol), *m*-CPBA (85%, 1.22 g, 6.0 mmol) and triflic acid (1.5 ml, 17 mmol), **1h** was obtained as a white solid (1.7 g, 86%). M.p. >300 °C. IR (KBr, cm⁻¹): 3098, 1801, 1718, 1644, 1598, 1322, 1231, 1138, 1074, 1021, 838, 634; ¹H NMR (500 MHz, DMSO-*d*₆) δ 8.71 (d, *J* = 8.3 Hz, 1H), 8.63 (dd, *J* = 7.9, 1.3 Hz, 1H), 8.55 (s, 1H), 8.28-8.24 (m, 2H), 7.93 (td, *J* = 8.1, 1.0 Hz, 1H), 7.82 (t, *J* = 8.5, 1.4 Hz, 1H); ¹⁹F NMR (470 MHz, DMSO-*d*₆) δ -61.0, -77.8; ¹³C NMR (125 MHz, DMSO-*d*₆): δ 145.6, 140.2, 132.3, 130.9, 130.6, 130.0 (q, $^2J_{C-F}$ = 33 Hz), 128.0, 127.6, 127.6 (q, $^3J_{C-F}$ = 4.0 Hz), 127.5 (q, $^3J_{C-F}$ = 3.8 Hz), 122.9, 123.3 (q, $^1J_{C-F}$ = 271 Hz), 122.0, 120.7 (q, $^1J_{C-F}$ = 321 Hz); MS (ESI): m/z 347 [M-OTf]⁺.

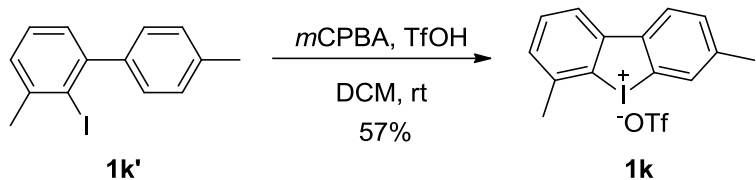


3-Cyanodibenzo[b,d]iodol-5-ium trifluoromethanesulfonate (1i):^{S2} Following the procedure for **1i**, with **1i'** (1.3 g, 4.2 mmol), *m*-CPBA (85%, 1.27 g, 6.3 mmol) and triflic acid (1.15 ml, 12.6 mmol), **1i** was obtained as a white solid (1.82 g, 96%). M.p. 286-288 °C. IR (KBr, cm⁻¹): 3084, 2229, 1589, 1235, 1176, 892, 834, 637; ¹H NMR (500 MHz, DMSO-*d*₆): δ 8.59 (d, *J* = 8.3 Hz, 1H), 8.54 (dd, *J* = 8.0, 1.3 Hz, 1H), 8.48 (d, *J* = 1.5 Hz, 1H), 8.28 (dd, *J* = 8.2, 1.5 Hz, 1H), 8.23 (d, *J* = 8.2 Hz, 1H), 7.91-7.87 (m, 1H), 7.78-7.76 (m, 1H); ¹³C NMR (125 MHz, DMSO-*d*₆): δ 145.9, 140.1, 134.2, 134.1, 132.5, 130.9, 130.6, 128.1, 127.2, 123.2, 121.7, 120.7 (q, $^1J_{C-F}$ = 318 Hz), 117.5, 112.4; MS (ESI): m/z 304 [M-OTf]⁺.

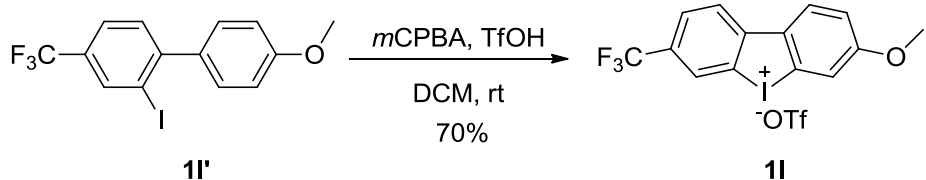


1-Methyldibenzo[b,d]iodol-5-ium trifluoromethanesulfonate (1j):^{S5} Following the procedure for **1a**, with **1j'** (1.9 g, 6.5 mmol), *m*-CPBA (85%, 2.0 g, 9.8 mmol) and triflic acid (1.7 ml, 19.5 mmol), **1j** was obtained as a white solid (2.6 g, 90%). M.p.

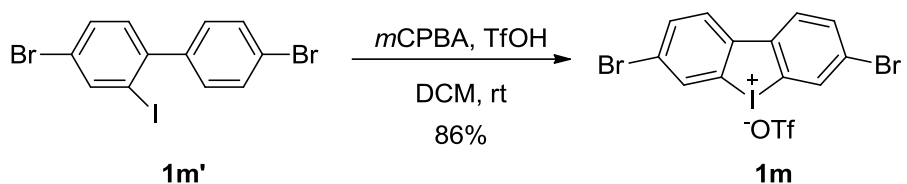
>300 °C. IR (KBr, cm⁻¹): 3052, 1586, 1247, 1168, 767, 641; ¹H NMR (500 MHz, DMSO-*d*₆): δ 8.49 (d, *J* = 8.3, 1.0 Hz, 1H), 8.30 (dd, *J* = 8.2, 1.2 Hz, 1H), 8.15 (d, *J* = 8.0 Hz, 1H), 7.88 (td, *J* = 8.3, 1.2 Hz, 1H), 7.73-7.68 (m, 2H), 7.57 (t, *J* = 7.9 Hz, 1H), 2.88 (s, 3H); ¹³C NMR (125 MHz, DMSO-*d*₆): δ 142.6, 139.8, 139.3, 134.4, 130.7, 130.6, 130.4, 130.1, 129.8, 128.5, 121.9, 120.7 (q, ¹*J*_{C-F} = 320 Hz), 120.5, 23.2; HRMS (ESI) Calcd for C₁₃H₁₀I [M-OTf]⁺ 292.9822, found 292.9821.



3,6-Dimethyldibenzo[*b,d*]iodol-5-ium trifluoromethanesulfonate (1k): Following the procedure for **1a**, with **1k'** (924 mg, 3.0 mmol), *m*-CPBA (85%, 914 mg, 4.5 mmol) and triflic acid (0.8 mL, 9.0 mmol), **1k** was obtained as a white solid (776 mg, 57%). M.p. 249-251 °C. IR (KBr, cm⁻¹): 3052, 2921, 2847, 1599, 1452, 1384, 1160, 1033, 830, 639; ¹H NMR (500MHz, DMSO-*d*₆): δ 8.24 (d, *J* = 8.1 Hz, 1H), 8.14 (d, *J* = 7.6 Hz, 1H), 8.04 (s, 1H), 7.71 (t, *J* = 7.6 Hz, 1H), 7.63 (d, *J* = 8.7 Hz, 1H), 7.50 (d, *J* = 7.2 Hz, 1H), 2.65 (s, 3H), 2.48 (s, 3H). ¹³C NMR (125 MHz, DMSO-*d*₆): δ 142.0, 141.7, 140.0, 139.3, 131.9, 130.9, 130.8, 130.7, 127.2, 125.7, 124.2, 121.7, 120.7 (q, ¹*J*_{C-F} = 321 Hz), 24.9, 21.3; HRMS (DART) [M-OTf]⁺ calcd for C₁₄H₁₂I⁺ 306.9978, found 306.9976.

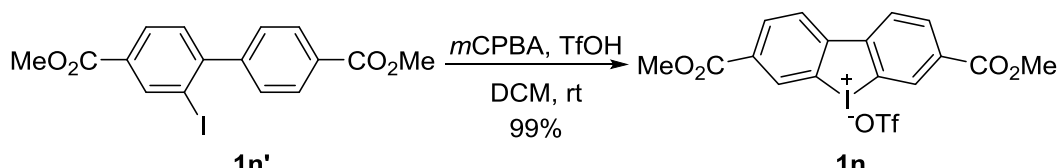


3-Methoxy-7-(trifluoromethyl)dibenzo[*b,d*]iodol-5-ium trifluoromethanesulfonate (1l):⁸⁵ Following the for **1a**, with **1l'** (1.3 g, 3.5 mmol), *m*-CPBA (85%, 1.1 g, 5.25 mmol) and triflic acid (0.9 ml, 10.5 mmol) **1l** was obtained as a white solid (1.3 g, 70%). M.p.>300 °C. IR (KBr, cm⁻¹): 3101, 2953, 2848, 1595, 1472, 1391, 1235, 1175, 1072, 1024, 828, 639; ¹H NMR (500MHz, DMSO-*d*₆): δ 8.44 (d, *J* = 8.3 Hz, 1H), 8.40 (s, 1H), 8.36 (d, *J* = 8.8 Hz, 1H), 8.09 (dd, *J* = 8.3, 1.1 Hz, 1H), 7.66 (d, *J* = 2.4 Hz, 1H), 7.38 (dd, *J* = 8.8, 2.4 Hz, 1H), 3.91 (s, 3H); ¹⁹F NMR (470 MHz, DMSO-*d*₆) δ -61.0, -77.8; ¹³C NMR (125 MHz, DMSO-*d*₆): δ 161.6, 145.3, 132.6, 128.8 (q, ²*J*_{C-F} = 32.5 Hz), 128.5, 127.5 (q, ³*J*_{C-F} = 3.8 Hz), 127.3 (q, ³*J*_{C-F} = 3.8 Hz), 126.7, 124.1, 123.4 (q, ¹*J*_{C-F} = 271 Hz), 121.1, 120.7 (q, ¹*J*_{C-F} = 320 Hz), 118.0, 114.8, 56.2. MS (ESI): m/z 377 [M-OTf]⁺.

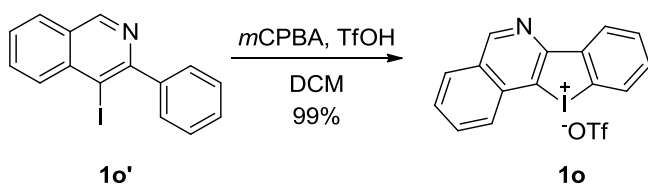


3,7-Dibromodibenzo[*b,d*]iodol-5-ium trifluoromethanesulfonate (1m):^{S6}

Following the procedure for **1a**, with **1m'** (1.3 g, 2.9 mmol), *m*-CPBA (85%, 888 mg, 4.3 mmol) and triflic acid (0.8 ml, 9 mmol), **1m** was obtained as an orange solid (1.45 g, 86%). M.p. > 300 °C. IR (KBr, cm⁻¹): 3095, 1570, 1217, 1175, 879, 633; ¹H NMR (500 MHz, DMSO-*d*₆): δ 8.30 (dd, *J* = 8.5, 1.4 Hz, 2H), 8.26-8.21 (m, 2H), 7.98 (dt, *J* = 8.5, 1.4 Hz, 2H); ¹³C NMR (125 MHz, DMSO-*d*₆): δ 139.9, 133.9, 132.4, 128.4, 123.3, 122.7, 120.7 (q, ¹*J*_{C-F} = 320 Hz); MS (ESI): m/z 437 [M-OTf]⁺.

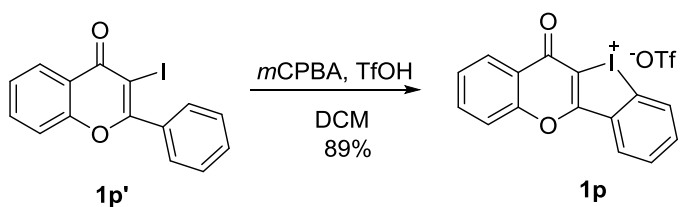


Dimethyl dibenzo[*b,d*]tellurophene-3,7-dicarboxylate (1n):^{S6} Following the procedure for **1a**, with **1n'** (673 mg, 1.7 mmol), *m*-CPBA (85%, 527 mg, 2.6 mmol) and triflic acid (0.46 ml, 5.1 mmol), **1n** was obtained as a white solid (928 mg, 99%). M.p. >300 °C. IR (KBr, cm⁻¹): 3097, 2959, 2360, 1713, 1433, 1378, 1285, 1172, 1114, 1029, 960, 841, 757, 640; ¹H NMR (500 MHz, DMSO-*d*₆): δ 8.77 (d, *J* = 1.6 Hz, 2H), 8.63 (d, *J* = 8.4 Hz, 2H), 8.32 (dd, *J* = 8.2, 1.6 Hz, 2H), 3.95 (s, 6H); ¹³C NMR (125 MHz, DMSO-*d*₆): δ 164.5, 144.4, 131.9, 131.4, 131.2, 127.8, 123.0, 120.7 (q, ¹*J*_{C-F} = 320 Hz), 52.9; MS (ESI): m/z 395 [M-OTf]⁺.



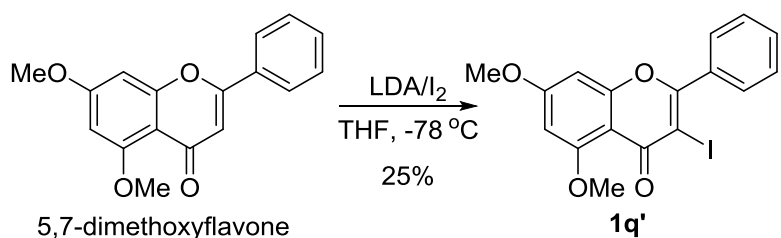
Benzo[4,5]iodolo[3,2-*c*]isoquinolin-11-ium trifluoromethanesulfonate (1o**):**^{S7} **1o'** was readily prepared according to the literature.^[S7] To a stirred solution of **1o'** (534 mg, 1.61 mmol) in CH₂Cl₂ (20 mL) was added TfOH (0.42 mL, 4.8 mmol), and then a solution of *m*-CPBA (85%, 488 mg, 2.4 mmol) in CH₂Cl₂ was added dropwise. The solution was stirred for 2 h at room temperature before CH₂Cl₂ was removed by rotary evaporation. Ether (15 mL) was added to the residue and a well-dispersed white solid was precipitated, and stirred for 10 min. After filtered, the solid was washed with ether (3×10 mL), affording **1o** as a white solid (765.2 mg, 99%). M.p. >300 °C. IR (KBr, cm⁻¹): 3009, 2356, 1629, 1557, 1262, 1036, 646, 580; ¹H NMR (500 MHz, DMSO-*d*₆) δ 9.75 (s, 1H), 8.62-8.52 (m, 2H), 8.49-8.39 (m, 2H), 8.15-8.12 (m, 1H), 8.03-7.93 (m, 2H), 7.89-7.85 (m, 1H); ¹³C NMR (125 MHz, DMSO-*d*₆): δ 155.5,

153.3, 140.5, 134.4, 133.6, 132.5, 131.1, 130.7, 130.0, 129.4, 129.2, 126.7, 122.0, 121.3, 120.7 (q, $^1J_{C-F} = 321$ Hz), 120.4; MS (ESI): m/z 330 [M-OTf]⁺.



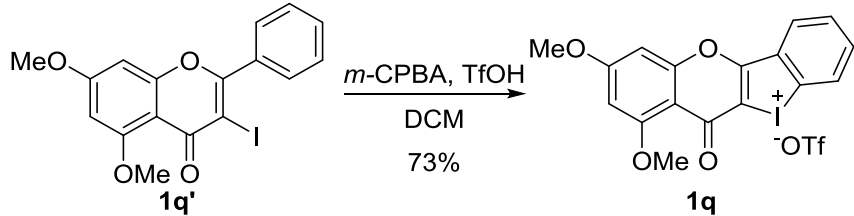
11-Oxo-11H-benzo[b]chromeno[3,2-d]iodol-5-iumtrifluoromethanesulfonate(1p):

^{s7} **1p'** was prepared according to the literature.^{s7} To a stirred solution of **1p'** (905 mg, 2.6 mmol) in CH₂Cl₂ (20 mL) was added TfOH (0.68 mL, 7.8 mmol), and then a solution of *m*-CPBA (85%, 787 mg, 3.88 mmol) in CH₂Cl₂ was added dropwise. The solution was stirred for 2 h at rt before CH₂Cl₂ was removed by rotary evaporation. Ether (15 mL) was added to the residue and a well-dispersed white solid precipitated, and stirred for 10 min. After filtered, the residue was washed with ether (3×10 mL), affording **1p** as a white solid (1.15 g, 89%). M.p. 290-292 °C. IR (KBr, cm⁻¹): 3075, 1653, 1601, 1551, 1290, 1230, 1165, 861, 637; ¹H NMR (500 MHz, DMSO-*d*₆): δ 8.45 (d, *J* = 8.1 Hz, 1H), 8.41 (dd, *J* = 7.8, 1.5 Hz, 1H), 8.21 (dd, *J* = 7.9, 1.6 Hz, 1H), 8.07-8.02 (m, 2H), 7.97-7.95 (m, 2H), 7.71 (td, *J* = 8.0, 0.9 Hz, 1H); ¹³C NMR (125 MHz, DMSO-*d*₆): δ 172.4, 164.1, 155.2, 136.0, 135.3, 134.7, 131.5, 131.3, 129.0, 127.1, 125.3, 122.5, 120.7 (q, $^1J_{C-F} = 318$ Hz), 119.7, 118.8, 108.5; MS (ESI): m/z 347 [M-OTf]⁺.

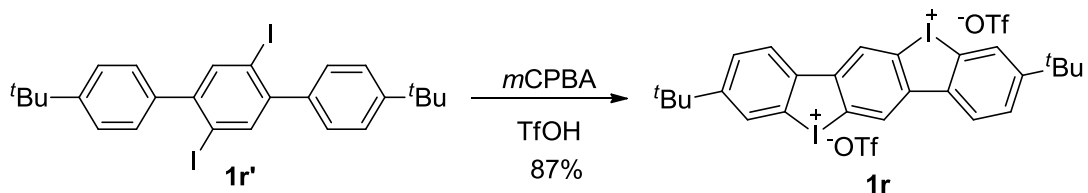


3-Iodo-5,7-dimethoxy-2-phenyl-4H-chromen-4-one (1q'): ^{s8} A 250 ml three-necked flask was charged with 5,7-dimethoxyflavone (1.77 g, 6.3 mmol) and THF (30 mL) under a nitrogen atmosphere. The mixture was cooled to -78 °C, and LDA (2.0 M in THF, 7.24 mL, 15.7 mmol) was added dropwise with stirring. The reaction mixture was stirred at -78 °C for 10 min. A solution of iodine (4.79 g, 18.9 mmol) in THF (6 mL) was added to the solution at -78 °C. The reaction mixture was stirred at -78 °C for 3 h, and allowed warmed up to room temperature slowly and stirred overnight. Then 1M aqueous Na₂S₂O₃ was added until the color of the mixture faded. The aqueous phase was extracted with EtOAc (3×30 mL). The combined organic layers were washed with H₂O (2×15 mL) and brine (10 mL), dried over anhydrous Na₂SO₄, concentrated in a vacuum. The residue was purified by column chromatography on silica gel (petroleum ether/DCM = 2:1 to PE : EA = 1 : 1) to provide **1q'** (644.7 mg, 25%) as a white solid. M.p. 179-180 °C. IR (KBr, cm⁻¹): 2941, 1622, 1461, 1424, 1314, 1103, 960, 821, 778, 691; ¹H NMR (500 MHz, CDCl₃): δ 7.77-7.75 (m, 2H),

7.54-7.48 (m, 3H), 6.47 (d, J = 2.3 Hz, 1H), 6.40 (d, J = 2.3 Hz, 1H), 3.95 (s, 3H), 3.87 (s, 3H); ^{13}C NMR (125 MHz, CDCl_3): δ 172.6, 164.5, 162.3, 160.9, 159.6, 135.1, 130.9, 129.6, 128.3, 105.9, 96.7, 92.2, 91.4, 56.6, 55.9; HRMS (ESI) calcd for $\text{C}_{17}\text{H}_{14}\text{IO}_4$ [$\text{M}+\text{H}]^+$ 408.9931, found 408.9928.

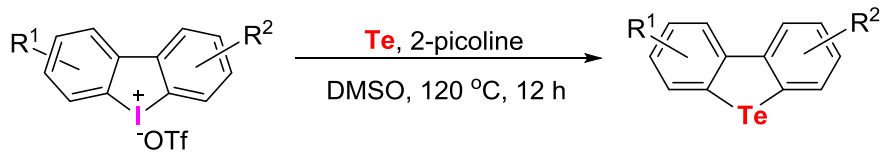


1,3,8-Tri methoxy-11-oxo-11*H*-benzo[*b*]chromeno[2,3-*d*]iodol-10-iumtrifluoromet hanesulfonate (1q): To a stirred solution of **1q'** (367.4 mg, 0.9 mmol) in CH_2Cl_2 (25 mL) was added TfOH (0.3 mL, 3.4 mmol) followed by addition of *m*-CPBA (85%, 274 mg, 1.35 mmol) slowly. The solution was stirred for 2 h at room temperature before CH_2Cl_2 was removed by rotary evaporation. Ether (15 mL) was added to the residue and a well-dispersed white solid precipitated, and stirred for 10 min. After filtered, the residue was washed with ether (3×10 mL), affording **1q** as a white solid (363.9 mg, 73%). M.p. > 300 °C. IR (KBr, cm^{-1}): 3081, 2846, 1628, 1509, 1426, 1393, 1223, 1169, 1068, 1031, 816, 638; ^1H NMR (500 MHz, $\text{DMSO}-d_6$): δ 8.44 (d, J = 8.4 Hz, 1H), 8.29 (dd, J = 7.7, 1.4 Hz, 1H), 8.03 (t, J = 7.4 Hz, 1H), 7.92 (td, J = 7.9, 1.4 Hz, 1H), 7.00 (d, J = 2.3 Hz, 1H), 6.73 (d, J = 2.3 Hz, 1H), 3.97 (s, 3H), 3.92 (s, 3H); ^{13}C NMR (125 MHz, $\text{DMSO}-d_6$): δ 170.0, 165.0, 161.1, 160.6, 158.8, 135.4, 134.0, 131.5, 131.1, 128.4, 120.7 (q, $^1J_{\text{C-F}} = 320$ Hz), 119.4, 111.5, 107.4, 97.4, 94.0, 56.7, 56.4; HRMS (ESI) calcd for $\text{C}_{17}\text{H}_{12}\text{IO}_4$ [$\text{M-OTf}]^+$ 406.9775, found 406.9775.

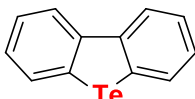


Bis-iodonium salt 1r: Compound 4,4''-di-*tert*-butyl-2',5'-diiodo-1,1':4',1''-terphenyl **1r'** was prepared according to the literature.^{S9} To a stirred solution of **1r'** (1.04 g, 1.75 mmol) in CH_2Cl_2 (30 mL) was added *m*-CPBA (85%, 1.06 g, 5.25 mmol) followed by TfOH (0.93 mL, 10.5 mmol). The solution was stirred for 2 h at room temperature before CH_2Cl_2 was removed by rotary evaporation. Ether (15 mL) was added to the residue and a well-dispersed white solid was precipitated, and stirred for 10 min. After filtered, the residue was washed with ether (3×10 mL), affording **1r** as a white solid (1.35 g, 87%). M.p. > 300 °C; IR (KBr, cm^{-1}): 3090, 2966, 1642, 1594, 1279, 1164, 837, 636; ^1H NMR (500 MHz, $\text{DMSO}-d_6$): δ 8.96 (s, 2H), 8.30 (d, J = 1.7 Hz, 2H), 8.24 (d, J = 8.5 Hz, 2H), 8.04 (dd, J = 8.3, 1.7 Hz, 2H); 1.42 (s, 18H); ^{13}C NMR (125 MHz, $\text{DMSO}-d_6$): δ 155.6, 142.6, 137.1, 129.0, 127.6, 127.0, 126.5, 124.6, 123.0, 120.7 (q, $^1J_{\text{C-F}} = 321$ Hz), 35.7, 30.8; HRMS (ESI) calcd for $\text{C}_{26}\text{H}_{27}\text{I}_2$ [$\text{M}+\text{H}-2\text{OTf}]^+$ 593.0197, found 593.0195.

2.2 The synthesis of tellurophene (DBTe's)

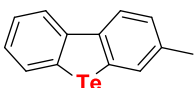


General Procedure: A 25 mL Schlenk tube was charged with cycloidal diaryliodonium salts **1** (0.3 mmol), tellurium (58 mg, 0.45 mmol), 2-picoline (1 mL) and DMSO (2 mL) under a nitrogen atmosphere. The reaction mixture was stirred at 120 °C for 12 h. After cooled to room temperature, the reaction mixture was diluted with H₂O (15 mL). The mixture extracted with dichloromethane (3 × 15 mL). The combined organic phase was washed with water and brine (20 mL), dried over anhydrous Na₂SO₄, filtered, and then evaporated under reduced pressure. The residue was purified by column chromatography on silica gel to give the desired product **2**.



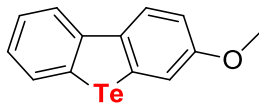
Dibenzo[b,d]tellurophene (2a):⁵¹⁰ Following the general procedure, the reaction of diaryliodonium salt **1a** (128.4 mg, 0.3 mmol), tellurium (58 mg, 0.45 mmol), 2-picoline (1 mL) and DMSO (2 mL) under a nitrogen atmosphere. After 12 h at 120 °C, purification by column chromatography on silica gel (petroleum ether) afforded **2a** (62 mg, 74 %) as a pale yellow solid. M.p. 94-95 °C. IR (KBr, cm⁻¹): 3030, 1701, 1550, 1416, 733; ¹H NMR (500 MHz, CDCl₃): δ 8.11 (dd, *J* = 8.0, 1.2 Hz, 2H), 7.89 (d, *J* = 7.8, 0.7 Hz, 2H), 7.47-7.44 (m, 2H), 7.32-7.28 (m, 2H); ¹³C NMR (125 MHz, CDCl₃): δ 144.1, 132.7, 128.8, 127.0, 125.8, 124.7; MS (DART): m/z 282.0 [M (Te)¹³⁰]⁺, 280.0 [M (Te)¹²⁸]⁺, 278.0 [M (Te)¹²⁶]⁺.

Synthesis of 2a on a 1.5 mmol scale: A 25 mL three-necked flask was charged with **1a** (642 mg, 1.5 mmol), tellurium (287 mg, 2.25 mmol), 2-picoline (5 mL) and DMSO (10 mL) under a nitrogen atmosphere. The reaction mixture was stirred at 120 °C for 12 h. After cooled to room temperature, the reaction mixture was diluted with H₂O (15 mL), and extracted with DCM (3 × 30 mL). The combined organic phase was washed with water (2 × 30 mL) and brine (20 mL), dried over anhydrous Na₂SO₄, filtered, and then evaporated under reduced pressure. Purification by column chromatography on silica gel (petroleum ether) afforded **2a** (223 mg, 54 %) as a yellow solid.

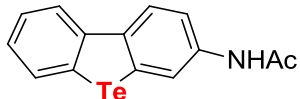


3-Methyldibenzob[b,d]tellurophene (2b): Following the general procedure, the reaction of diaryliodonium salt **1b** (132.6 mg, 0.3 mmol), tellurium (58 mg, 0.45 mmol), 2-picoline (1 mL) and DMSO (2 mL) under a nitrogen atmosphere. After 12 h at 120 °C, purification by column chromatography on silica gel (petroleum ether) afforded **2b** (65.6 mg, 74%) as a yellow solid. M.p. 68-69 °C. IR (KBr, cm⁻¹): 3042,

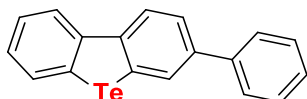
2921, 1587, 1430, 1231, 1201, 806, 748, 708; ^1H NMR (500 MHz, CDCl_3) δ 8.05 (dd, $J = 8.0, 1.3$ Hz, 1H), 7.98 (d, $J = 8.1$ Hz, 1H), 7.86 (dd, $J = 7.8, 0.6$ Hz, 1H), 7.77 (s, 1H), 7.44-7.41 (m, 1H), 7.31-7.23 (m, 2H), 2.43 (s, 3H); ^{13}C NMR (125 MHz, CDCl_3) δ 144.2, 141.8, 137.1, 132.9, 132.7, 128.8, 128.2, 127.2, 126.6, 125.8, 124.4, 124.4, 21.5; HRMS (ESI) m/z calcd for $\text{C}_{13}\text{H}_{10}\text{Te}^+ [\text{M}]^+$ 295.9845, found 295.9839.



3-Methoxydibenzo[*b,d*]tellurophene (2c): Following the general procedure, the reaction of diaryliodonium salt **1c** (137.4 mg, 0.3 mmol), tellurium (58 mg, 0.45 mmol), 2-picoline (1 mL) and DMSO (2 mL) under a nitrogen atmosphere. After 12 h at 120 °C, purification by column chromatography on silica gel (petroleum ether/EtOAc = 200/1) afforded **2c** (71 mg, 76%) as a yellow solid. M.p. 134-135 °C. IR (KBr, cm^{-1}): 3050, 2923, 2856, 1585, 1454, 1253, 1217, 1023, 825, 759, 719; ^1H NMR (500 MHz, CDCl_3): δ 7.96 (m, 2H), 7.83 (dd, $J = 8.0, 1.2$ Hz, 1H), 7.43-7.40 (m, 1H), 7.38 (d, $J = 2.5$ Hz, 1H), 7.25-7.22 (m, 1H), 7.03 (dd, $J = 8.8$ Hz, $J = 2.5$ Hz, 1H), 3.88 (s, 3H); ^{13}C NMR (125 MHz, CDCl_3): δ 158.8, 143.9, 137.5, 132.5, 129.9, 127.6, 126.0, 125.9, 125.3, 124.0, 116.1, 114.1, 55.7; HRMS (DART) calcd for $\text{C}_{13}\text{H}_{11}\text{OTe} [\text{M}+\text{H}]^+$ 312.9872, found 312.9867.

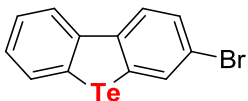


N-(Dibenzo[*b,d*]tellurophen-3-yl)acetamide (2d): Following the general procedure, the reaction of diaryliodonium salt **1d** (145.6 mg, 0.3 mmol), tellurium (58 mg, 0.45 mmol), 2-picoline (1 mL) and DMSO (2 mL) under a nitrogen atmosphere. After 12 h at 120 °C, purification by column chromatography on silica gel (petroleum ether/EtOAc = 3/1) afforded **2d** (35.4 mg, 35%) as a yellow solid. M.p. 176-177 °C. IR (KBr, cm^{-1}): 3240, 3049, 1659, 1585, 1520, 1480, 1439, 1378, 1315, 1273, 1010, 867, 717; ^1H NMR (500 MHz, CDCl_3): δ 8.32 (d, $J = 2.0$ Hz, 1H), 8.04-8.01 (m, 2H), 7.88 (d, $J = 8.3$ Hz, 1H), 7.46 (t, $J = 7.6$ Hz, 1H), 7.41 (dd, $J = 8.6, 2.1$ Hz, 1H), 7.31-7.26 (m, 1H), 2.25 (s, 3H); ^{13}C NMR (125 MHz, CDCl_3): δ 168.5, 143.6, 140.4, 136.7, 132.6, 129.7, 128.6, 126.6, 125.9, 124.7, 124.4, 123.0, 118.0, 24.9; HRMS (ESI) m/z calcd for $\text{C}_{13}\text{H}_7\text{TeN}^+ [\text{M}+\text{H}]^+$ 339.9976, found 339.9977.

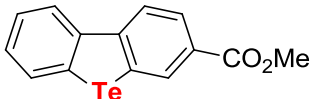


3-Phenyldibenzo[*b,d*]tellurophene (2e): Following the general procedure, the reaction of **1e** (151.2 mg, 0.3 mmol), tellurium (58 mg, 0.45 mmol), 2-picoline (1 mL) and DMSO (2 mL) under a nitrogen atmosphere. After 12 h at 120 °C, purification by column chromatography on silica gel (petroleum ether) afforded **2e** (56.3 mg, 53%) as a yellow solid. M.p. 146-147 °C. IR (KBr, cm^{-1}): 3043, 2921, 2856, 1588, 1445, 1376,

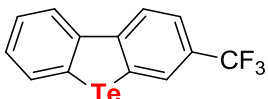
1242, 883, 752, 688, 590; ^1H NMR (500 MHz, CDCl_3): δ 8.18-8.09 (m, 3H), 7.90 (d, $J = 7.7$ Hz, 1H), 7.69-7.67 (m, 3H), 7.52-7.44 (m, 3H), 7.41-7.35 (m, 1H), 7.34-7.28 (m, 1H); ^{13}C NMR (125 MHz, CDCl_3): δ 143.8, 143.2, 140.6, 140.0, 132.8, 131.0, 129.4, 129.0, 128.9, 127.6, 127.3, 127.0, 125.9, 125.2, 124.9, 124.8. HRMS (ESI) m/z calcd for $\text{C}_{18}\text{H}_{12}\text{Te}^+ [\text{M}]^+$ 357.9996, found 358.0001.



3-Bromodibenzo[b,d]tellurophene (2f): Following the general procedure, the reaction of diaryliodonium salt **1f** (152.1 mg, 0.3 mmol), tellurium (58 mg, 0.45 mmol), 2-picoline (1 mL) and DMSO (2 mL) under a nitrogen atmosphere. After 12 h at 120 °C, purification by column chromatography on silica gel (petroleum ether) afforded **2f** (74.9 mg, 70%) as a yellow solid; M.p. 118-119 °C. IR (KBr, cm^{-1}): 3039, 2916, 1562, 1430, 1368, 1280, 1234, 1069, 1027, 860, 751, 710, 680, 566; ^1H NMR (500 MHz, CDCl_3): δ 8.05 (d, $J = 8.0$ Hz, 1H), 7.99 (d, $J = 2.4$ Hz, 1H), 7.93 (d, $J = 8.6$ Hz, 1H), 7.87 (d, $J = 7.8$ Hz, 1H), 7.56 (dd, $J = 8.4, 1.8$ Hz, 1H), 7.51-7.40 (m, 1H), 7.39-7.28 (m, 1H); ^{13}C NMR (125 MHz, CDCl_3): δ 143.1, 143.0, 134.8, 132.6, 130.4, 129.2, 128.8, 127.4, 126.0, 125.7, 124.8, 120.9; HRMS (ESI) m/z calcd for $\text{C}_{12}\text{H}_7\text{BrTe}^+ [\text{M}]^+$ 359.8788, found 359.8784.

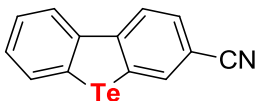


Methyl dibenzo[b,d]tellurophene-3-carboxylate (2g): Following the general procedure, the reaction of diaryliodonium salt **1g** (145.8 mg, 0.3 mmol), tellurium (58 mg, 0.45 mmol), 2-picoline (1 mL) and DMSO (2 mL) under a nitrogen atmosphere. After 12 h at 120 °C, purification by column chromatography on silica gel (petroleum ether/EtOAc = 40/1) afforded **2g** (57.3 mg, 57%) as a yellow solid. M.p. 135-136 °C. IR (KBr, cm^{-1}): 3050, 2986, 2941, 1702, 1583, 1427, 1378, 1282, 1243, 1105, 963, 911, 744, 522; ^1H NMR (500 MHz, CDCl_3): δ 8.57 (d, $J = 1.2$ Hz, 1H), 8.18-8.09 (m, 3H), 7.92 (d, $J = 7.8$ Hz, 1H), 7.49 (t, $J = 8.2$ Hz, 1H), 7.36 (td, $J = 8.5, 1.3$ Hz, 1H), 3.96 (s, 3H); ^{13}C NMR (125 MHz, CDCl_3): δ 166.8, 147.9, 143.0, 134.2, 132.8, 130.5, 128.6, 128.1, 127.9, 126.9, 126.0, 125.7, 124.3, 52.4; HRMS (DART) calcd for $\text{C}_{14}\text{H}_{10}\text{O}_2\text{Te} [\text{M}+\text{H}]^+$ 340.9821, found 340.9816.

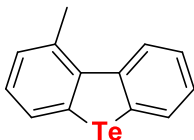


3-(Trifluoromethyl)dibenzo[b,d]tellurophene (2h): Following the general procedure, the reaction of diaryliodonium salt **1h** (148.8 mg, 0.3 mmol), tellurium (58 mg, 0.45 mmol), 2-picoline (1 mL) and DMSO (2 mL) under a nitrogen atmosphere. After 12 h at 120 °C, purification by column chromatography on silica gel (petroleum ether) afforded **2h** (84.6 mg, 81%) as a yellow solid. M.p. 92-93 °C. IR (KBr, cm^{-1}):

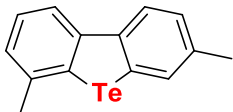
3061, 2920, 1764, 1590, 1389, 1317, 1247, 1069, 883, 822, 764, 725, 670, 461; ^1H NMR (500 MHz, CDCl_3): δ 8.18-8.15 (m, 3H), 7.92 (dd, $J = 7.9, 0.6$ Hz, 1H), 7.69 (dd, $J = 8.3, 1.0$ Hz, 1H), 7.50 (td, $J = 7.7, 1.1$ Hz, 1H), 7.37 (td, $J = 7.4, 1.1$ Hz, 1H); ^{19}F NMR (CDCl_3 , 470 MHz): δ -61.75; ^{13}C NMR (125 MHz, CDCl_3): δ 146.9, 142.7, 132.7, 130.1, 129.5 ($q, ^3J_{\text{C}-\text{F}} = 3.8$ Hz), 129.0, 128.5 ($q, ^2J_{\text{C}-\text{F}} = 32.5$ Hz), 127.9, 126.1, 125.5, 124.2 (d, $^1J_{\text{C}-\text{F}} = 271$ Hz), 124.5, 122.7 ($q, ^3J_{\text{C}-\text{F}} = 3.8$ Hz); HRMS (DART) calcd for $\text{C}_{13}\text{H}_7\text{F}_3\text{Te} [\text{M}]^+$ 349.9557, found 349.9557.



Dibenzo[*b,d*]tellurophene-3-carbonitrile (2i): Following the general procedure, the reaction of diaryliodonium salt **1i** (135.9 mg, 0.3 mmol), tellurium (58 mg, 0.45 mmol), 2-picoline (1 mL) and DMSO (2 mL) under a nitrogen atmosphere. After 12 h at 120 °C, purification by column chromatography on silica gel (petroleum ether/EtOAc = 10/1) afforded **2i** (62.8 mg, 69 %) as a yellow solid. M.p. 157-158 °C. IR (KBr, cm^{-1}): 3045, 2920, 2206, 1734, 1378, 1272, 1230, 1184, 1014, 887, 759, 712, 643; ^1H NMR (500 MHz, CDCl_3): δ 8.19-8.11 (m, 3H), 7.93 (dd, $J = 7.8, 0.6$ Hz, 1H), 7.70 (dd, $J = 8.3, 1.6$ Hz, 1H), 7.52 (td, $J = 8.2, 1.1$ Hz, 1H), 7.40 (td, $J = 8.1, 1.3$ Hz, 1H); ^{13}C NMR (125 MHz, CDCl_3): δ 147.6, 142.3, 136.4, 132.7, 130.8, 129.3, 128.9, 128.4, 126.3, 125.8, 124.7, 118.9, 109.8; HRMS (DART) calcd for $\text{C}_{13}\text{H}_8\text{NTE} [\text{M}+\text{H}]^+$ 307.9713, found 307.9713.

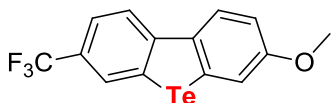


1-Methyldibenzo[*b,d*]tellurophene (2j): Following the general procedure, the reaction of diaryliodonium salt **1j** (132.6 mg, 0.30 mmol), tellurium (58 mg, 0.45 mmol), 2-picoline (1 mL) and DMSO (2 mL) under a nitrogen atmosphere. After 12 h at 120 °C, purification by column chromatography on silica gel (petroleum ether) afforded **2j** (54.2 mg, 62%) as a yellow solid. M.p. 73-74 °C. IR (KBr, cm^{-1}): 3053, 2919, 2855, 1759, 1563, 1439, 1370, 1020, 816, 776, 715, 575; ^1H NMR (500 MHz, CDCl_3): δ 8.41 (d, $J = 8.3$ Hz, 1H), 7.95 (dd, $J = 7.7, 1.0$ Hz, 1H), 7.81 (d, $J = 8.3$ Hz, 1H), 7.48-7.44 (m, 1H), 7.29-7.26 (m, 2H), 7.16 (t, $J = 7.5$ Hz, 1H), 2.92 (s, 3H); ^{13}C NMR (125 MHz, CDCl_3): δ 145.7, 142.3, 137.8, 133.0, 130.8, 130.0, 129.8, 129.1, 128.9, 125.9, 125.9, 125.5, 24.7; HRMS (ESI) m/z calcd for $\text{C}_{13}\text{H}_{10}\text{Te}^+ [\text{M}]^+$ 295.9839, found 295.9841.

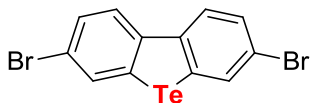


3,6-Dimethyldibenzo[*b,d*]tellurophene (2k): Following the general procedure, the reaction of diaryliodonium salt **1k** (136.8 mg, 0.3 mmol), tellurium (58 mg, 0.45

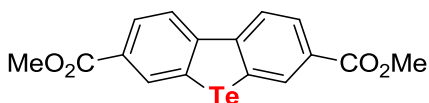
mmol), 2-picoline (1 mL) and DMSO (2 mL) under a nitrogen atmosphere. After 12 h at 120 °C, purification by column chromatography on silica gel (petroleum ether) afforded **2k** (66.6 mg, 72%) as a yellow solid. M.p. 59–60 °C. IR (KBr, cm⁻¹): 3035, 2921, 2863, 1595, 1454, 1381, 1251, 1159, 825, 633; ¹H NMR (500 MHz, CDCl₃): δ 7.96 (d, *J* = 8.1 Hz, 1H), 7.89 (d, *J* = 7.9 Hz, 1H), 7.73 (s, 1 H), 7.40 (t, *J* = 7.5 Hz, 1H), 7.26 (d, *J* = 8.0 Hz, 1H), 7.16 (d, *J* = 7.5 Hz, 1H), 2.50 (s, 3 H), 2.44 (s, 3H); ¹³C NMR (125 MHz, CDCl₃): δ 144.1, 142.6, 140.1, 136.9, 132.8, 131.8, 128.6, 127.2, 126.4, 126.0, 124.7, 121.6, 26.4, 21.4; HRMS (ESI) m/z calcd for C₁₄H₁₂Te⁺ [M]⁺ 309.9995, found 309.9999.



3-Methoxy-7-(trifluoromethyl)dibenzo[b,d]tellurophene (2l): Following the general procedure, the reaction of diaryliodonium salt **1l** (157.8 mg, 0.3 mmol), tellurium (58 mg, 0.45 mmol), 2-picoline (1 mL) and DMSO (2 mL) under a nitrogen atmosphere. After 12 h at 120 °C, purification by column chromatography on silica gel (petroleum ether/EtOAc = 100/1) afforded **2l** (64.2 mg, 57%) as a yellow solid. M.p. 89–90 °C. IR (KBr, cm⁻¹): 3095, 2954, 2847, 2606, 1596, 1476, 1322, 1276, 1232, 1139, 1077, 1024, 826, 637; ¹H NMR (500 MHz, CDCl₃): δ 8.08 (s, 1H), 8.02 (d, *J* = 8.4 Hz, 1H), 8.01 (d, *J* = 8.9 Hz, 1H), 7.64 (dd, *J* = 8.4, 1.1 Hz, 1H), 7.40 (d, *J* = 2.5 Hz, 1H), 7.07 (dd, *J* = 8.8, 2.5 Hz, 1H), 3.90 (s, 3H); ¹³C NMR (125 MHz, CDCl₃) δ 159.5, 146.9, 136.1, 131.4, 129.4 (q, ³J_{C-F} = 3.8 Hz), 127.7, 127.6 (²J_{C-F} = 31 Hz), 126.1, 124.3 (¹J_{C-F} = 270 Hz), 123.8, 122.8 (q, ³J_{C-F} = 3.8 Hz), 116.1, 114.5, 55.7; HRMS (DART) calcd for C₁₄H₁₀F₃OTe [M+H]⁺ 380.9746, found 380.9741.

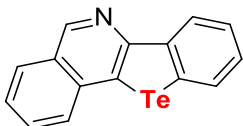


3,7-Dibromodibenzo[b,d]tellurophene (2m):^{S11} Following the general procedure, the reaction of diaryliodonium salt **1m** (175.1 mg, 0.3 mmol), tellurium (58 mg, 0.45 mmol), 2-picoline (1 mL) and DMSO (2 mL) under a nitrogen atmosphere. After 12 h at 120 °C, purification by column chromatography on silica gel (petroleum ether) afforded **2m** (96.2 mg, 73 %) as a yellow solid. M.p. 213–214 °C. IR (KBr, cm⁻¹): 2922, 2858, 1723, 1559, 1436, 1361, 1259, 1079, 863, 804, 702; ¹H NMR (500 MHz, CDCl₃): δ 7.98 (d, *J* = 1.9 Hz, 2H), 7.86 (d, *J* = 8.5 Hz, 2H), 7.56 (dd, *J* = 8.5, 1.9 Hz, 2H); ¹³C NMR (125 MHz, CDCl₃): δ 141.9, 134.8, 130.4, 129.4, 125.8, 121.3; HRMS (DART) calcd for C₁₂H₇Br₂OTe⁺ [M+OH]⁺ 456.7905, found 458.7900.

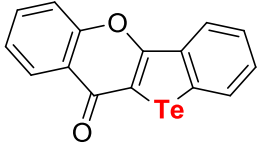


Dimethyl dibenzo[b,d]tellurophene-3,7-dicarboxylate (2n): Following the general procedure, the reaction of diaryliodonium salt **1n** (163.1 mg, 0.3 mmol), tellurium (58

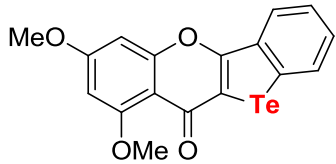
mg, 0.45 mmol), 2-picoline (1 mL) and DMSO (2 mL) under a nitrogen atmosphere. After 12 h at 120 °C, purification by column chromatography on silica gel (petroleum ether/EtOAc = 10/1) afforded **2n** (67.8 mg, 57%) as a yellow solid. M.p. 225-226 °C. IR (KBr, cm⁻¹): 3070, 2940, 1712, 1583, 1431, 1383, 1277, 1111, 975, 836, 755, 695; ¹H NMR (500 MHz, CDCl₃): δ 8.60 (d, *J* = 1.5 Hz, 2H), 8.20 (d, *J* = 8.3 Hz, 2H), 8.13 (dd, *J* = 8.4, 1.6 Hz, 2H), 3.97 (s, 6H); ¹³C NMR (125 MHz, CDCl₃): δ 166.6, 146.7, 134.3, 130.3, 128.9, 127.1, 125.3, 52.5. HRMS (DART) calcd for C₁₆H₁₃O₄Te [M+H]⁺ 398.9876, found 398.9870.



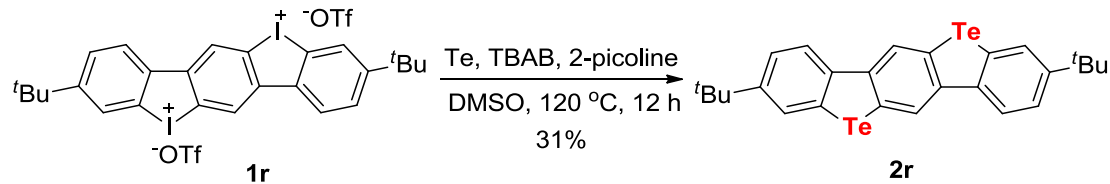
Benzo[4,5]telluropheno[3,2-c]isoquinoline (2o) Following the general procedure, the reaction of diaryliodonium salt **1o** (143.8 mg, 0.3 mmol), tellurium (58 mg, 0.45 mmol), 2-picoline (1 mL) and DMSO (2 mL) under a nitrogen atmosphere. After 12 h at 120 °C, purification by column chromatography on silica gel (petroleum ether/EtOAc = 10/1) afforded **2o** (43.9 mg, 44%) as a yellow solid. M.p. 149-150 °C. IR (KBr, cm⁻¹): 3049, 2926, 2356, 1701, 1532, 1441, 1305, 1094, 949, 904, 751; ¹H NMR (500 MHz, CDCl₃): δ 9.31 (s, 1H), 8.62 (dd, *J* = 8.8, 0.9 Hz, 1H), 8.10 (d, *J* = 8.0 Hz, 1H), 8.00 (d, *J* = 7.4 Hz, 1H), 7.81-7.77 (m, 1H), 7.74-7.64 (m, 2H), 7.61-7.58 (m, 1H), 7.45-7.41 (m, 1H); ¹³C NMR (125 MHz, CDCl₃): δ 154.7, 151.4, 144.1, 138.7, 132.3, 131.2, 128.9, 128.3, 127.9, 127.6, 127.5, 127.5, 126.8, 126.2, 125.1; HRMS (ESI) m/z calcd for C₁₅H₁₀NTe [M+H]⁺ 333.9870, found 333.9873.



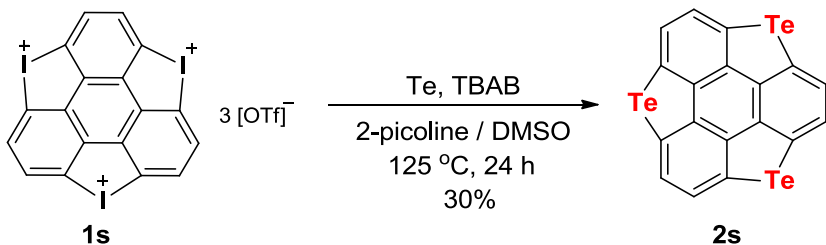
11*H*-benzo[4,5]telluropheno[2,3-*b*]chromen-11-one (2p) Following the general procedure, the reaction of diaryliodonium salt **1p** (148.9 mg, 0.3 mmol), tellurium (58 mg, 0.45 mmol), 2-picoline (1 mL) and DMSO (2 mL) under a nitrogen atmosphere. After 12 h at 120 °C, purification by column chromatography on silica gel (petroleum ether/ EtOAc = 10:1 to 5:1) afforded **2p** (47.4 mg, 46%) as a yellow solid. M.p. 236-237 °C. IR (KBr, cm⁻¹): 3055, 2922, 2859, 2360, 1603, 1557, 1513, 1459, 1377, 1261, 1209, 1087, 859, 713; ¹H NMR (500 MHz, CDCl₃): δ 8.32 (dd, *J* = 8.0, 1.7 Hz, 1H), 8.24 (d, *J* = 7.9 Hz, 1H), 7.99 (d, *J* = 7.9 Hz, 1H), 7.80-7.74 (m, 1H), 7.66 (d, *J* = 7.9 Hz, 1H), 7.56 (t, *J* = 7.6 Hz, 1H), 7.50 (t, *J* = 7.0 Hz, 1H), 7.45-7.41 (m, 1H); ¹³C NMR (125 MHz, CDCl₃): δ 177.3, 159.7, 156.3, 137.6, 134.0, 133.1, 129.4, 128.8, 127.1, 126.1, 126.0, 125.3, 121.6, 118.1, 113.3; HRMS (ESI) m/z calcd for C₁₅H₉O₂Te [M+H]⁺ 350.9665, found 350.9662.



2,4-Dimethoxy-11*H*-benzo[4,5]telluropheno[2,3-*b*]chromen-11-one (2q): A 25 mL Schlenk tube was charged with diaryliodonium salt **1q** (111.2 mg, 0.2 mmol), tellurium (51 mg, 0.4 mmol), 2-picoline (0.7 mL) and DMSO (1.4 mL) under a nitrogen atmosphere. The reaction mixture was stirred at 120 °C for 12 h. After cooled to room temperature, the reaction mixture was diluted with H₂O (15 mL), and extracted with DCM (3×15 mL). The combined organic phase was washed with water (2×10 mL) and brine (20 mL), dried over anhydrous Na₂SO₄, and then evaporated under reduced pressure. Purification by column chromatography on silica gel (petroleum ether/ EtOAc = 2 : 1) afforded **2q** (35.5 mg, 44%) as a yellow solid. M.p. 204-205 °C .IR (KBr, cm⁻¹): 2923, 2855, 1615, 1458, 1388, 1349, 1270, 1074, 813, 762; ¹H NMR (500 MHz, CDCl₃): δ 8.13 (d, J = 8.0 Hz, 1H), 7.96 (d, J = 7.9 Hz, 1H), 7.55-7.45 (m, 1H), 7.41 -7.33 (m, 1H), 6.67 (d, J = 2.3 Hz, 1H), 6.45 (d, J = 2.3 Hz, 1H), 3.98 (s, 3H), 3.95 (s, 3H); ¹³C NMR (125 MHz, CDCl₃): δ 176.1, 164.3, 161.1, 160.2, 157.3, 137.6, 133.1, 128.7, 128.5, 126.5, 125.8, 116.1, 107.3, 96.4, 93.0, 56.6, 56.0 ; HRMS (ESI) m/z calcd for C₁₇H₁₃O₄Te [M+H]⁺ 410.9871, found 410.9873.



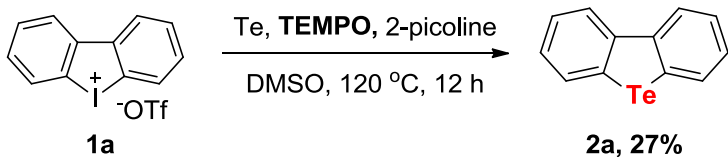
3,9-Bis(tert-butyl)benzo[1,2-b:4,5-b']bis[b]benzotellurophene (2r): A 25 mL Schlenk tube was charged with diaryliodonium salt **1r** (88.9 mg, 0.10 mmol), TBAB (193.2 mg, 0.6 mmol), tellurium (102.1 mg, 0.8 mmol), 2-picoline (0.7 mL) and DMSO (1.4 mL) under a nitrogen atmosphere. The reaction mixture was stirred at 120 °C for 12 h. After cooled to room temperature, the reaction mixture was diluted with H₂O (15 mL), extracted with DCM/CS₂ (9:1, 3×15 mL). The combined organic phase was washed with water (2×10 mL) and brine (20 mL), dried over anhydrous Na₂SO₄, and then evaporated under reduced pressure. Purification by column chromatography on silica gel (petroleum ether/DCM = 50:1 to 20:1) afforded **2r** (18.5 mg, 31%) as a yellow solid. M.p.>300 °C. IR (KBr, cm⁻¹): 3049, 2953, 2862, 1642, 1586, 1547, 1469, 1387, 1255, 1040, 862, 735; ¹H NMR (500 MHz, CDCl₃): δ 8.48 (s, 2H), 8.01 (d, J = 8.5 Hz, 2H), 7.90 (d, J = 1.8 Hz, 2H), 7.49 (dd, J = 8.4, 1.9 Hz, 2H), 1.41 (s, 18H); ¹³C NMR (125 MHz, CDCl₃): δ 150.6, 143.0, 140.6, 129.2, 128.5, 128.2, 125.4, 124.2, 124.0, 35.1, 31.5; HRMS (MALDI-FT/DHB) m/z calcd for C₂₆H₂₆Te₂ [M]⁺ 594.0130, found 594.0126.



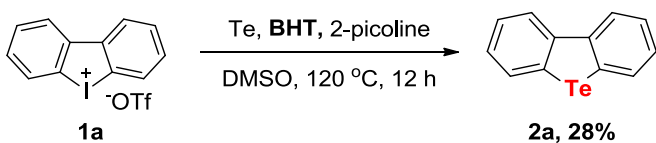
Triphenylene[1,12-bcd:4,5-b'c'd':8,9-b''c''d'']tris(tellurophene) (2s): **1s** was prepared by our recently developed method.^{S12} A 100 mL Schlenk tube was charged with diaryliodonium salt **1s** (315mg, 0.3 mmol), tellurium (760 mg, 6.0 mmol), TBAB (1.93 g, 6.0 mmol), 2-picoline (8 mL) and DMSO (12 mL) under a nitrogen atmosphere. The reaction mixture was stirred at 125 °C for 24 h. After the reaction, water (60 mL) were added, followed by vigorously stirring for 3 min, The solid was filtered and washed with water (2×60 mL), extracted with DCM/CS₂(10:1, 2×55 mL). After filtered, the combined organic phase was dried over anhydrous Na₂SO₄, and then evaporated under reduced pressure. Purification by column chromatography on silica gel (DCM) afforded **2s** (54.7 mg, 30%) as a yellow solid. M.p.>300 °C. IR (KBr, cm⁻¹): 3050, 2923, 2855, 1615, 1458, 1388, 1349, 1270, 1074, 813, 762; ¹H NMR (500 MHz, DMSO-*d*₆): δ 8.31 (s, 6H); ¹³C NMR (125 MHz, DMSO-*d*₆) δ 140.3, 129.9, 126.6; HRMS (MALDI-FT/DHB) m/z calcd for C₁₈H₆Te₃ [M]⁺ 605.7609, found 605.7615.

3. Mechanistic Studies

3.1 Reaction with radical inhibitors TEMPO and BHT



A 25 mL Schlenk tube was charged with diaryliodonium salt **1a** (128.4 mg, 0.3 mmol), tellurium (58 mg, 0.45 mmol), 2,2,6,6-tetramethylpiperidine-1-oxyl (TEMPO) (93.6 mg, 0.6 mmol), 2-picoline (1 mL) and DMSO (2 mL) under a nitrogen atmosphere. The reaction mixture was stirred at 120 °C for 12 h. After cooled to room temperature, the reaction mixture was diluted with H₂O (15 mL), and extracted with DCM (3×15 mL). The combined organic phase was washed with water (2×10 mL) and brine (20 mL), dried over anhydrous Na₂SO₄, and then evaporated under reduced pressure. Purification by column chromatography on silica gel (petroleum ether) afforded **2a** (22.4 mg, 27 %) as a yellow solid.

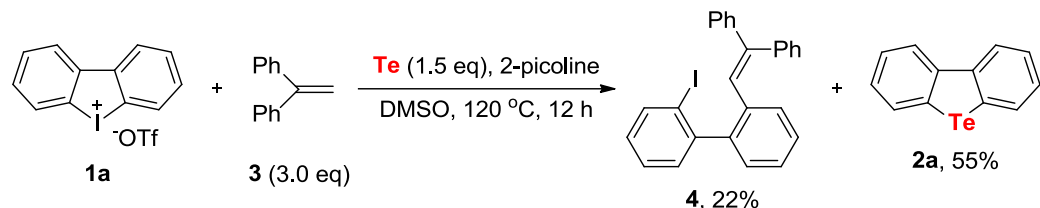


A 25 mL Schlenk tube was charged with diaryliodonium salt **1a** (128.4 mg, 0.3 mmol), tellurium (58 mg, 0.45 mmol), butylated hydroxytoluene (BHT) (132.2 mg, 0.6 mmol), 2-picoline (1 mL) and DMSO (2 mL) under a nitrogen atmosphere. The

reaction mixture was stirred at 120 °C for 12 h. After cooled to room temperature, the reaction mixture was diluted with H₂O (15 mL), and extracted with DCM (3×15mL). The combined organic phase was washed with water (2×10 mL) and brine (20 mL), dried over anhydrous Na₂SO₄, and then evaporated under reduced pressure. Purification by column chromatography on silica gel (petroleum ether) afforded **2a** (23.1 mg, 28%) as a yellow solid.

3.2 Radical-trapping experiments with 1,1-diphenylethylene **3**

(a) Under standard conditions



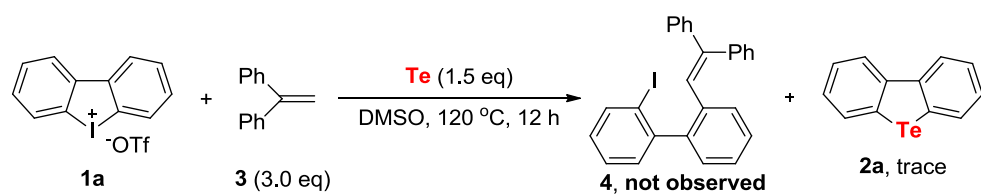
A 25 mL Schlenk tube was charged with diaryliodonium salt **1a** (128.4 mg, 0.3 mmol), tellurium (58 mg, 0.45 mmol), ethene-1,1-diylbenzene **3** (162 mg, 0.9 mmol) 2-picoline (1 mL) and DMSO (2 mL) under a nitrogen atmosphere. The reaction mixture was stirred at 120 °C for 12 h. After cooled to room temperature, the reaction mixture was diluted with H₂O (15 mL), and extracted with DCM (3×15 mL). The combined organic phase was washed with water (2×10 mL) and brine (20 mL), dried over anhydrous Na₂SO₄, and then evaporated under reduced pressure. Purification by column chromatography on silica gel (petroleum ether) afforded **4** (29.9 mg, 22%) and **2a** (46.1 mg, 55%). Characterization of compound **4**: M.p. 141-142 °C. IR (KBr, cm⁻¹): 3214, 3054, 2957, 1550, 1491, 1442, 1261, 1001, 880, 761, 698, 648; ¹H NMR (500 MHz, CDCl₃): δ 7.98 (dd, *J* = 8.0, 1.1 Hz, 1H), 7.34-6.96 (m, 17H), 6.69 (s, 1H); ¹³C NMR (125 MHz, CDCl₃): δ 146.3, 144.7, 143.6, 143.1, 140.5, 139.1, 135.8, 130.8, 130.4, 130.0, 129.9, 128.9, 128.4, 128.1(9), 128.1(7), 128.1(5), 127.5, 127.4, 127.3, 126.7, 126.5, 100.1; MS (DART, m/z): 458 [M]⁺.

(b) Without tellurium



The same procedure as (a) except without addition of tellurium.

(c) Without 2-picoline

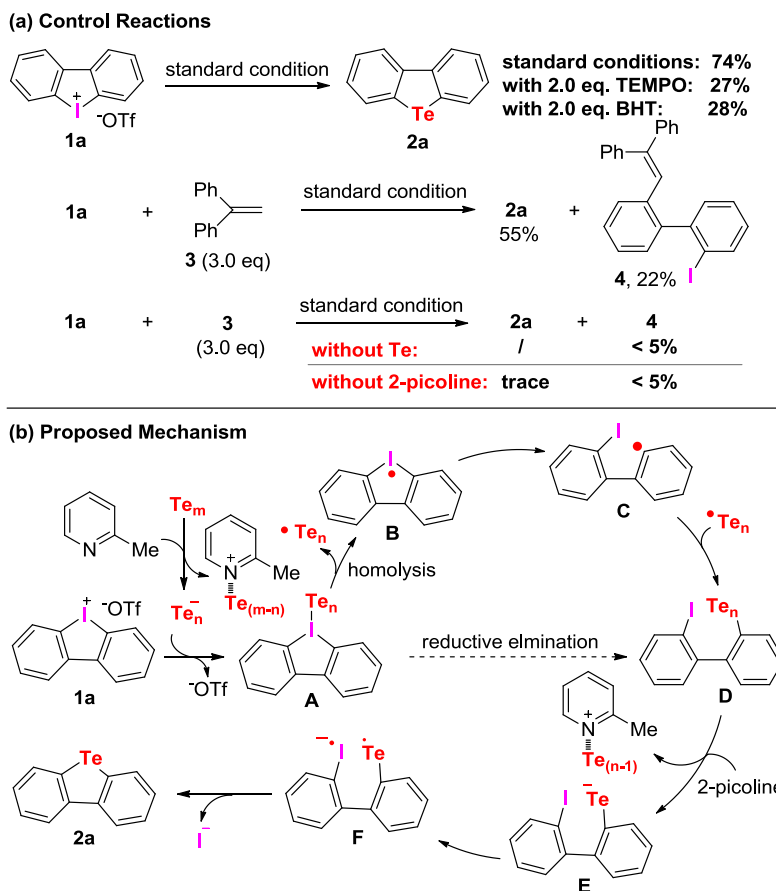


The same procedure as (a) except without addition of 2-picoline.

3.3 Proposed Mechanism

Based on the results of the control reactions, the reaction was significantly inhibited by radical scavengers (TEMPO or BHT) indicating a radical pathway might be involved. According to the experimental results and literature,^{S13,S14} a plausible mechanism was proposed as shown in Scheme S1. Chalcogens were reported to form anions under bases.^{S13} In the presence of 2-picoline, polymeric tellurium (Te_m) generated tellurium anions, which exchanged with the anion of **1a** to give intermediate **A**. The cationic complex between 2-picoline and tellurium formed was probably stabilized by the aromatic pyridine ring; while other organic bases such trialkyl amines did not have such an effect. Homolysis of **A** led to intermediate **B**, which then rearranged to **C**.^{S15} Radical coupling between **C** and tellurium radical gave **D**, which afforded intermediate **E** with the aid of 2-picoline. The intermolecular coupling between aryl iodide and tellurium anions under transitional-metal free conditions was well documented possibly via a single electron transfer mechanism.^{S14} Therefore, **E** transformed to the desired product **2a** possibly through intermediate **F**. Radical trapping reaction of **C** with olefin **3** under the standard condition gave the expected olefin product **4** (Scheme S1a). However, **4** could not be isolated in the absence of either tellurium or base indicating their vital roles for generation of radical species. Direct transformation of intermediate **A** to **D** through reductive elimination could not be ruled out at this stage.^{S15}

Scheme S1. Reaction Mechanism Studies



4. X-ray Crystallographic Data

The data can be obtained free of charge from The Cambridge Crystallographic Data Centre via www.ccdc.cam.ac.uk/data_request/cif.

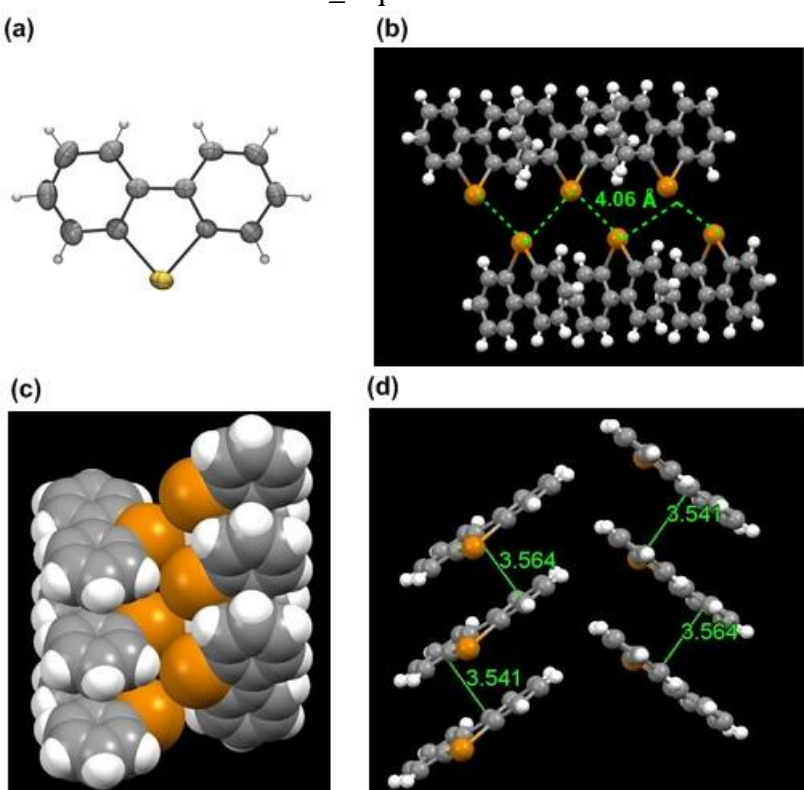


Figure S1. X-ray structure of **2a**. (a) ORTEP drawing (thermal ellipsoids set at 50% probability); (b) Packing with Te-Te distance; (c) Packing in a spacefill model; (d) Packing with π - π interactions. The crystal suitable for X-ray crystallographic analysis was obtained as a yellow needle by slow evaporation from a toluene solution; CCDC 1892105.

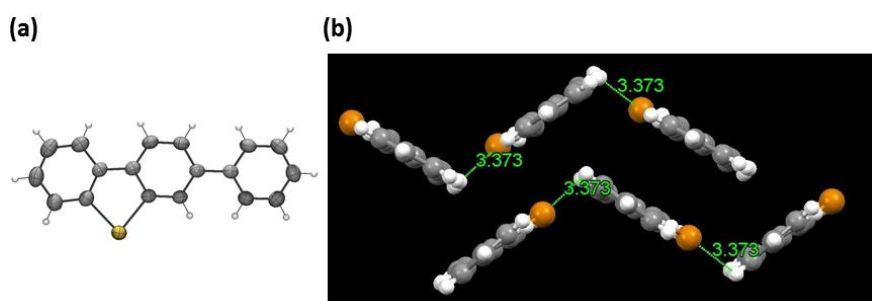


Figure S2. X-ray structure of **2e**. (a) ORTEP drawing (thermal ellipsoids set at 50% probability); (b) Packing with Te-H distances. The crystal suitable for X-ray crystallographic analysis was obtained as a yellow needle by slow evaporation from a toluene solution; CCDC 1942804.

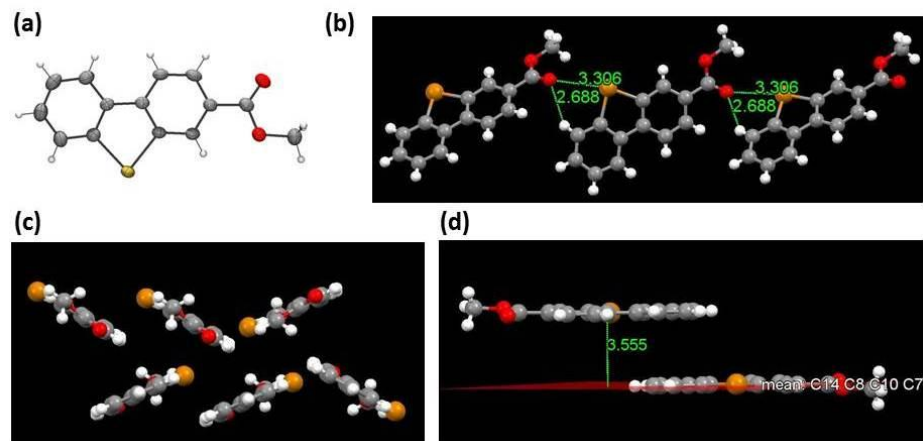


Figure S3. X-ray structure of **2g**. (a) ORTEP drawing (thermal ellipsoids set at 50% probability); (b) Packing with Te-O and O-H distances; (c) Packing model; (d) Packing with π - π interactions. The crystal suitable for X-ray crystallographic analysis was obtained as a yellow needle by slow evaporation from a toluene solution; CCDC 1892106.

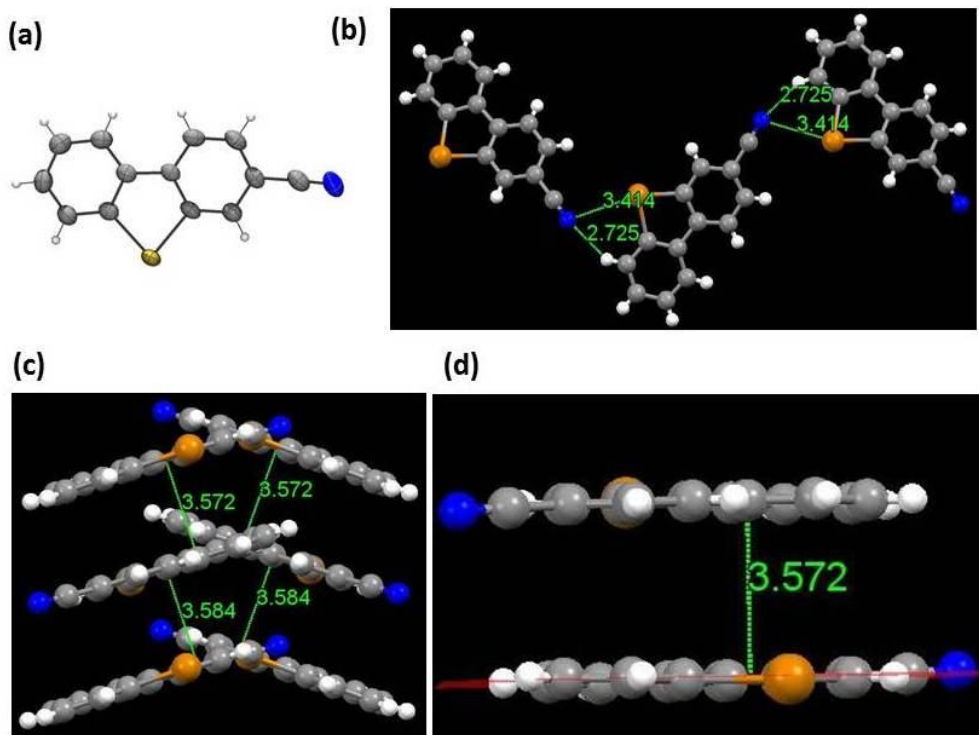


Figure S4. X-ray structure of **2i**. (a) ORTEP drawing (thermal ellipsoids set at 50% probability); (b) Packing with Te-N and N-H distances; (c) Packing with π - π interactions; (d) Packing between two molecular in the adjacent layer. The crystal suitable for X-ray crystallographic analysis was obtained as a yellow prism by slow evaporation from a toluene solution; CCDC 1942805.

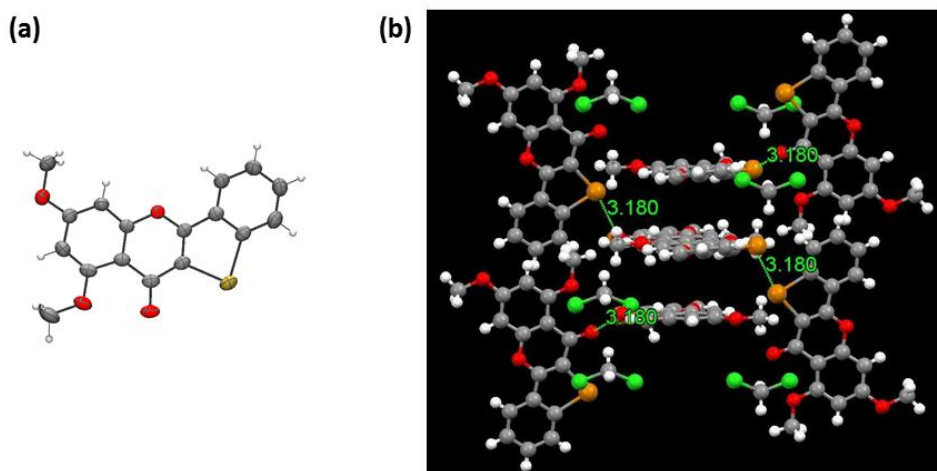


Figure S5. X-ray structure of **2q**. (a) ORTEP drawing (thermal ellipsoids set at 50% probability); (b) Packing with Te-O distances. The crystal suitable for X-ray crystallographic analysis was obtained as yellow block by slow evaporation from a dichloromethane solution; CCDC 1892119.

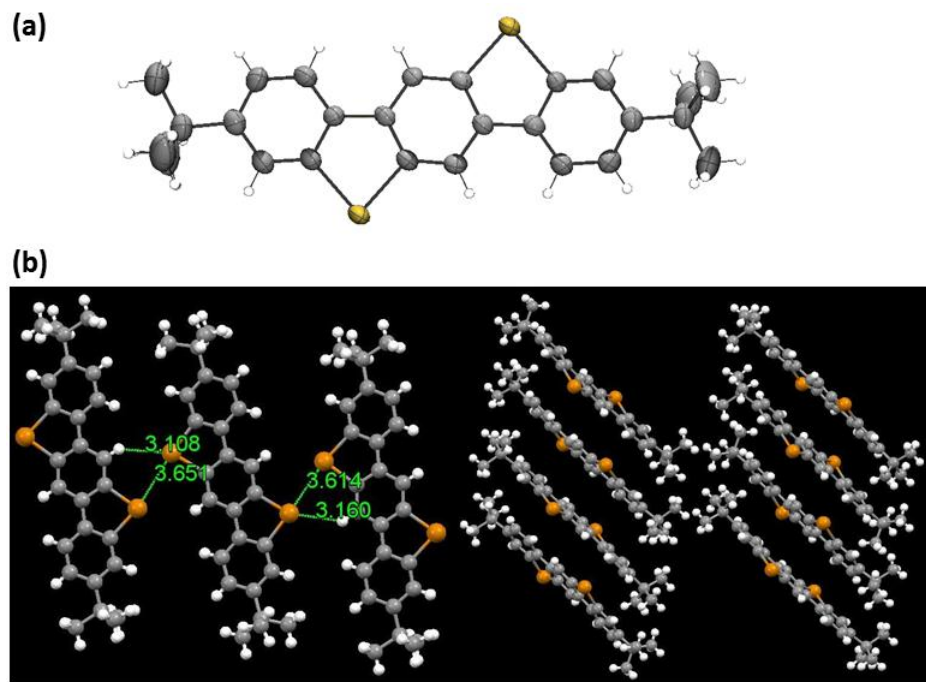


Figure S6. X-ray structure of **2r**. (a) ORTEP drawing (thermal ellipsoids set at 50% probability); (b) Packing with Te-Te and Te-H distances; The crystal suitable for X-ray crystallographic analysis was obtained as yellow needle by slow evaporation from a chloroform solution; CCDC 1942806.

5. Electrochemical Properties

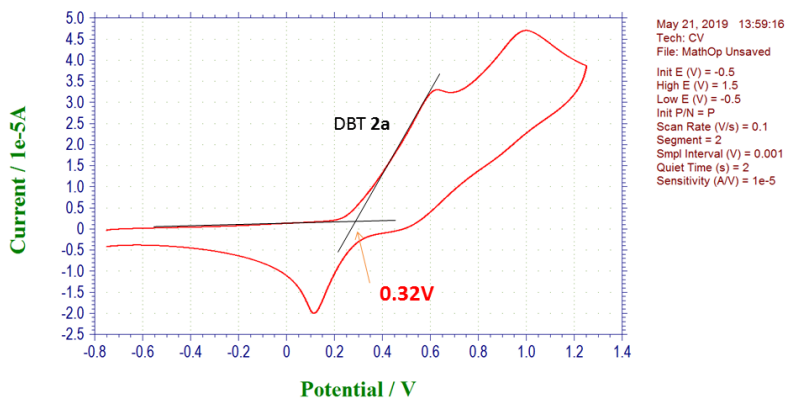


Figure S7. Cyclic voltammograms of DBTe **2a** in dichloromethane containing 0.10 M *n*-Bu₄NClO₄. The potentials were calibrated using the ferrocene/ferrocenium (Fc/Fc⁺) redox couple (0.25 V vs. Ag/Ag⁺) as an external standard which was measured under the same condition. The arrows indicate the onset of oxidative potentials. The HOMO level was estimated to be -5.12 eV ($E_{\text{HOMO}} = -E_{\text{ox(onset)}} - 4.80$).

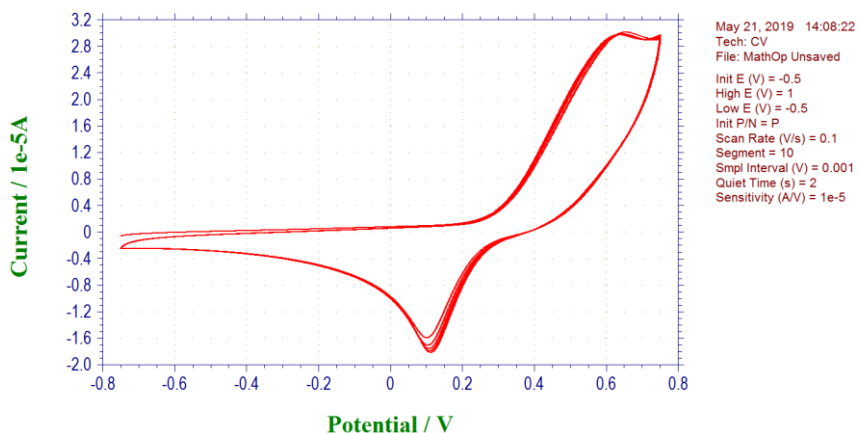


Figure S8. Cyclic voltammograms of DBTe **2a** (five scanning circles) in dichloromethane containing 0.10 M *n*-Bu₄NClO₄.

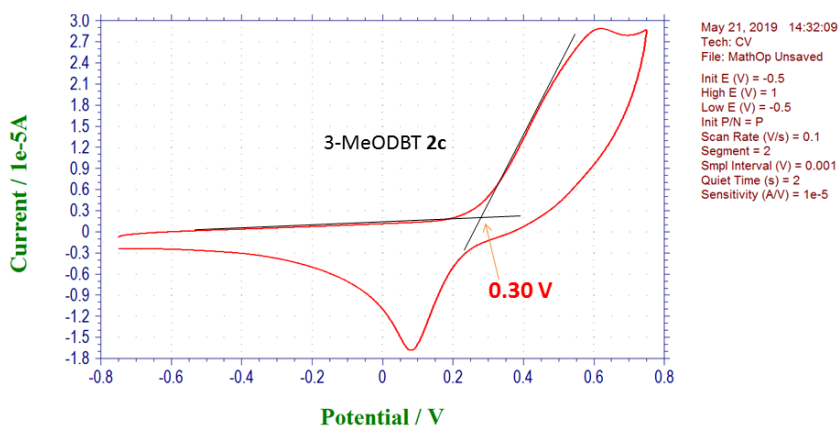


Figure S9. Cyclic voltammograms of DBTe **2c** in dichloromethane containing 0.10 M *n*-Bu₄NClO₄.

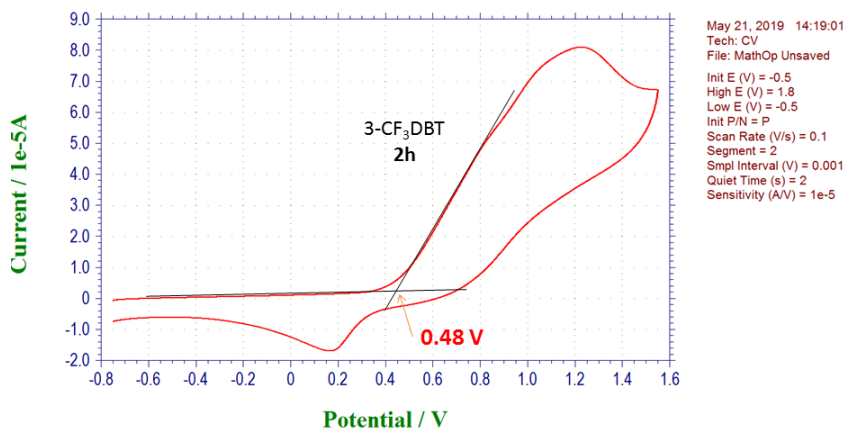


Figure S10. Cyclic voltammograms of DBTe **2h** in dichloromethane containing 0.10 M *n*-Bu₄NClO₄.

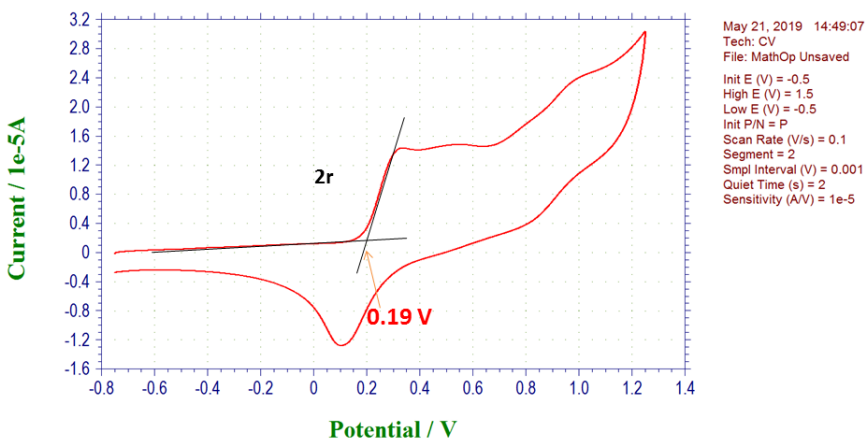


Figure S11. Cyclic voltammograms of DBTe **2r** in dichloromethane containing 0.10 M *n*-Bu₄NClO₄.

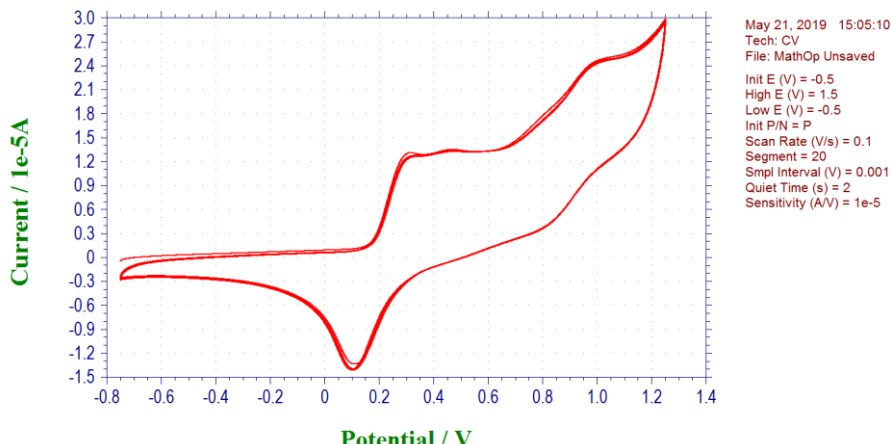


Figure S12. Cyclic voltammograms of DBTe **2r** (ten scanning circles) in dichloromethane containing 0.10 M *n*-Bu₄NClO₄.

6. Studies of the Photophysical Properties

Table S1. Photographs of DBTe's taken under 365 nm lamp at room temperature

Entry	Structure	Photo	Entry	Structure	Photo
2a			2k		
2b			2l		
2c			2m		
2d			2n		
2e			2o		
2f			2p		
2g			2q		
2h			2r		
2i			2s		
2j			-	-	-

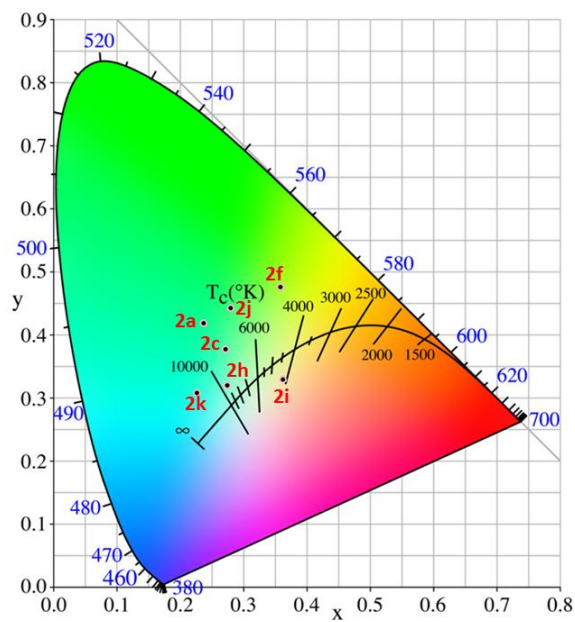


Figure S13. CIE chromaticity diagrams of DBTe's with strong RTP emission.

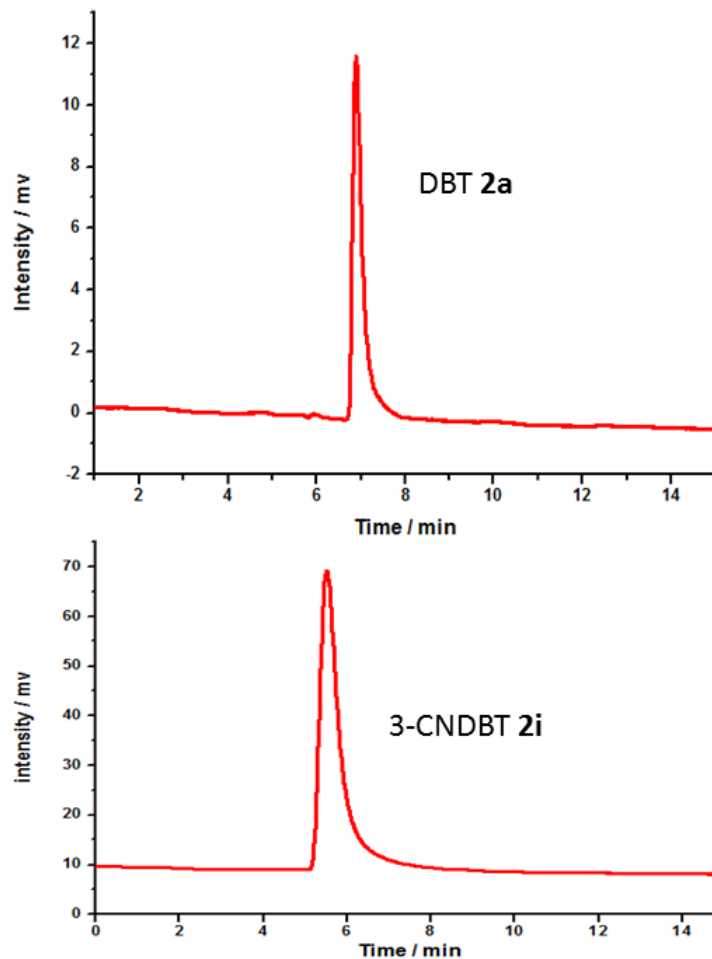


Figure S14. High-performance liquid chromatogram (HPLC) spectra of DBTe **2a** and 3-CNDBT **2i**. The sample was purified by preoperative HPLC and exhibited similar emission as those purified by normal chromatography.

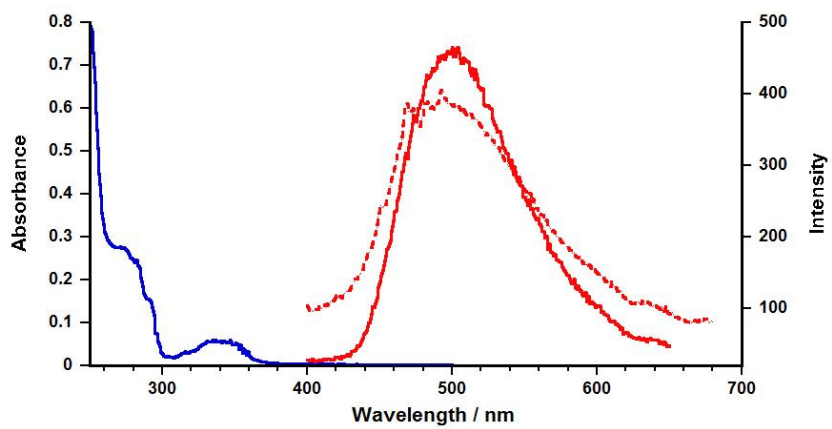


Figure S15. UV-Vis absorption spectrum (in THF, $c = 2 \times 10^{-5}$ M, blue line) and emission spectrum ($\lambda_{\text{exc}} = 350$ nm; red solid line for powder; red dashed line for crystals) of **2a** (DBTe) at room temperature.

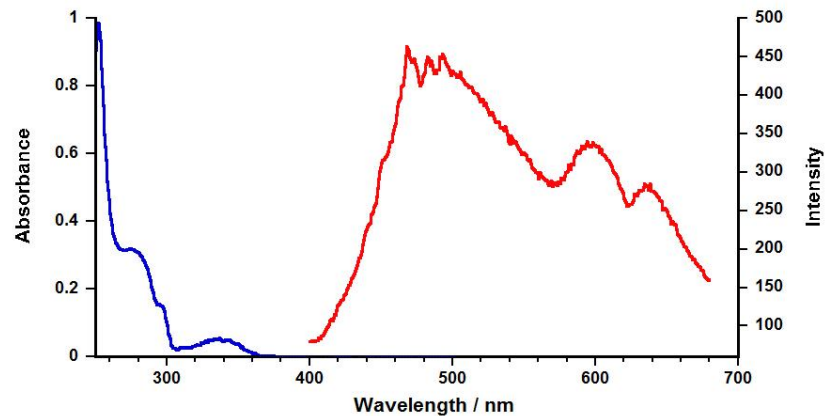


Figure S16. UV-Vis absorption spectrum (in THF, $c = 1.5 \times 10^{-5}$ M, blue line) and emission spectrum (powder, $\lambda_{\text{exc}} = 350$ nm, red line) of **2b** (3-MeDBTe) at room temperature.

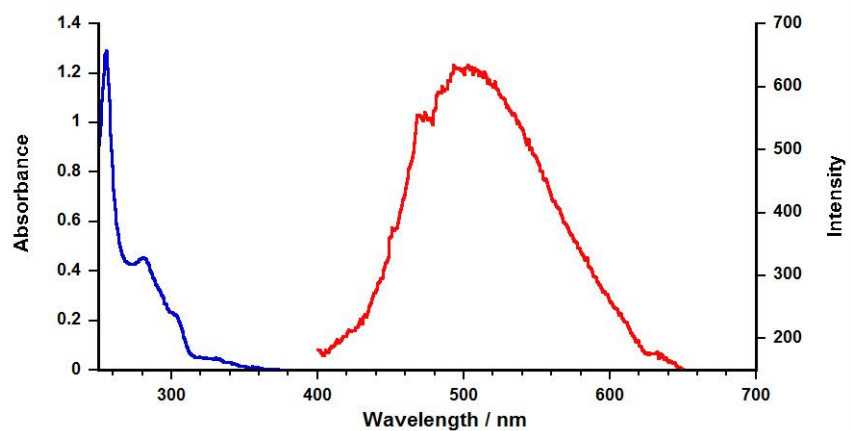


Figure S17. UV-Vis absorption spectrum (in THF, $c = 2 \times 10^{-5}$ M, blue line) and emission spectrum (powder, $\lambda_{\text{exc}} = 350$ nm, red line) of **2c** (3-MeODBTe) at room temperature.

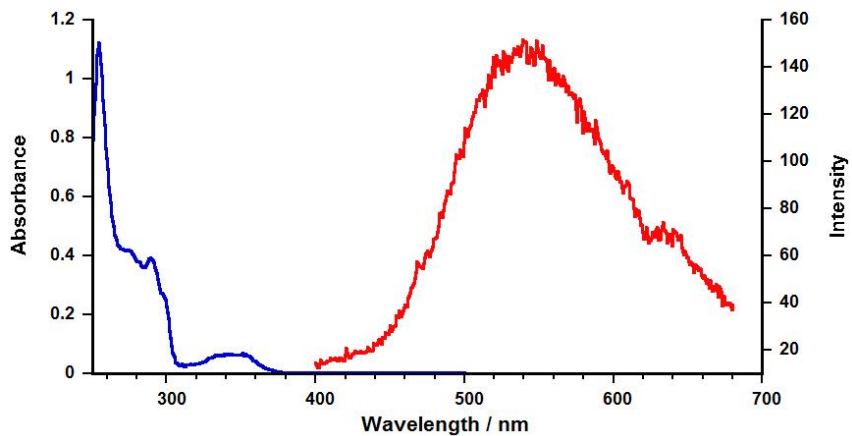


Figure S18. UV-Vis absorption spectrum (in THF, $c = 2 \times 10^{-5}$ M, blue line) and emission spectrum (powder, $\lambda_{\text{exc}} = 350$ nm, red line) of **2f** (3-BrDBTe) at room temperature.

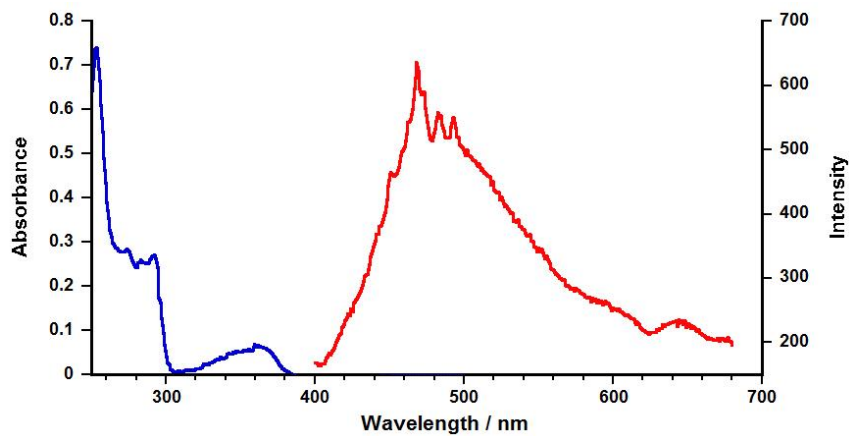


Figure S19. UV-Vis absorption spectrum (in THF, $c = 2 \times 10^{-5}$ M, blue line) and emission spectrum (powder, $\lambda_{\text{exc}} = 350$ nm, red line) of **2h** (3-CF₃DBTe) at room temperature.

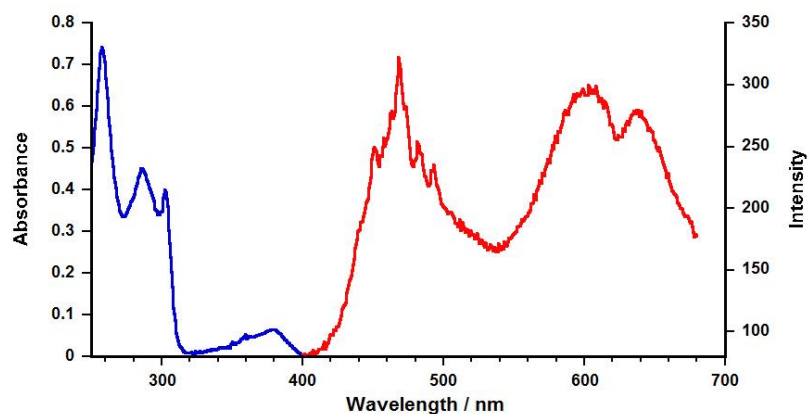


Figure S20. UV-Vis absorption spectrum (in THF, $c = 2 \times 10^{-5}$ M, blue line) and emission spectrum (powder, $\lambda_{\text{exc}} = 350$ nm, red line) of **2i** (3-CNDBTe) at room temperature.

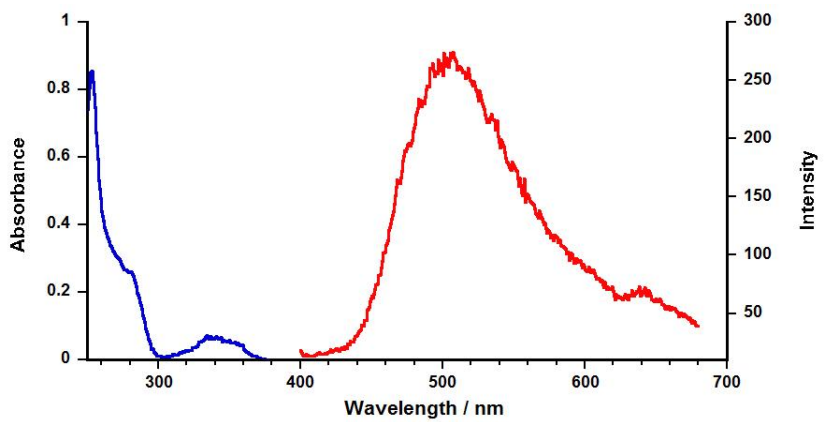


Figure S21. UV-Vis absorption spectrum (in THF, $c = 2 \times 10^{-5}$ M, blue line) and emission spectrum (powder, $\lambda_{\text{exc}} = 365$ nm, red line) of **2j** (2-MeDBTe) at room temperature.

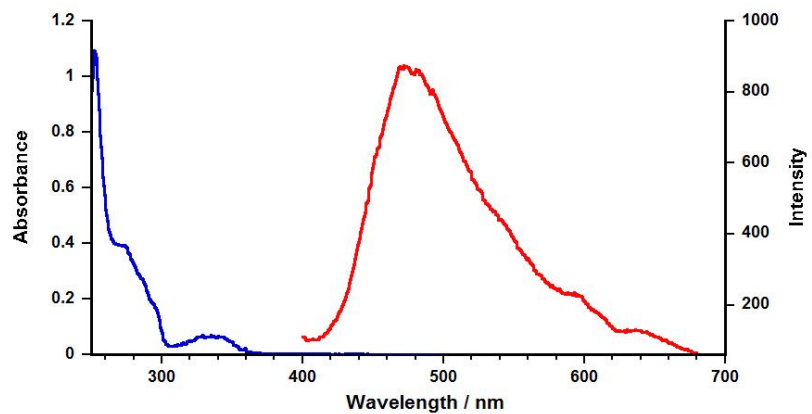


Figure S22. UV-Vis absorption spectrum (in THF, $c = 2.5 \times 10^{-5}$ M, blue line) and emission spectrum (powder, $\lambda_{\text{exc}} = 365$ nm, red line) of **2k** (3,6-diMeDBTe) at room temperature.

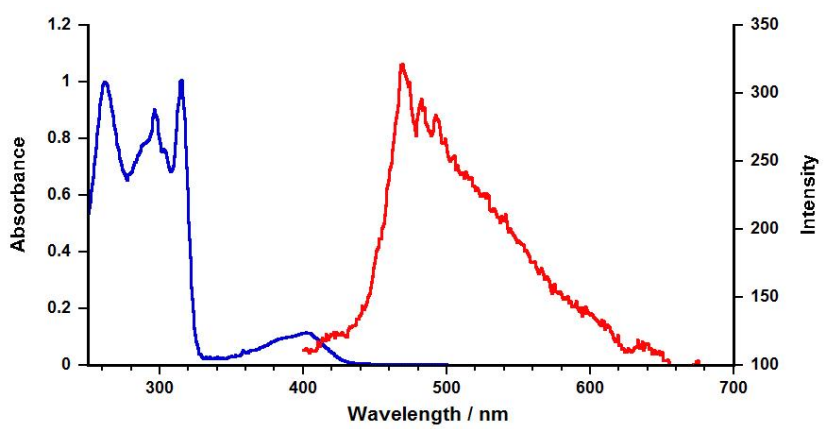


Figure S23. UV-Vis absorption spectrum (in THF, $c = 4 \times 10^{-5}$ M, blue line) and eEmission spectrum (powder, $\lambda_{\text{exc}} = 365$ nm, red line) of **2n** (3,7-diCO₂Me-DBTe) at room temperature.

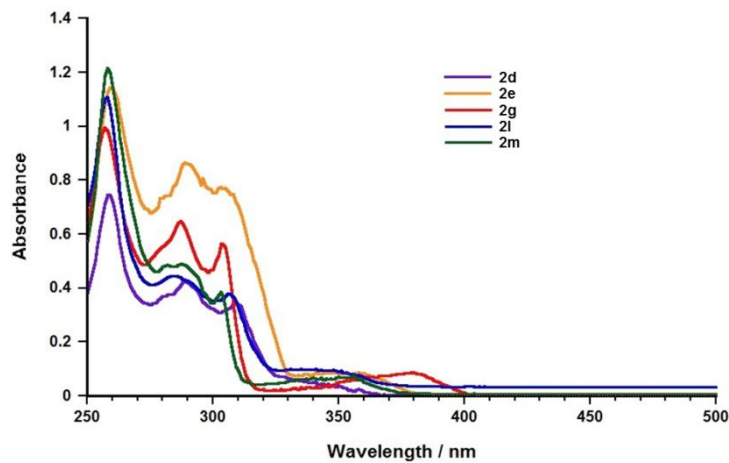


Figure S24. UV-Vis spectra of non-emissive or weak emissive DBTe's (**2d**, **2e**, **2g**, **2l** and **2m**) in dichloromethane.

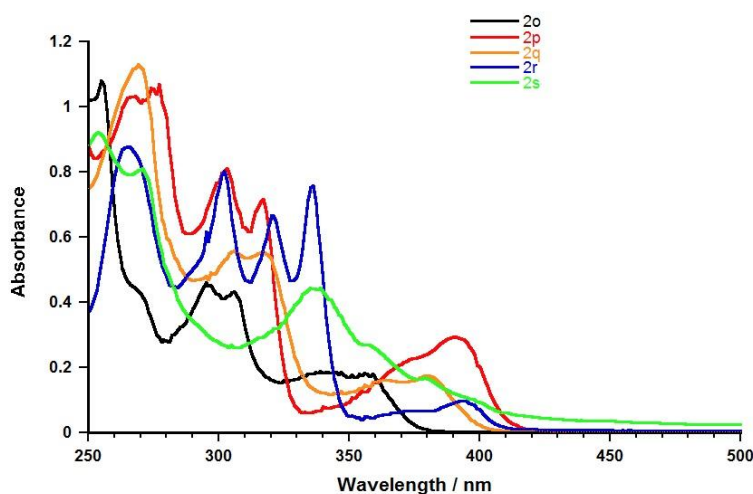


Figure S25. UV-Vis spectra of non-emissive or weak emissive DBTe's (**2o**, **2p**, **2q**, **2r** and **2s**) in dichloromethane.

(a) At 293 K



(b) At 77 K

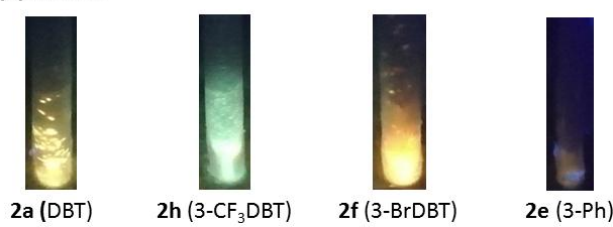


Figure S26. Photographs of representative DBTe's powder under a 365 nm lamp at room temperature or at 77 K.

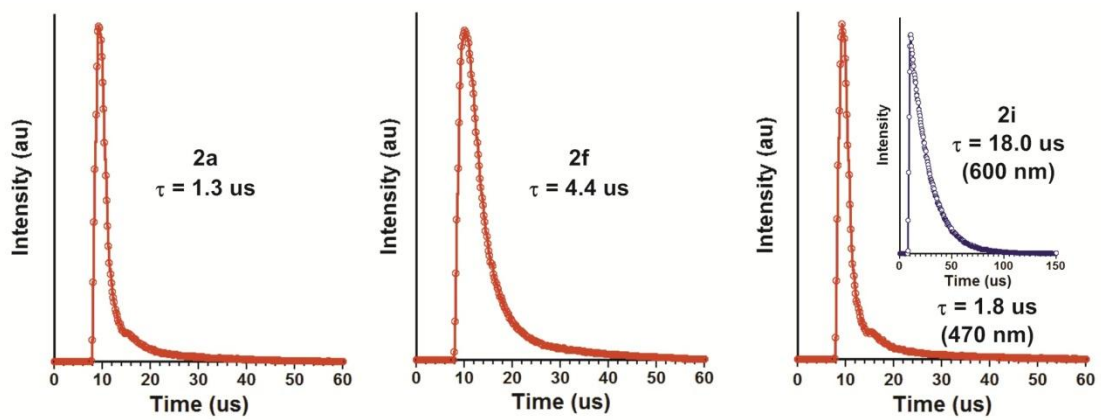


Figure S27. Decay curves for **2a** and **2f** (measured at 500 nm and 550 nm), **2i** (red curve for 468 nm, and blue curve for 600 nm).

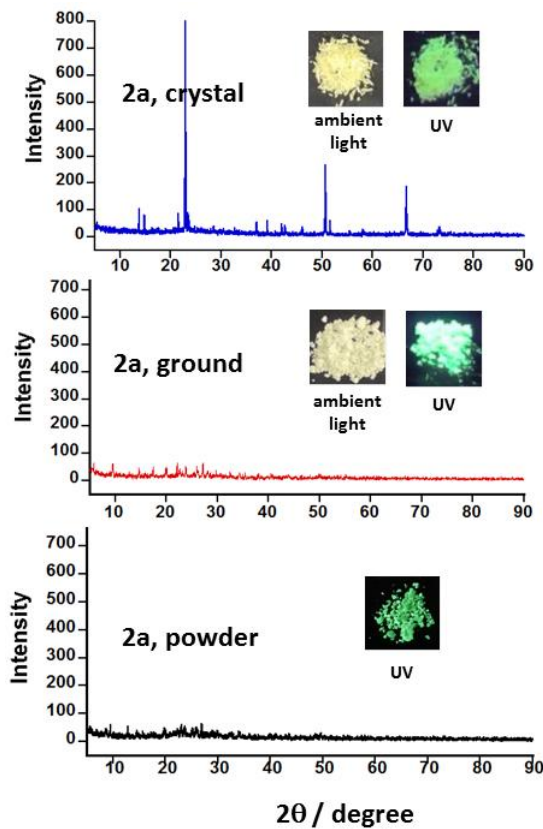


Figure S28. XRD pattern of **2a** for crystal, powder and ground samples (inset: the photographs of the sample at ambient light and UV irradiation (365 nm)).

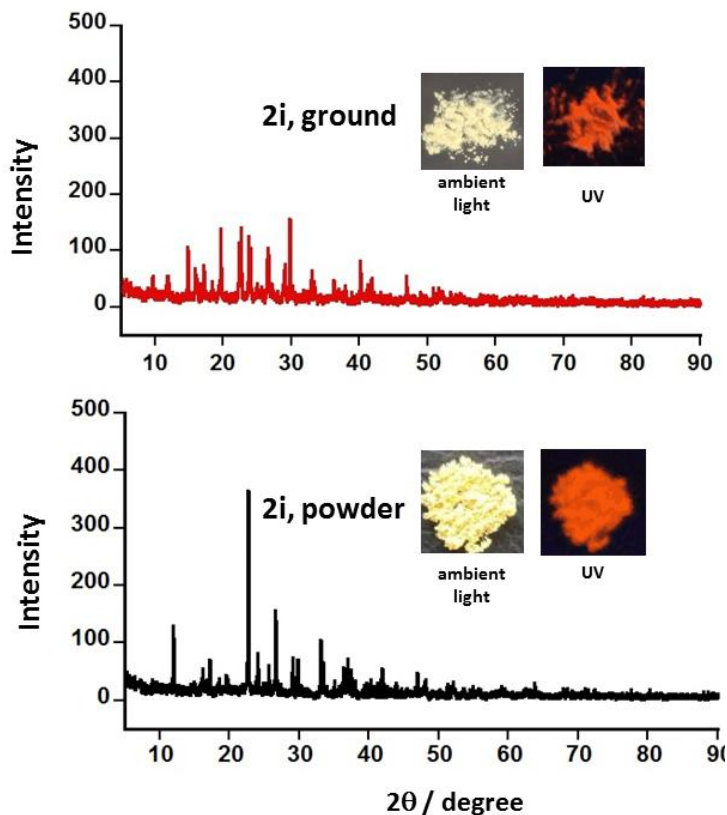


Figure S29. XRD pattern of **2i** for powder and ground samples (inset: the photographs of the sample at ambient light and UV irradiation (365 nm)).

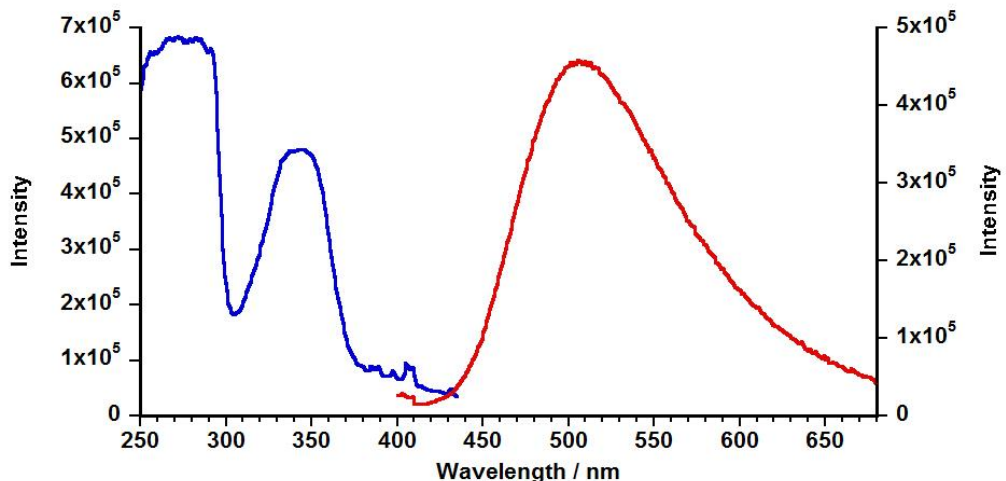


Figure S30. Excitation (blue line) and Emission (red line) spectra of **2a** as film (1wt% in PMMA) at room temperature. The film was prepared as followed: PMMA (200 mg) was dissolved in CHCl_3 (5.0 g) by stirred at 40 °C for 5 h. **2a** (2 mg) was added to the solution and stirred at rt for 30 min. A small amount of the solution was dropped on a glass slide by a dropper and the solvent volatized slowly at rt. The formed film was then dried at 60 °C for 8 h under a nitrogen atmosphere. Emission spectrum was excited at 350 nm. The emission spectrum in PMMA has no significant difference from the powder sample.

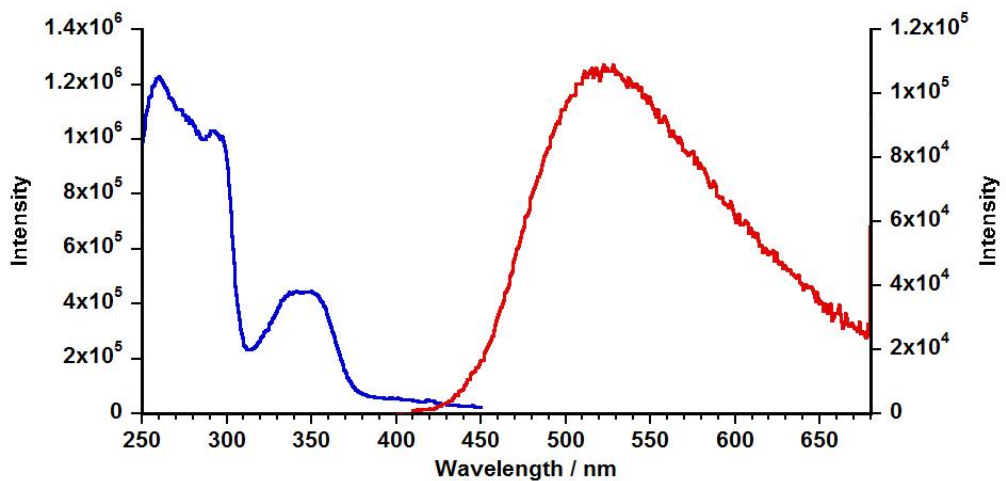


Figure S31. Excitation (blue lines) and Emission (red lines) spectra of **2f** as film (1wt% in PMMA) at room temperature. The film was prepared as for **2a**. Emission spectrum was excited at 350 nm. The emission spectrum in PMMA has no significant difference from the powder sample.

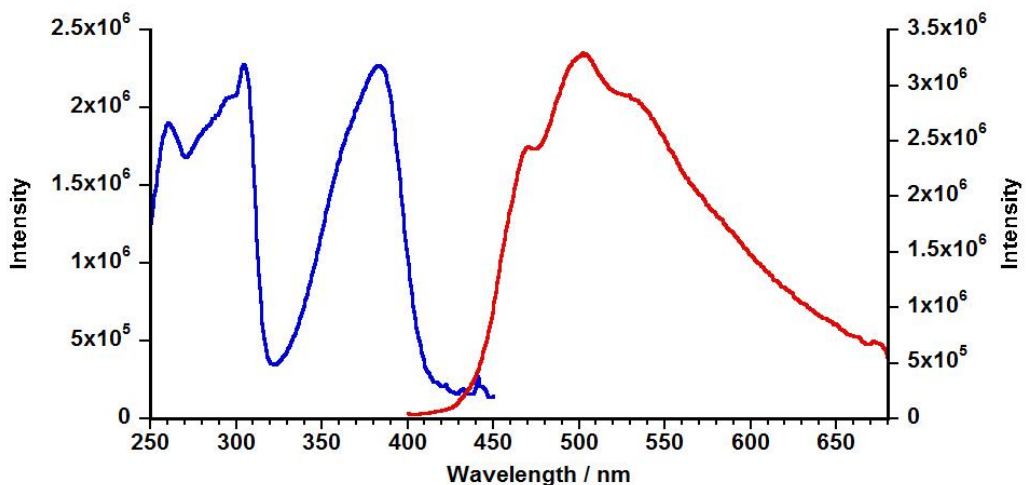
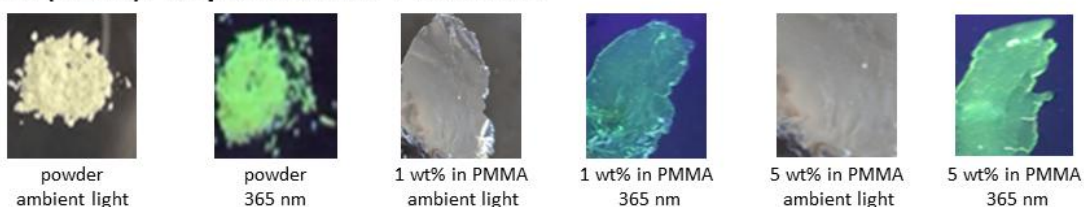
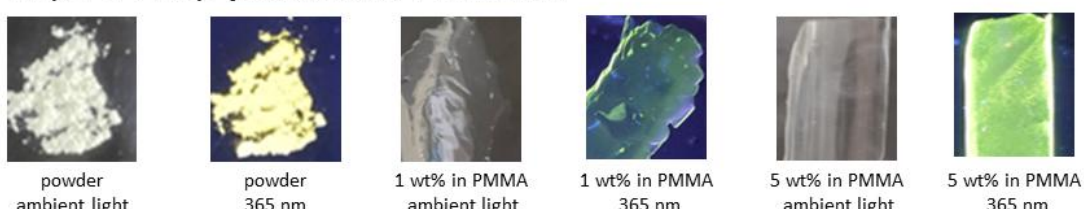


Figure S32. Excitation (blue line) and Emission (red line) spectra of **2i** as film (1wt% in PMMA) at room temperature. The film was prepared as for **2a**. Emission spectrum was excited at 380 nm. The emission spectrum in PMMA has a big difference from the powder sample. The main peak around 600 nm in powder sample disappeared, which indicates that it may attribute to excimer emission.^{S16}

2a (DBTe): as powder and PMMA film



2f (3-BrDBTe): powder and PMMA film



2i (3-CNDBTe): powder and PMMA film



Figure S33. The photographs of powder sample and PMMA films for **2a**, **2f** and **2i** under ambient light and UV.

7. Theoretic Calculations

7.1. Computational Methods

Ground state (S_0) geometry optimizations were performed in the gas-phase using density functional theory (DFT) at the B3LYP/cc-pVTZ (cc-pVTZ-pp for Te) level of theory,^{S17-S20} which was revealed by Rivard *et al.* to be suitable for tellurium-containing heterocycles.^{S21} The obtained optimized geometries were confirmed to be a local energy minimum structure by performing a vibrational frequency analysis using the same level of theory. The basis sets and corresponding effective core potential (ECP) for tellurium were obtained from the Basis Set Exchange library. The absorption (vertical excitation) energies were predicted at their optimized S_0 geometries using time-dependent density functional theory (TD-DFT) at the B3LYP/cc-pVTZ-(PP) level of theory. The calculated results are in good agreement with the experimental UV-vis spectra. For phosphorescence energies, the lowest energy triplet state (T_1) was optimized at the B3LYP/cc-pVTZ-(PP) level of theory. The phosphorescence energies were estimate from the singlet to triplet energy gap at the optimized T_1 geometry (E_{vertical}). Similar to previous reports,^[S21] the phosphorescence energies are under-estimated by these two methods. All of the present computations were carried out using Gaussian09.^{S22}

7.2 Computed UV-vis Spectra for Representative DBTe's

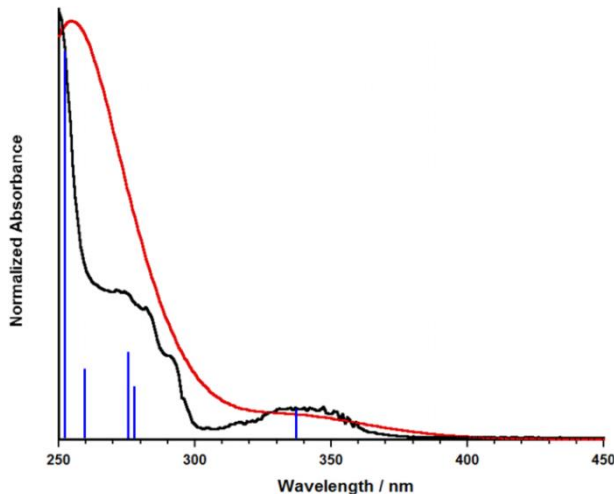


Figure S34. Calculated UV-vis spectra and oscillator strengths for **2a** at TD-B3LYP/cc-pVTZ [cc-pVTZ-pp for Te] level of theory in the gas-phase based on optimized S_0 geometry, and experimental UV-vis spectra (black line).

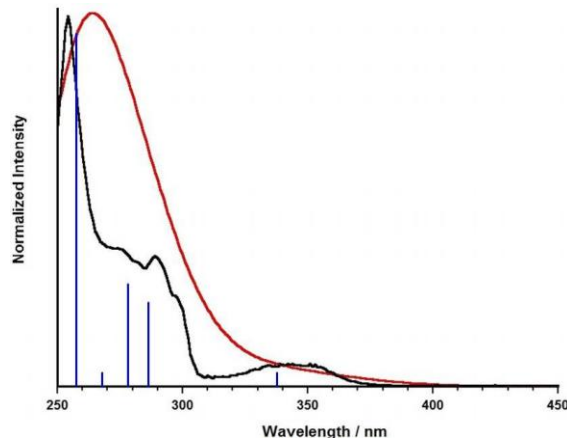


Figure S35. Calculated UV-vis spectra and oscillator strengths for 3-BrDBTe **2f** at TD-B3LYP/cc-pVTZ [cc-pVTZ-pp for Te] level of theory in the gas-phase based on optimized S_0 geometry, and experimental UV-vis spectra (black line).

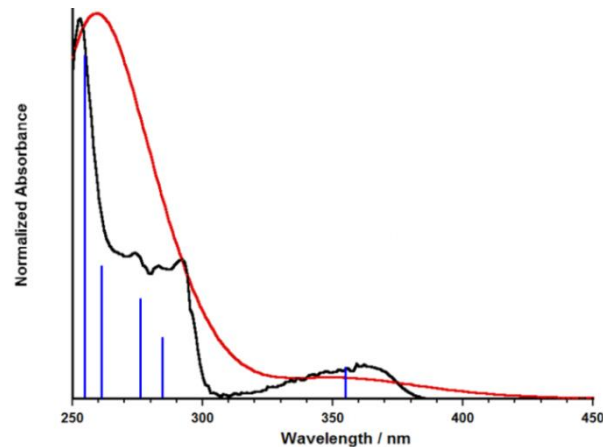


Figure S36. Calculated UV-vis spectra and oscillator strengths for 3-CF₃DBTe **2h** at TD-B3LYP/cc-pVTZ [cc-pVTZ-pp for Te] level of theory in the gas-phase based on optimized S_0

geometry, and experimental UV-vis spectra (black line).

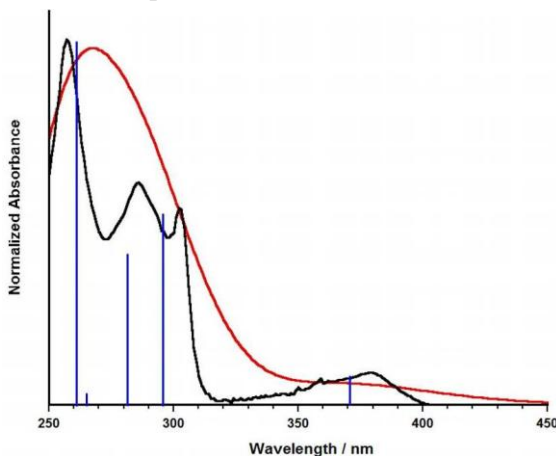


Figure S37. Calculated UV-vis spectra and oscillator strengths for 3-CNDBTe **2i** at TD-B3LYP/cc-pVTZ [cc-pVTZ-pp for Te] level of theory in the gas-phase based on optimized S_0 geometry, and experimental UV-vis spectra (black line).

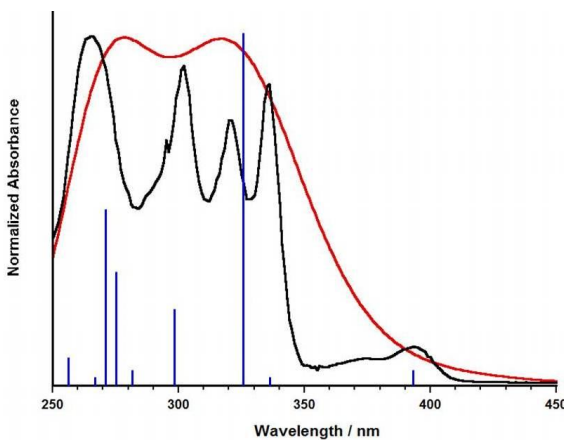


Figure S38. Calculated UV-vis spectra and oscillator strengths for **2r** at TD-B3LYP/cc-pVTZ [cc-pVTZ-pp for Te] level of theory in the gas-phase based on optimized S_0 geometry, and experimental UV-vis spectra (black line).

7.3 Molecular Orbitals for Representative DBTe's

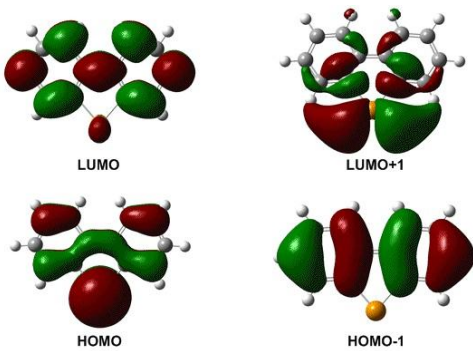


Figure S39. Calculated molecular orbitals of **2a** (DBTe) at the S_0 equilibrium geometry as determined at the B3LYP/cc-pVTZ (cc-pVTZ-pp for Te) level of theory.

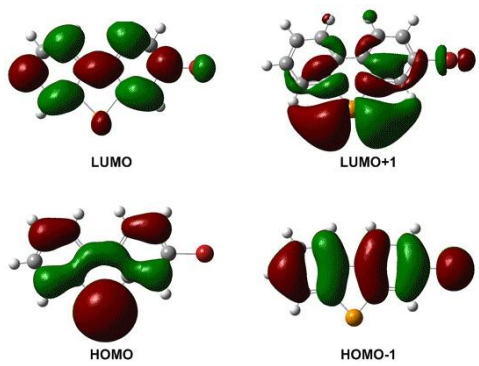


Figure S40. Calculated molecular orbitals of **2f** (3-BrDBTe) at the S_0 equilibrium geometry as determined at the B3LYP/cc-pVTZ (cc-pVTZ-pp for Te) level of theory.

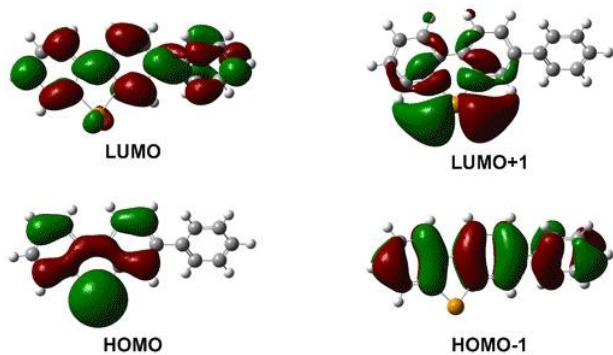


Figure S41. Calculated molecular orbitals of **2e** (3-PhDBTe) at the S_0 equilibrium geometry as determined at the B3LYP/cc-pVTZ (cc-pVTZ-pp for Te) level of theory.

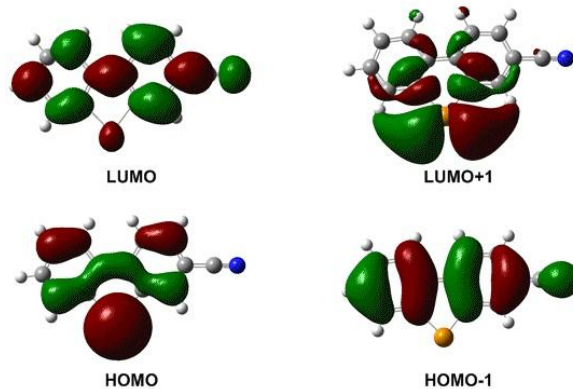


Figure S42 Calculated molecular orbitals of **2i** (3-CNDBTe) at the S_0 equilibrium geometry as determined at the B3LYP/cc-pVTZ (cc-pVTZ-pp for Te) level of theory.

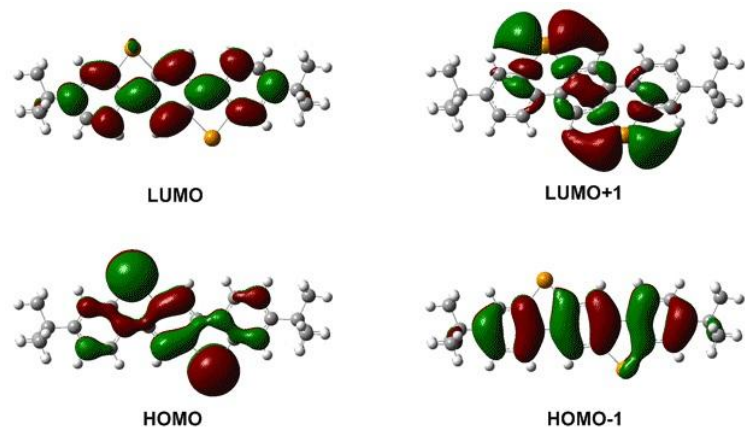


Figure S43. Calculated molecular orbitals of **2r** at the S_0 equilibrium geometry as determined at the B3LYP/cc-pVTZ (cc-pVTZ-pp for Te) level of theory.

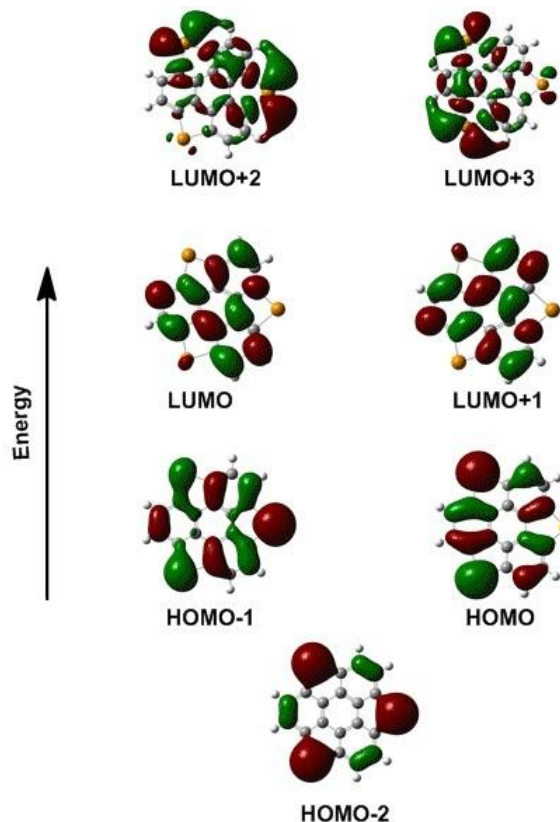


Figure S44. Calculated molecular orbitals of **2s** at the S_0 equilibrium geometry as determined at the B3LYP/cc-pVTZ (cc-pVTZ-pp for Te) level of theory. The energy for HOMO-1 and HOMO, LUMO and LUMO+1, LUMO+2 and LUMO+3 orbitals are degenerate.

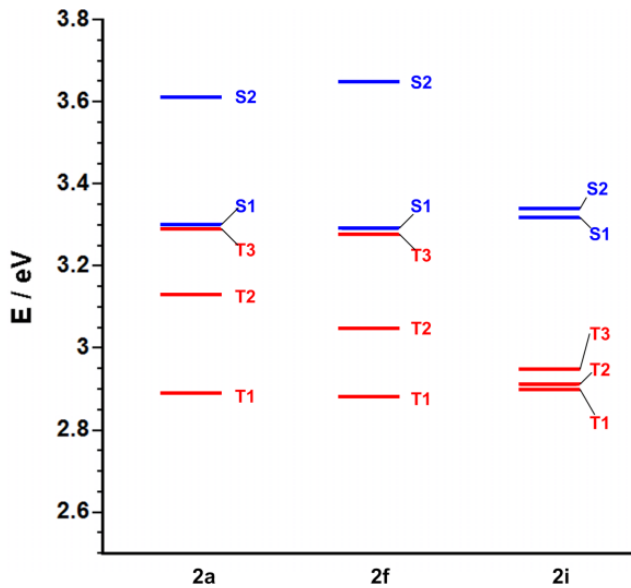


Figure S45. Computed vertical excitation energies for both singlet (S_n) and triplet (T_n) states at their S_0 geometries in the gas phase for **2a**, **2f** and **2i**.

Table S2. Nature of the lowest-lying singlet states for DBTe **2a** at the TD-B3LYP/cc-pVTZ-(PP) levels of theory in the gas-phase. All computations at the S_0 geometry (as determined at the B3LYP/cc-pVTZ-(PP) level of theory).

Excited State	Energy (eV)	Wavelength (nm)	f_{os}	Major contributions
S1	3.30	375	0	HOMO \rightarrow LUMO+1 (99.5%)
S2	3.68	337	0.027	HOMO \rightarrow LUMO (96.0%)
S3	4.20	295	0	HOMO-1 \rightarrow LUMO+1 (99.2%)
S4	4.46	278	0.039	HOMO-1 \rightarrow LUMO (53.8%) HOMO \rightarrow LUMO+3 (44.0%)
S5	4.48	277	0.071	HOMO \rightarrow LUMO+2 (94.4%)
S6	4.77	260	0.068	HOMO-2 \rightarrow LUMO (-17.3%) HOMO-1 \rightarrow LUMO+2 (53.0%) HOMO \rightarrow LUMO+3 (-16.7%)
S7	4.91	253	0.358	HOMO-1 \rightarrow LUMO (-32.8%) HOMO-1 \rightarrow LUMO+2 (17.4%) HOMO \rightarrow LUMO+3 (35.1%)

Table S3. Nature of the lowest-lying singlet states for 3-BrDBTe **2f** at the TD-B3LYP/cc-pVTZ-(PP) levels of theory in the gas-phase. All computations at the S₀ geometry (as determined at the B3LYP/cc-pVTZ-(PP) level of theory).

Excited State	Energy (eV)	Wavelength (nm)	f _{os}	Major contributions
S1	3.29	377	0	HOMO → LUMO+1 (99.2%)
S2	3.65	339	0.024	HOMO → LUMO (95.7%)
S3	4.04	307	0	HOMO-1→LUMO+1 (99.1%)
S4	4.32	287	0.109	HOMO-1→LUMO (55.5%) HOMO→LUMO+2 (23.3%) HOMO→LUMO+3 (-18.0%)
S5	4.45	278	0.150	HOMO-1→LUMO (-17.6%) HOMO→LUMO+2 (70.6%)
S6	4.64	267	0.023	HOMO-1→LUMO+2 (66.9%) HOMO→LUMO+3 (15.3%)
S7	4.80	258	0.441	HOMO-1→LUMO (21.0%) HOMO→LUMO+3 (56.6%)

Table S4. Nature of the lowest-lying singlet states for 3-CNDBTe **2i** at the TD-B3LYP/cc-pVTZ-(PP) levels of theory in the gas-phase. All computations at the S₀ geometry (as determined at the B3LYP/cc-pVTZ-(PP) level of theory).

Excited State	Energy (eV)	Wavelength (nm)	f _{os}	Major contributions
S1	3.32	373	0	HOMO→LUMO+1 (99.5%)
S2	3.34	372	0.032	HOMO→LUMO (96.7%)
S3	4.21	294	0.208	HOMO-1→LUMO (69.5%) HOMO→LUMO+2 (-14.3%) HOMO→LUMO+3 (13.5%)
S4	4.25	292	0	HOMO-1→LUMO+1 (99.2%)
S5	4.42	280	0.158	HOMO-1→LUMO (11.5%) HOMO→LUMO+2 (81%)
S6	4.67	266	0.01	HOMO-2→LUMO (-34.5%) HOMO-1→LUMO+2 (51.4%)
S7	4.76	261	0.37	HOMO-1→LUMO (-13.6%) HOMO→LUMO+3 (70.2%)

Table S5. Computational and experimental phosphorescence emission wavelengths of DBTe's **2a**, **2f** and **2i**. The wavelengths computed (TD-DFT) at the T₁ geometry optimized at B3LYP/cc-pVTZ-(pp) levels of theory.

Compound	B3LYP/cc-pVTZ-(pp)		Experiment results	
2a (DBTe)	2.22 eV	558 nm	2.47 eV	501 nm
2f (3-BrDBTe)	2.26	548 nm	2.30 eV	538 nm
2i (3-CNDBTe)	2.19 eV	567 nm	2.06 eV, 2.65 eV,	468 nm, 600 nm

Table S6. Calculated coordinates of optimized S₀ and T₁ geometry of **2a** (DBTe)

S ₀ Geometry					T ₁ Geometry				
Row	Symbol	X	Y	Z	Row	Symbol	X	Y	Z
1	C	0.7316780	1.1568550	-0.0000040	1	C	-0.7404710	1.2377460	0.0000000
2	C	1.3741790	-0.0967070	-0.0000280	2	C	-1.3622860	-0.0128140	0.0000020
3	Te	-0.0000010	-1.6917990	0.0000000	3	Te	-0.0000030	-1.7953560	-0.0000010
4	C	-1.3741810	-0.0967070	0.0000270	4	C	1.3622870	-0.0128170	-0.0000030
5	C	-0.7316760	1.1568570	-0.0000020	5	C	0.7404750	1.2377450	0.0000010
6	C	1.5368060	2.3041970	0.0000400	6	C	-1.5435750	2.3776620	-0.0000050
7	C	2.9172720	2.2029300	0.0000380	7	C	-2.9319550	2.2578480	-0.0000050
8	C	3.5323710	0.9510300	-0.0000060	8	C	-3.5365850	1.0054850	-0.0000010
9	C	2.7609650	-0.2019480	-0.0000360	9	C	-2.7415860	-0.1384690	0.0000020
10	C	-2.7609640	-0.2019450	0.0000400	10	C	2.7415870	-0.1384750	-0.0000020
11	C	-3.5323690	0.9510360	0.0000140	11	C	3.5365880	1.0054770	0.0000020
12	C	-2.9172690	2.2029320	-0.0000350	12	C	2.9319610	2.2578410	0.0000060
13	C	-1.5368010	2.3041980	-0.0000460	13	C	1.5435810	2.3776590	0.0000060
14	H	1.0777410	3.2834410	0.0000840	14	H	-1.1005980	3.3649730	-0.0000090
15	H	3.5208970	3.1005700	0.0000770	15	H	-3.5429040	3.1509240	-0.0000080
16	H	4.6116320	0.8756240	-0.0000130	16	H	-4.6156120	0.9221610	-0.0000010
17	H	3.2418390	-1.1710620	-0.0000680	17	H	-3.1964490	-1.1234460	0.0000040
18	H	-3.2418430	-1.1710570	0.0000630	18	H	3.1964470	-1.1234530	-0.0000050
19	H	-4.6116300	0.8756280	0.0000290	19	H	4.6156160	0.9221510	0.0000010
20	H	-3.5208900	3.1005750	-0.0000700	20	H	3.5429130	3.1509160	0.0000100
21	H	-1.0777370	3.2834420	-0.0000960	21	H	1.1006070	3.3649700	0.0000110

Table S7. Calculated coordinates of optimized S₀ and T₁ geometry of **2f** (3-BrDBTe)

S ₀ Geometry					T ₁ Geometry				
Row	Symbol	X	Y	Z	Row	Symbol	X	Y	Z
1	C	-2.5021070	0.0528670	0.0000220	1	C	1.6467990	1.2235840	0.0000010
2	C	-1.7077590	1.2159930	0.0000050	2	C	2.5066930	0.0470820	0.0000020
3	C	-0.2573850	1.0311230	0.0000080	3	Te	1.3604270	-1.7292810	0.0000020
4	C	0.2216850	-0.2935310	-0.0000160	4	C	-0.2307710	-0.3352090	0.0000000
5	Te	-1.3404040	-1.7034680	0.0000020	5	C	0.2810030	1.0350310	0.0000000
6	C	-3.8909730	0.1218280	0.0000240	6	C	2.3138060	2.5128910	0.0000010
7	C	-4.5112490	1.3626660	-0.0000050	7	C	3.6810610	2.5920260	0.0000020
8	C	-3.7441450	2.5276120	-0.0000420	8	C	4.4767340	1.4332020	0.0000030
9	C	-2.3620040	2.4556060	-0.0000370	9	C	3.8644400	0.1519850	0.0000030
10	C	0.6885110	2.0642670	0.0000520	10	C	-1.5552470	-0.6103960	-0.0000010
11	C	2.0462170	1.7958990	0.0000490	11	C	-2.4916810	0.4808810	-0.0000020
12	C	2.4803110	0.4727900	0.0000050	12	C	-2.0520960	1.8207240	-0.0000020
13	C	1.5823340	-0.5814170	-0.0000210	13	C	-0.7193100	2.1058410	-0.0000010
14	Br	4.3561700	0.1034060	-0.0000110	14	H	1.7215470	3.4156050	0.0000000
15	H	-4.4899410	-0.7790120	0.0000510	15	H	4.1591380	3.5626060	0.0000020
16	H	-5.5913500	1.4233740	-0.0000030	16	H	5.5544580	1.5111000	0.0000040

17	H	-4.2306660	3.4936410	-0.0000790	17	H	4.4916500	-0.7293840	0.0000040
18	H	-1.7844240	3.3699060	-0.0000740	18	H	-1.9329470	-1.6221360	-0.0000010
19	H	0.3636670	3.0956820	0.0000940	19	H	-2.7816090	2.6175680	-0.0000030
20	H	2.7636950	2.6027240	0.0000860	20	H	-0.3945850	3.1350800	-0.0000010
21	H	1.9434520	-1.5993810	-0.0000400	21	Br	-4.3396700	0.0938950	-0.0000030

Table S8. Calculated coordinates of optimized S_0 and T_1 geometry of **2i** (3-CNDBTe)

S ₀ Geometry					T ₁ Geometry				
Row	Symbol	X	Y	Z	Row	Symbol	X	Y	Z
1	C	-1.0875090	1.2054470	0.0000000	1	C	-1.8599770	0.0185160	-0.0000550
2	C	-1.8492260	0.0205350	0.0000040	2	C	-3.2217840	0.0672690	-0.0001030
3	Te	-0.6439150	-1.7046070	0.0000000	3	H	-3.8139650	-0.8379270	-0.0001620
4	C	0.8787670	-0.2537890	-0.0000020	4	C	-3.8832700	1.3238620	-0.0000760
5	C	0.3659970	1.0601010	0.0000010	5	H	-4.9634130	1.3578970	-0.0001140
6	C	-1.7733880	2.4282610	-0.0000070	6	C	-3.1377930	2.5006410	0.0000000
7	C	-3.1562050	2.4631780	-0.0000070	7	H	-3.6446240	3.4560160	0.0000210
8	C	-3.8913730	1.2770860	0.0000000	8	C	-1.7575020	2.4628560	0.0000500
9	C	-3.2397750	0.0530840	0.0000050	9	H	-1.1986590	3.3870550	0.0001080
10	C	2.2431800	-0.4997960	-0.0000030	10	C	-1.0551260	1.2117110	0.0000240
11	C	3.1330250	0.5758650	0.0000010	11	C	0.3296290	1.0669130	0.0000680
12	C	2.6419870	1.8906900	0.0000080	12	C	0.8880140	-0.2987600	0.0000190
13	C	1.2815810	2.1219010	0.0000080	13	C	2.2226490	-0.5334020	0.0000400
14	C	4.5405100	0.3357740	-0.0000010	14	H	2.6235200	-1.5367380	0.0000030
15	N	5.6772030	0.1426360	-0.0000070	15	C	3.1424720	0.5695750	0.0001130
16	H	-1.2205100	3.3575330	-0.0000140	16	C	2.6189780	1.9231860	0.0001820
17	H	-3.6689820	3.4151880	-0.0000130	17	H	3.3239940	2.7422380	0.0002540
18	H	-4.9725660	1.3093000	0.0000020	18	C	1.2932250	2.1607050	0.0001620
19	H	-3.8149400	-0.8628350	0.0000090	19	H	0.9344460	3.1792120	0.0002200
20	H	2.6326830	-1.5078520	-0.0000060	20	C	4.5208510	0.3489190	0.0001200
21	H	3.3371160	2.7175750	0.0000140	21	N	5.6700890	0.1674220	0.0001170
22	H	0.9249410	3.142165	0.0000140	22	Te	-0.6452710	-1.727917	-0.000085

Table S9 Calculated coordinates of the optimized S_0 geometry of **2r**

Row	Symbol	X	Y	Z	Row	Symbol	X	Y	Z
1	C	1.3825370	0.3215470	-0.0001630	28	C	-7.643984	-1.590374	1.258839
2	C	0.9188550	-1.0124190	-0.0001330	29	H	-0.755802	-2.347088	-0.000069
3	C	-0.4312660	-1.3155500	-0.0001130	30	H	0.753818	2.376016	-0.000107
4	C	-1.3850190	-0.2924270	-0.0001200	31	H	2.902313	2.675583	-0.000422
5	C	-0.9212510	1.0416550	-0.0001170	32	H	5.312169	2.827223	-0.000364
6	C	0.4290780	1.3445350	-0.0001370	33	H	5.615415	-1.445176	0.000128
7	C	2.8300040	0.5241840	-0.0001630	34	H	-2.904427	-2.648941	-0.000263
8	C	3.6441360	-0.6239380	-0.0000530	35	H	-5.317861	-2.795751	-0.000153
9	Te	2.5064930	-2.3994130	-0.0000240	36	H	-5.616301	1.476211	0.000203
10	C	-2.8319930	-0.4939060	-0.0000820	37	H	7.405345	2.761543	-0.884281

11	C	-3.6446400	0.6506060	0.0000170	38	H	7.405255	2.762064	0.883467
12	Te	-2.5096810	2.4265410	-0.0000040	39	H	8.820783	2.203146	-0.000154
13	C	3.4801070	1.7609820	-0.0002810	40	H	7.384567	0.540318	-2.16584
14	C	4.8633320	1.8458000	-0.0002380	41	H	8.844003	0.10118	-1.271632
15	C	5.6723240	0.7029000	-0.0000750	42	H	7.460005	-0.988814	-1.293991
16	C	5.0281360	-0.5370860	0.0000030	43	H	7.383694	0.541836	2.166369
17	C	-3.4830330	-1.7349010	-0.0001490	44	H	8.843444	0.101886	1.273062
18	C	-4.8614180	-1.8156550	-0.0000870	45	H	7.459261	-0.987917	1.29562
19	C	-5.6741710	-0.6693950	0.0000600	46	H	-7.674629	1.133683	0.88526
20	C	-5.0341170	0.5672550	0.0000990	47	H	-8.999022	0.386947	0.000584
21	C	-7.2023200	-0.8140990	0.0001290	48	H	-7.674575	1.134429	-0.883373
22	C	7.206954	0.767009	0.000152	49	H	-7.203066	-2.585104	-1.297889
23	C	7.730134	2.21144	-0.000227	50	H	-7.350617	-1.059024	-2.166014
24	C	7.753024	0.060122	-1.258358	51	H	-8.729642	-1.705382	-1.269966
25	C	7.752465	0.060948	1.259382	52	H	-7.350342	-1.060654	2.166113
26	C	-7.919661	0.544122	0.000687	53	H	-8.729466	-1.706347	1.269739
27	C	-7.644156	-1.589427	-1.259107	54	H	-7.202888	-2.58608	1.296826

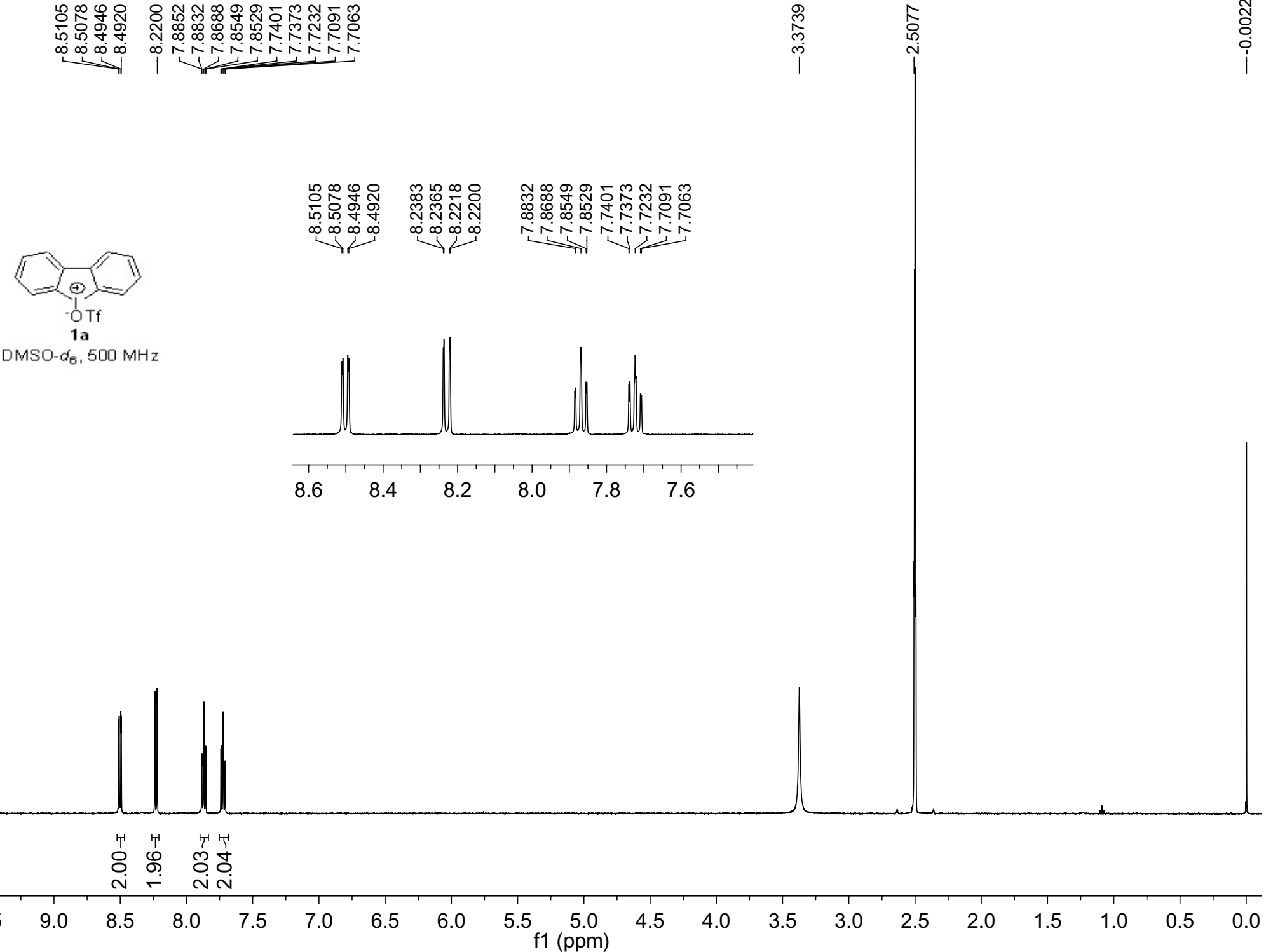
Table S10. Calculated coordinates of the optimized S₀ geometry of **2s** (tritellurasumanene)

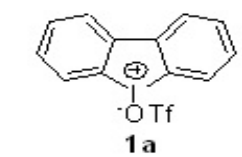
Row	Symbol	X	Y	Z	Row	Symbol	X	Y	Z
1	C	-1.2422990	-0.6790290	0.0010620	15	C	0.0497500	2.8140870	0.0004490
2	C	-1.2167960	0.7236240	0.0010670	16	C	1.2739700	3.4777550	-0.0000280
3	C	0.0336200	1.4155050	0.0010680	17	C	2.4763030	2.7542210	-0.0000260
4	C	1.2355050	0.6921520	0.0010620	18	C	2.4636290	1.3616100	0.0004470
5	C	1.2096210	-0.7366370	0.0010560	19	Te	-2.0804410	-3.4558170	-0.0003260
6	C	-0.0179330	-1.4159510	0.0010590	20	Te	-1.9534760	3.5290970	-0.0003300
7	C	2.4126030	-1.4501490	0.0004330	21	Te	4.0335230	-0.0732690	-0.0003220
8	C	2.3746810	-2.8422500	-0.0000420	22	H	3.2861000	-3.4250520	-0.0004330
9	C	1.1468500	-3.5217180	-0.0000310	23	H	1.1561510	-4.6035280	-0.0004270
10	C	-0.0525370	-2.8142320	0.0004470	24	H	-4.6085690	-1.1339940	-0.0004050
11	C	-2.4617740	-1.3641340	0.0004470	25	H	-4.5641960	1.3010210	-0.0003970
12	C	-3.6484230	-0.6354000	-0.0000170	26	H	1.3219750	4.5585630	-0.0004260
13	C	-3.6228880	0.7676870	-0.0000130	27	H	3.4083300	3.3034620	-0.0004250
14	C	-2.4104360	1.4526870	0.0004500					

8. Reference

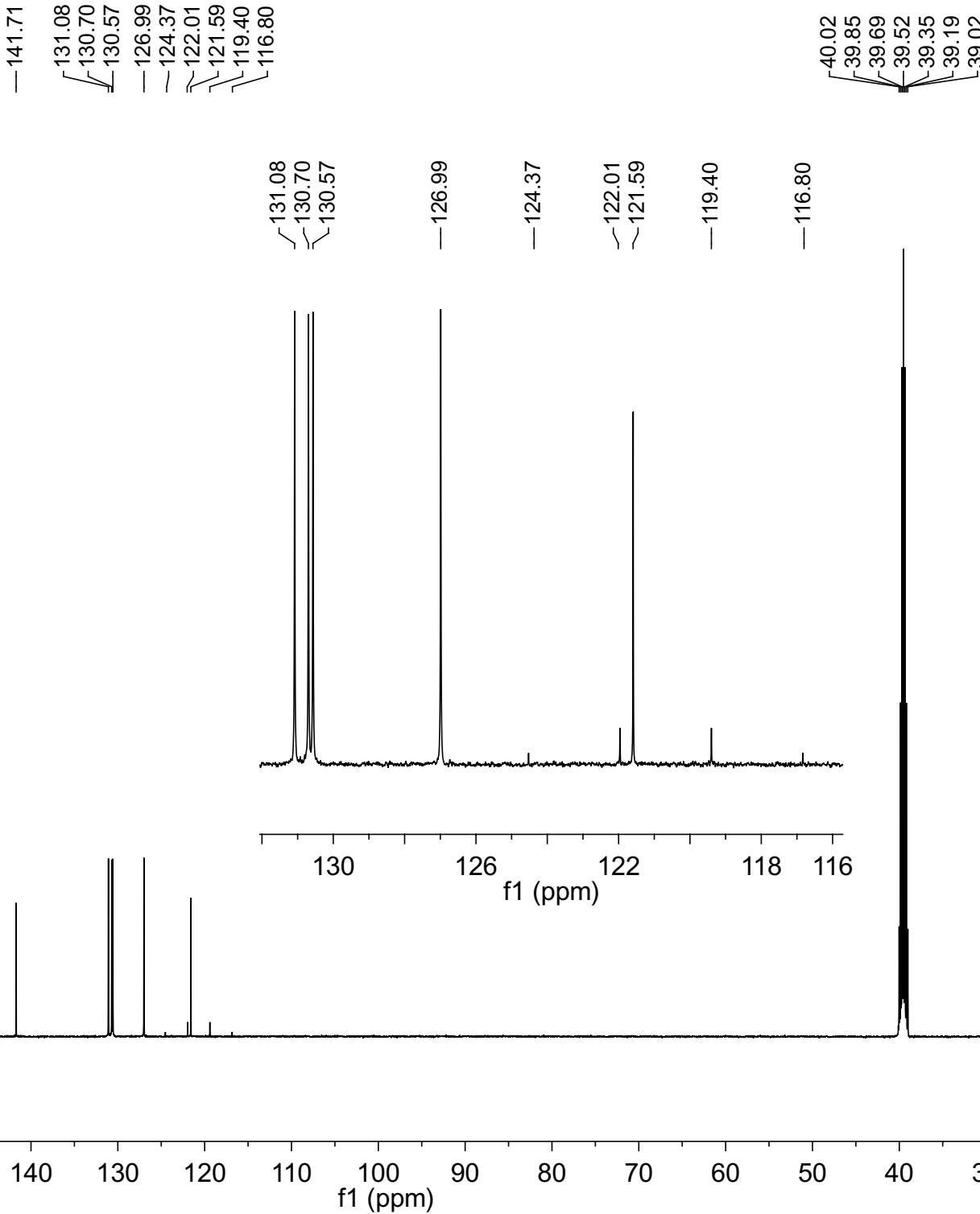
- (1) Zhang, T.; Deng, G.; Li, H.; Liu, B.; Tan, Q.; Xu, B. *Org. Lett.* **2018**, *20*, 5439.
- (2) Zhu, D.; Liu, Q.; Luo, B.; Chen, M.; Pi, R.; Huang, P.; Wen, S. *Adv. Synth. Catal.* **2013**, *355*, 2172.
- (3) Luo, B.; Cui, Q.; Luo, H.; Hu, Y.; Huang, P.; Wen, S. *Adv. Synth. Catal.* **2016**, *358*, 2733.
- (4) Wang, M.; Fan, Q.; Jiang, X. *Org. Lett.* **2018**, *20*, 216.
- (5) Wu, B.; Yoshikai, N. *Angew. Chem. Int. Ed.* **2015**, *54*, 8736.

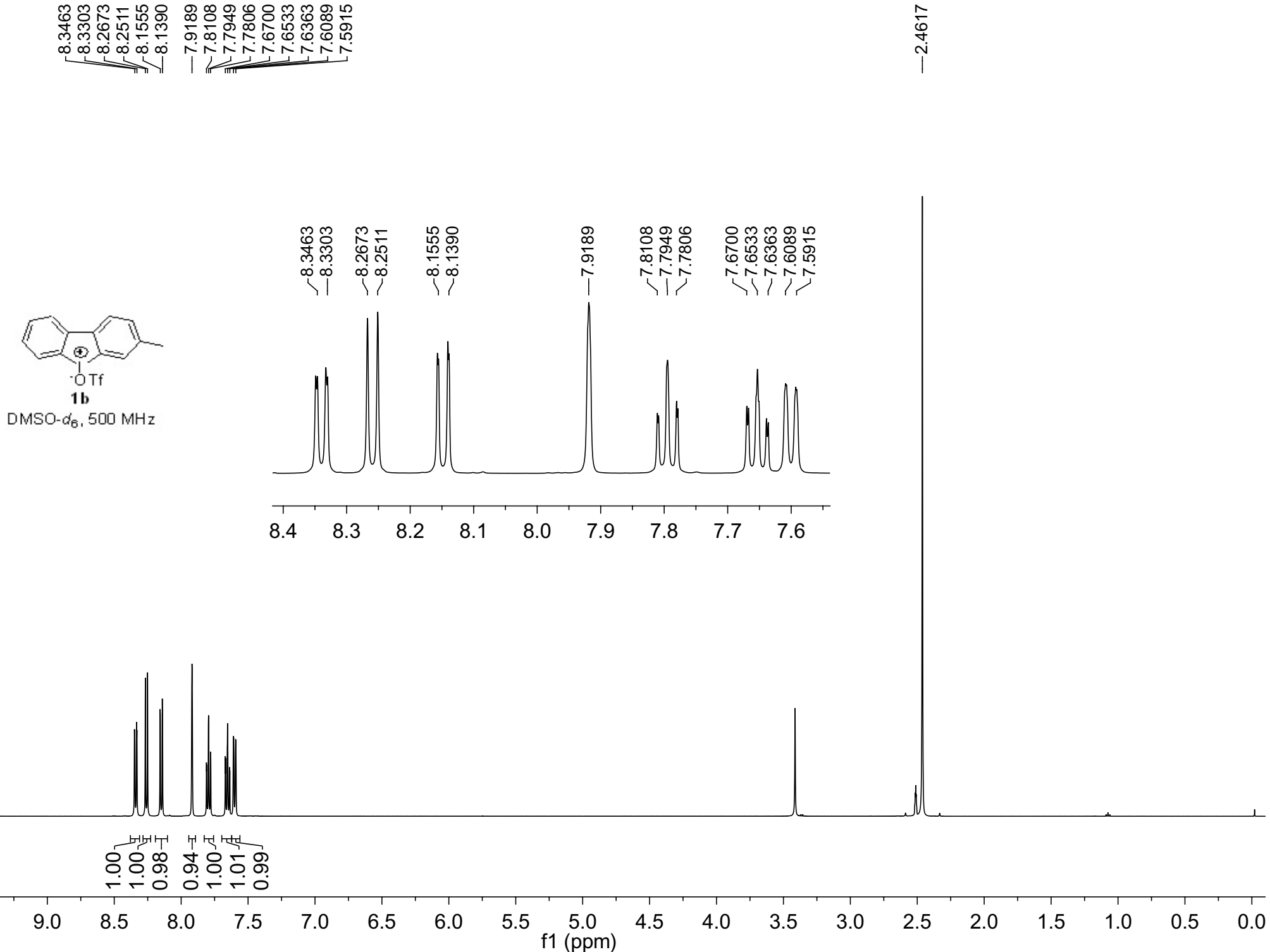
- (6) Akimoto, G.; Otsuka, M.; Miyamoto, K.; Muranaka, A.; Hashizume, D.; Takita, R.; Uchiyama, M. *Chem. Asian J.* **2018**, *13*, 913.
- (7) Zhu, D.; Wu, Z.; Luo, B.; Du, Y.; Liu, P.; Chen, Y.; Hu, Y.; Huang, P.; Wen, S. *Org. Lett.* **2018**, *20*, 4815.
- (8) Wang, C. L.; Li, H. Q.; Meng, W. D.; Qing, F. L. *Bioorg. Med. Chem. Lett.* **2005**, *15*, 4456.
- (9) Feng, X.; Pisula, W.; Müllen, K. *J. Am. Chem. Soc.* **2007**, *129*, 14116.
- (10) Murata, S.; Suzuki, T.; Yanagisawa, A.; Suga, S. *J. Heterocyclic Chem.* **1991**, *28*, 433.
- (11) Fell, V. H. K.; Mikosch, A.; Steppert, A. K.; Ogieglo, W.; Senol, E.; Cannesson, D.; Bayer, M.; Schoenebeck, F.; Greilich, A.; Kuehne, A. J. C. *Macromolecules* **2017**, *50*, 2338.
- (12) Tan, Q.; Zhou, D.; Zhang, T.; Liu, B.; Xu, B. *Chem. Commun.* **2017**, *53*, 10279.
- (13) (a) Hojo, M.; Sawyer, D. T. *Inorg. Chem.* **1989**, *28*, 1201. (b) Lindner, G. G.; Witke, K.; Schlaich, H.; Reinen, D. *Inorg. Chim. Acta* **1996**, *252*, 39. (c) Sheldrick, W. S. Z. *Anorg. Allg. Chem.* **2012**, *638*, 2401. (d) Chivers, T.; Elder, P. J. W. *Chem. Soc. Rev.* **2013**, *42*, 5996.
- (14) (a) Bunnett, J. F.; Wamser, C. C. *J. Am. Chem. Soc.* **1967**, *89*, 6712. (b) Grushin, V. V. *Acc. Chem. Res.* **1992**, *25*, 529. (c) Zhang, S.; Karra, K.; Koe, A.; Jin, J. *Tetrahedron Lett.* **2013**, *54*, 2452.
- (15) (a) Grushin, V. V. *Chem. Soc. Rev.* **2000**, *29*, 315. (b) Yoshimura, A.; Zhdankin, V. V. *Chem. Rev.* **2016**, *116*, 3328.
- (16) (a) Förster, T. *Angew. Chem., Int. Ed.* **1969**, *8*, 333. (b) Han, G.; Kim, D.; Park, Y.; Bouffard, J.; Kim, Y. *Angew. Chem., Int. Ed.* **2015**, *54*, 3912. (c) An, B.; Hua, C.; Ma, H.; Pan, Q.; Li, M. *J. Lumin.* **2007**, *127*, 297.
- (17) Becke, A. D. *J. Chem. Phys.* **1993**, *98*, 5648.
- (18) Lee, C.; Yang, W.; Parr, R. G. *Phys. Rev. B* **1988**, *37*, 785.
- (19) Dunning, T. H. *J. Chem. Phys.* **1989**, *90*, 1007.
- (20) Dunning, J. T. H.; Woon, D. E. *J. Chem. Phys.* **1993**, *98*, 1358.
- (21) Braun, C. A.; Zomerman, D.; de Aguiar, I.; Qi, Y.; Delgado, W. T.; Ferguson, M. J.; McDonald, R.; de Souza, G. L. C.; He, G.; Brown, A.; Rivard, E. *Faraday Discuss.* **2017**, *196*, 255.
- (22) Gaussian 09, M. J. Frisch, G. W. Trucks, H. B. Schlegel, G. E. Scuseria, M. A. C. Robb, J. R.; Scalmani, G.; Barone, V.; Mennucci, B.; Petersson, G. A.; Nakatsuji, H.; Caricato, M.; Li, X.; Hratchian, H. P.; Izmaylov, A. F.; Bloino, J.; Zheng, G.; Sonnenberg, J. L.; Hada, M.; Ehara, M.; Toyota, K.; Fukuda, R.; Hasegawa, J.; Ishida, M.; Nakajima, T.; Honda, Y.; Kitao, O.; Nakai, H.; Vreven, T.; J. A. Montgomery, J.; Peralta, J. E.; Ogliaro, F.; Bearpark, M.; Heyd, J. J.; Brothers, E.; Kudin, K. N.; Staroverov, V. N.; Keith, T.; Kobayashi, R.; Normand, J.; Raghavachari, K.; Rendell, A.; Burant, J. C.; Iyengar, S. S.; Tomasi, J.; Cossi, M.; Rega, N.; Millam, J. M.; Klene, M.; Knox, J. E.; Cross, J. B.; Bakken, V.; Adamo, C.; Jaramillo, J.; Gomperts, R.; Stratmann, R. E.; Yazyev, O.; Austin, A. J.; Cammi, R.; Pomelli, C.; Ochterski, J. W.; Martin, R. L.; Morokuma, K.; Zakrzewski, V. G.; Voth, G. A.; Salvador, P.; Dannenberg, J. J.; Dapprich, S.; Daniels, A. D.; Farkas, O.; Foresman, J. B.; Ortiz, J. V.; Cioslowski, J.; Fox, D. J., Gaussian, Inc.: Wallingford CT, 2010.

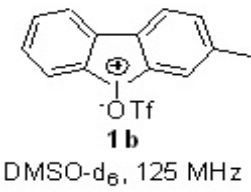




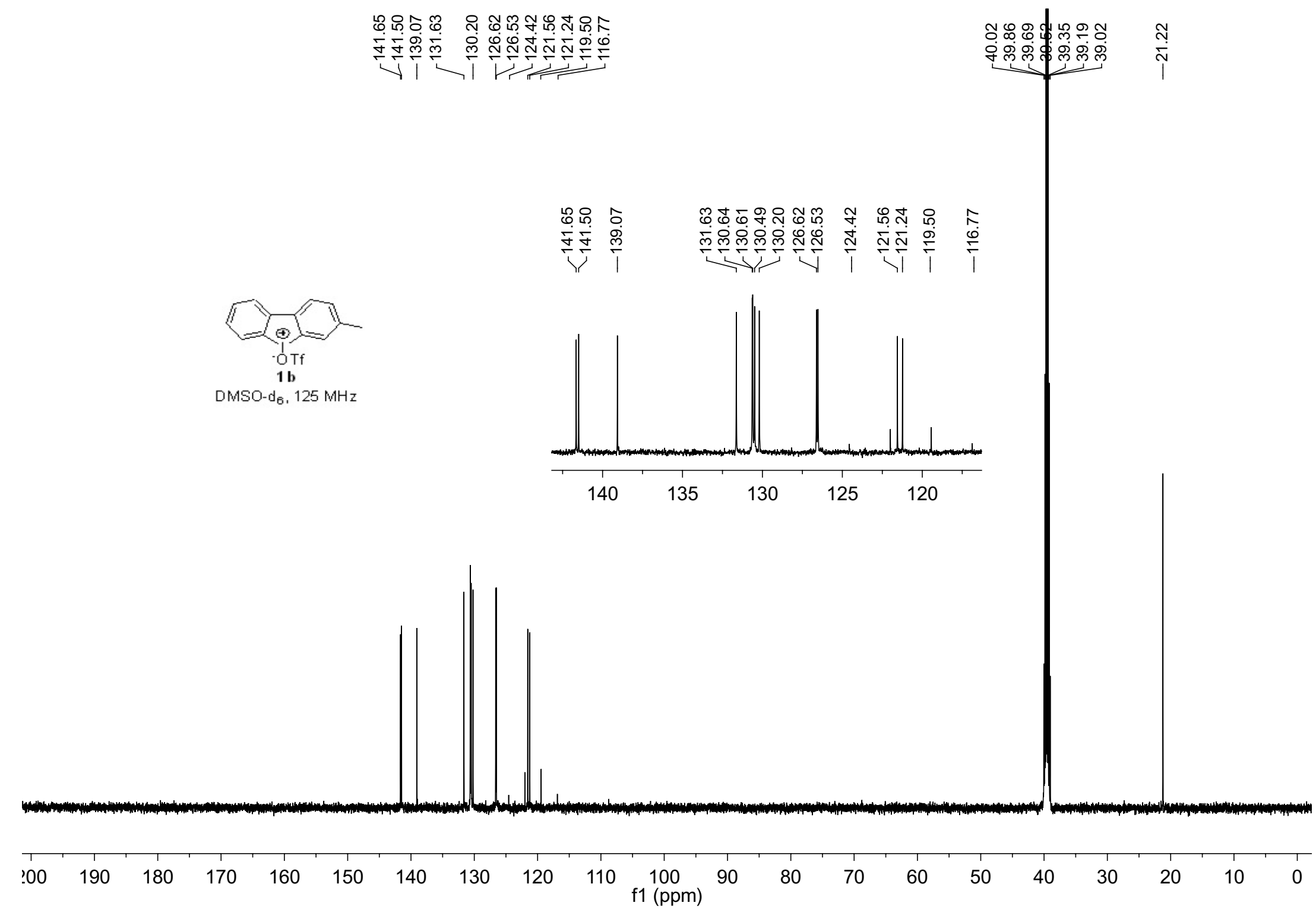
DMSO- d_6 , 125 MHz

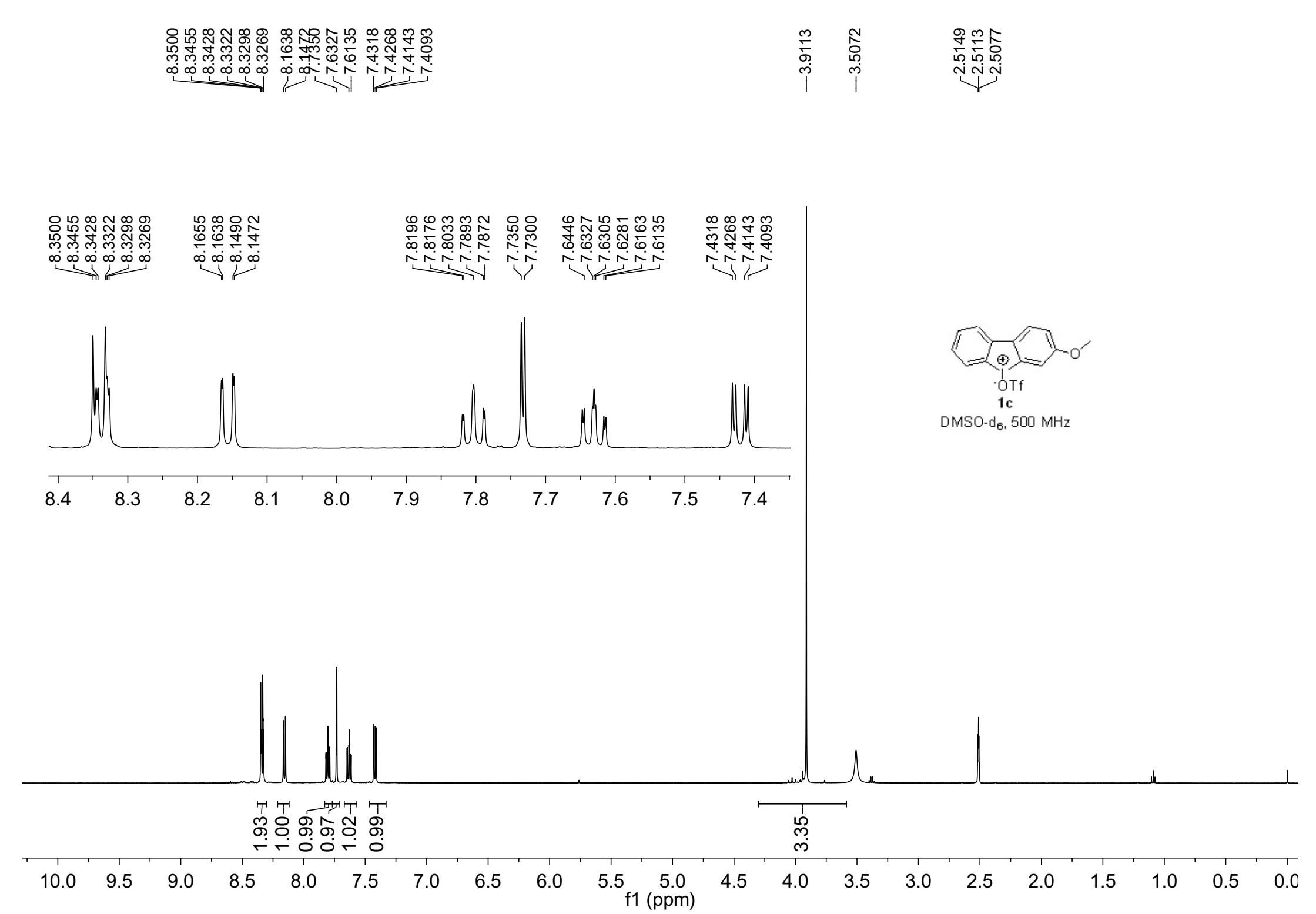


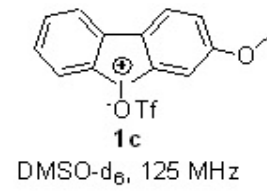




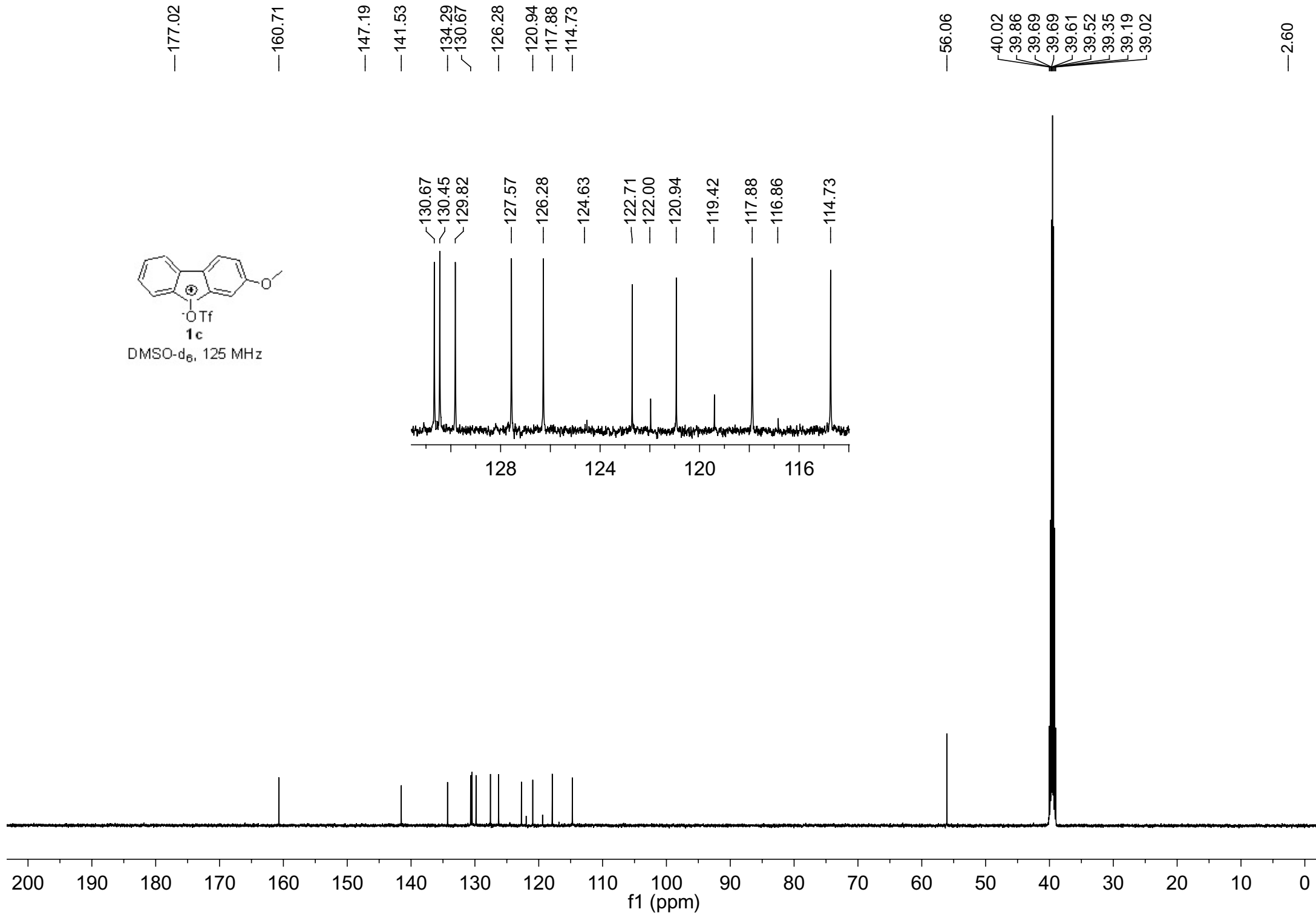
DMSO-d₆, 125 MHz

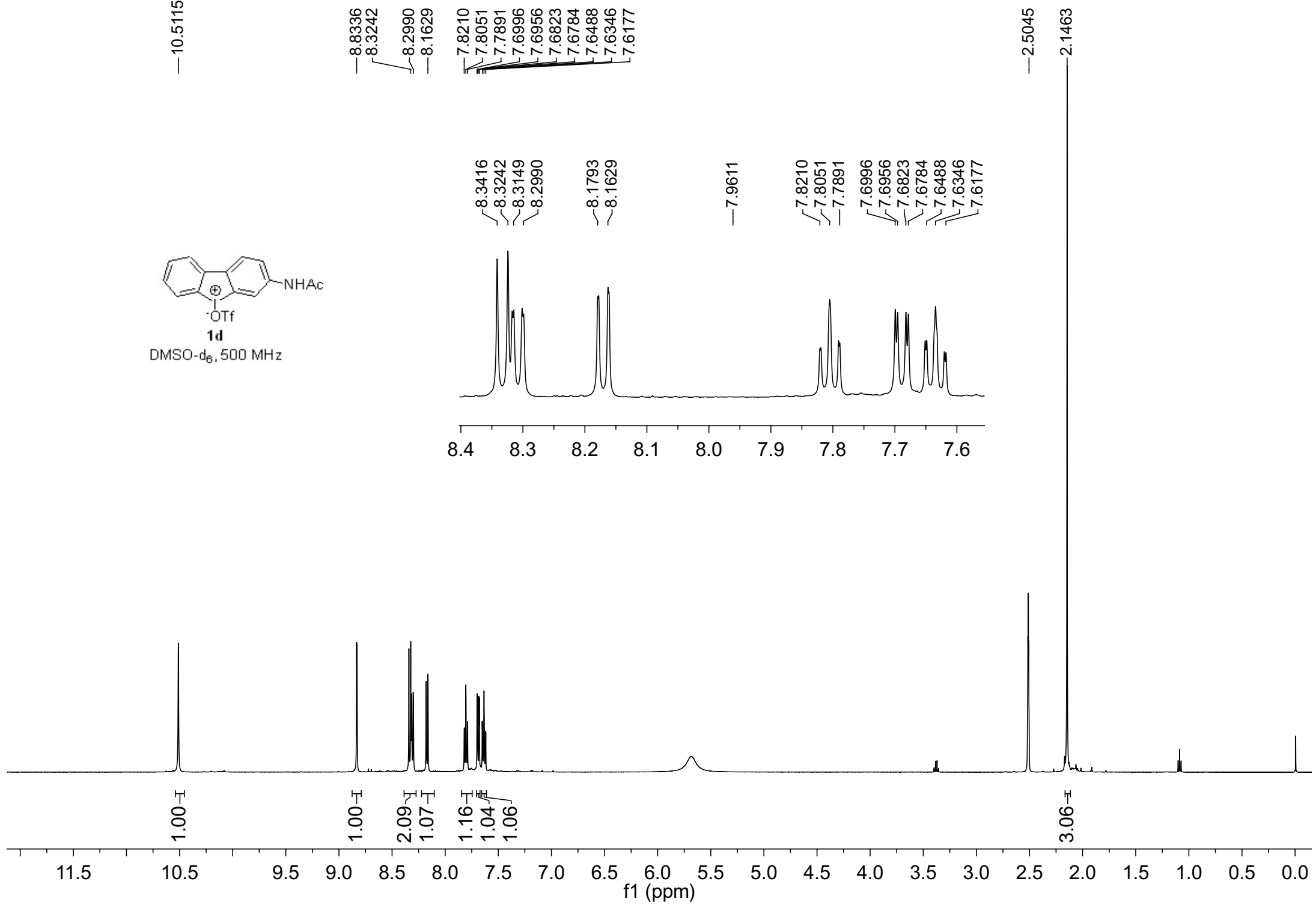
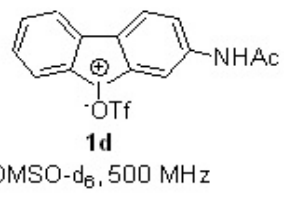


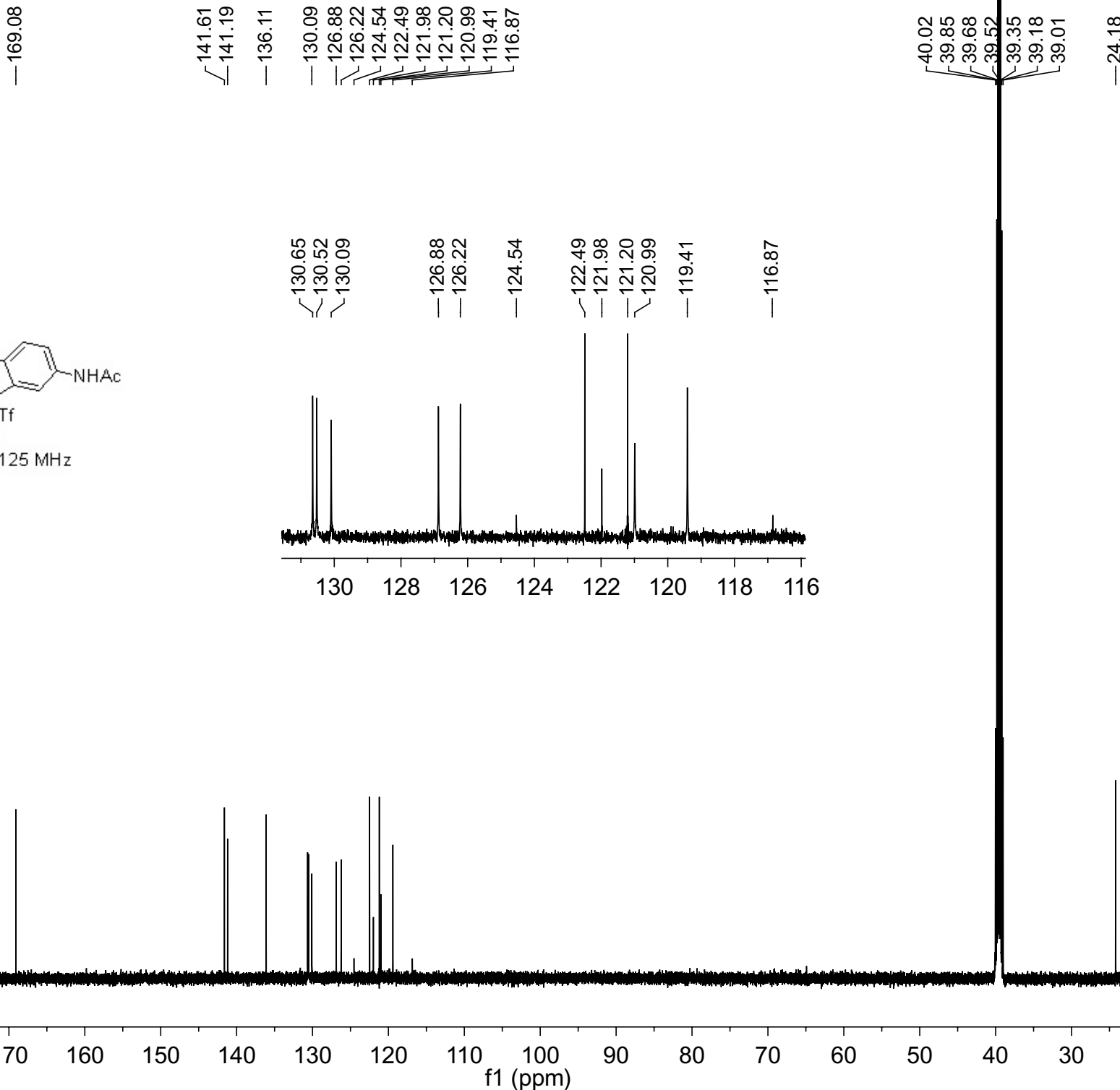
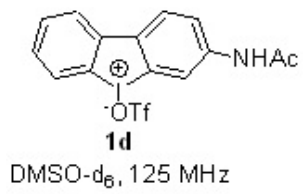


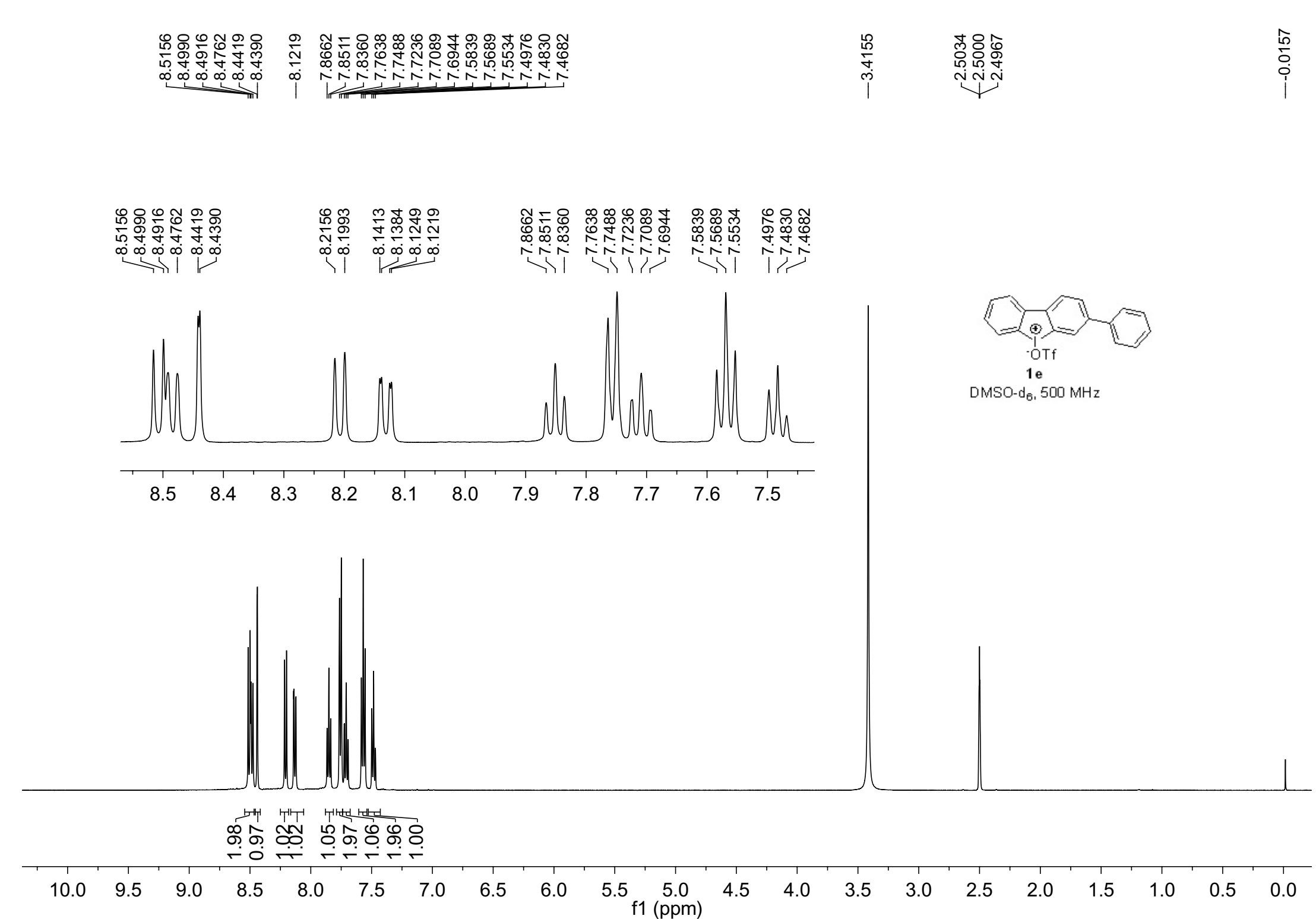


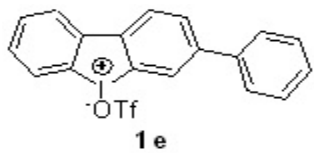
DMSO-d₆, 125 MHz



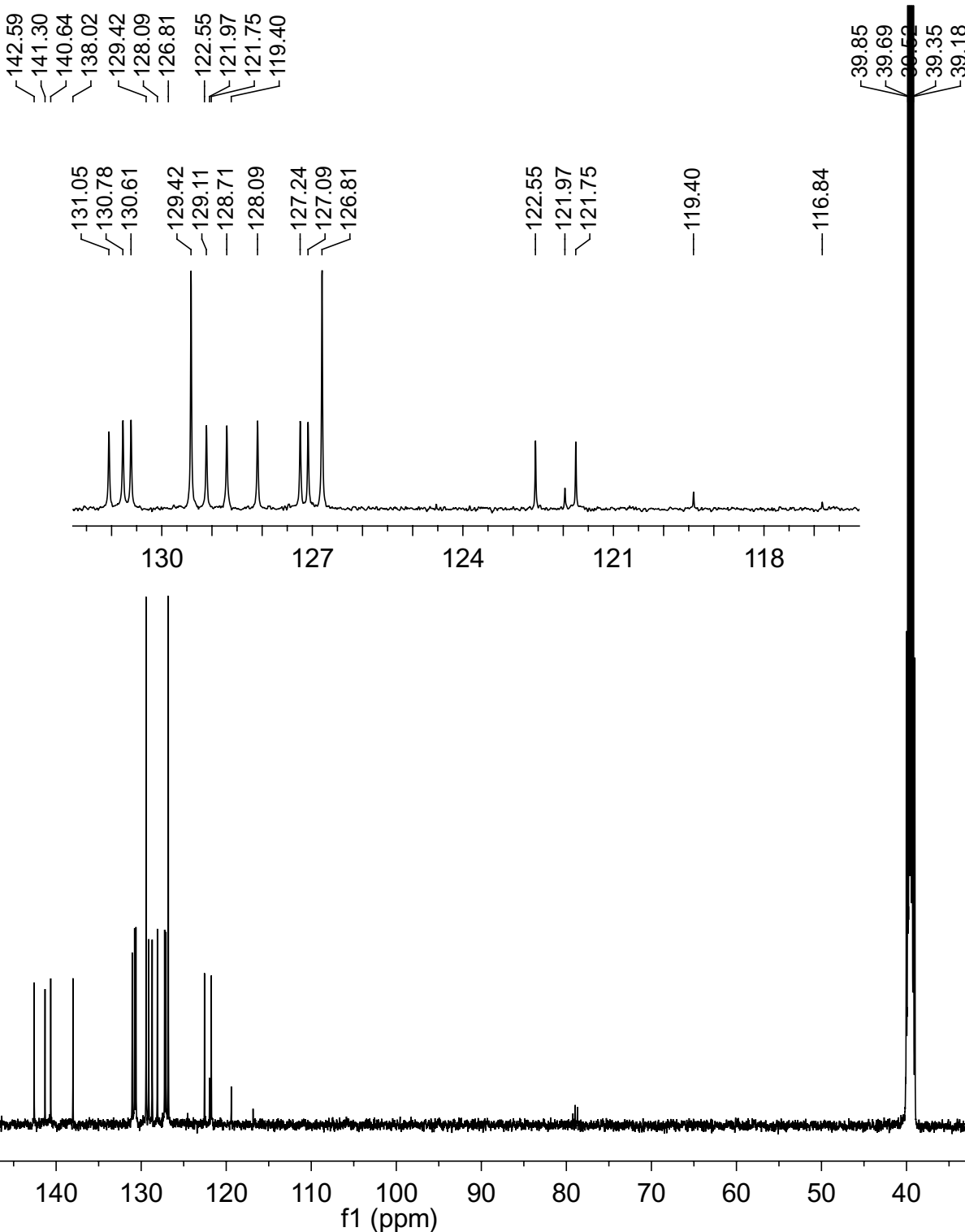


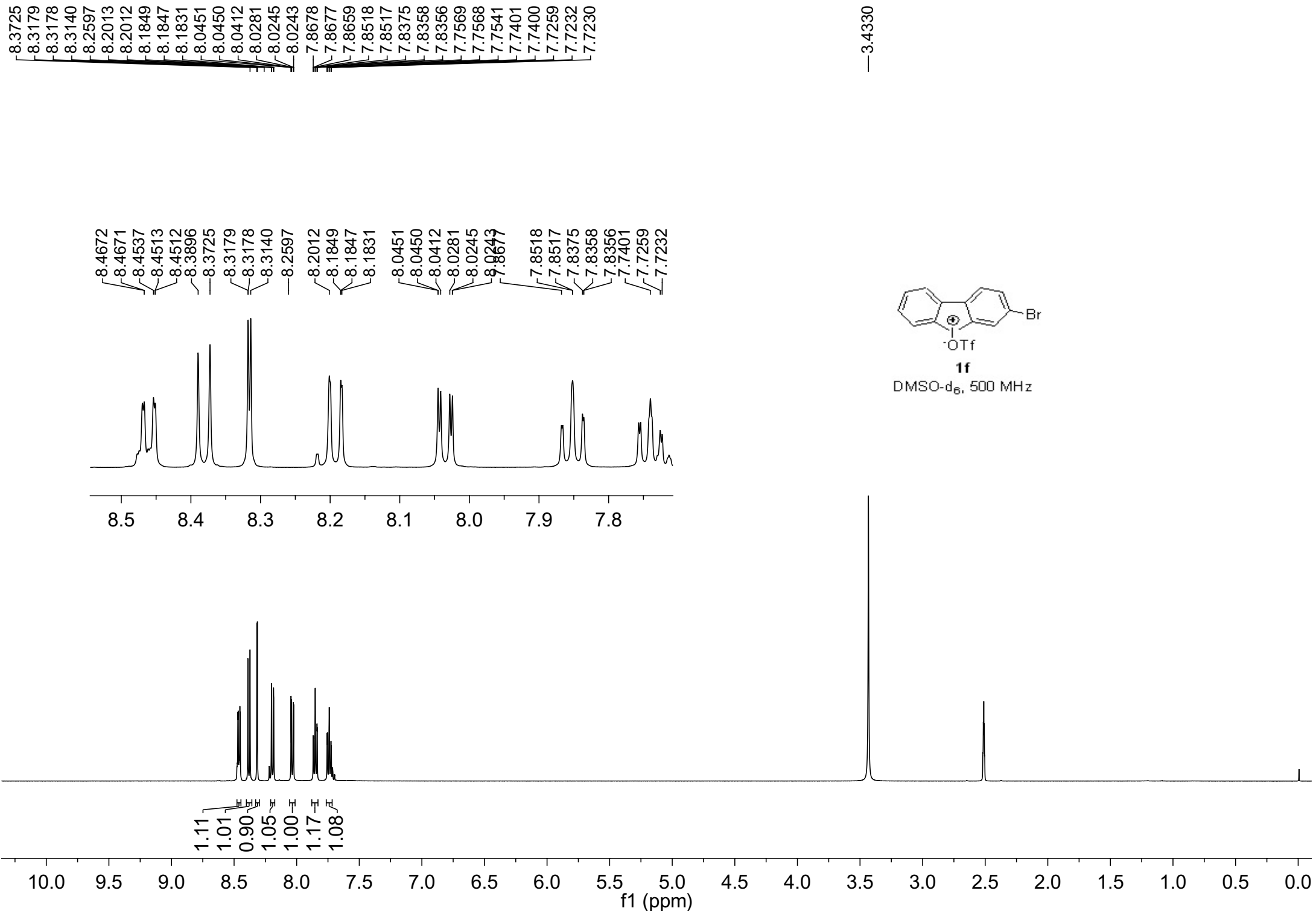


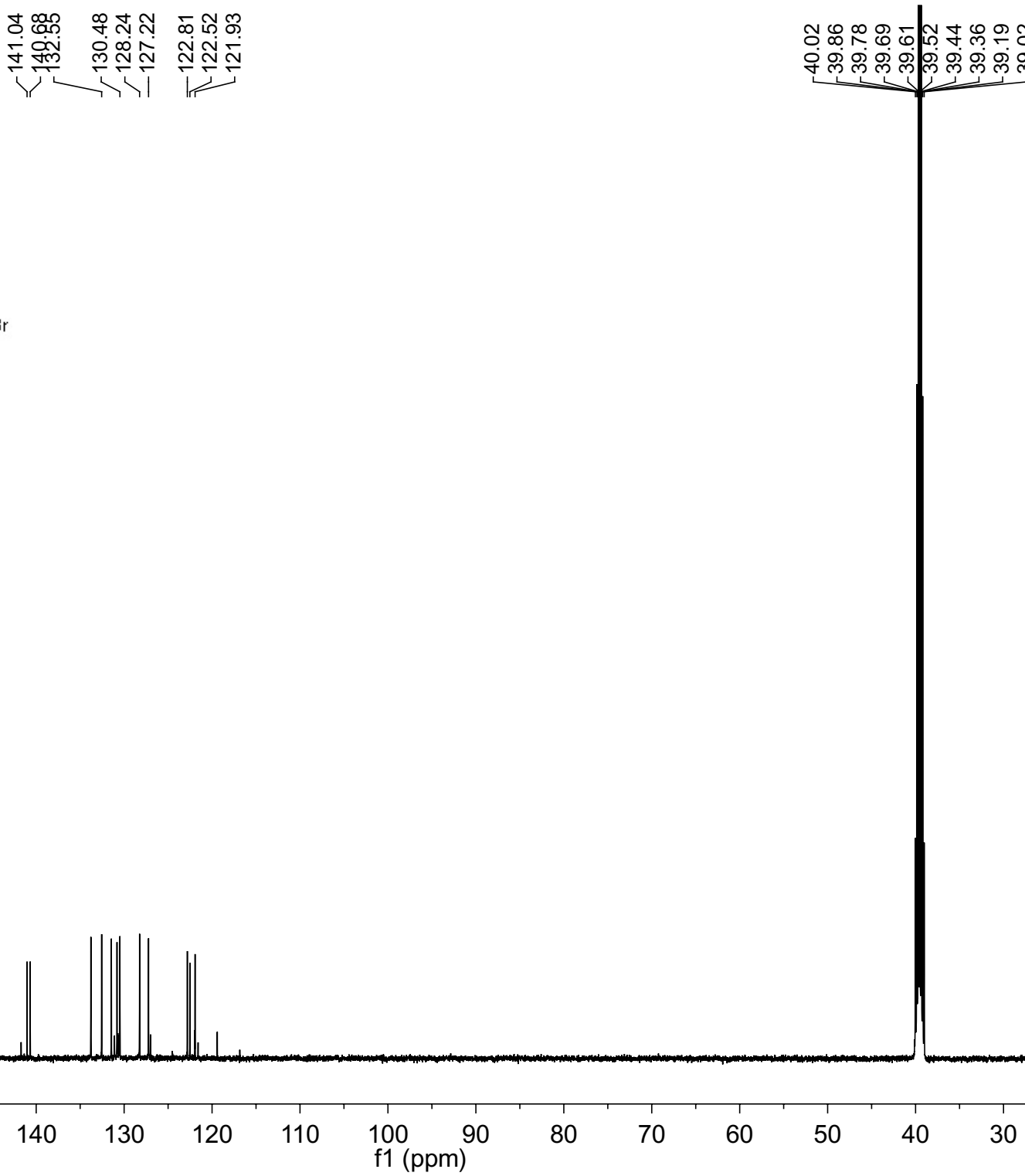
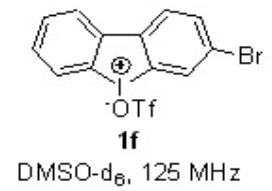


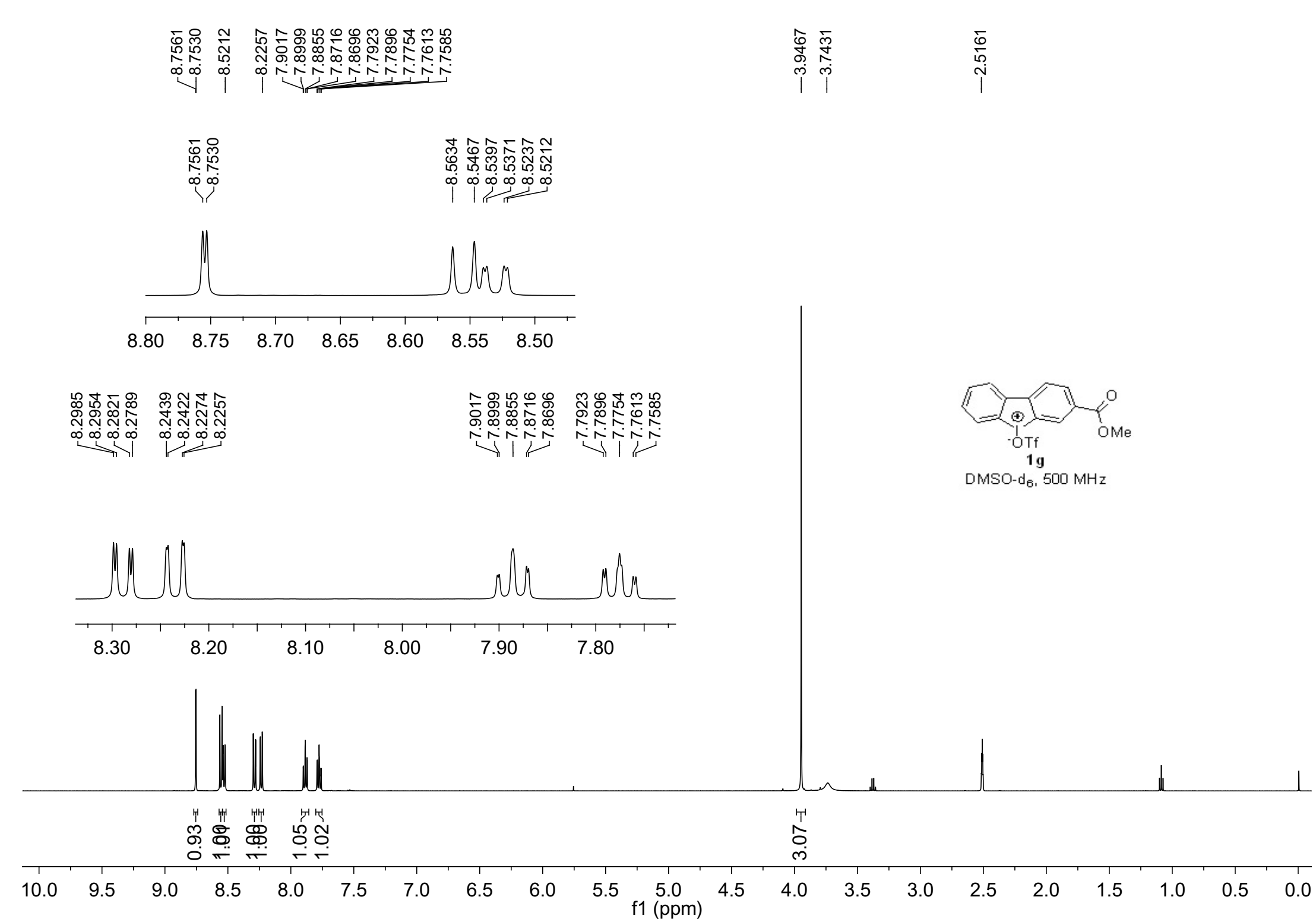


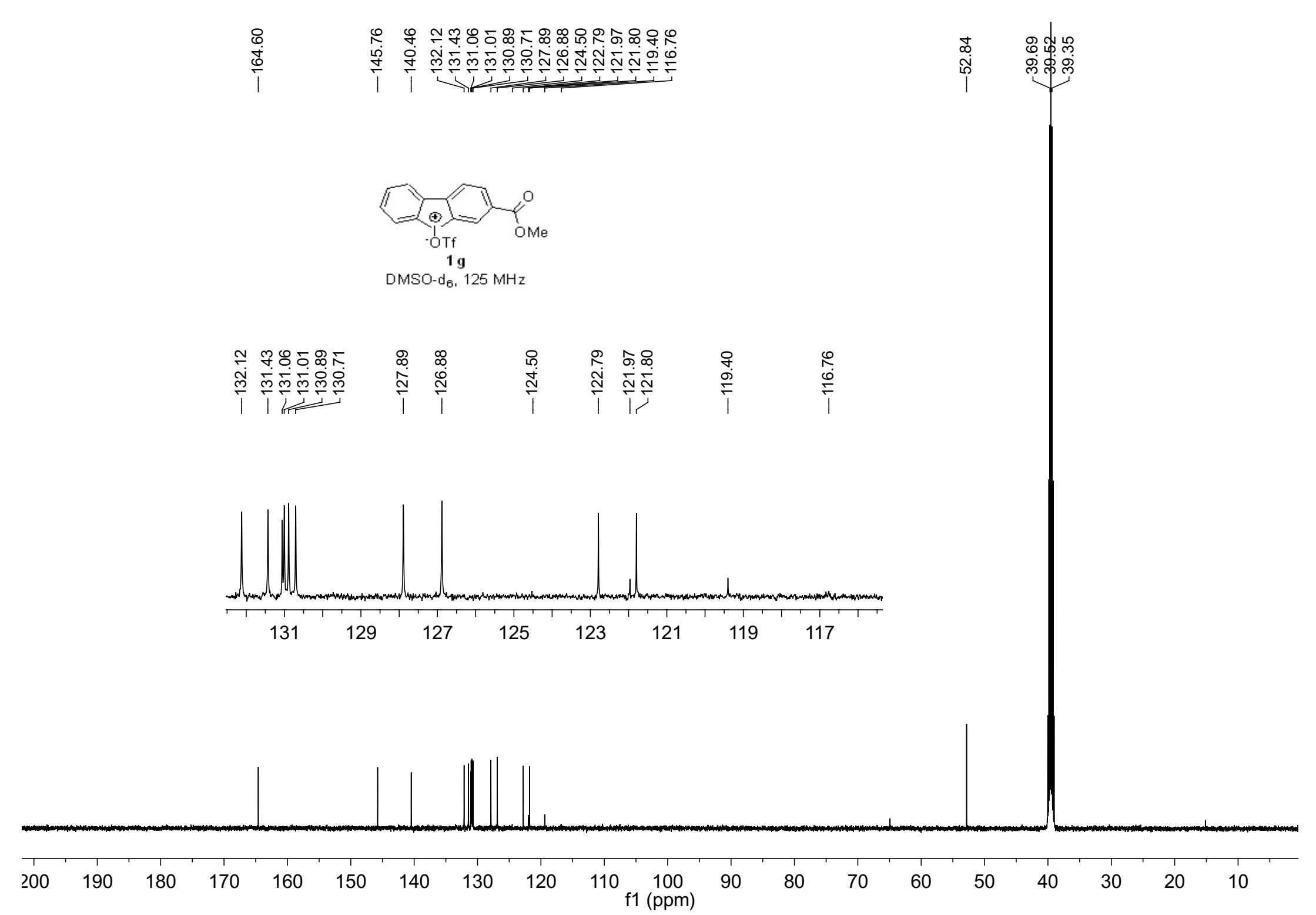
DMSO-d₆, 125 MHz

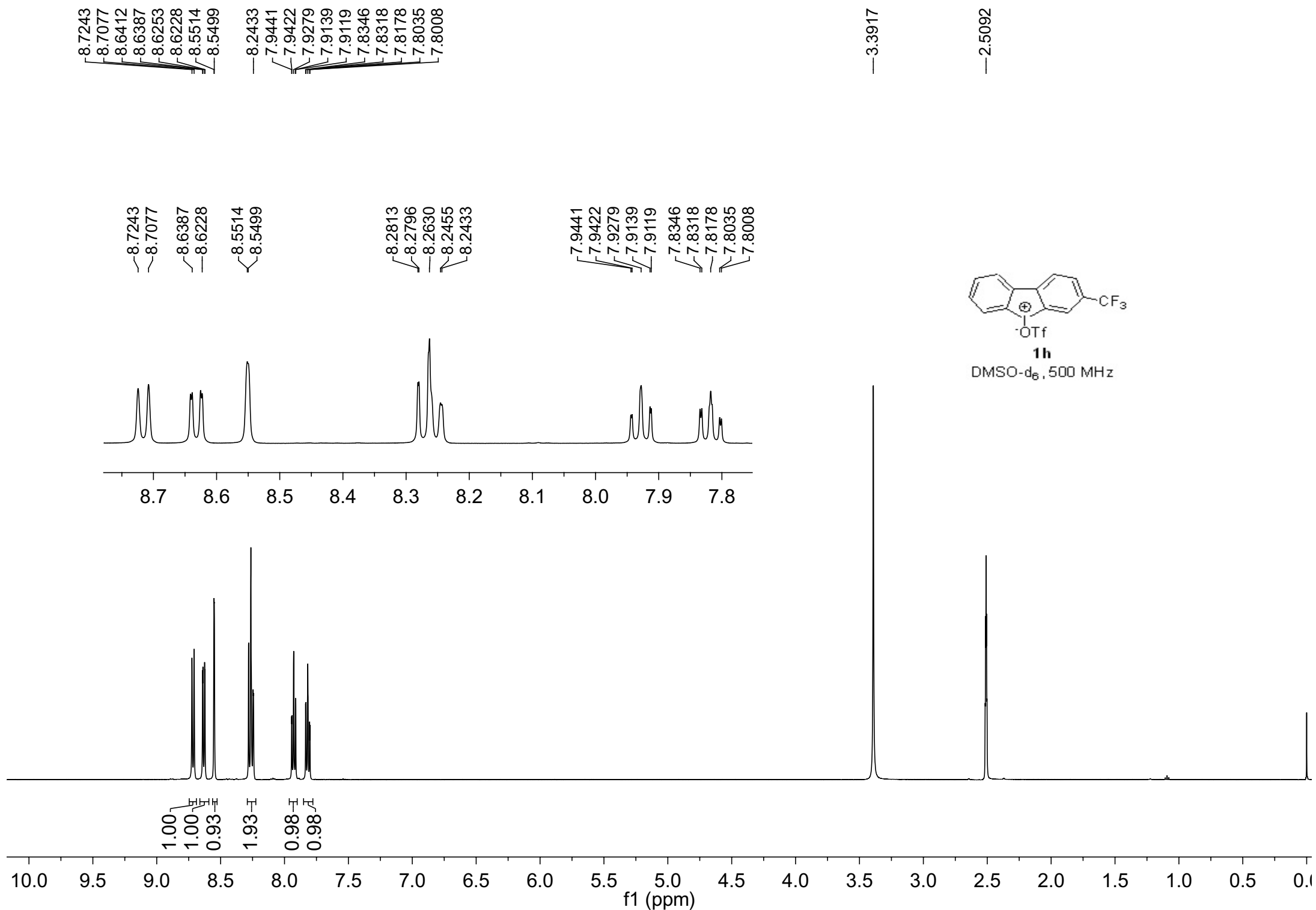






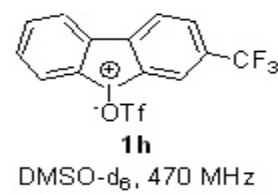


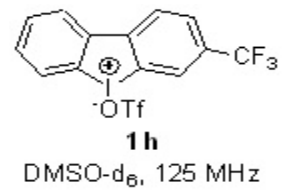
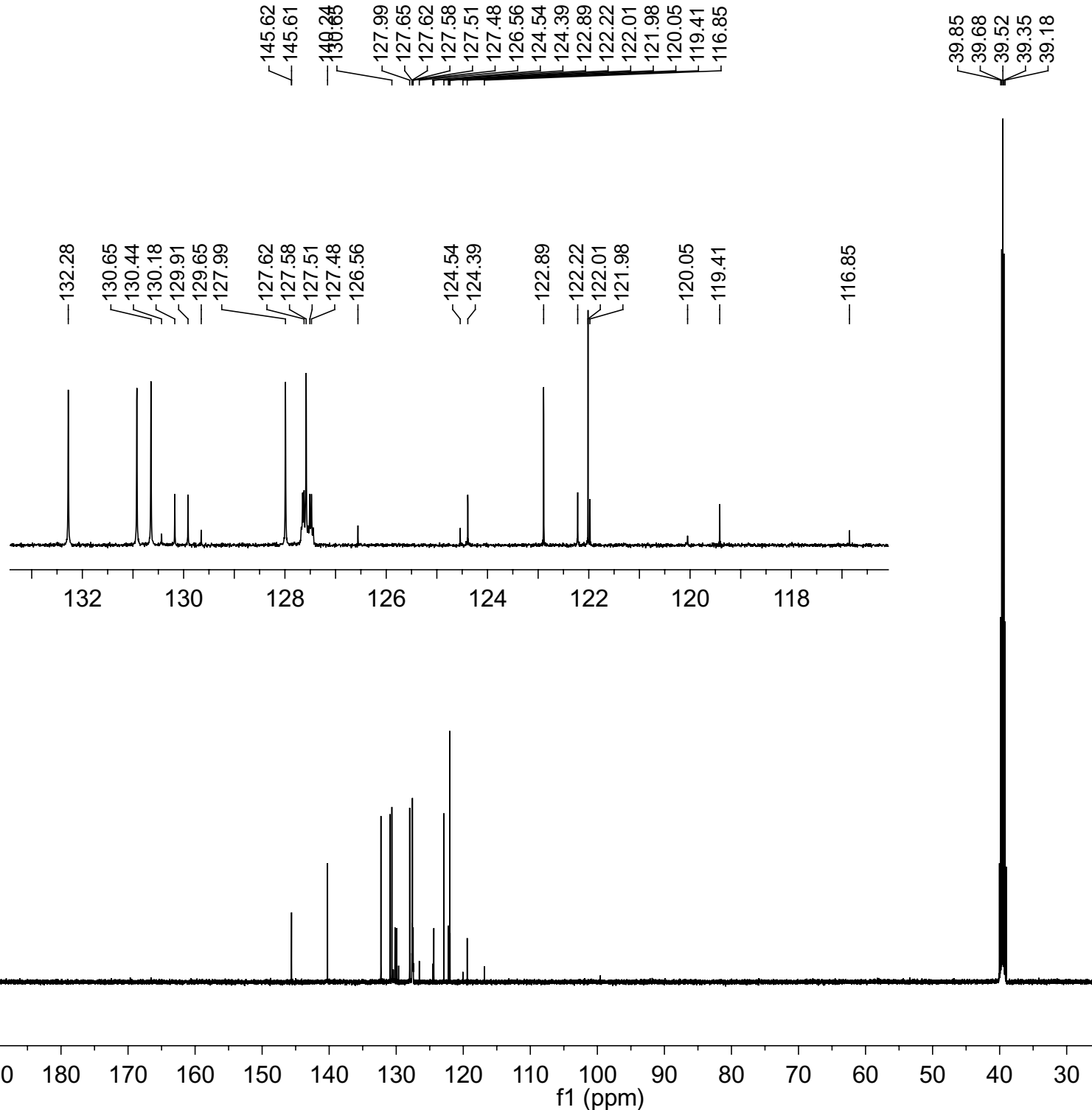




— -60.9925

— -77.7636





8.6113
 8.5947
 8.5570
 8.5545
 8.5410
 8.5386
 8.4860
 8.4831

-8.2152
 7.9021
 7.9003
 7.8861

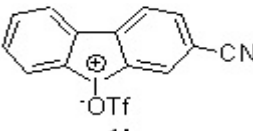
7.8719
 7.8700
 7.8115
 7.8088
 7.7947
 7.7805
 7.7778

-3.8010
 3.3890
 3.3750
 3.3610
 3.3470

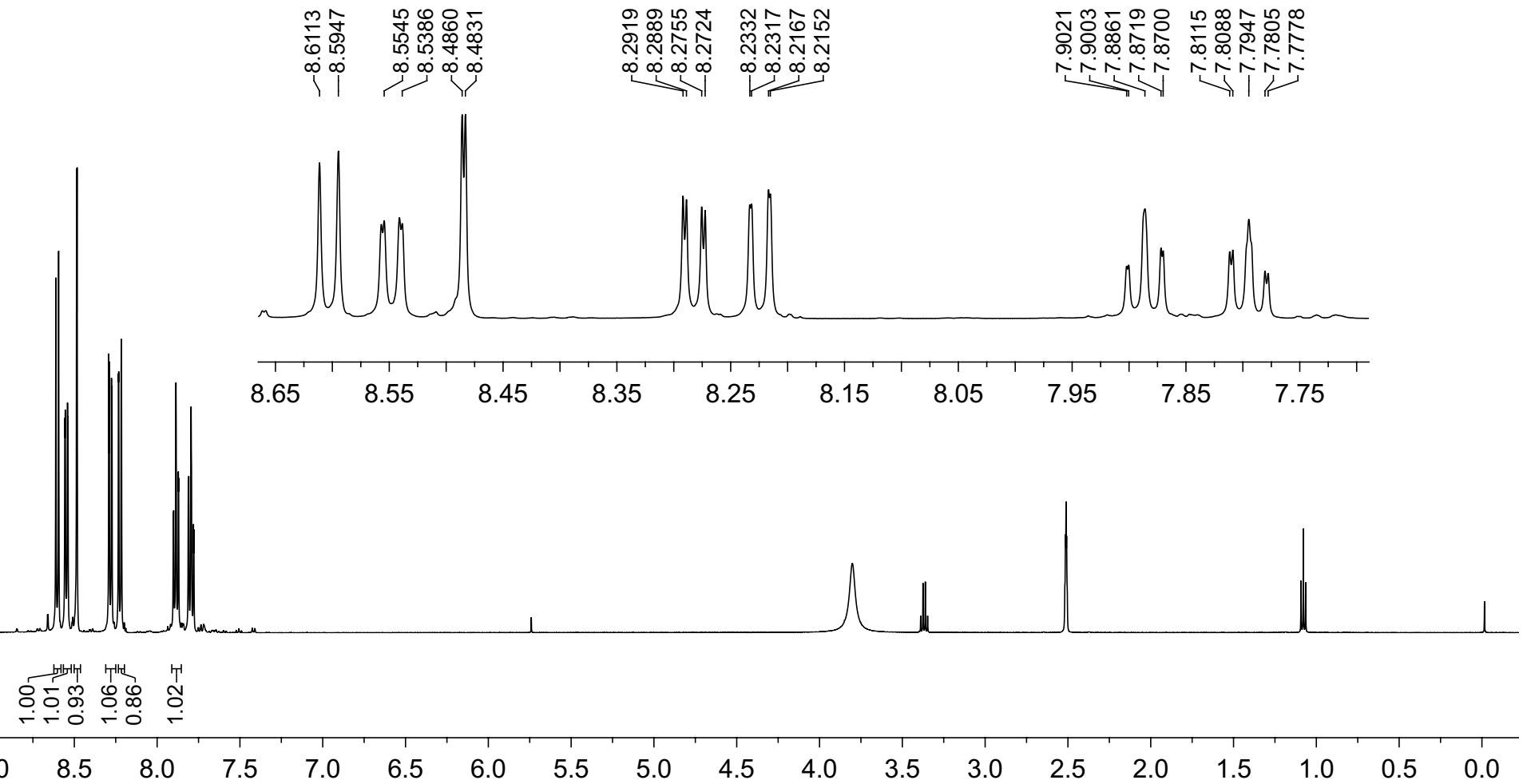
2.5147
 2.5112
 2.5077

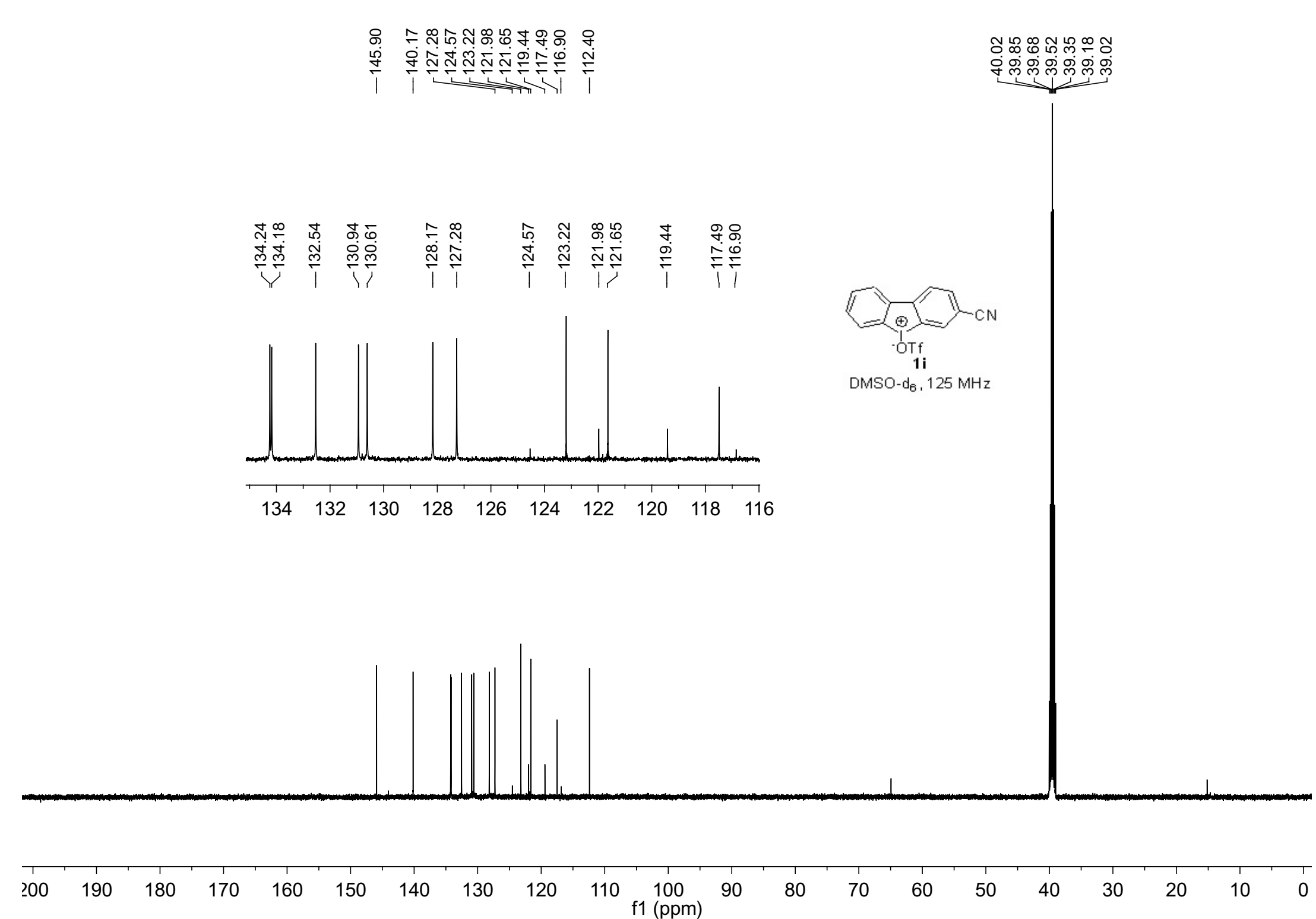
1.0923
 1.0783
 1.0643

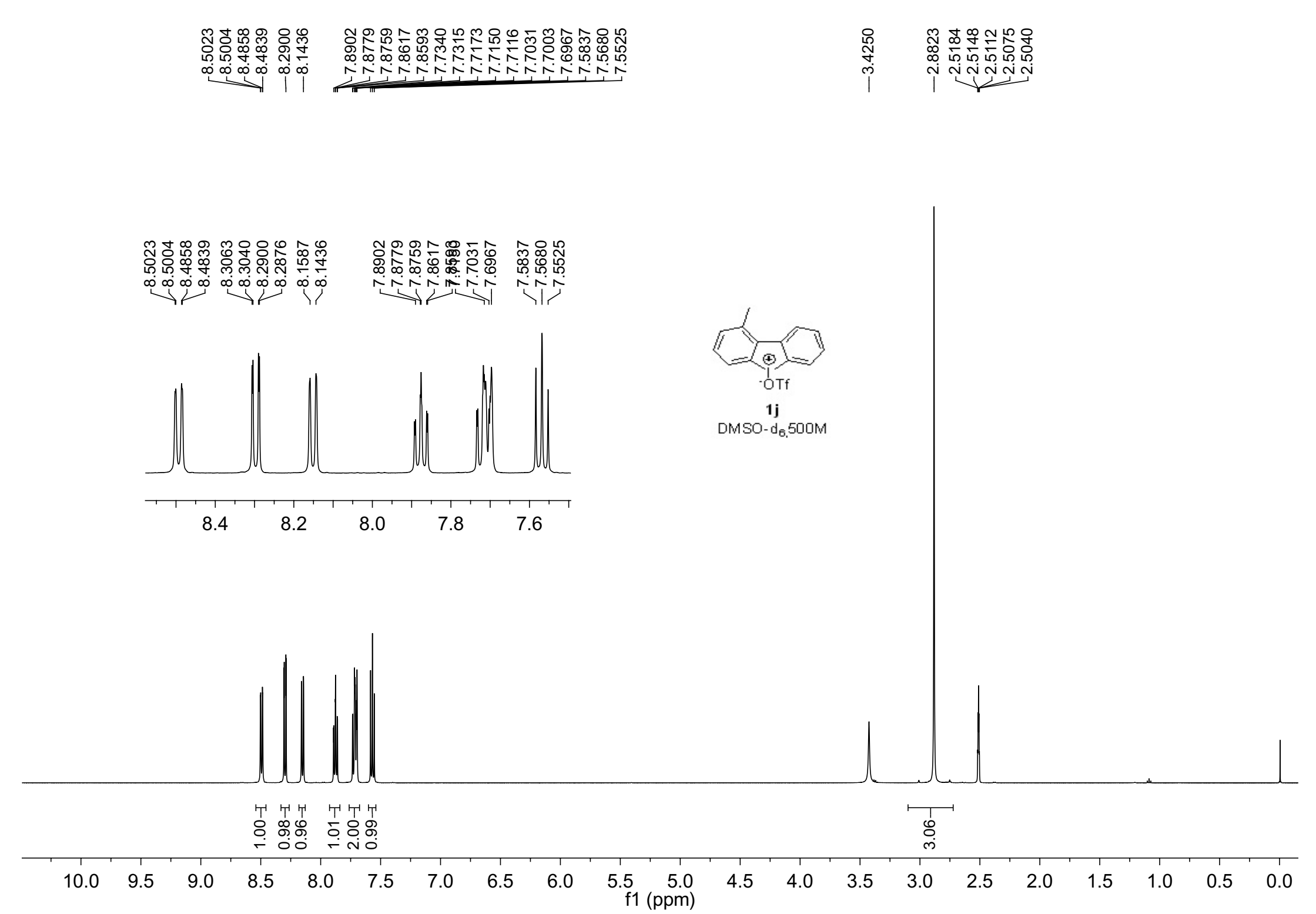
-0.0156

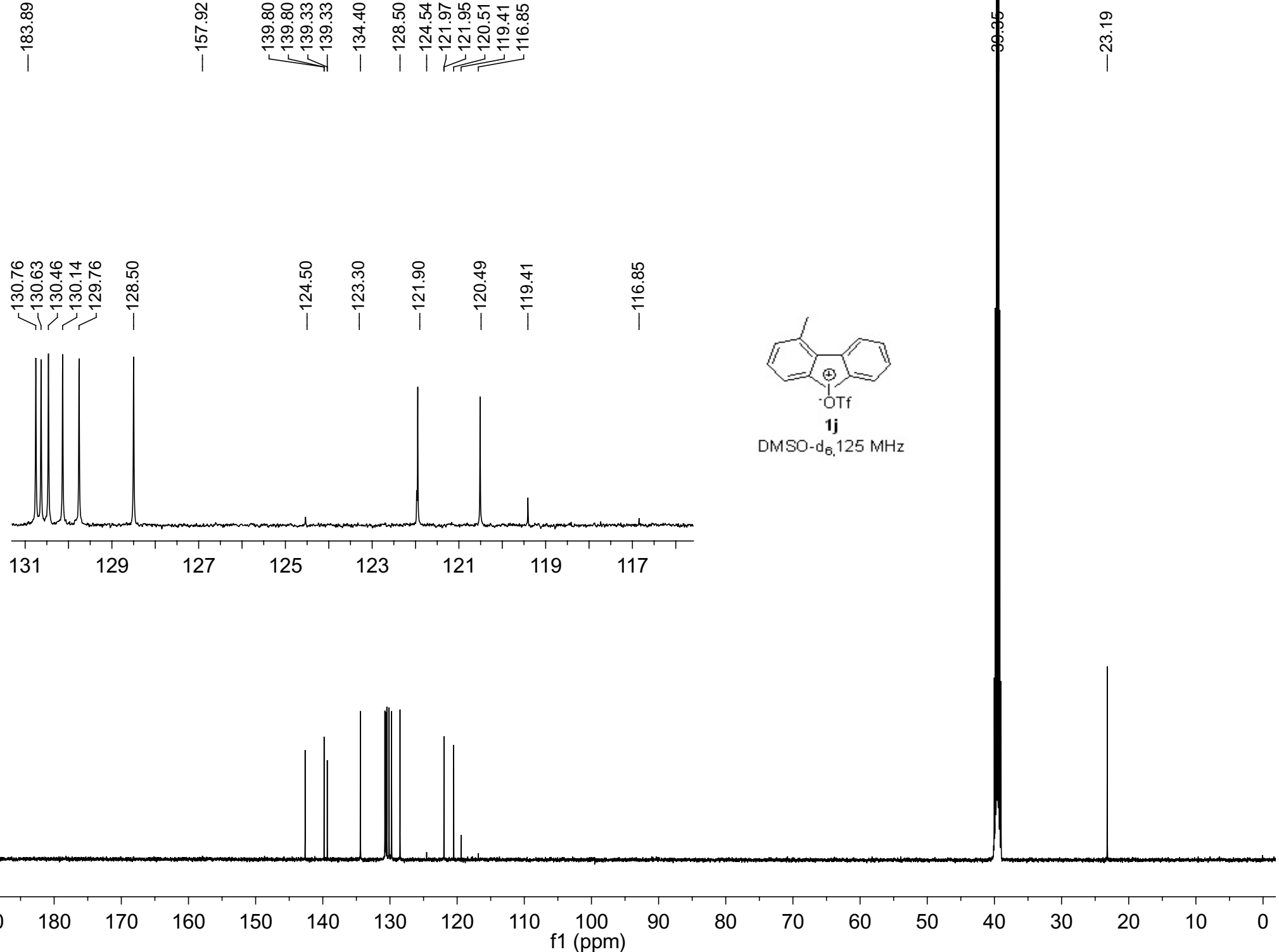


DMSO-d₆, 500 MHz







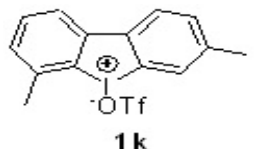


8.2450
8.2288
8.1512
8.1360
8.0454
8.0440
8.0430
7.7207
7.7055
7.6903
7.6414
7.6401
7.6387
7.6253
7.6241
7.6226
7.5024
7.4879

-3.5086

-2.6517
-2.4792

-0.0094



1k

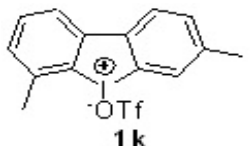
DMSO- d_6 , 500 MHz

1.00
1.00
0.96
1.02
0.99
1.02

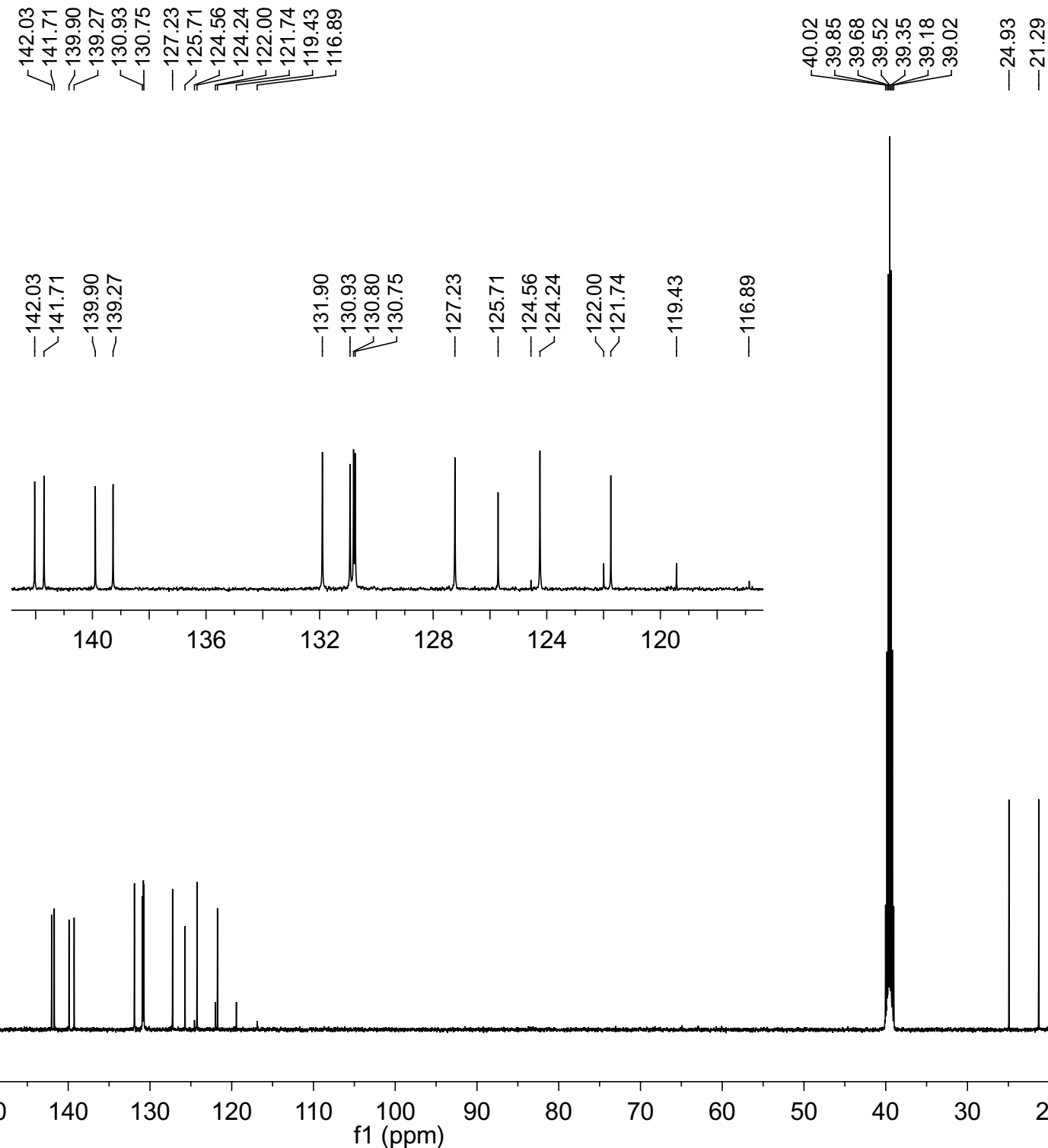
3.03
3.28

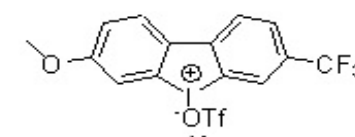
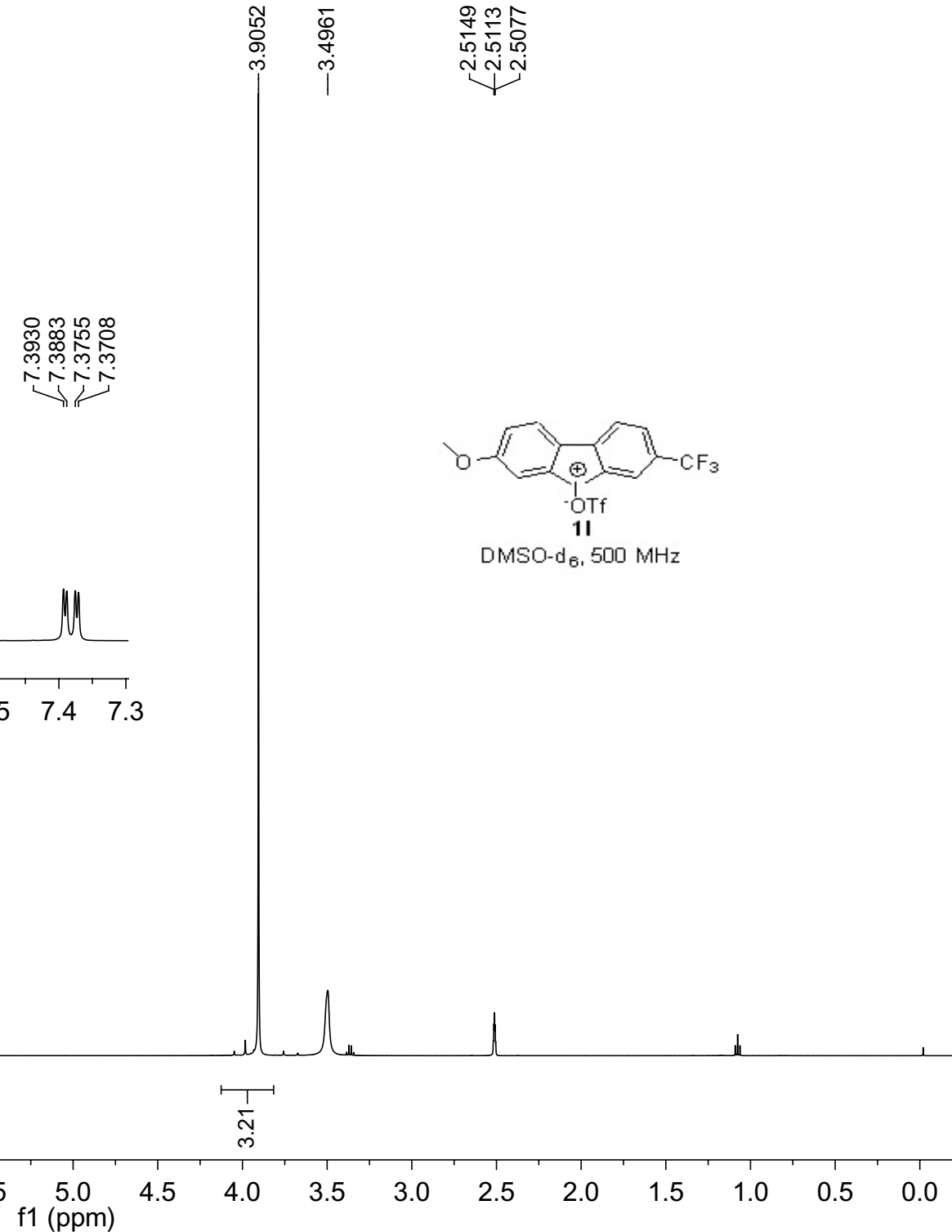
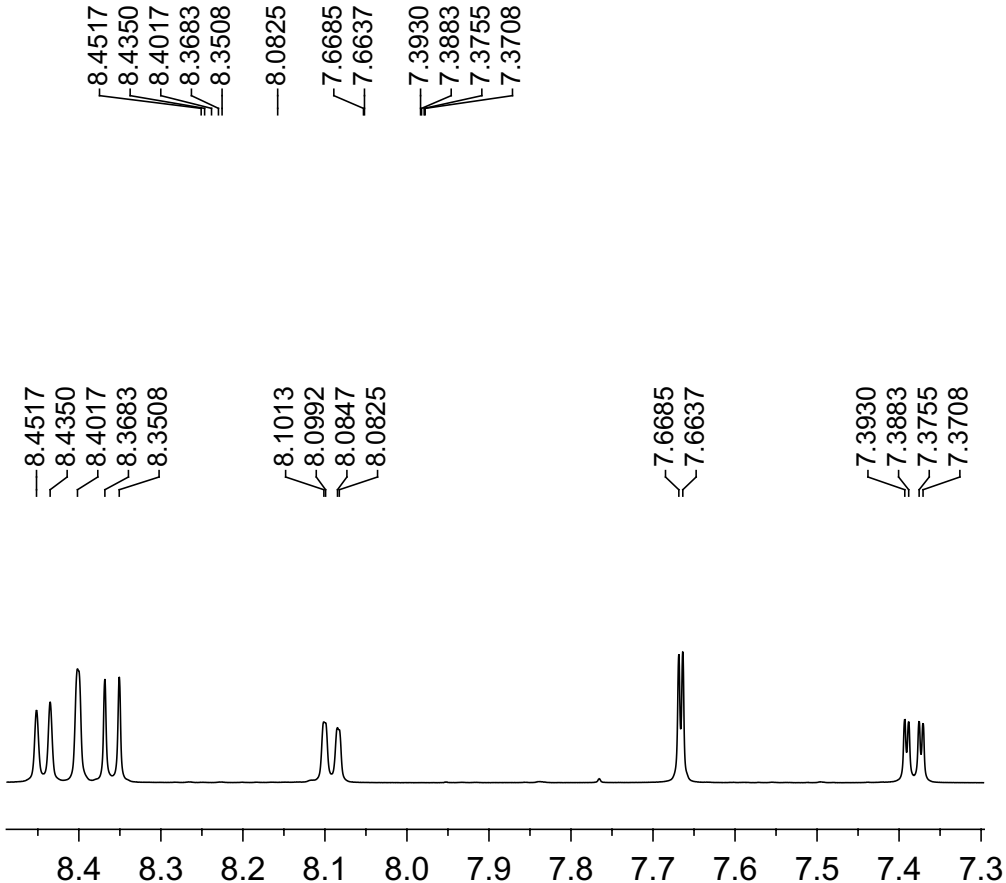
10.0 9.5 9.0 8.5 8.0 7.5 7.0 6.5 6.0 5.5 5.0 4.5 4.0 3.5 3.0 2.5 2.0 1.5 1.0 0.5 0.0

f1 (ppm)

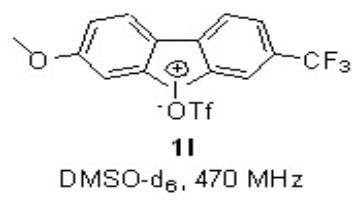


DMSO-d₆, 125 MHz





DMSO- d_6 , 500 MHz

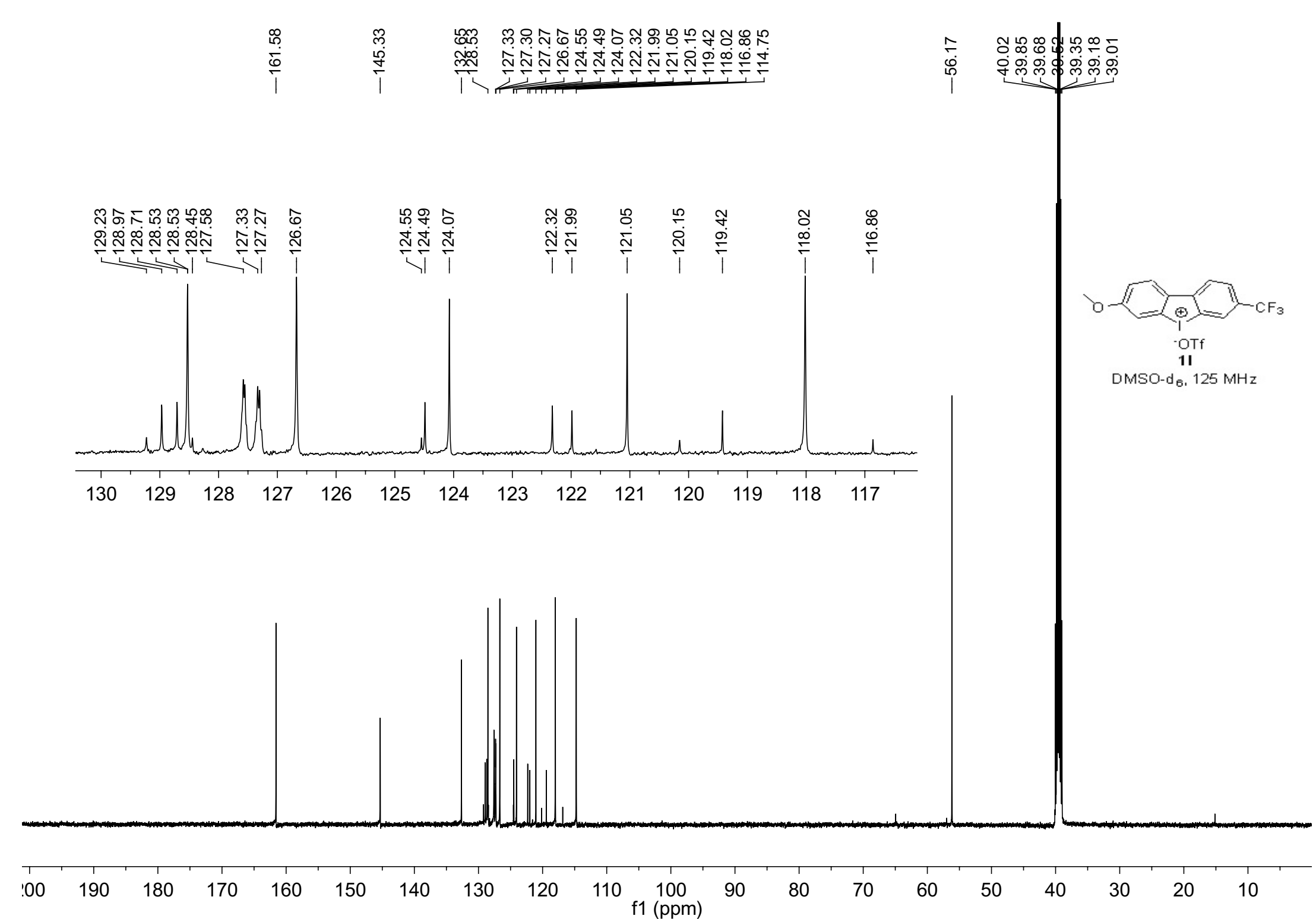


DMSO-d₆, 470 MHz

—60.9868

—77.8209

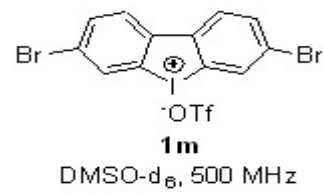
0 -10 -20 -30 -40 -50 -60 -70 -80 -90 -100 -110 -120 -130 -140 -150 -160 -170 -180 -190 -200
f1 (ppm)



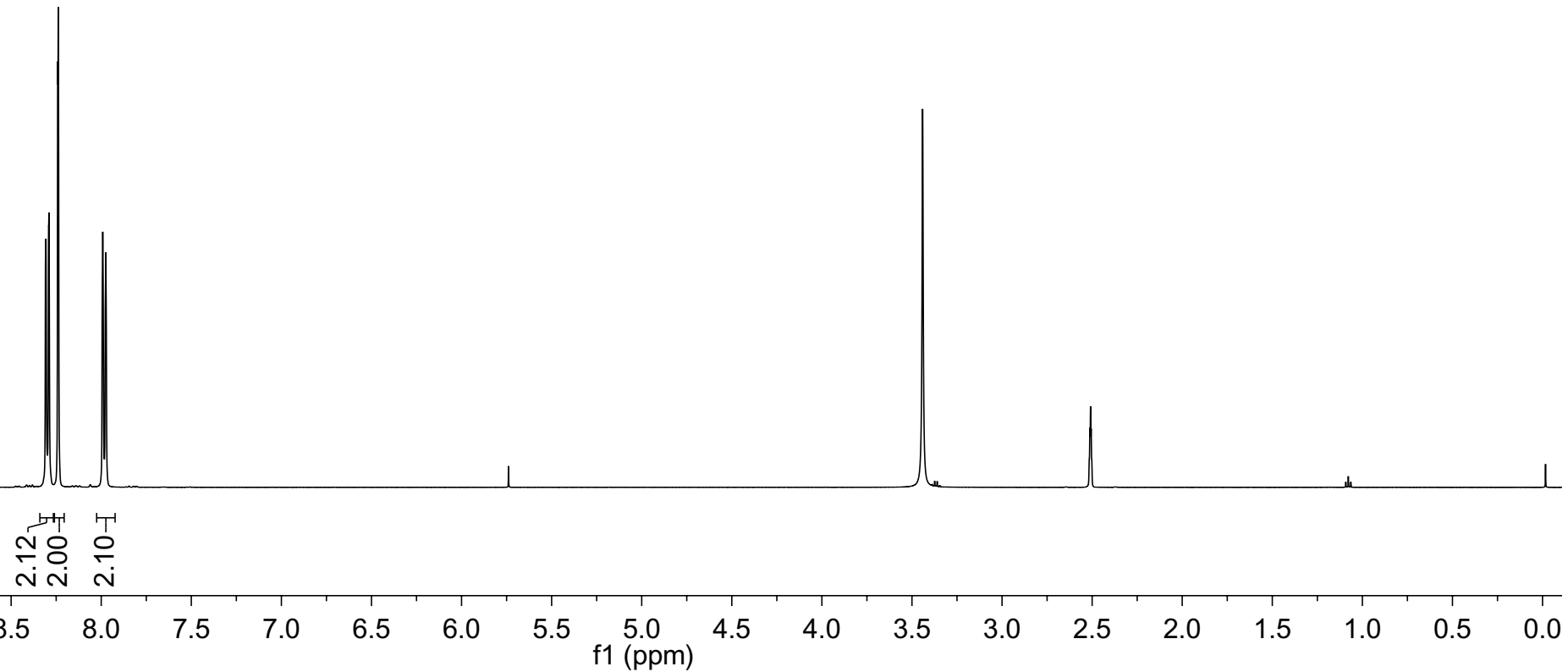
8.3068
8.2899
8.2405
8.2385
7.9912
7.9743

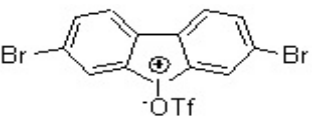
—3.4405

2.5122
2.5087
2.5052



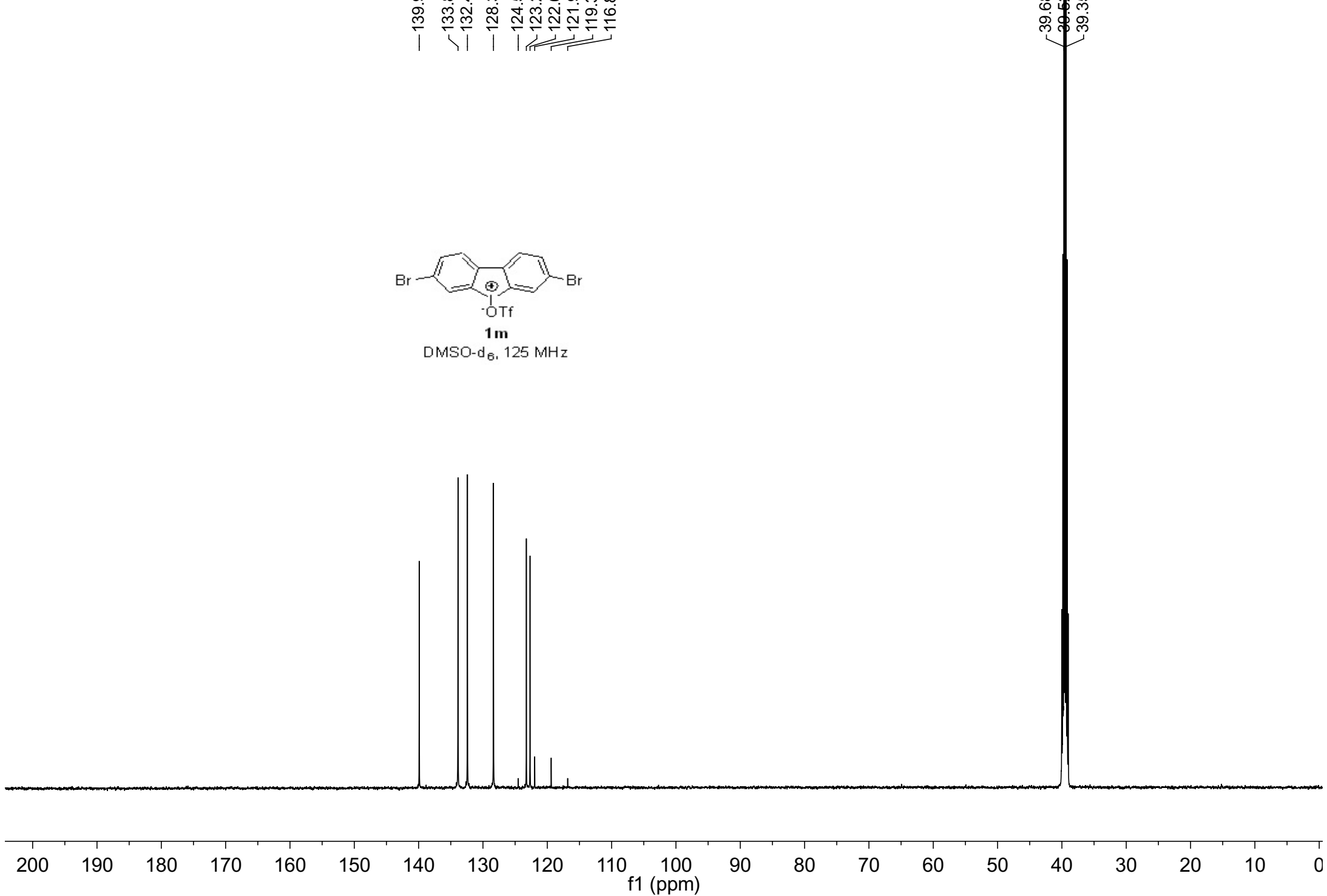
DMSO-d₆, 500 MHz





1m

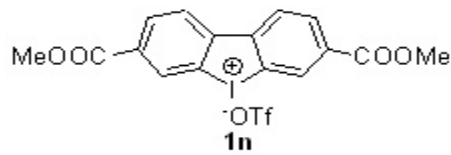
DMSO-d₆, 125 MHz



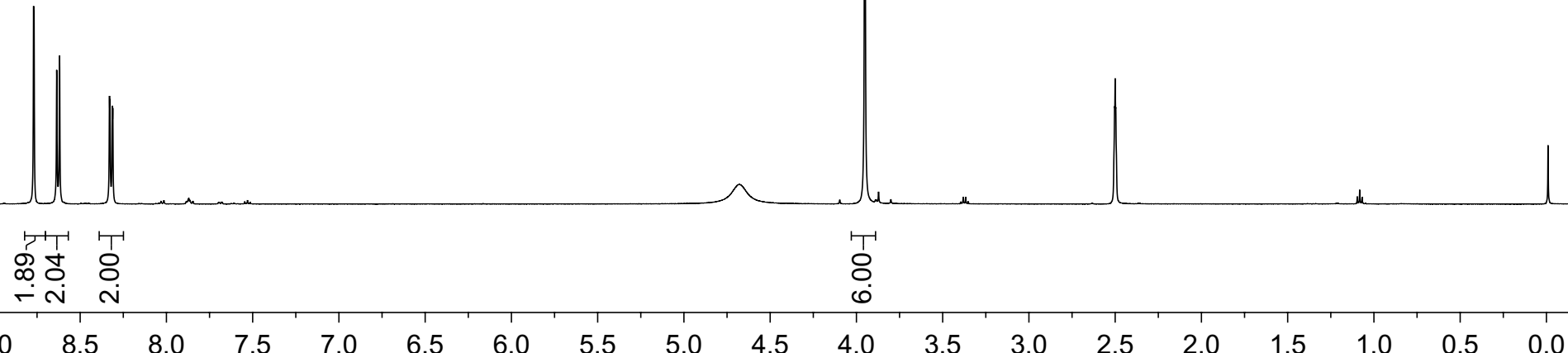
8.7700
8.7673
8.6359
8.6193
8.3300
8.3274
8.3137
8.3110

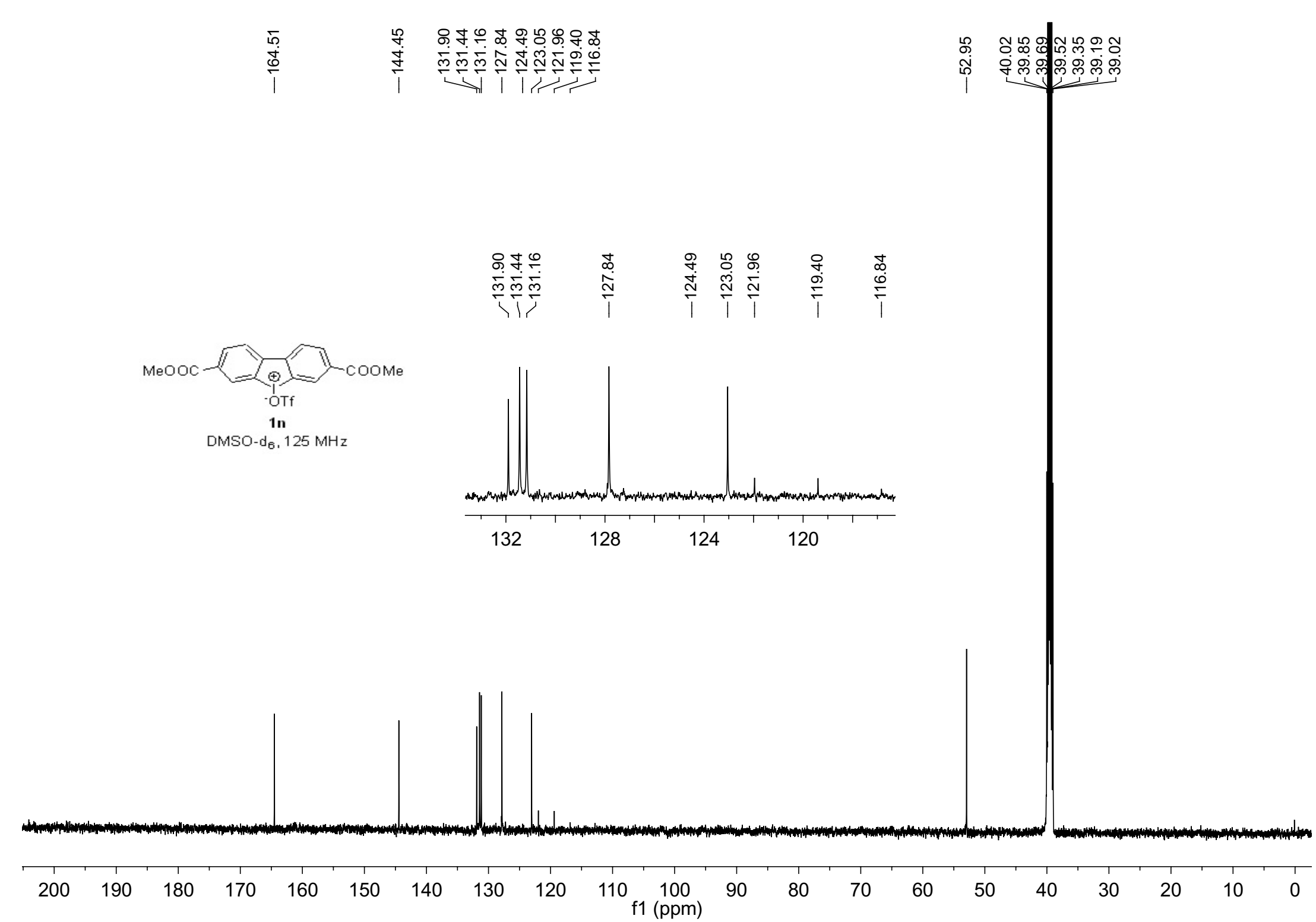
-3.9510

-2.5000



DMSO-d₆, 500 MHz





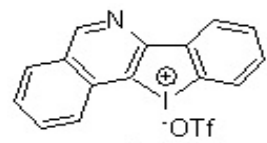
-9.7466

8.5506
8.4639
8.4476
8.4392
8.4225

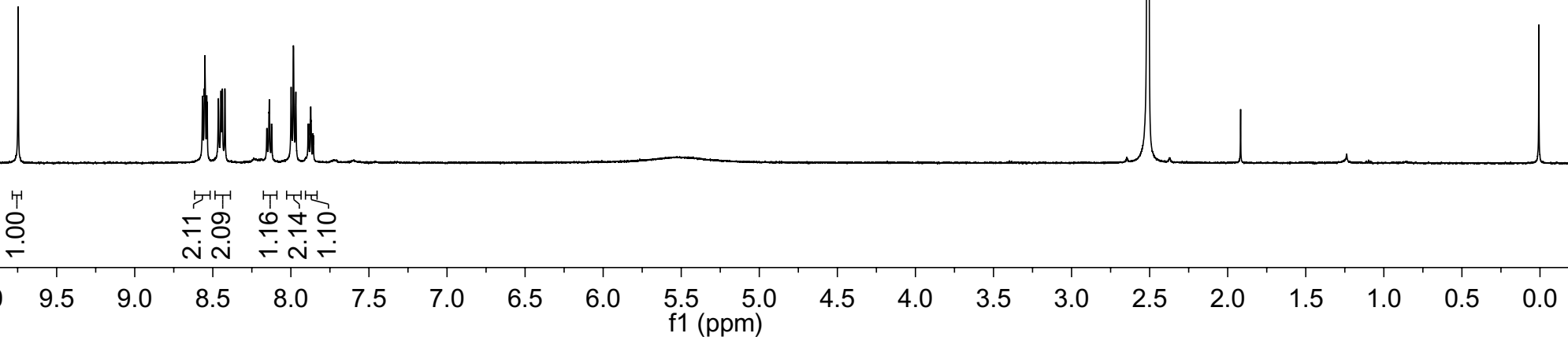
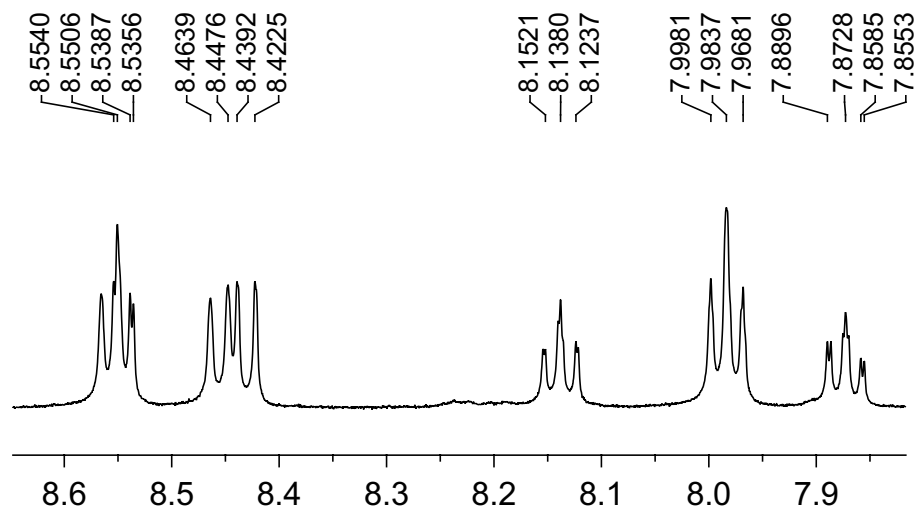
8.1521
8.1380
8.1237
7.9981
7.9837
7.9681
7.8896
7.8864
7.8728
7.8585
7.8553

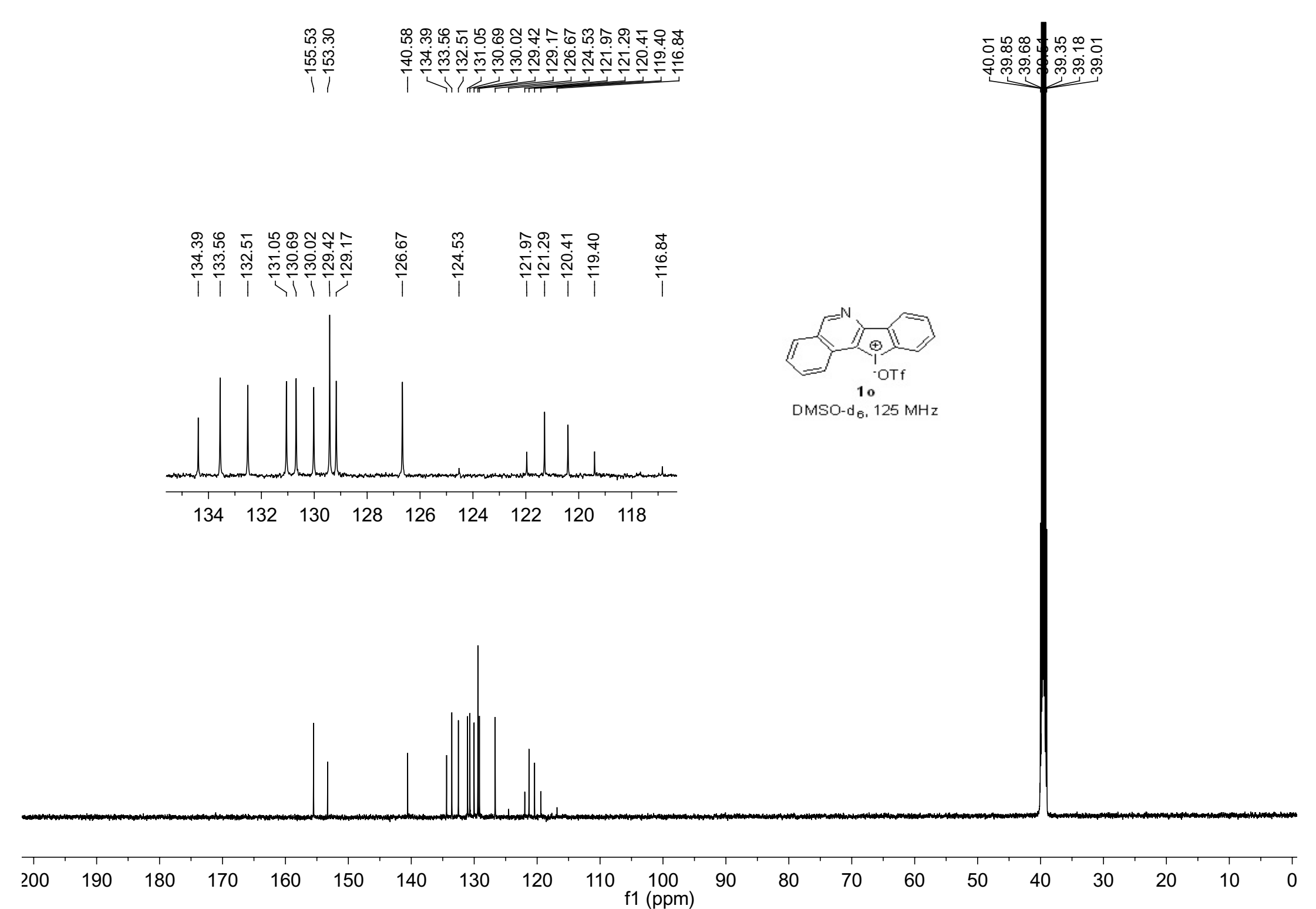
2.5142
2.5107
2.5071

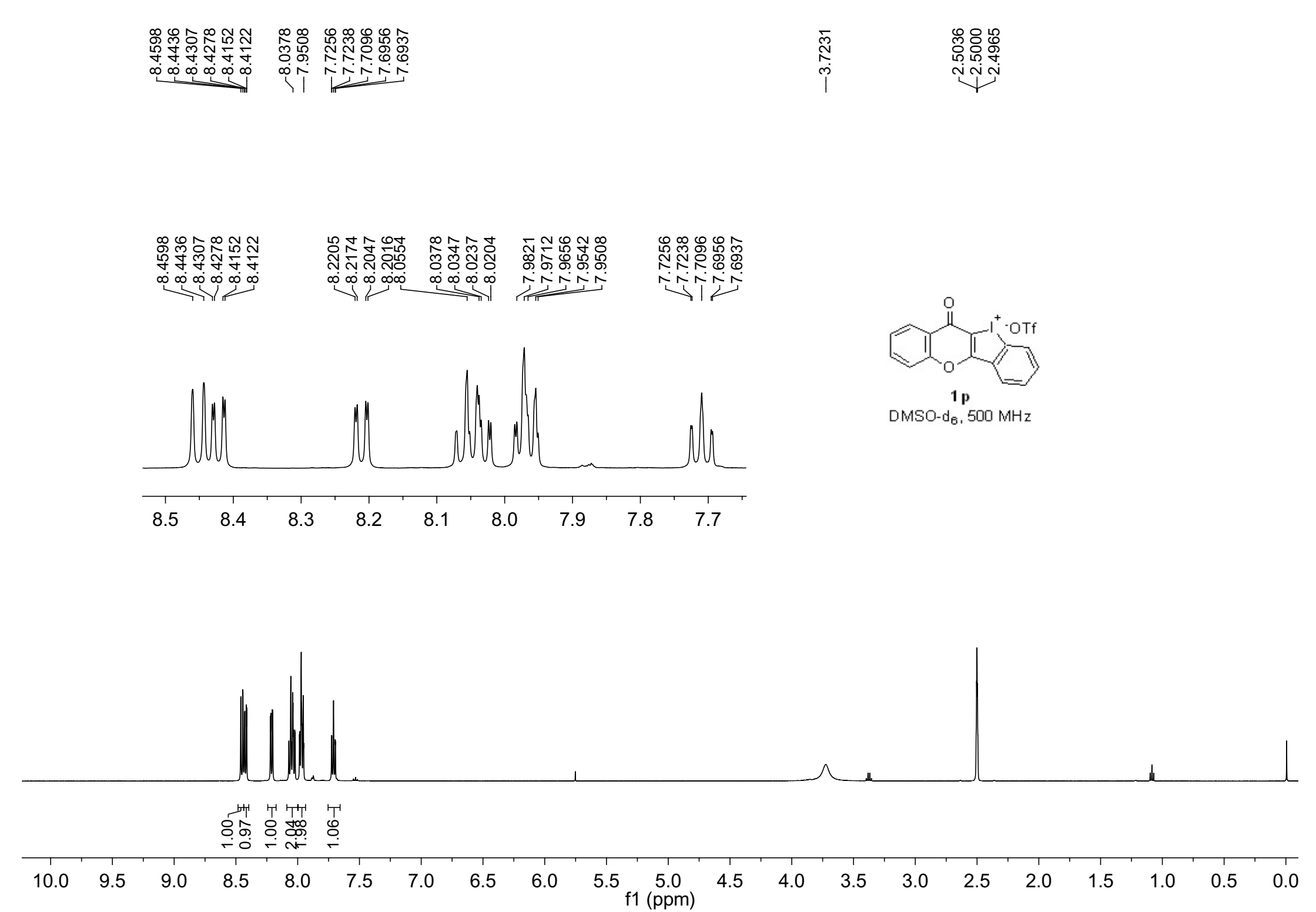
-0.0069

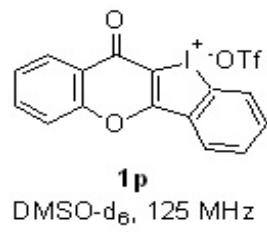


DMSO-d₆, 500 MHz









-172.37
-164.08
-155.20

135.96
135.27
134.70

125.27
124.53
122.51
121.96

119.66
119.42
118.80

119.42
118.80

118.80

135.96
135.27
134.70

131.45
131.28

128.96

127.05

125.27
124.53

122.51
121.96

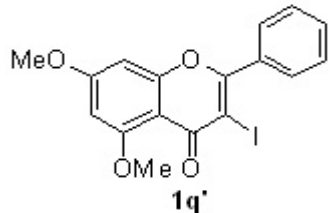
119.66
119.42
118.80

40.02
39.85
39.68
39.54

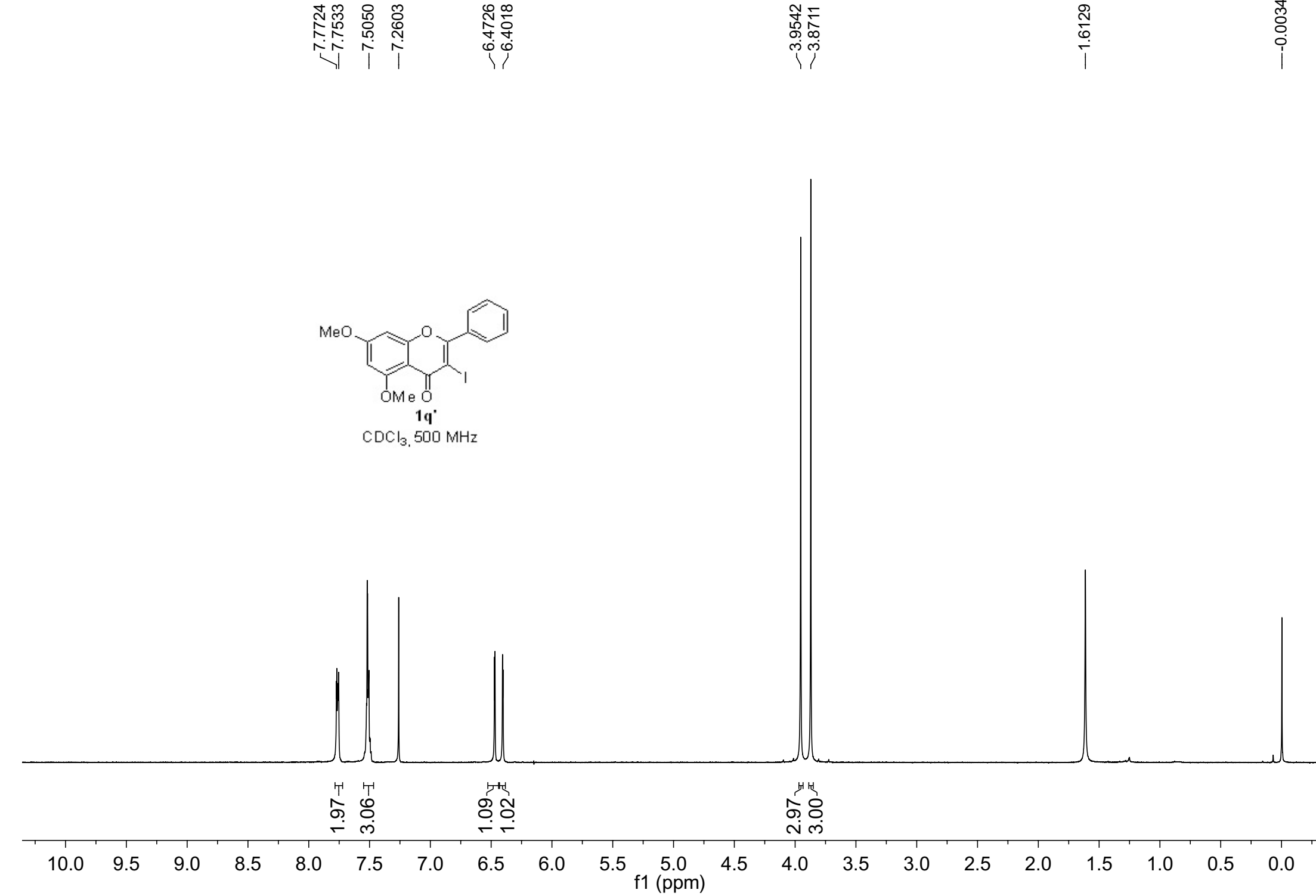
39.35
39.18
39.01

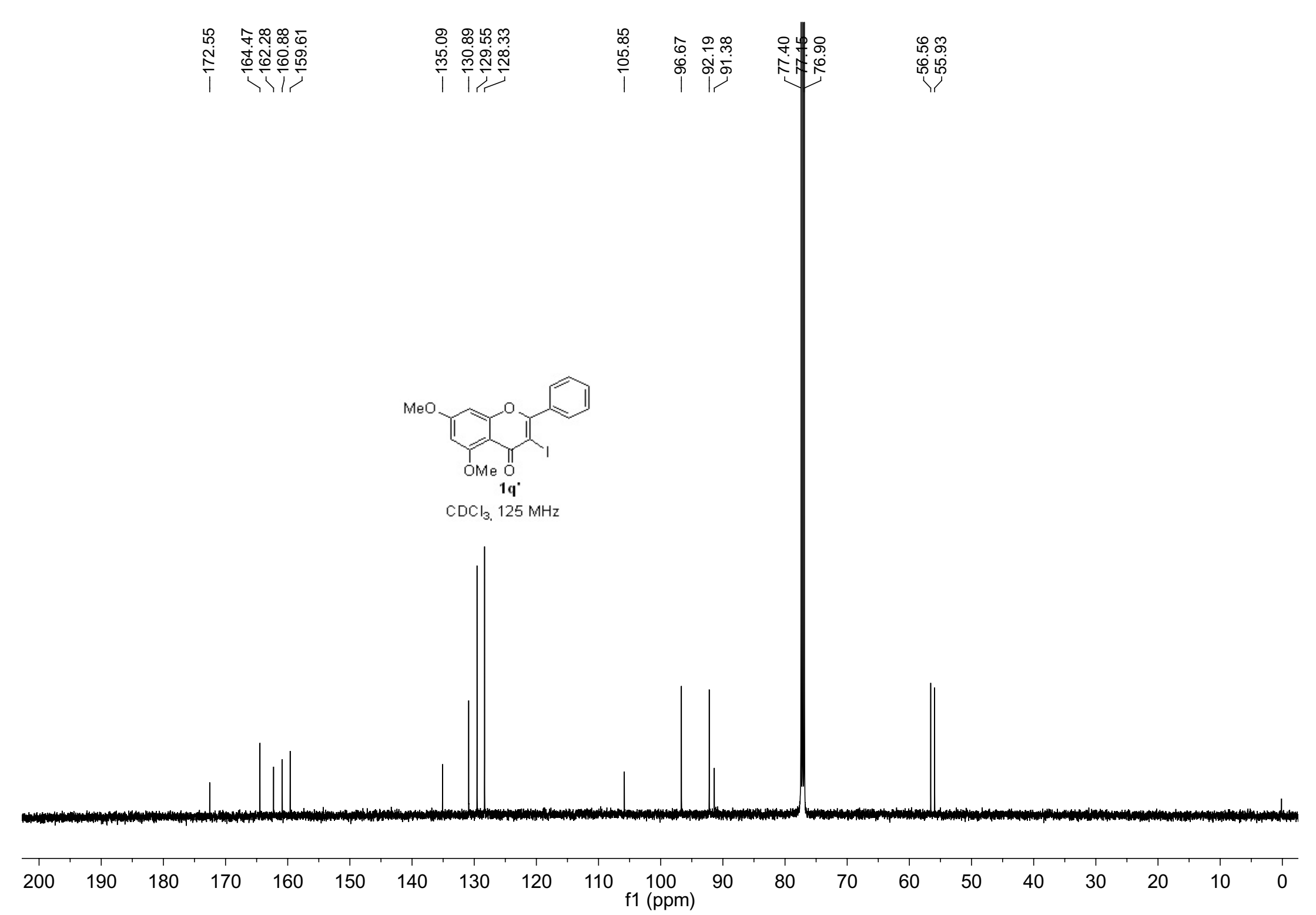
200 190 180 170 160 150 140 130 120 110 100 90 80 70 60 50 40 30 20 10 0

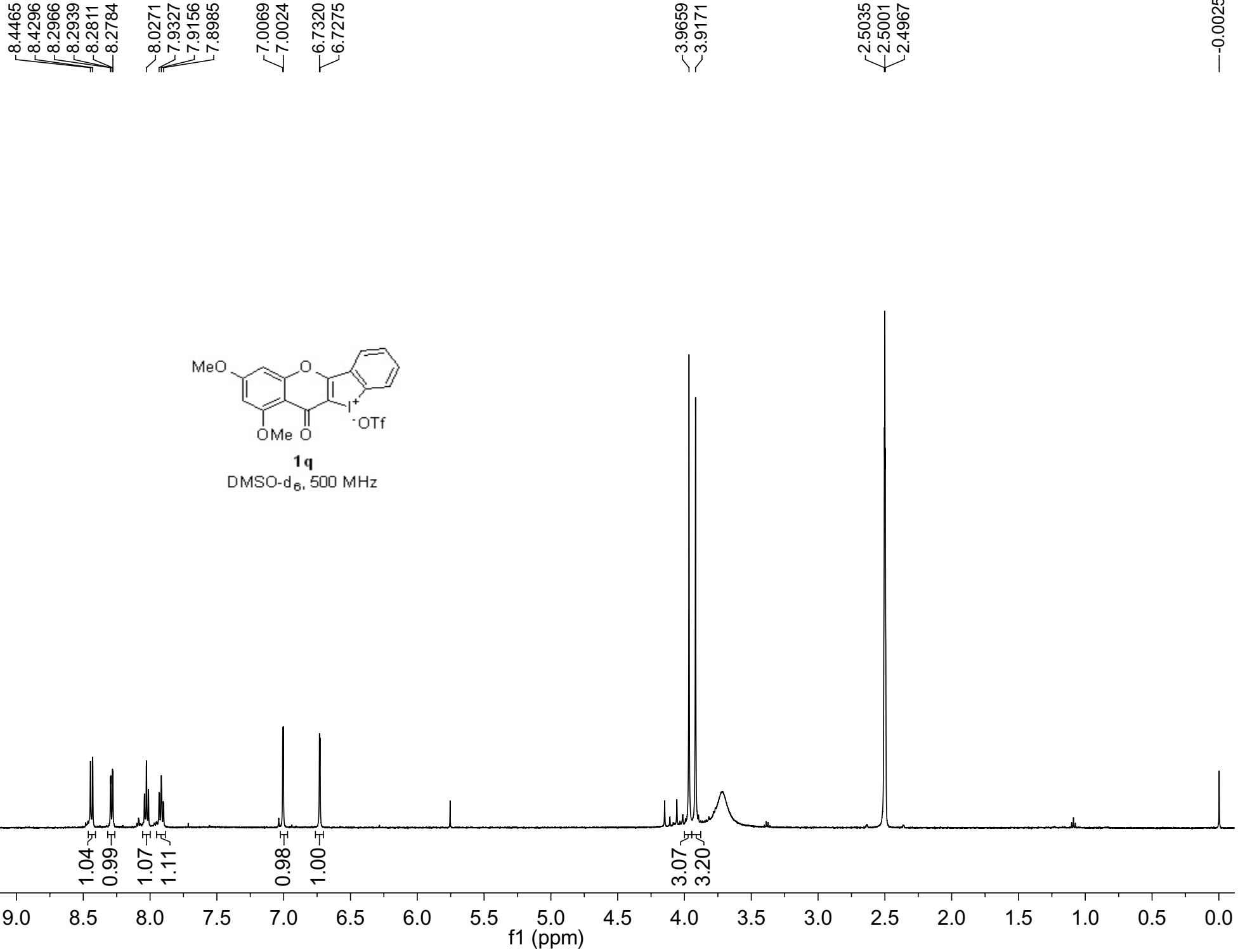
f1 (ppm)

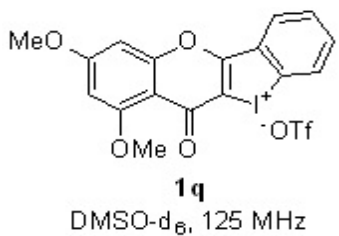


CDCl_3 , 500 MHz









—170.00

—164.97

—161.09

—160.56

—158.83

—135.35

—134.00

—131.46

—131.14

—128.39

—121.96

—119.35

—116.83

—111.48

—107.35

—97.43

—93.97

—119.40

—119.35

—116.83

—56.68

—56.35

—40.02

—39.94

—39.85

—39.69

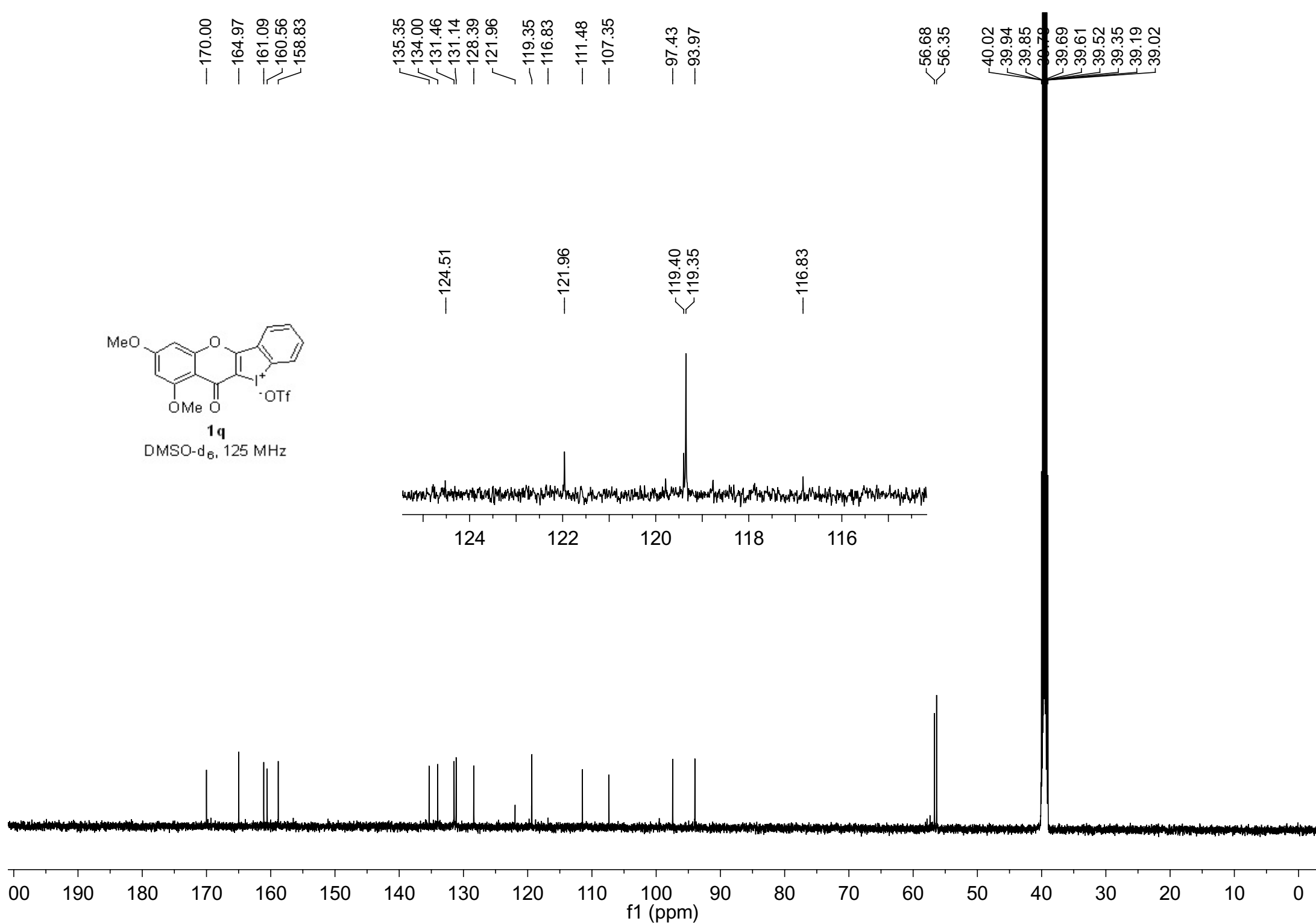
—39.61

—39.52

—39.35

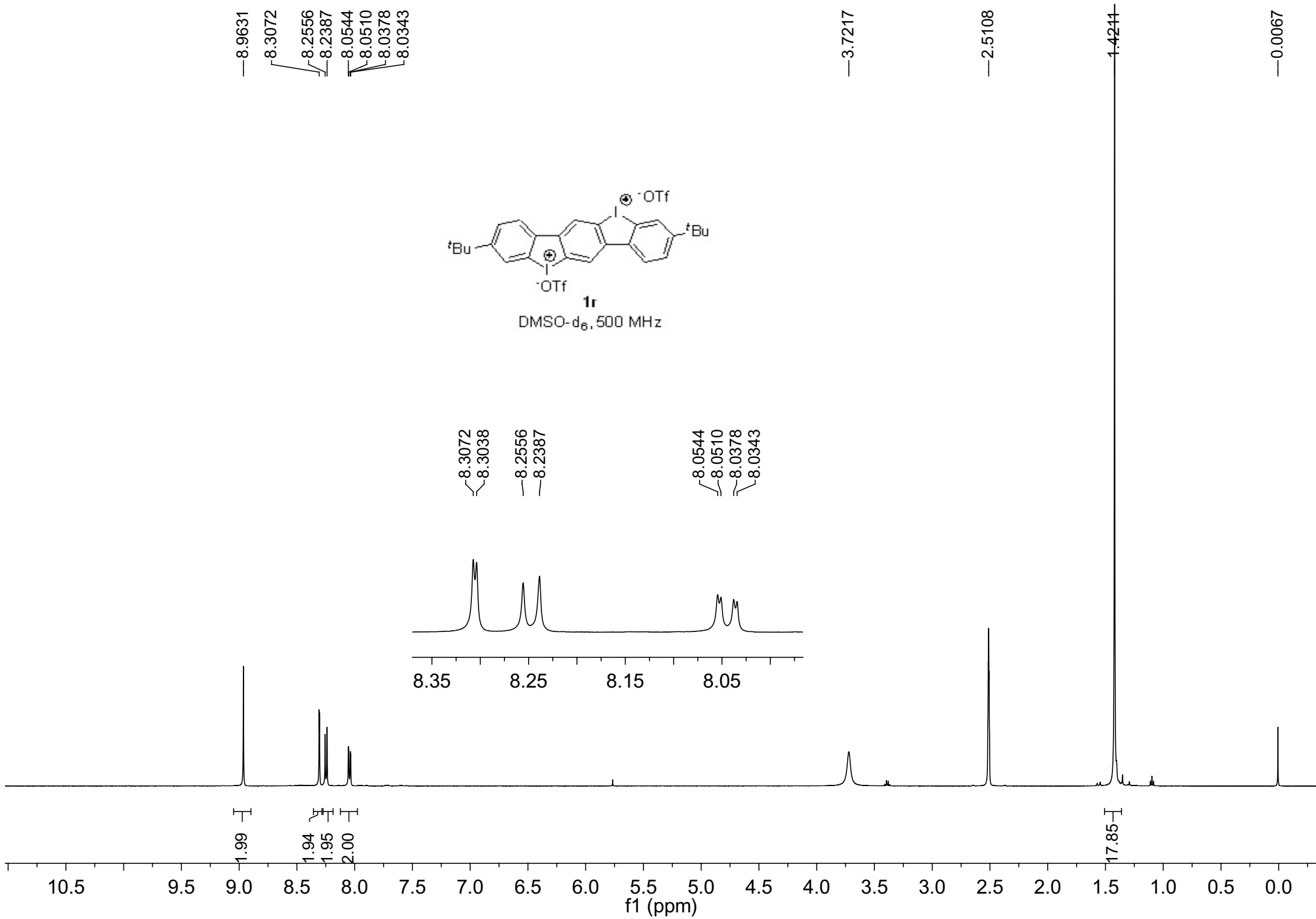
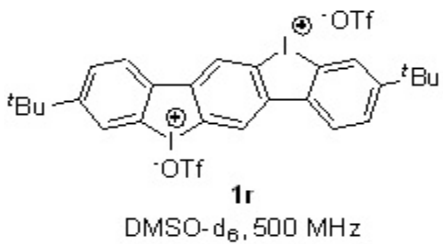
—39.19

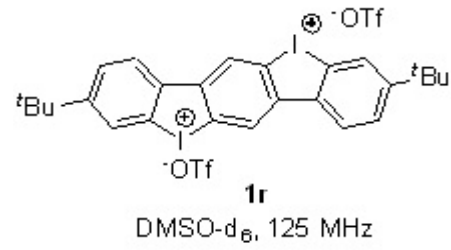
—39.02



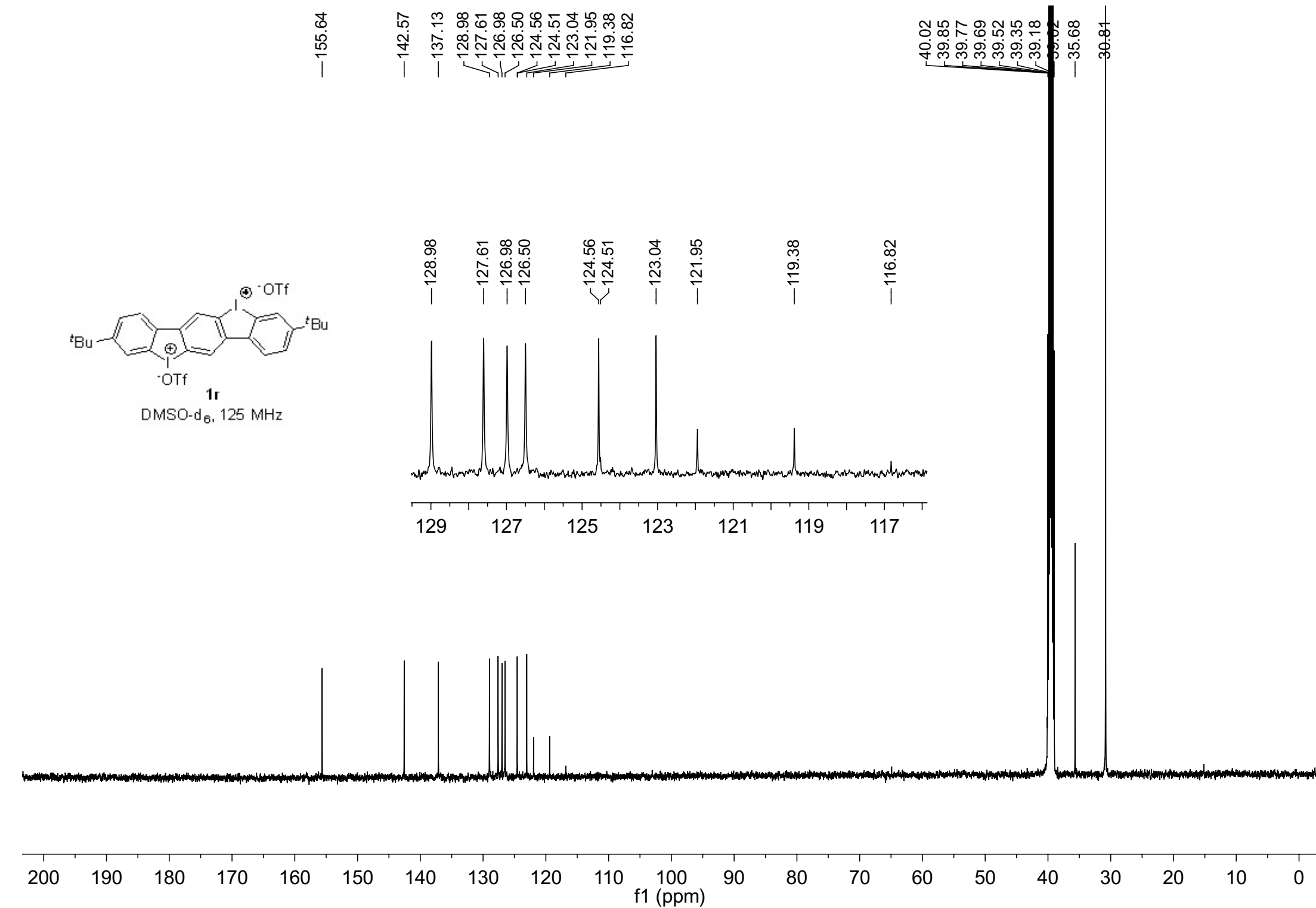
-8.9631
-8.3072
-8.2556
-8.2387
-8.0544
-8.0510
-8.0378
-8.0343

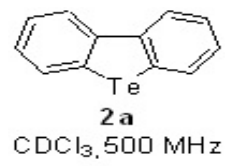
-3.7217
-2.5108
-1.4244
-0.0067



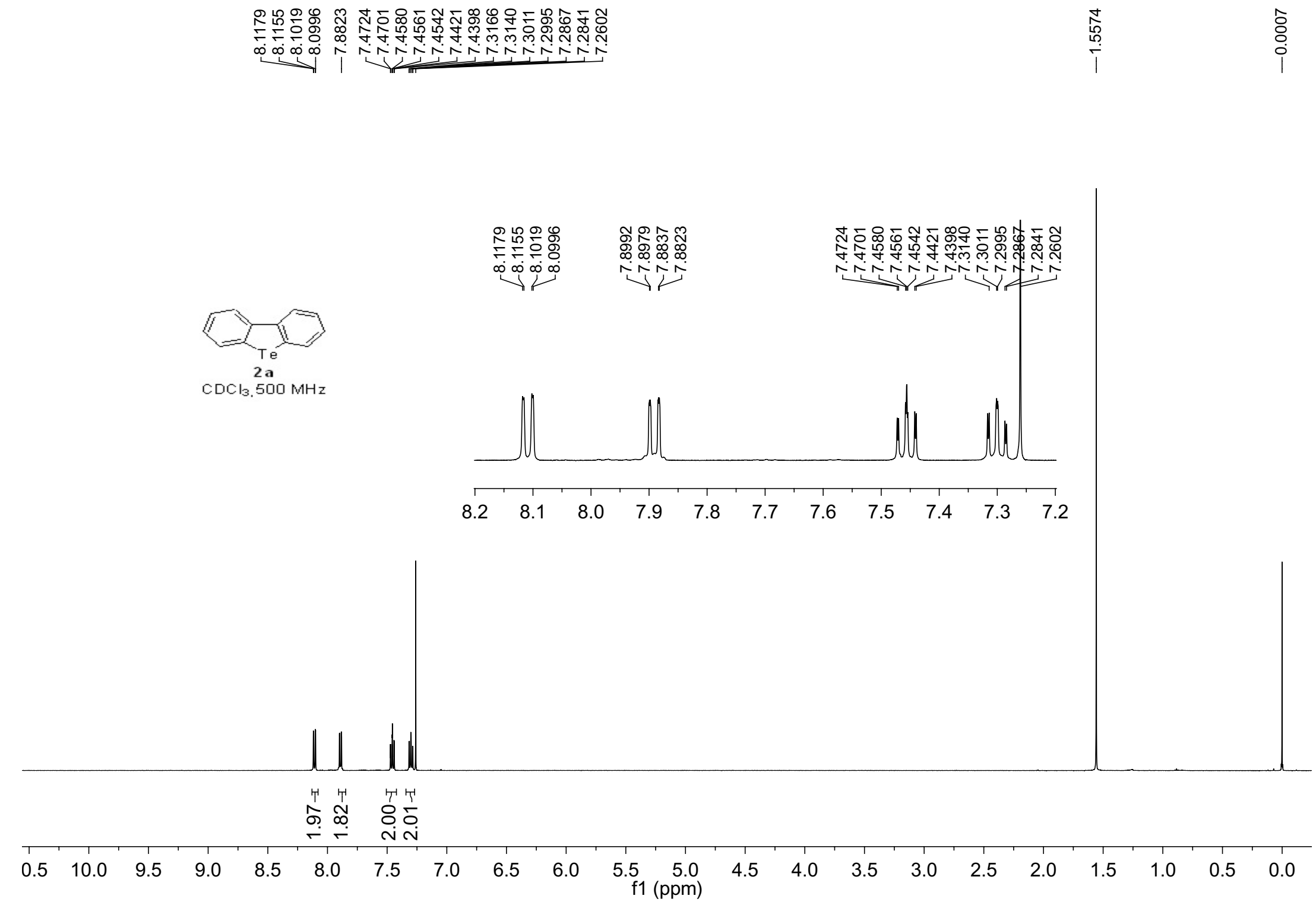


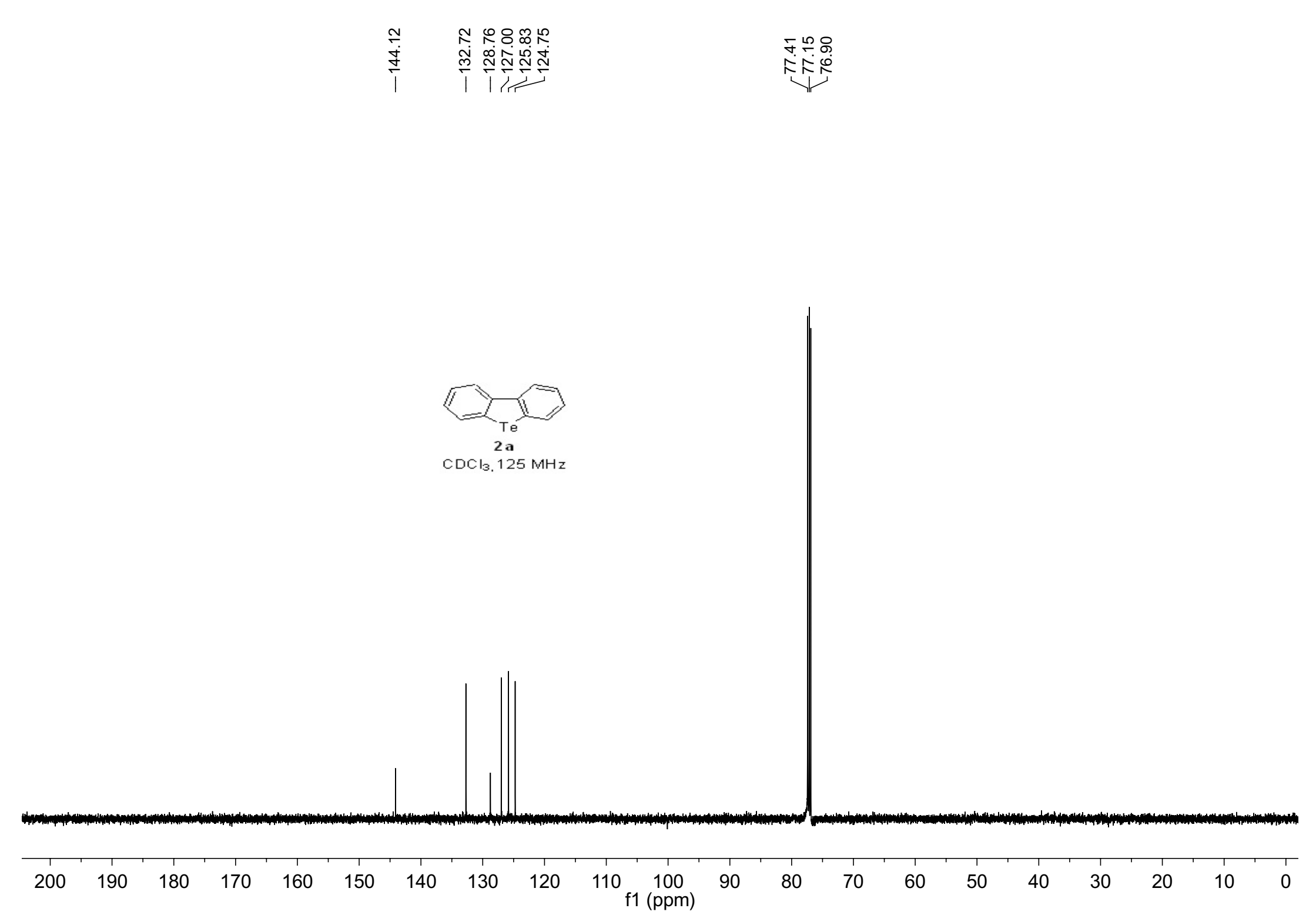
DMSO- d_6 , 125 MHz

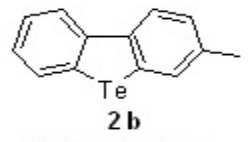




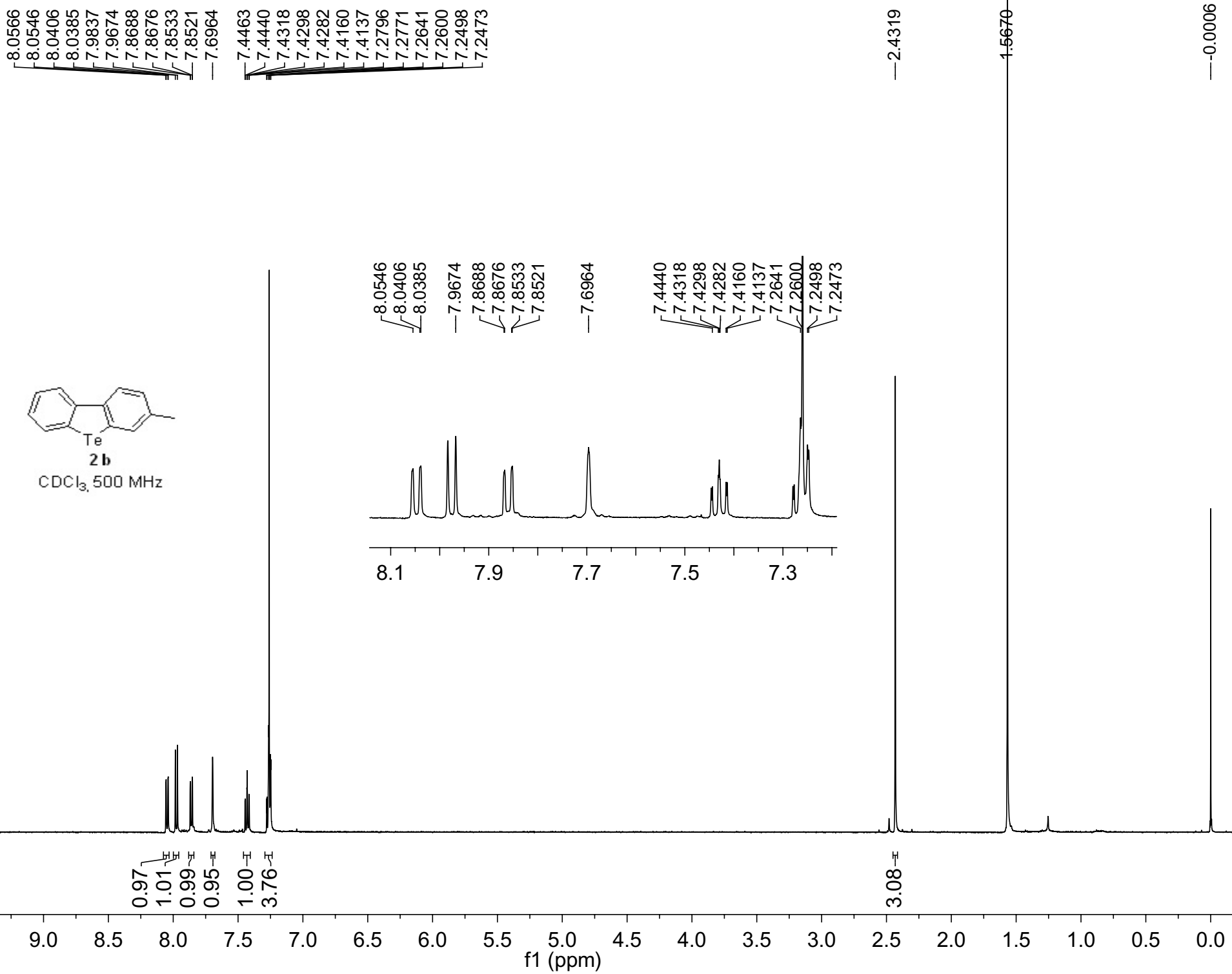
$\text{CDCl}_3, 500 \text{ MHz}$

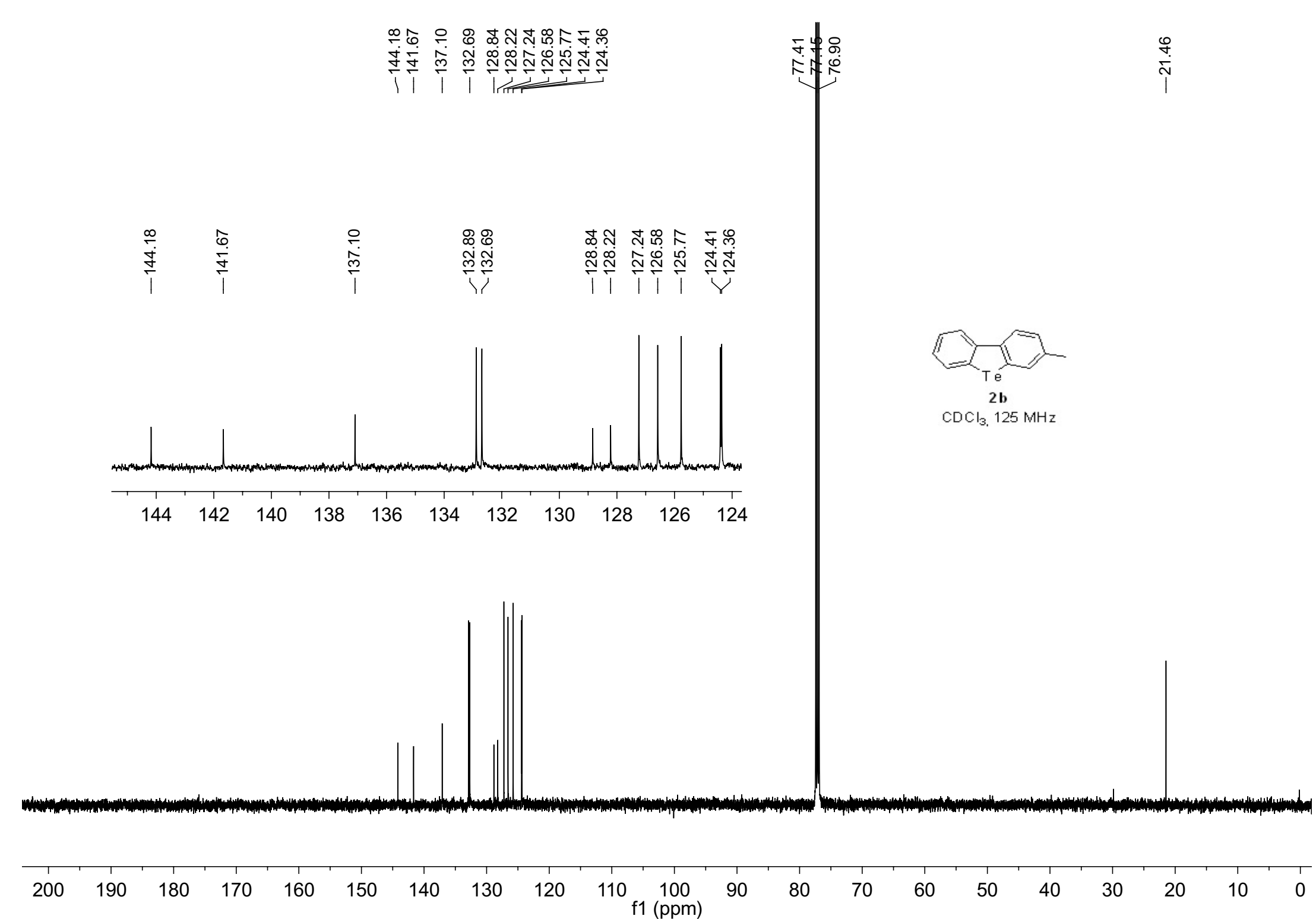


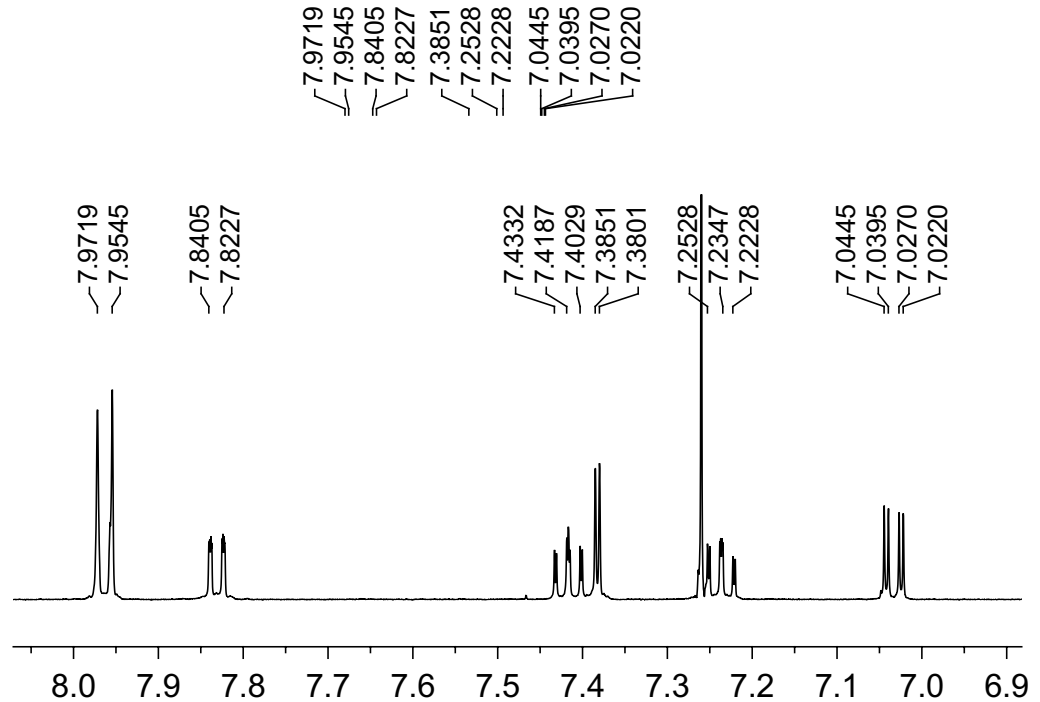




$\text{CDCl}_3, 500 \text{ MHz}$

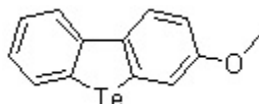
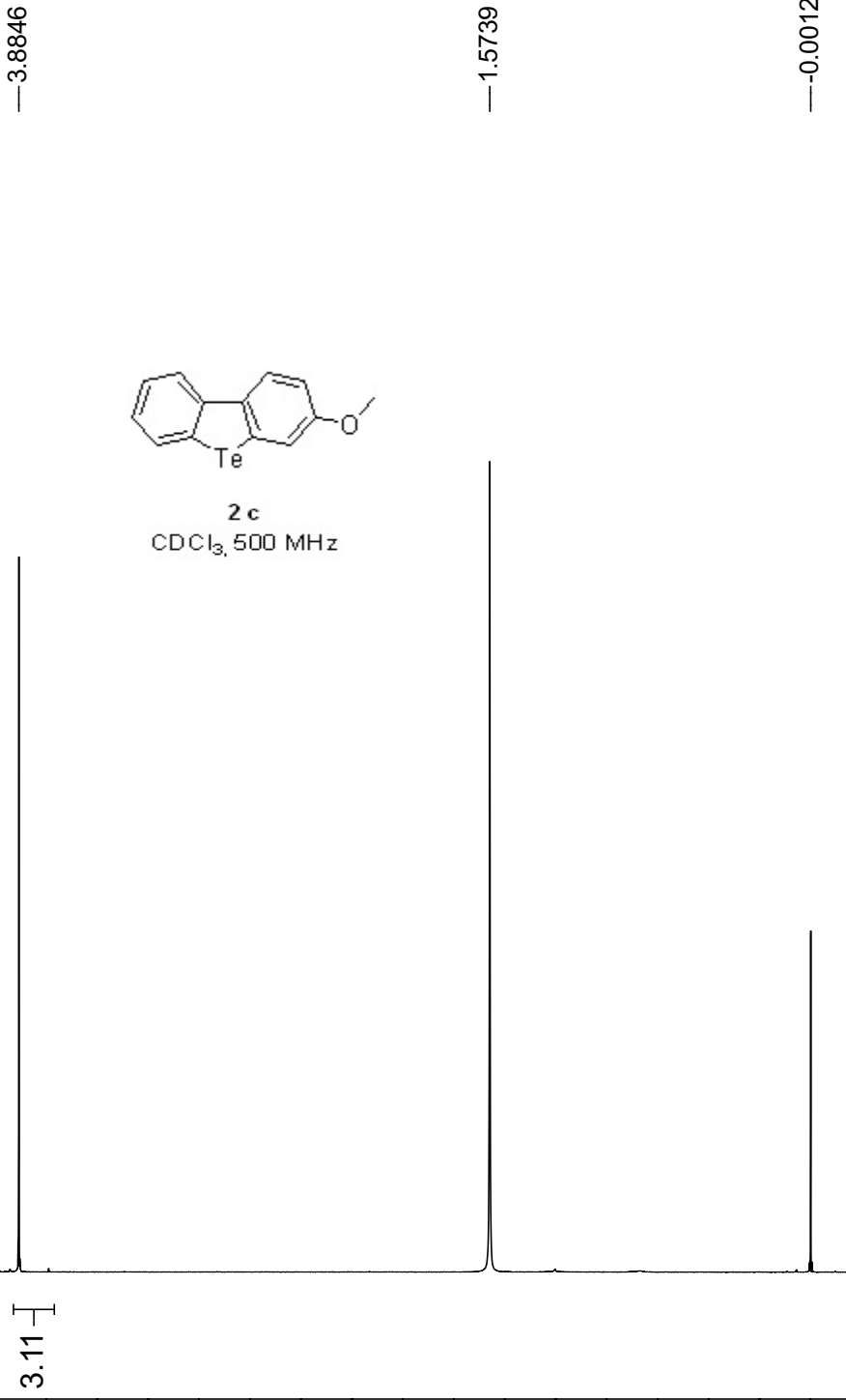




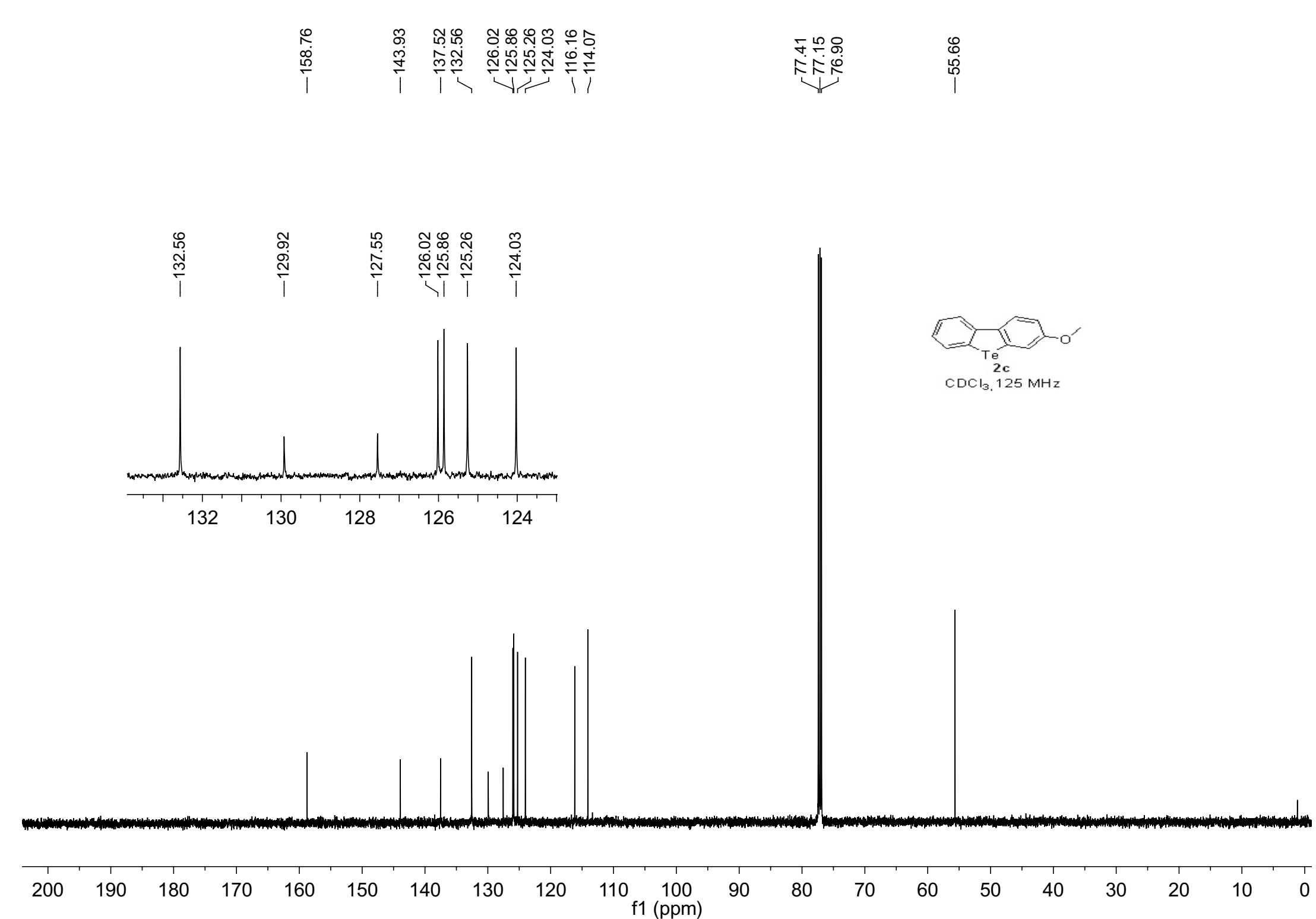


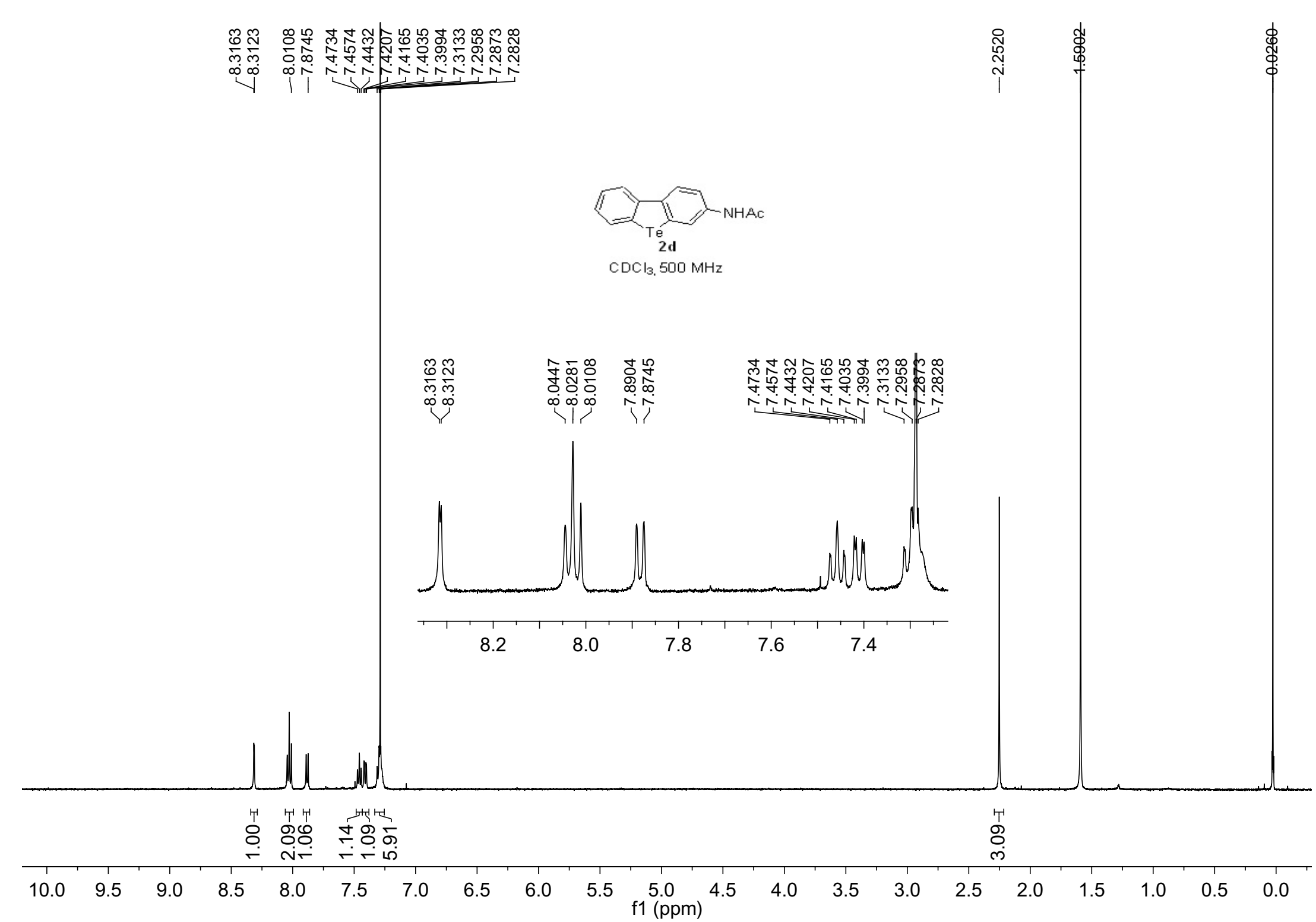
8.0 7.9 7.8 7.7 7.6 7.5 7.4 7.3 7.2 7.1 7.0 6.9

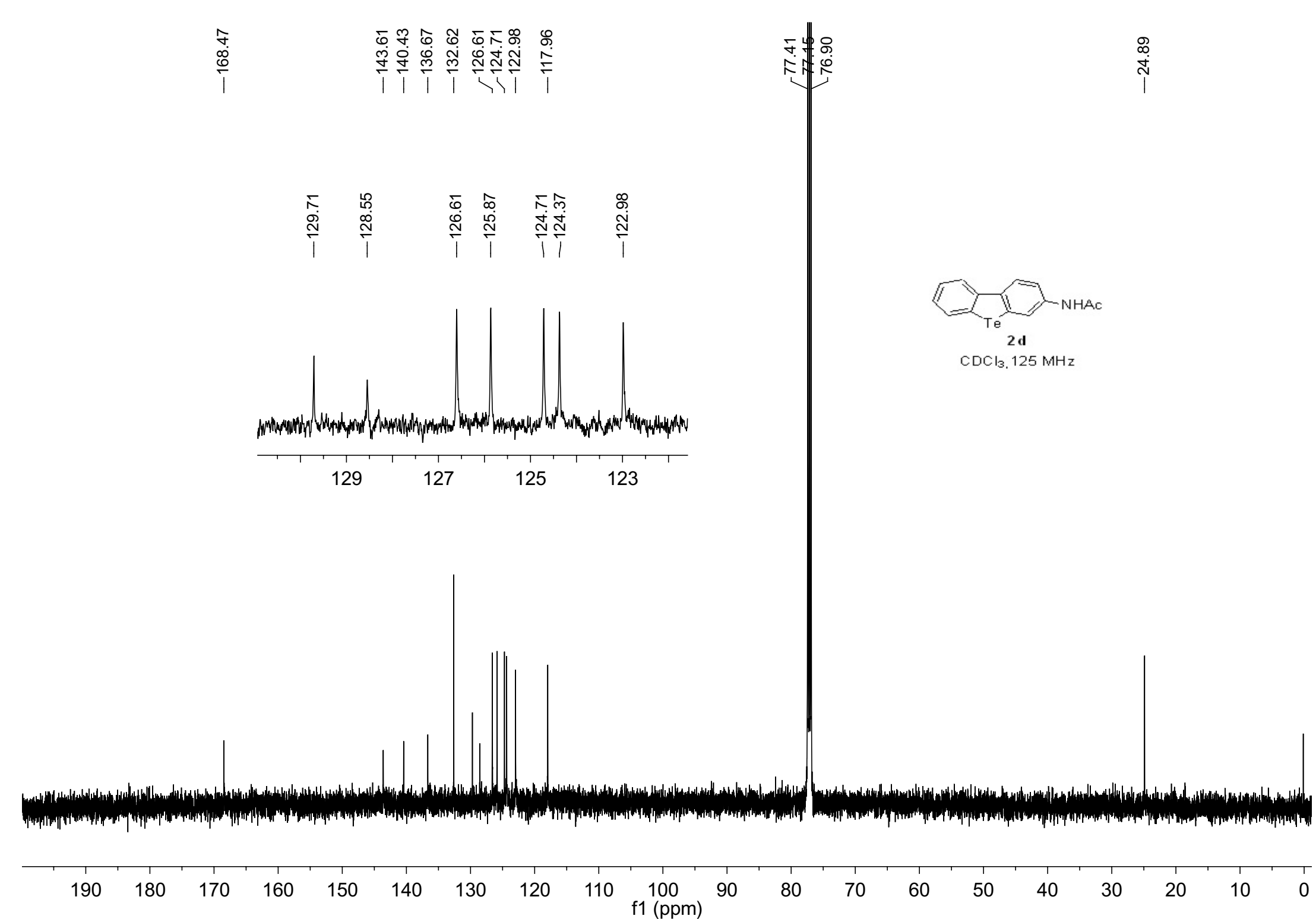
1.98
0.95
1.00
0.94
0.98
0.99

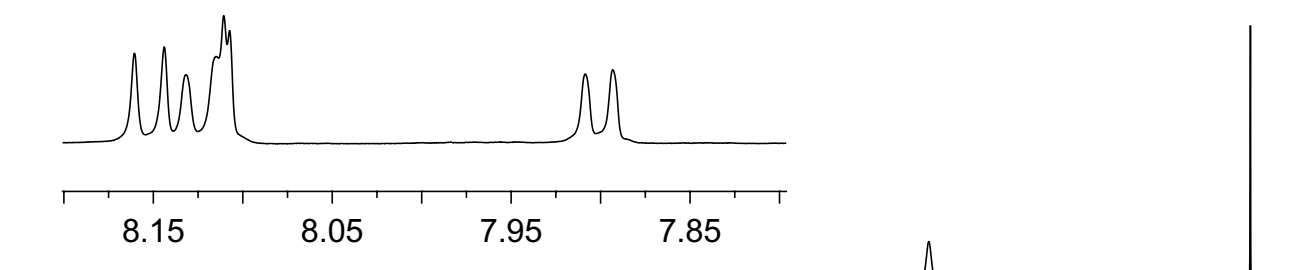
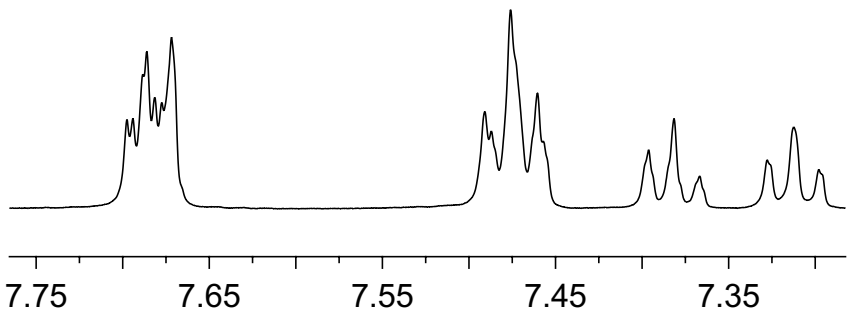


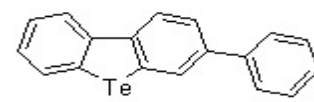
2c
 $\text{CDCl}_3, 500 \text{ MHz}$



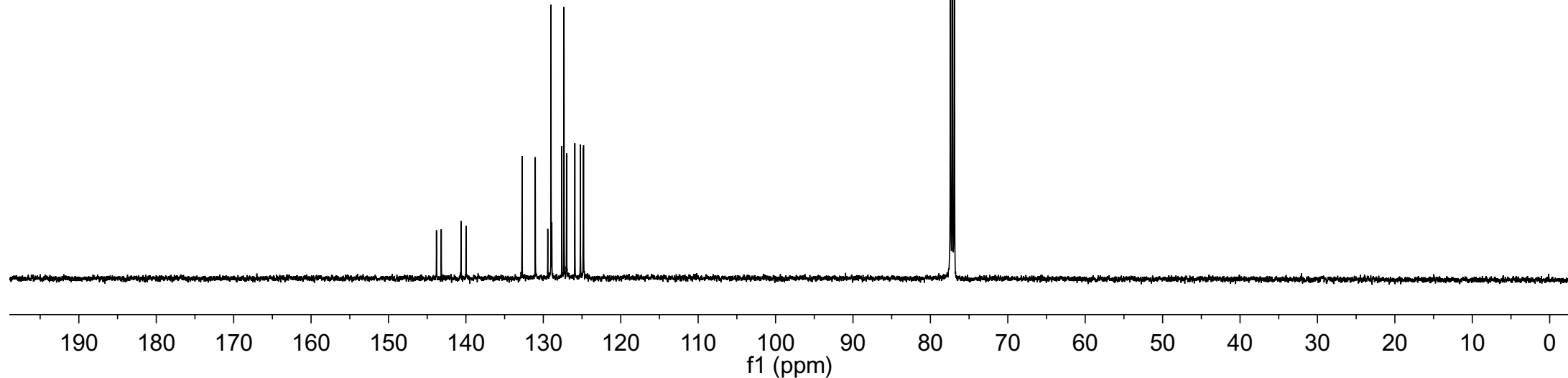
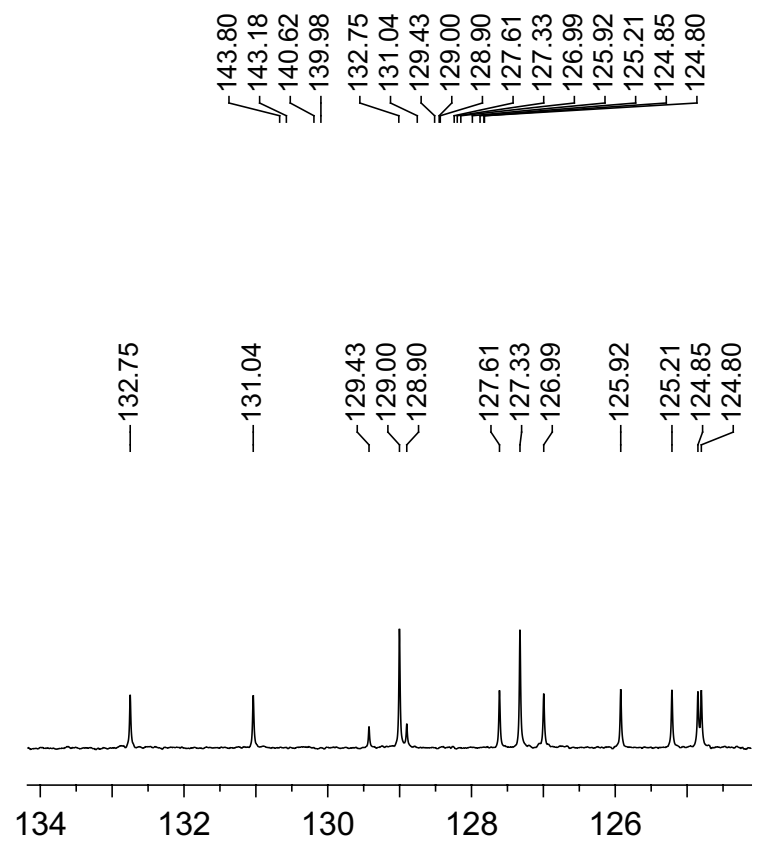


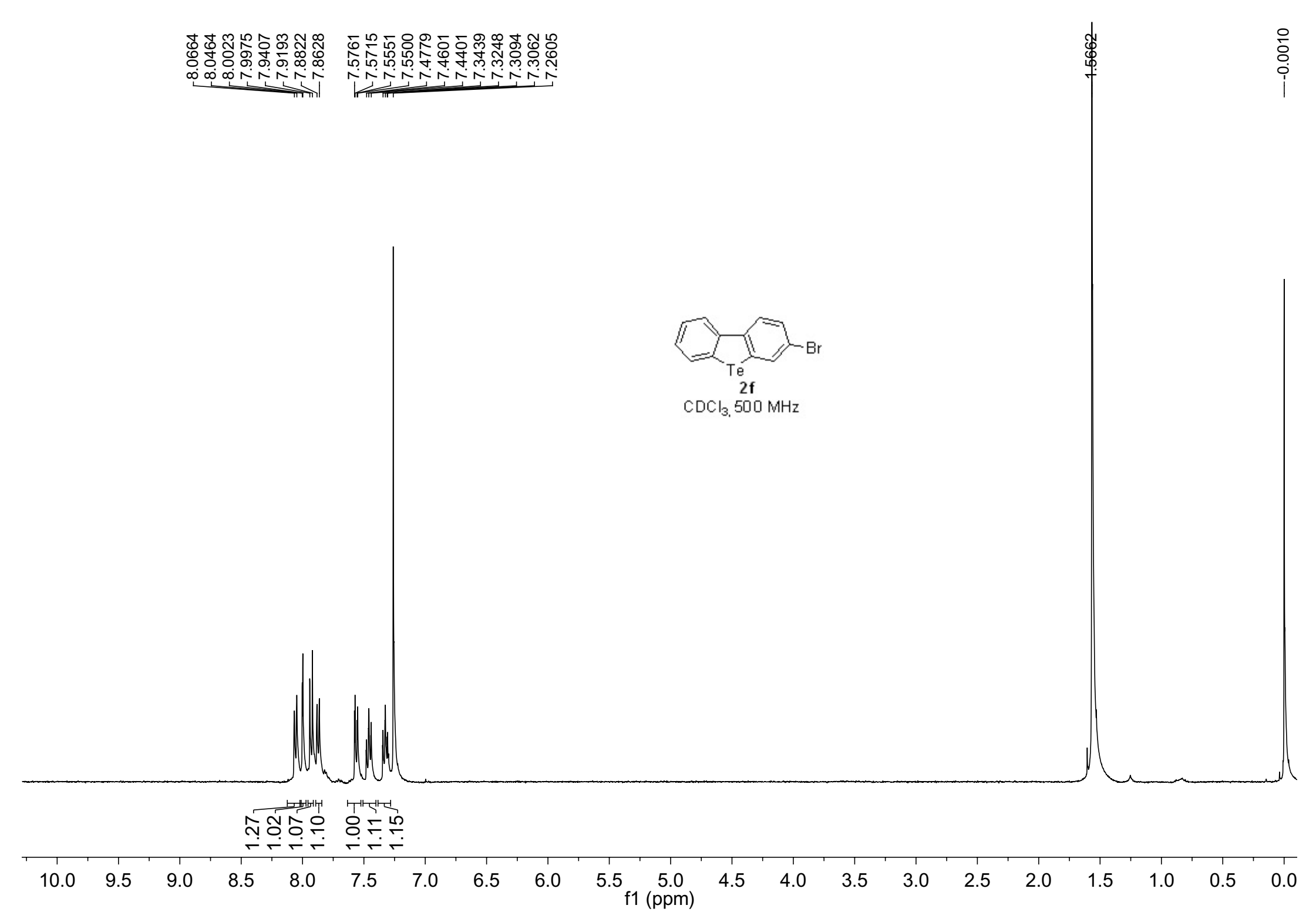


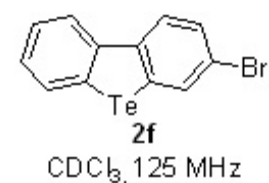
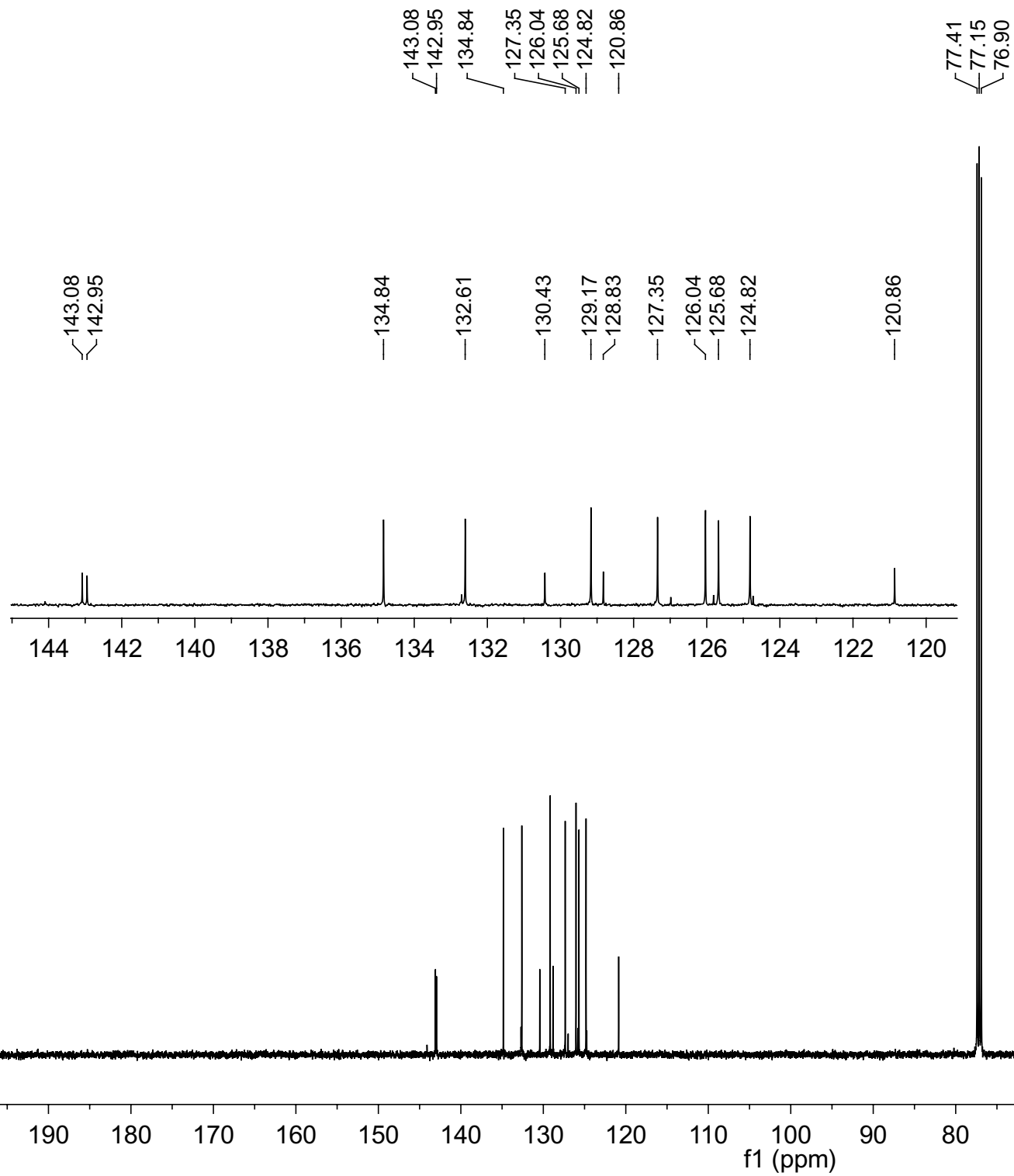


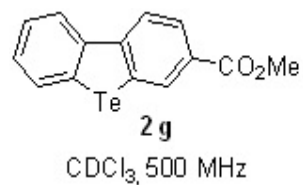
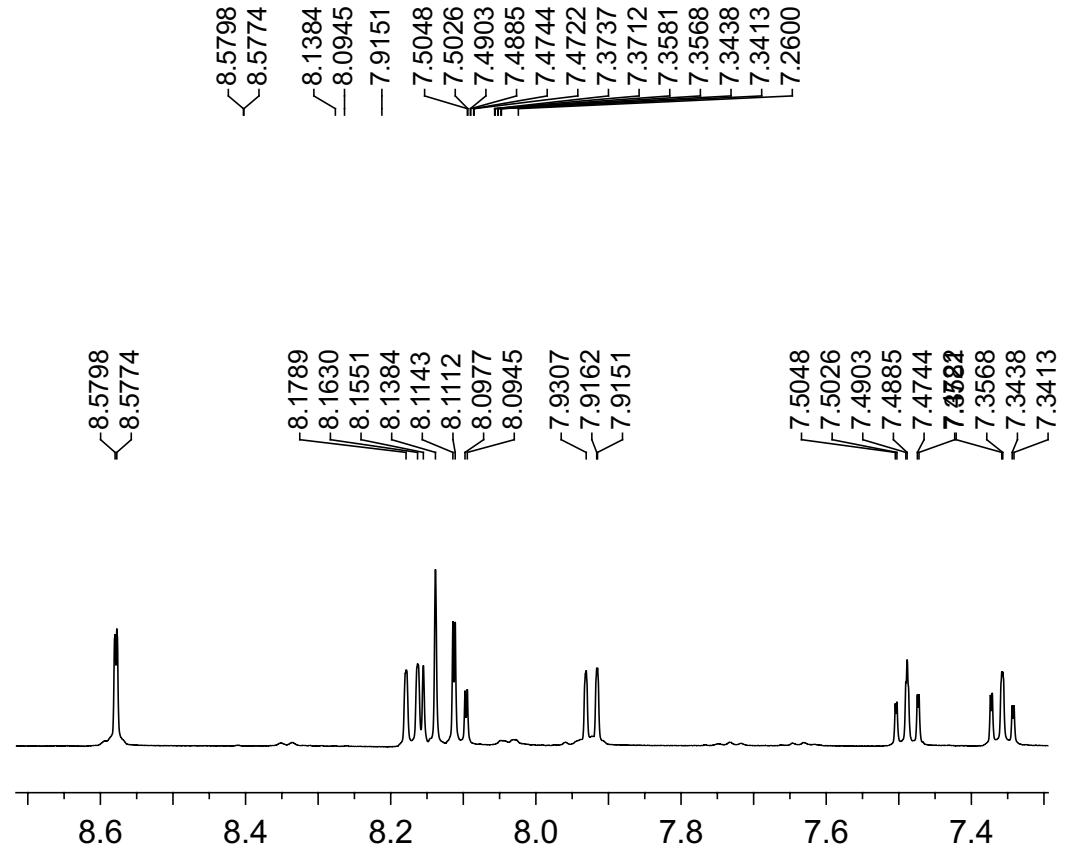


CDCl₃, 125 MHz

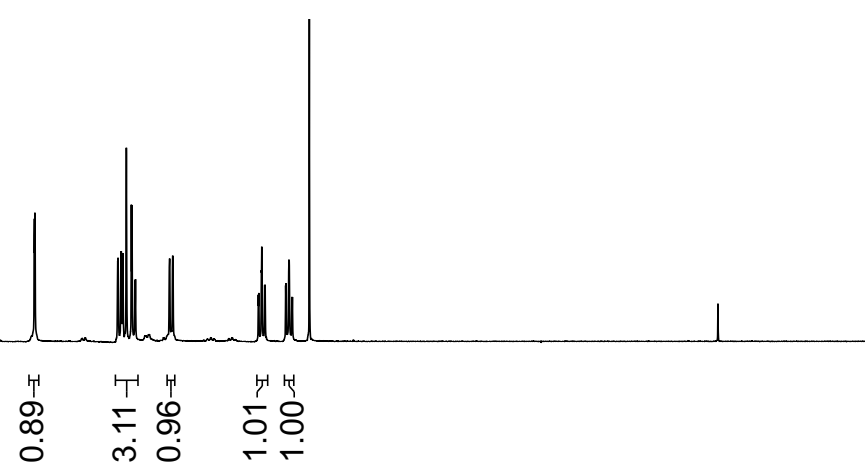


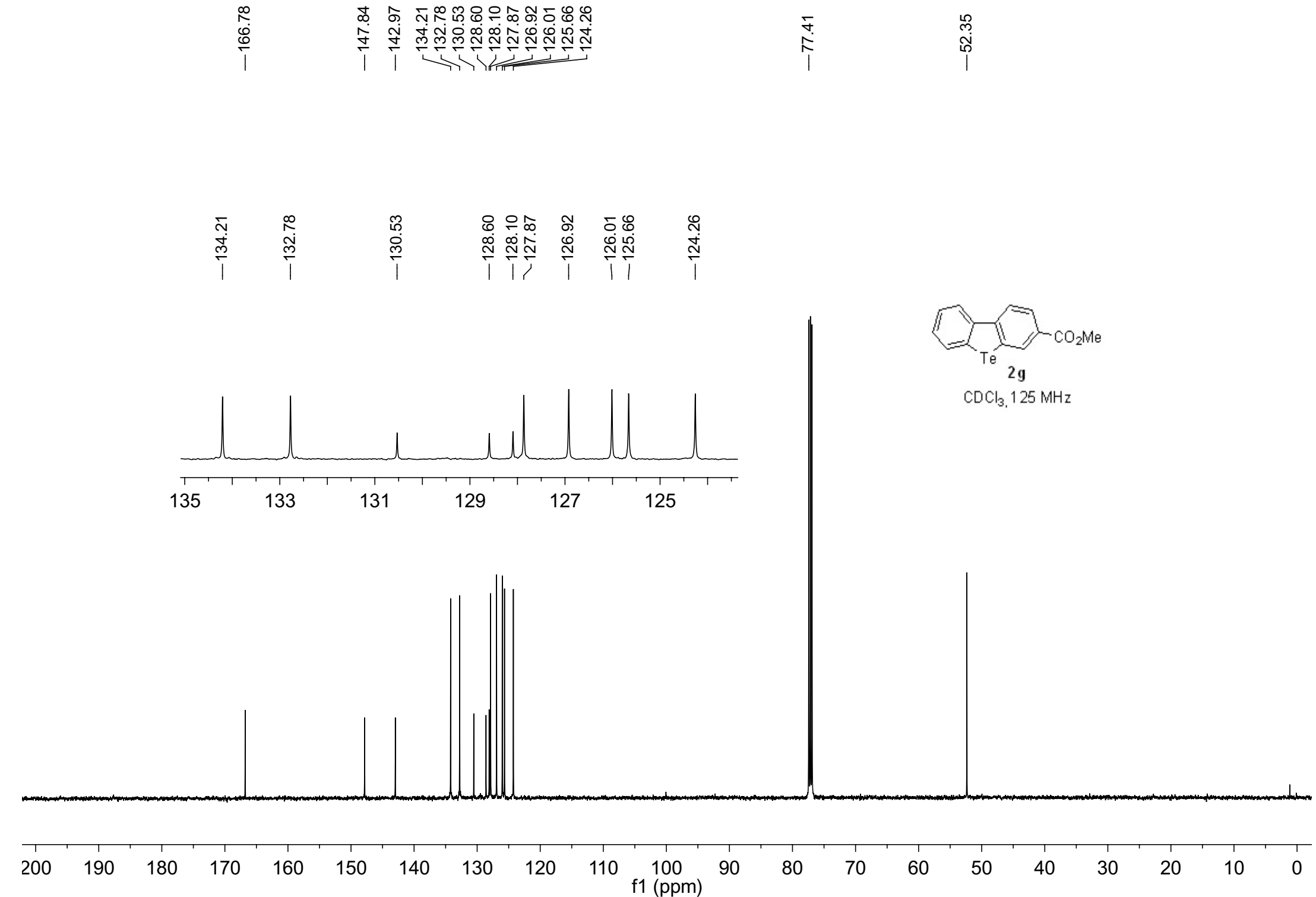


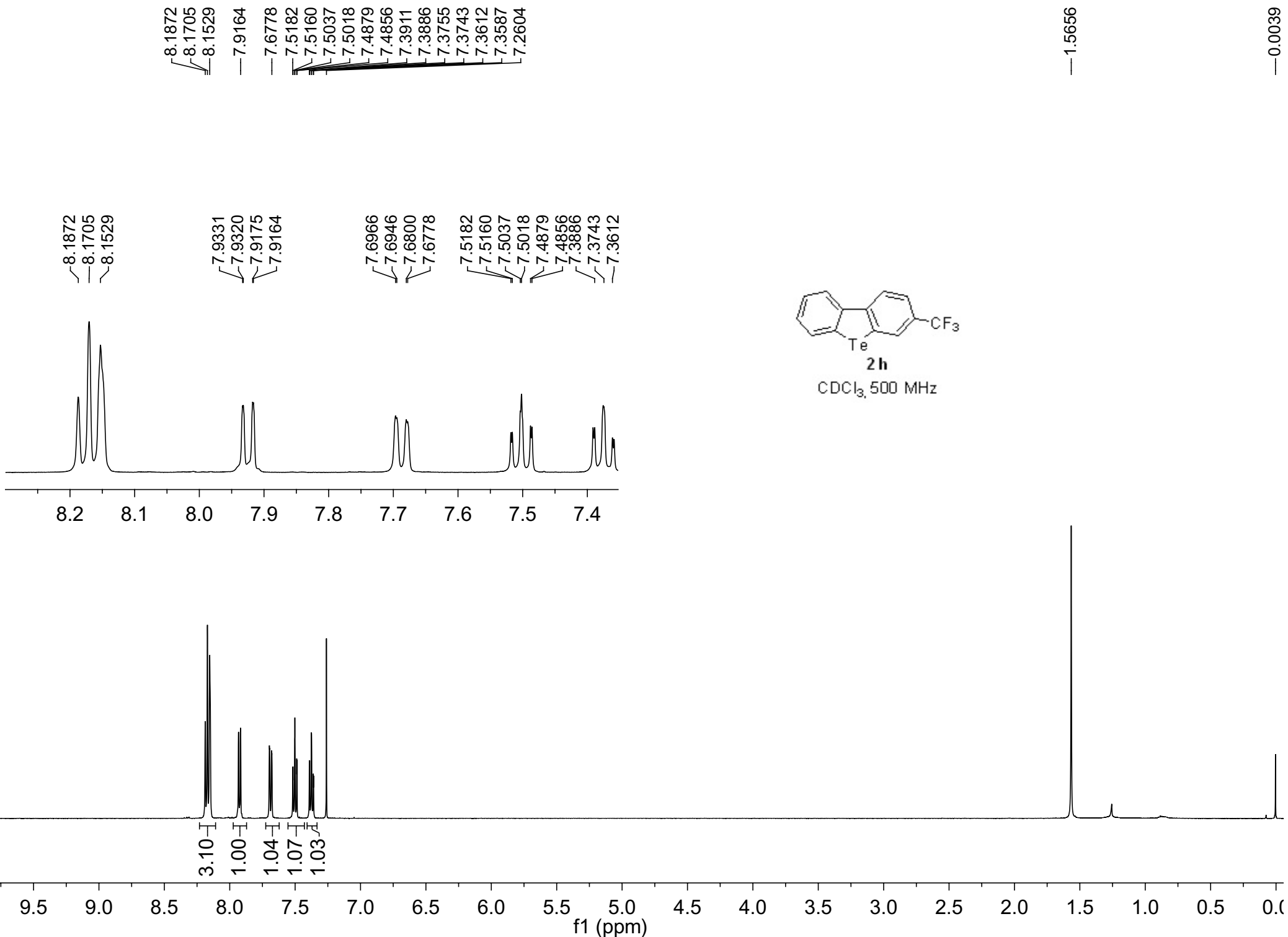




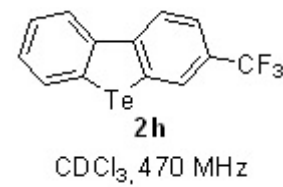
$\text{CDCl}_3, 500 \text{ MHz}$





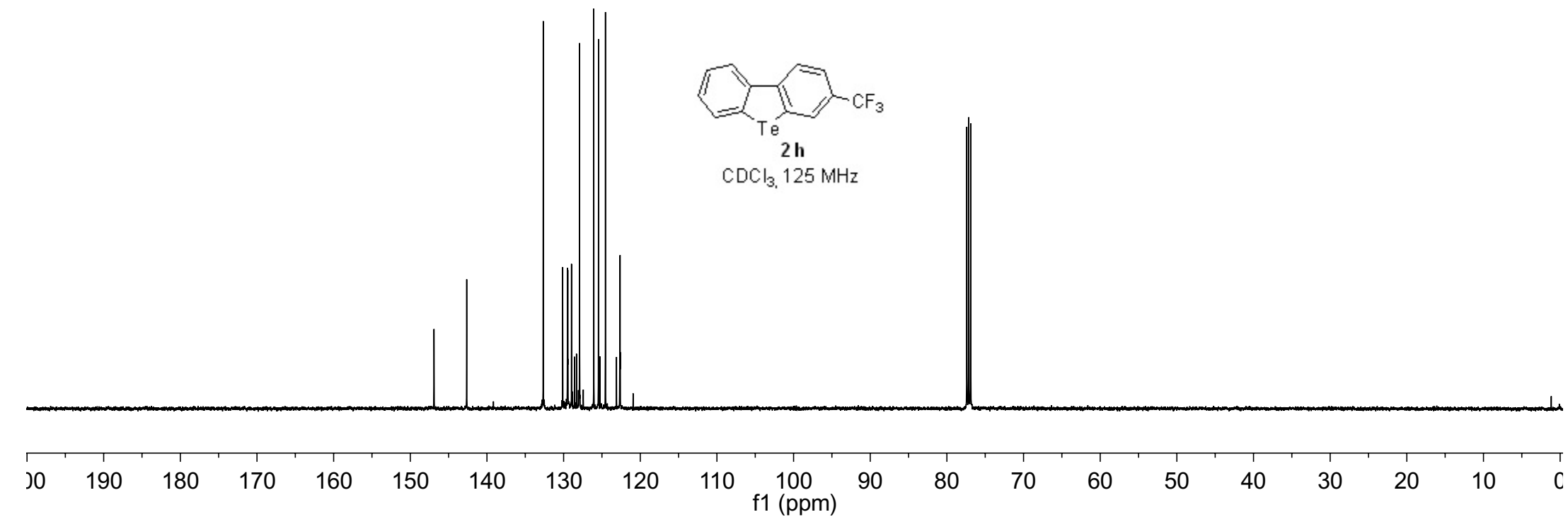
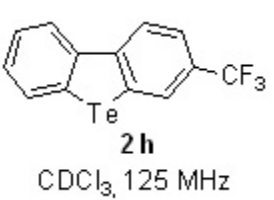
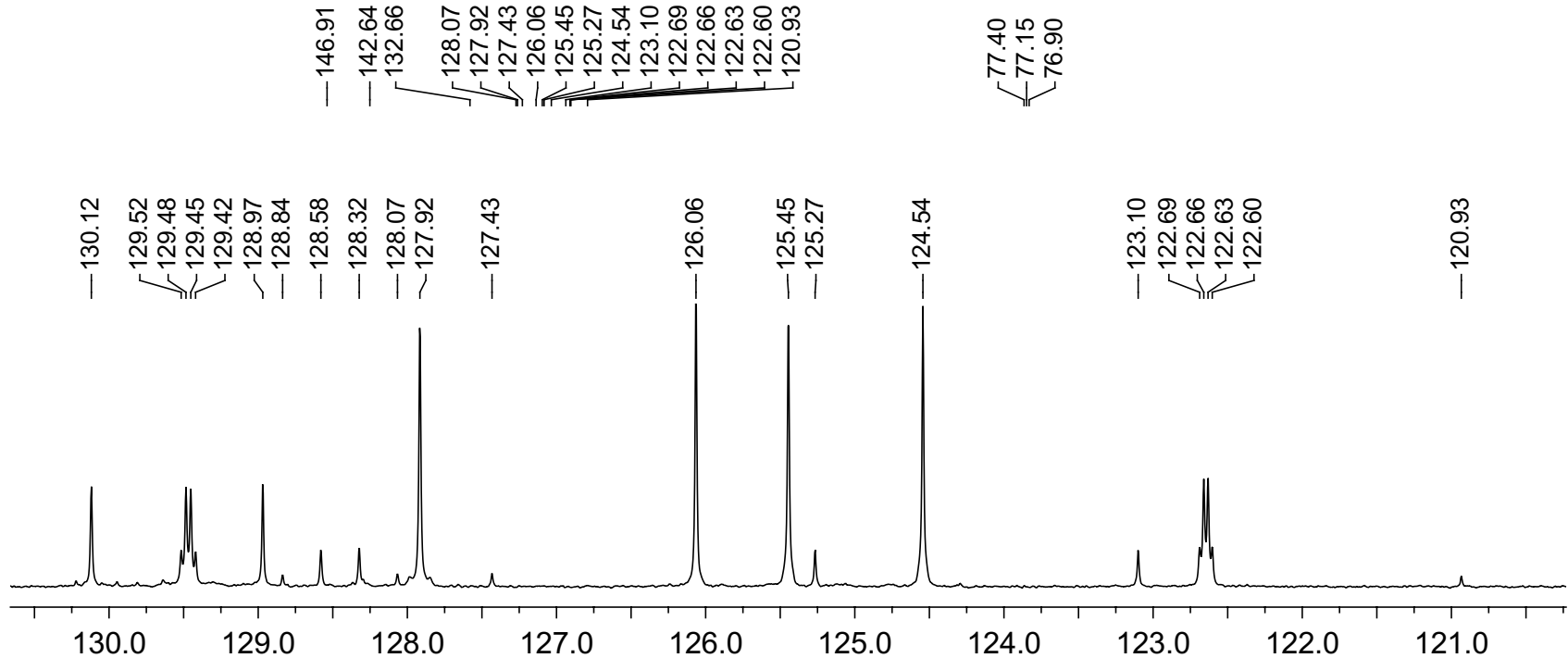


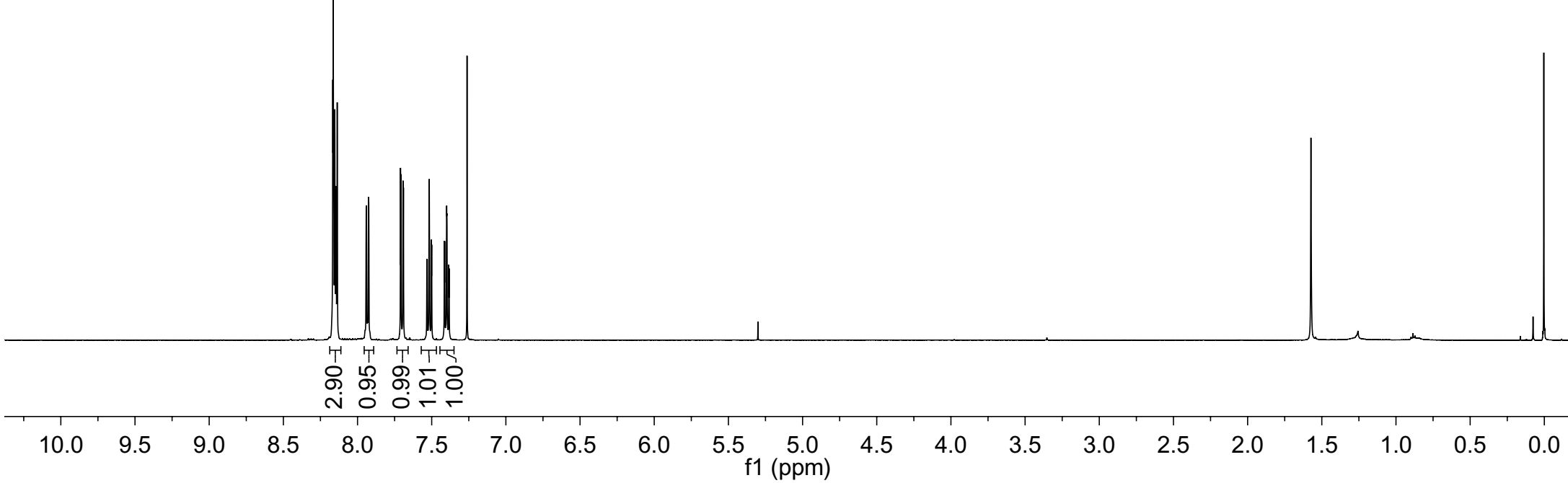
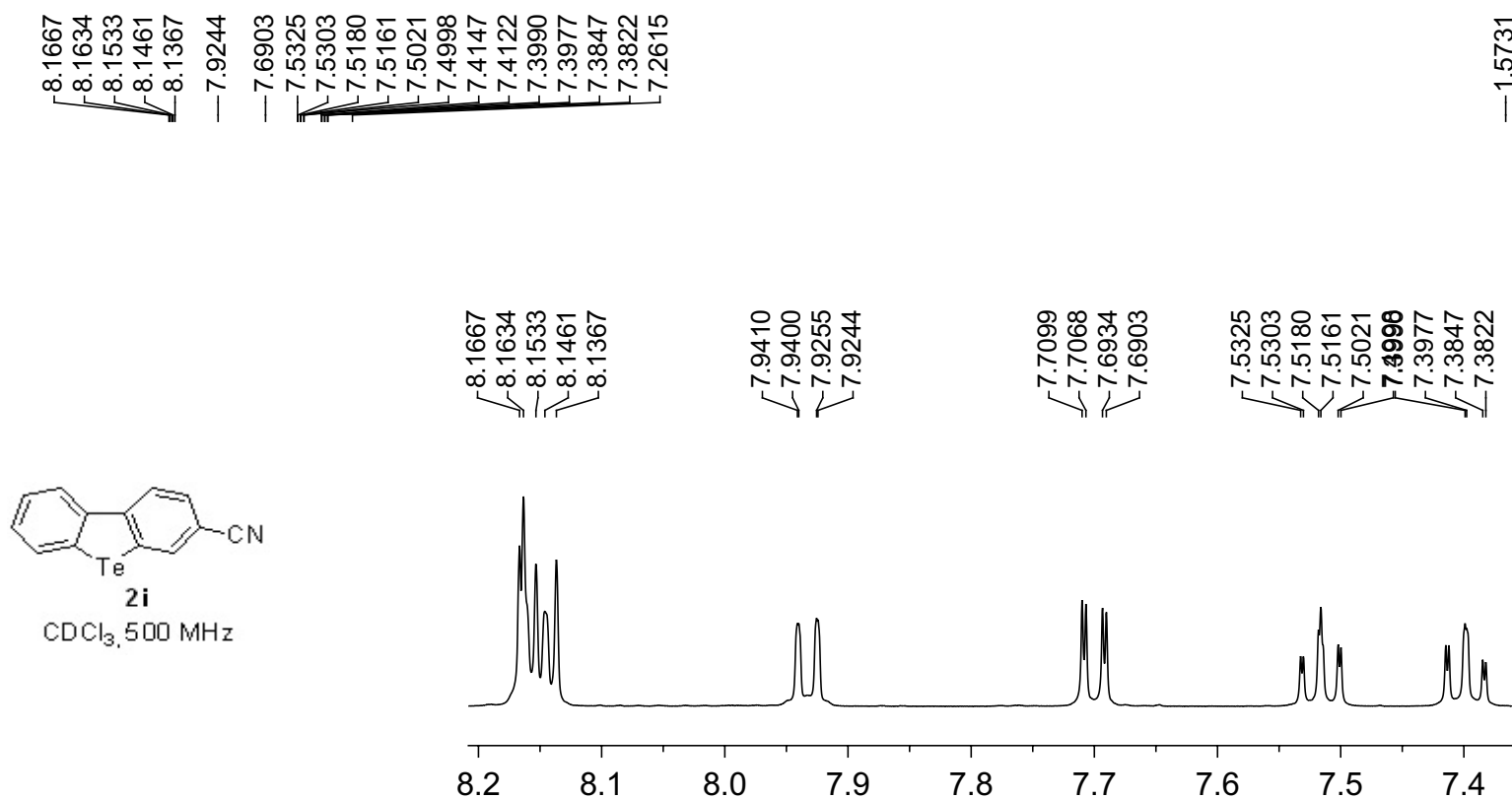
-61.75



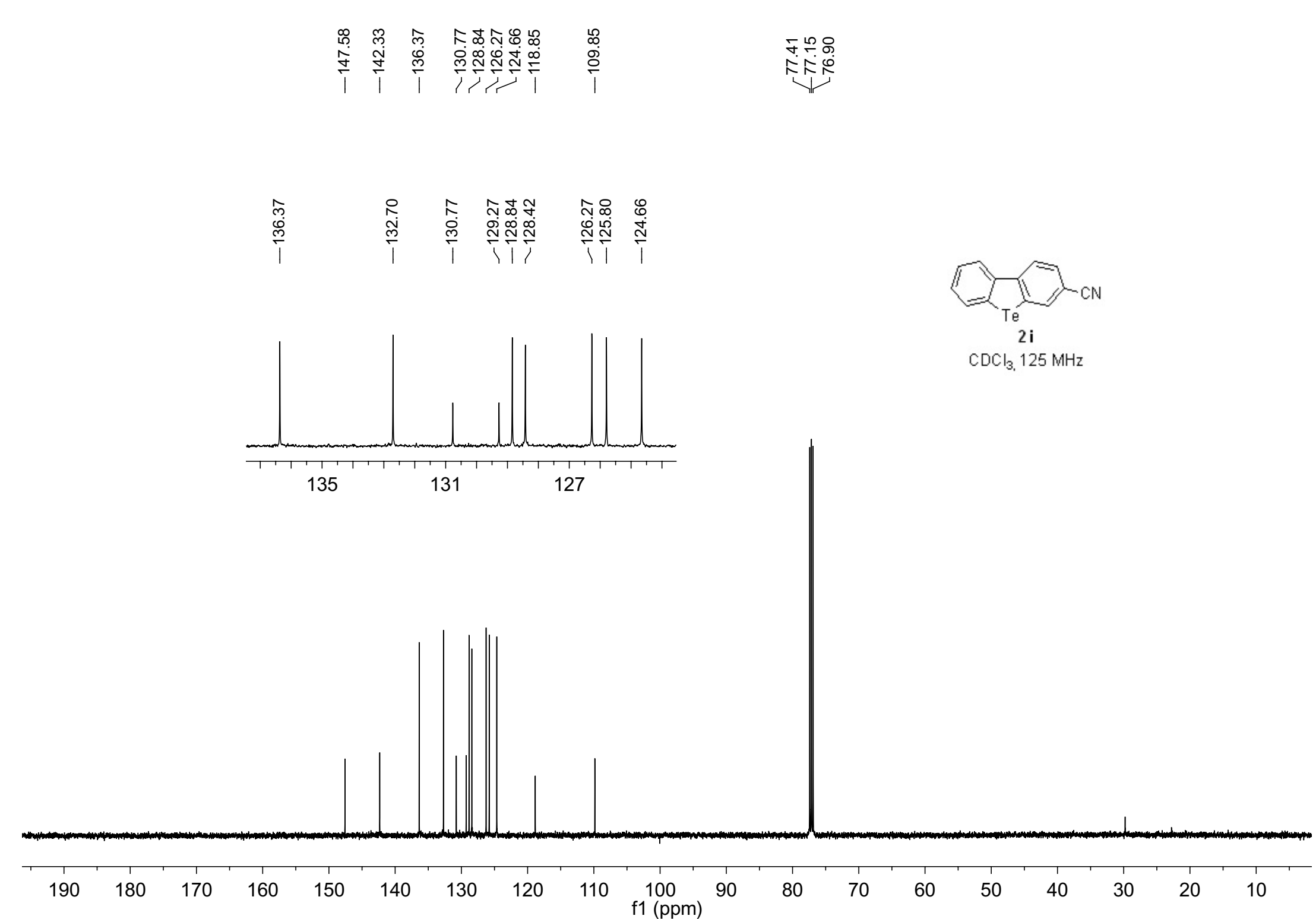
$\text{CDCl}_3, 470 \text{ MHz}$

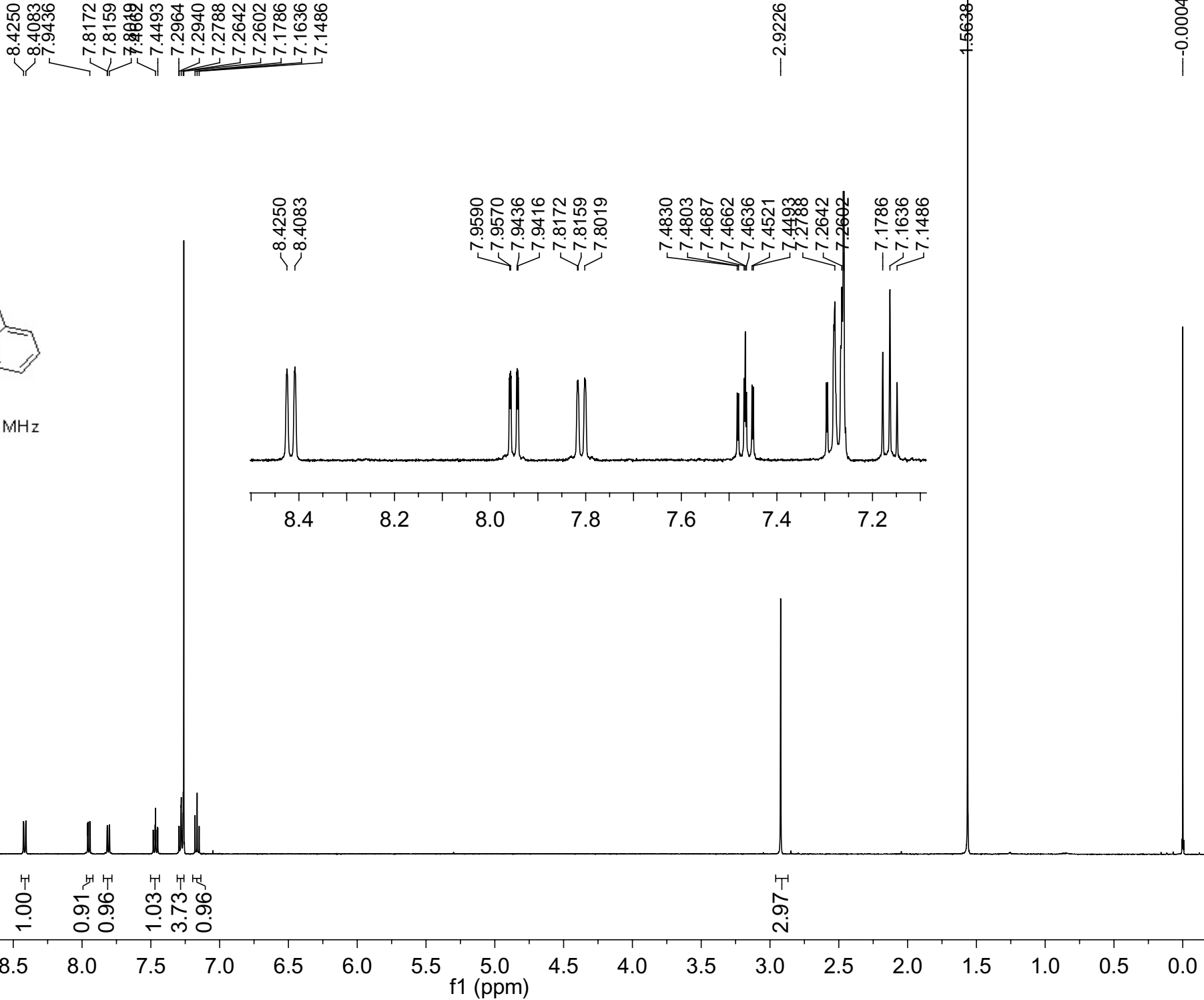
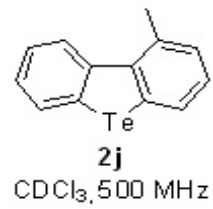
0 -10 -20 -30 -40 -50 -60 -70 -80 -90 -100 -110 -120 -130 -140 -150 -160 -170 -180 -190 -200
f1 (ppm)

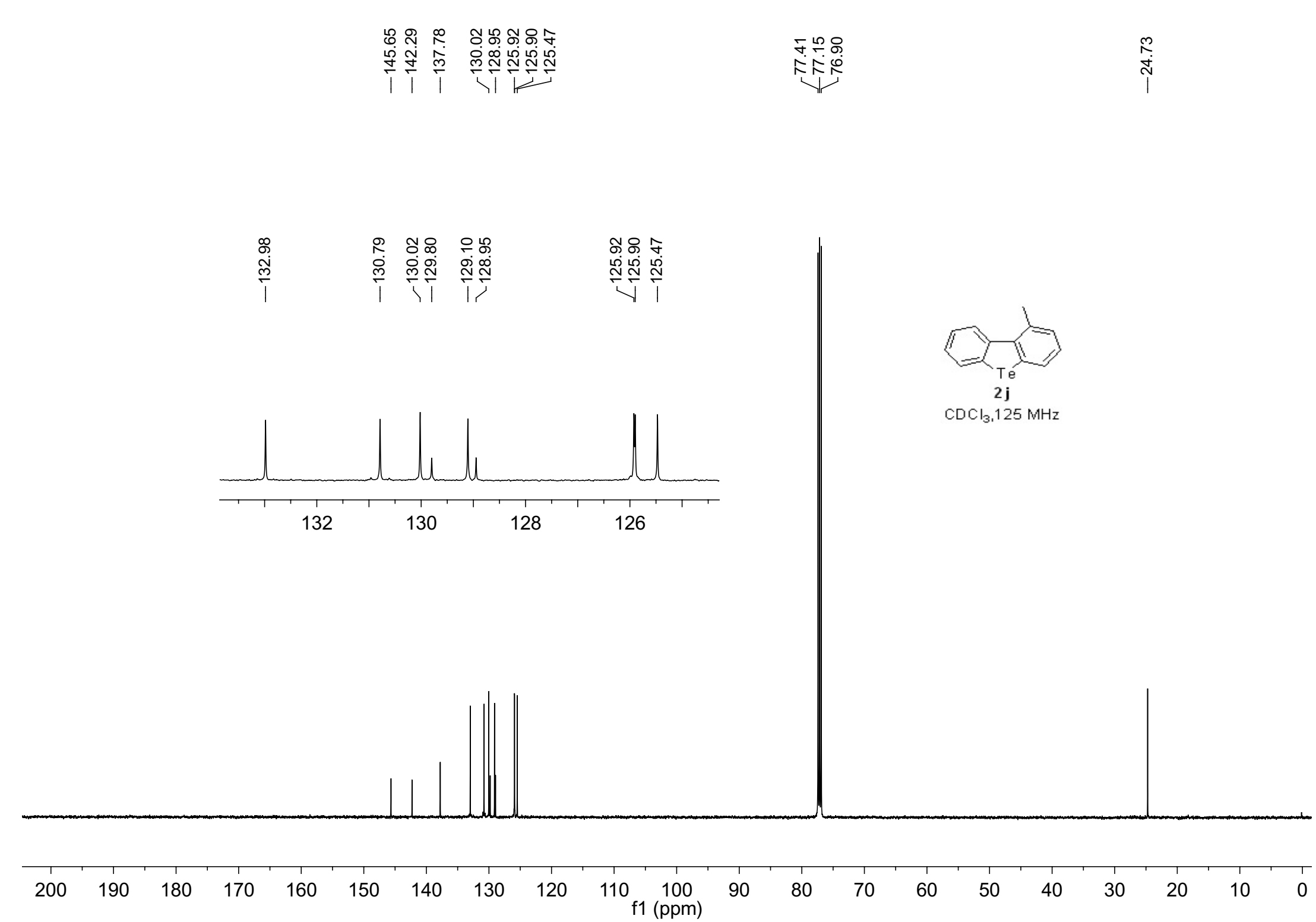


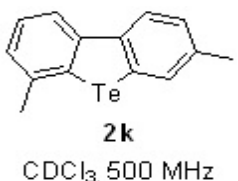


-0.0031



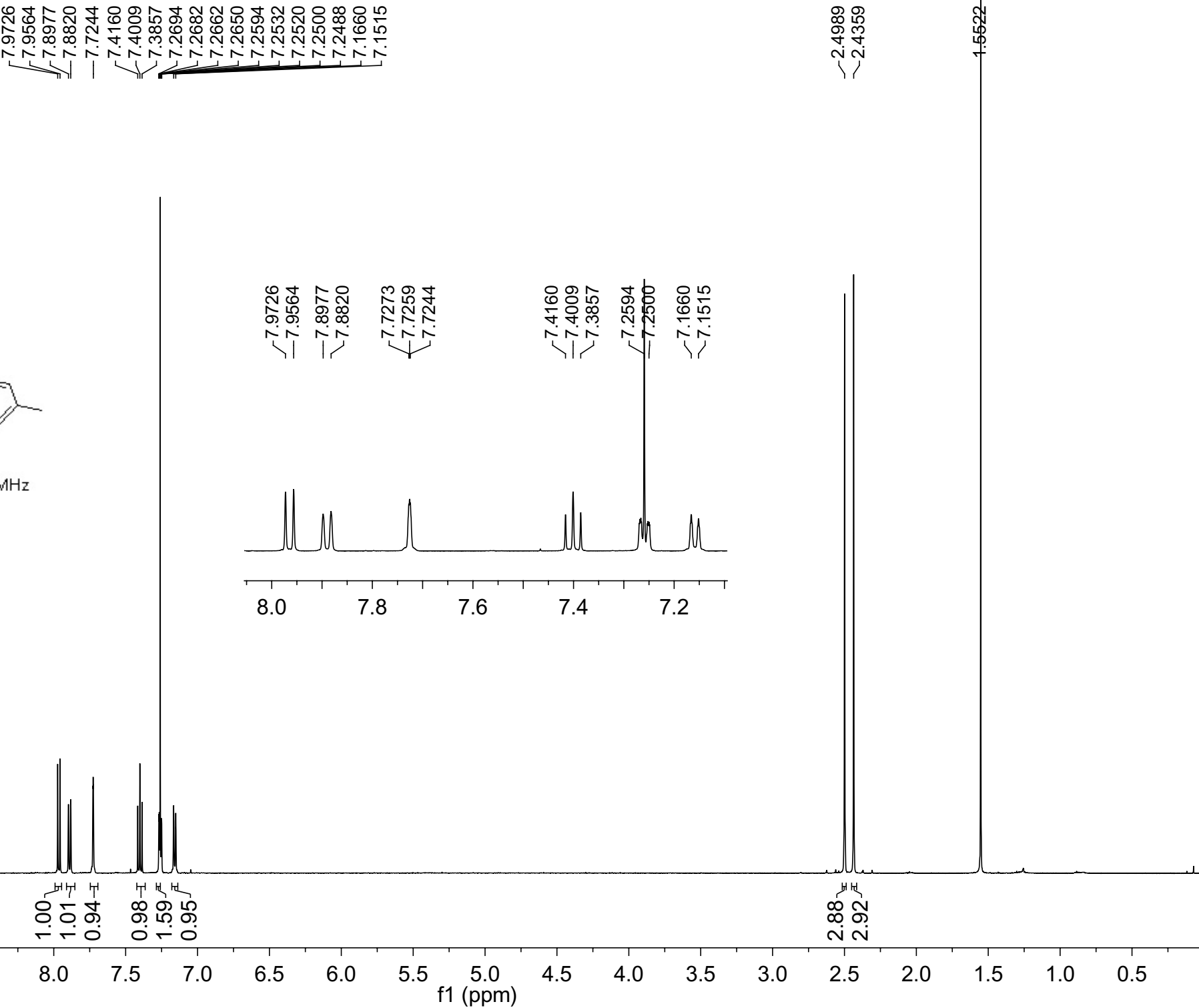


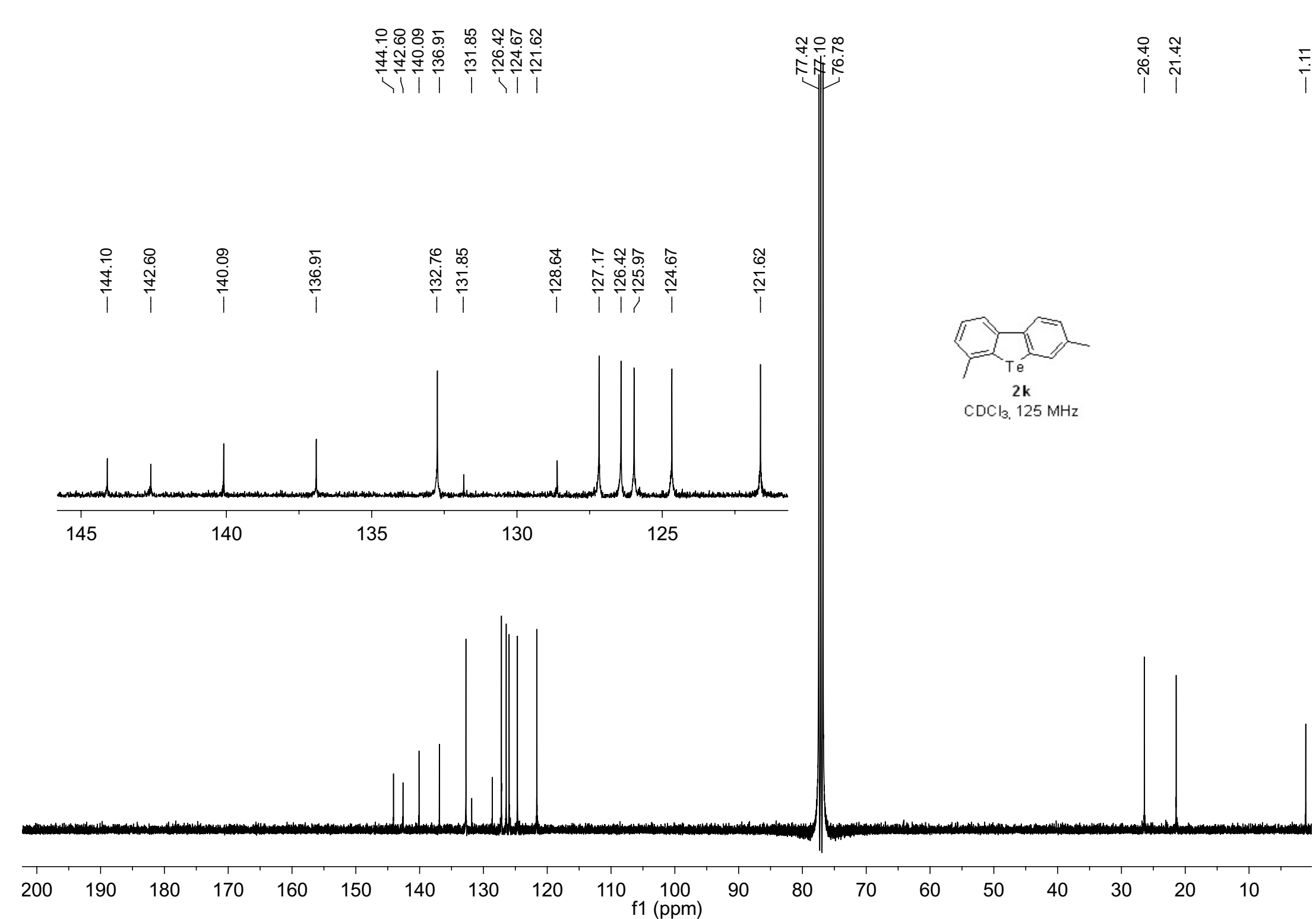


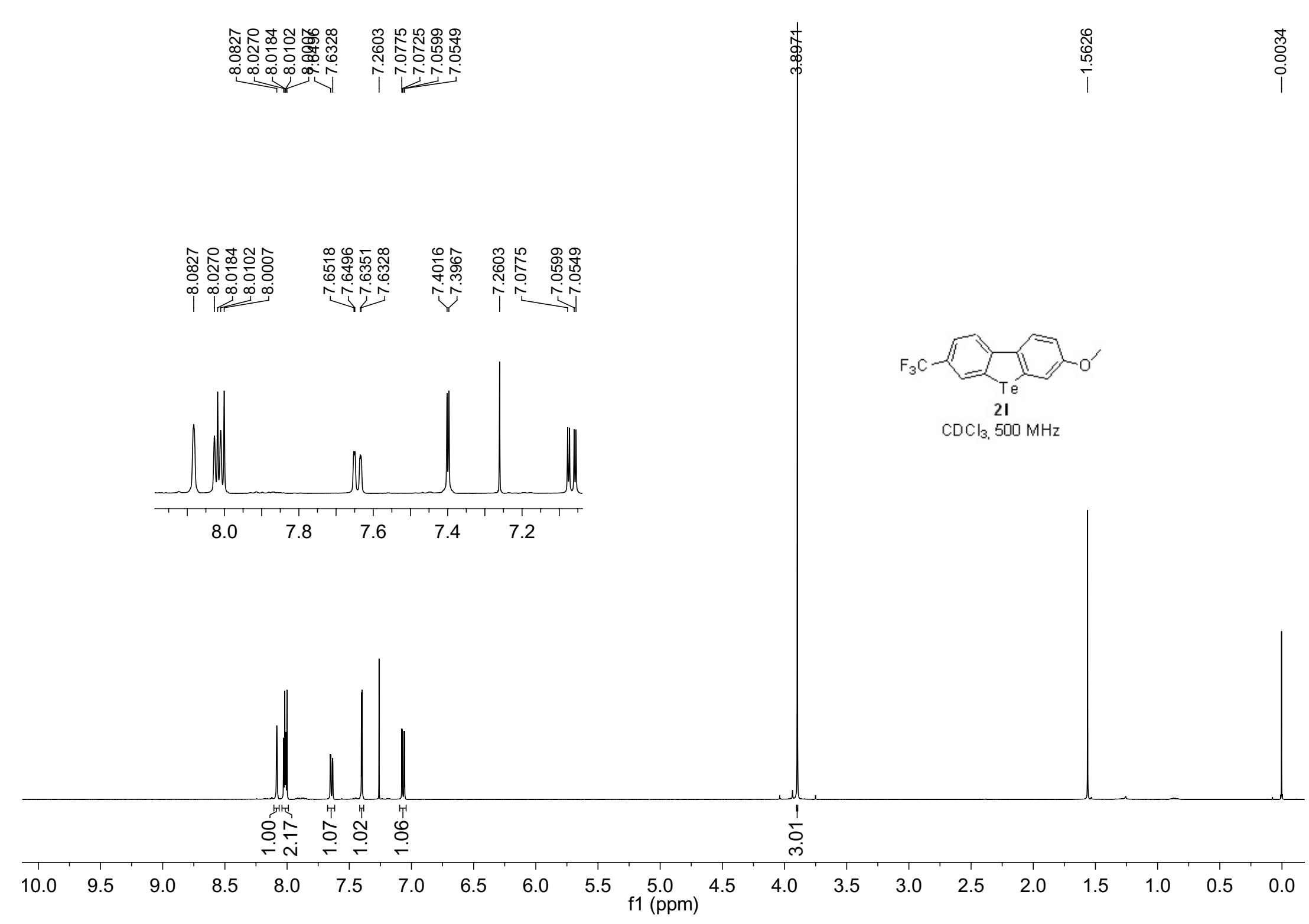


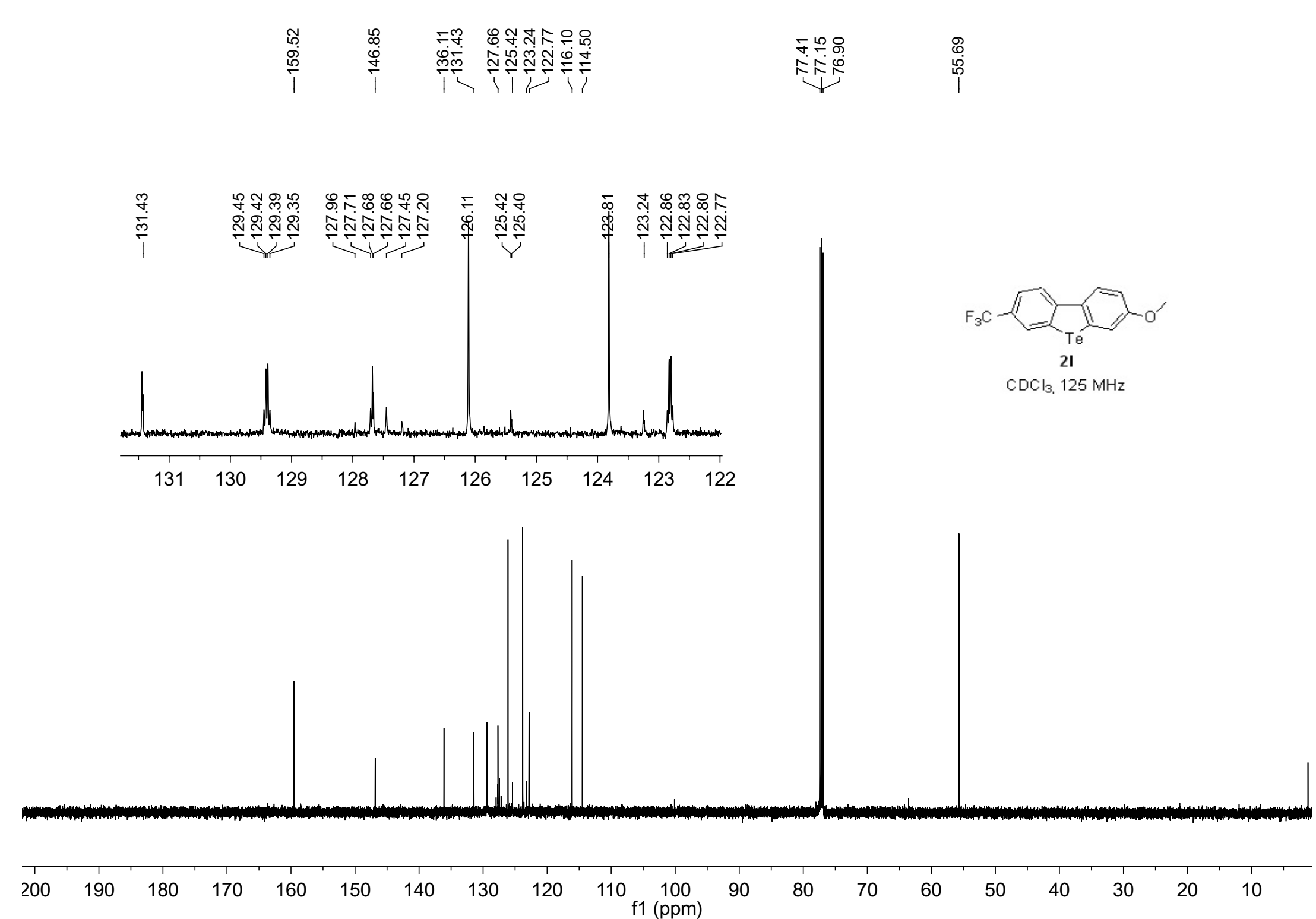
2k

$\text{CDCl}_3, 500 \text{ MHz}$



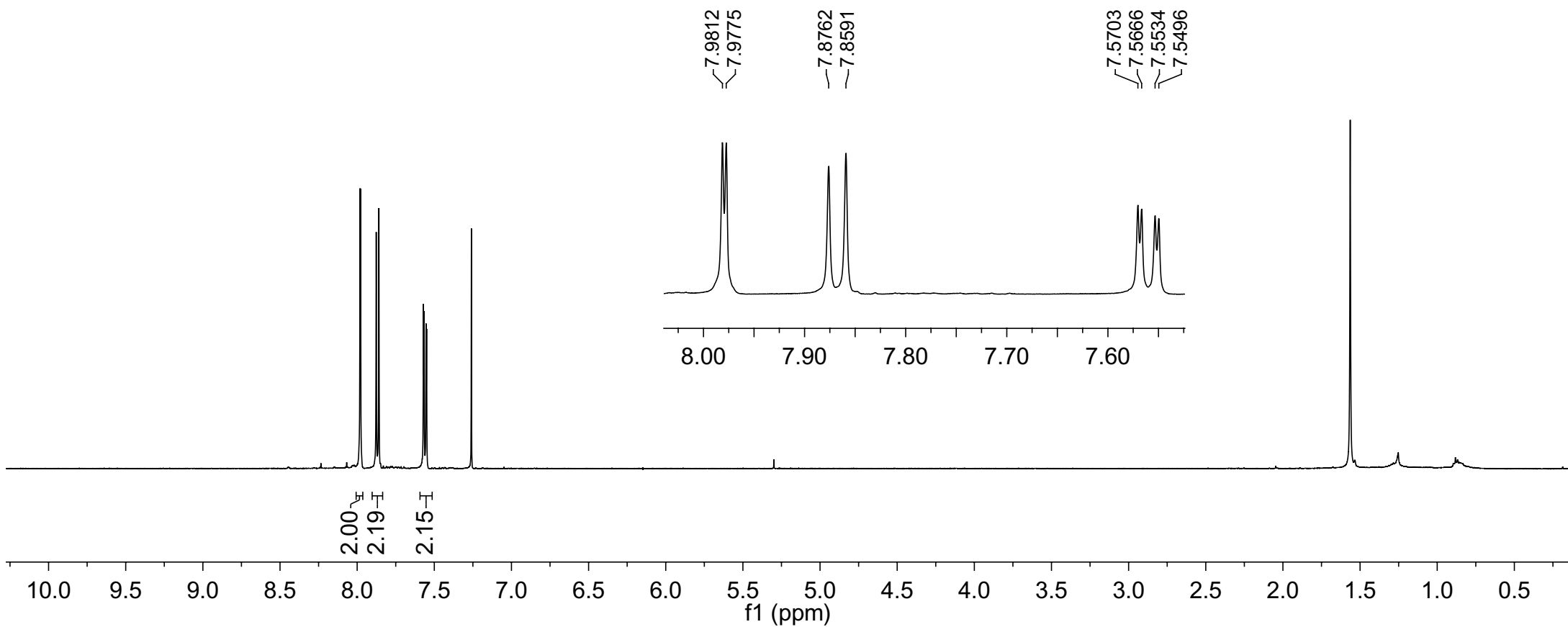
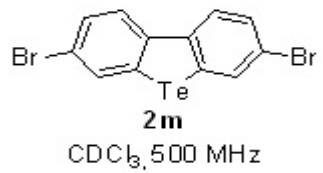


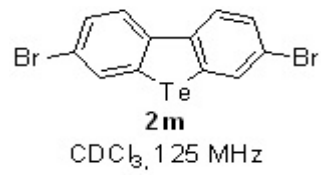




7.9812
7.9775
7.8762
7.8503
7.5534
7.5496
—7.2594

—1.5635

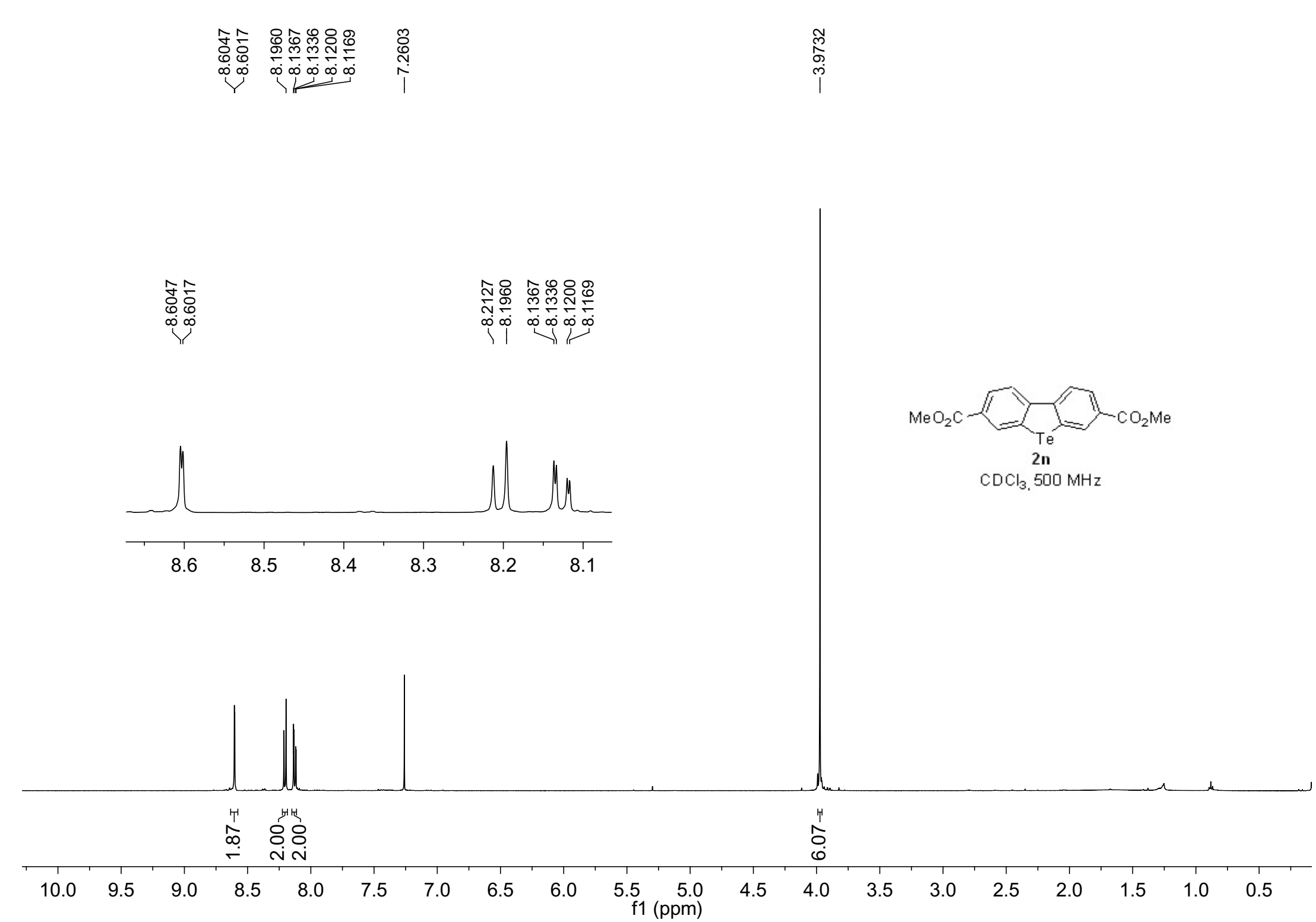


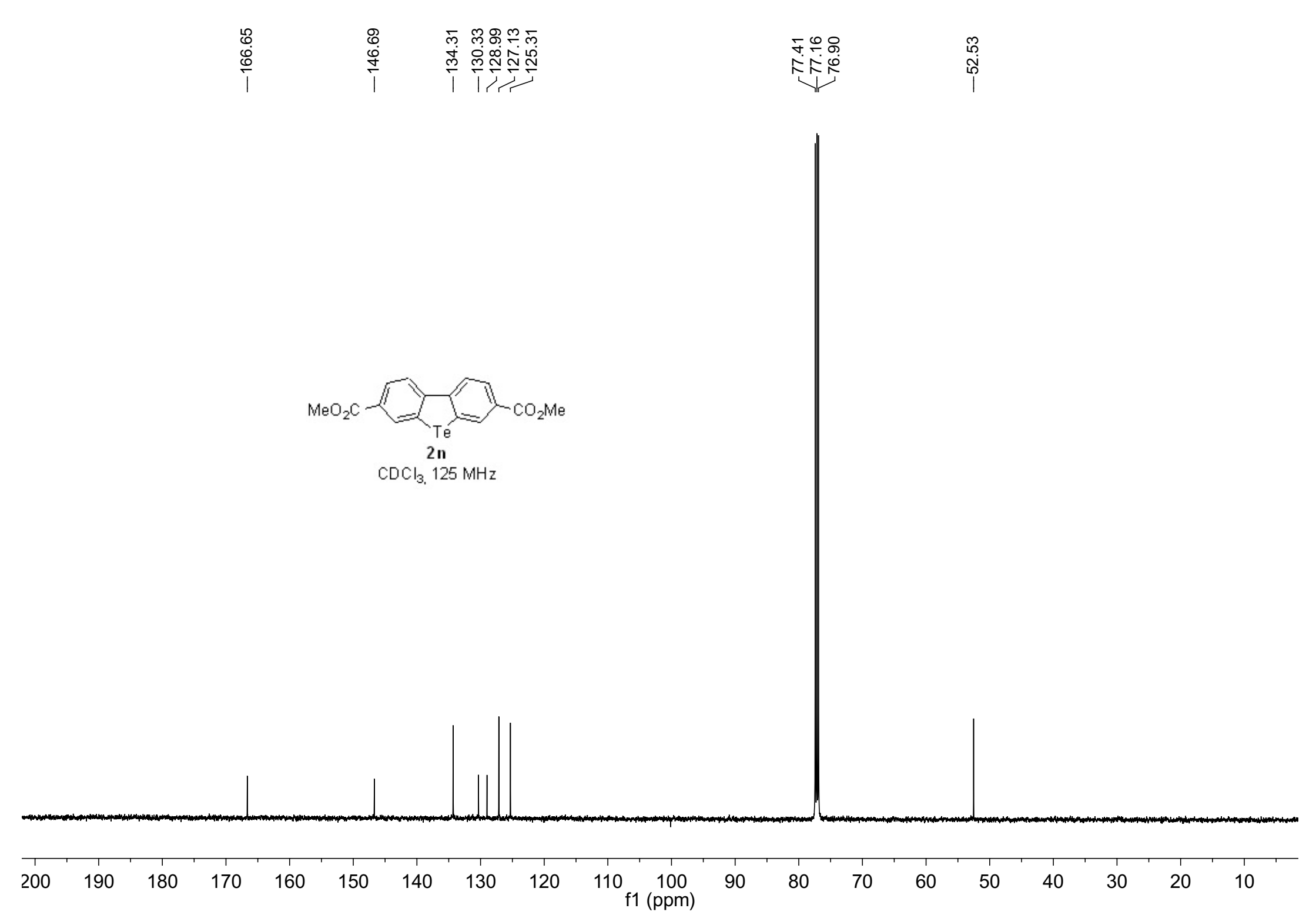


—141.97
—134.80
—129.45
—125.78
—121.31
77.41
77.45
76.90

190 180 170 160 150 140 130 120 110 100 90 80 70 60 50 40 30 20 10

f1 (ppm)





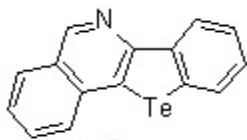
-9.3089

8.6282
8.6264
8.6123
8.6106
8.0916
8.0084
7.9935
7.8882

7.7744
7.7719
7.7044
7.7023
7.6904
7.6883
7.6862
7.6744
7.6722
7.6602
7.6439
7.6125
7.6104
7.5963
7.5823
7.5802
7.4482
7.4454
7.4327
7.4311
7.4183
7.4156
7.2875

-1.6092

-0.0980



CDCl₃, 500 MHz

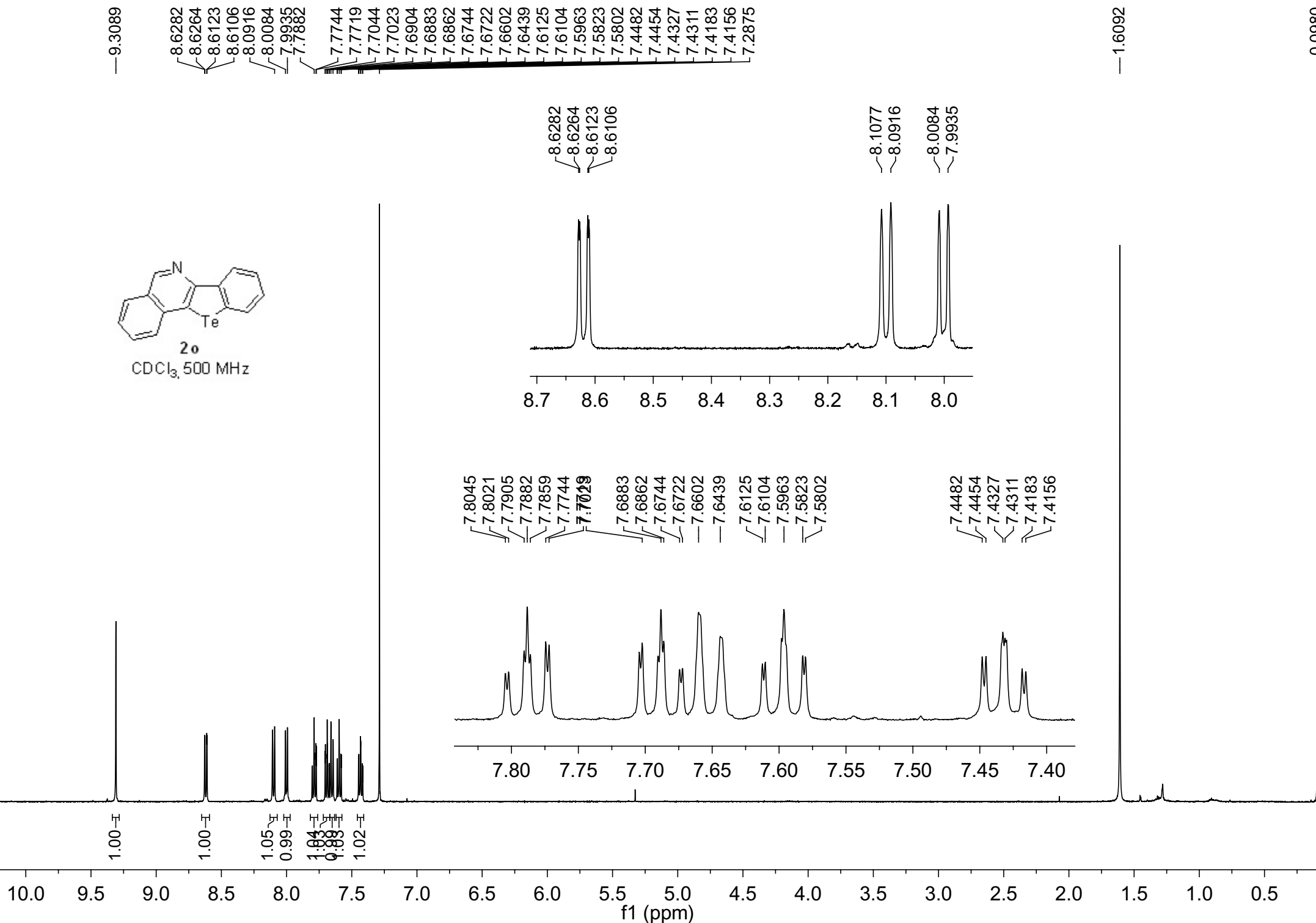
1.00
1.00
1.05
0.99
1.04
0.88
0.98
1.02

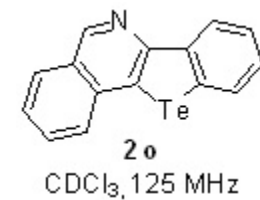
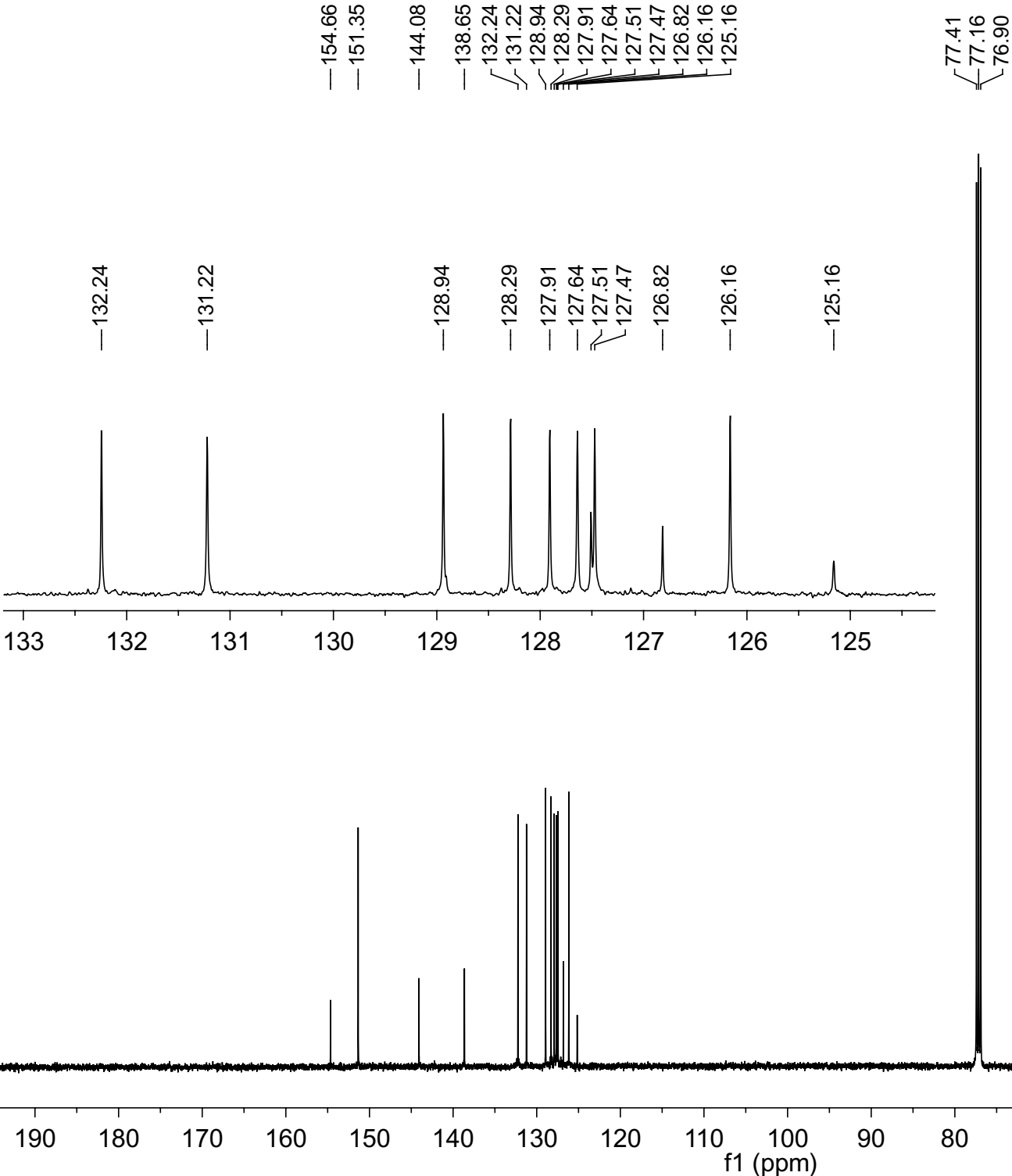
7.8045
7.8021
7.7905
7.7882
7.7859
7.7744
7.7029
7.6883
7.6862
7.6744
7.6722
7.6602
7.6439
7.6439
7.6125
7.6104
7.5963
7.5823
7.5802
7.4482
7.4454
7.4327
7.4311
7.4183
7.4156
7.2875

7.4482
7.4454
7.4327
7.4311
7.4183
7.4156

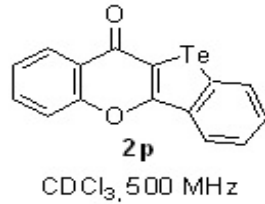
8.6282
8.6264
8.6123
8.6106

8.107
~8.0916
8.0084
~7.9935

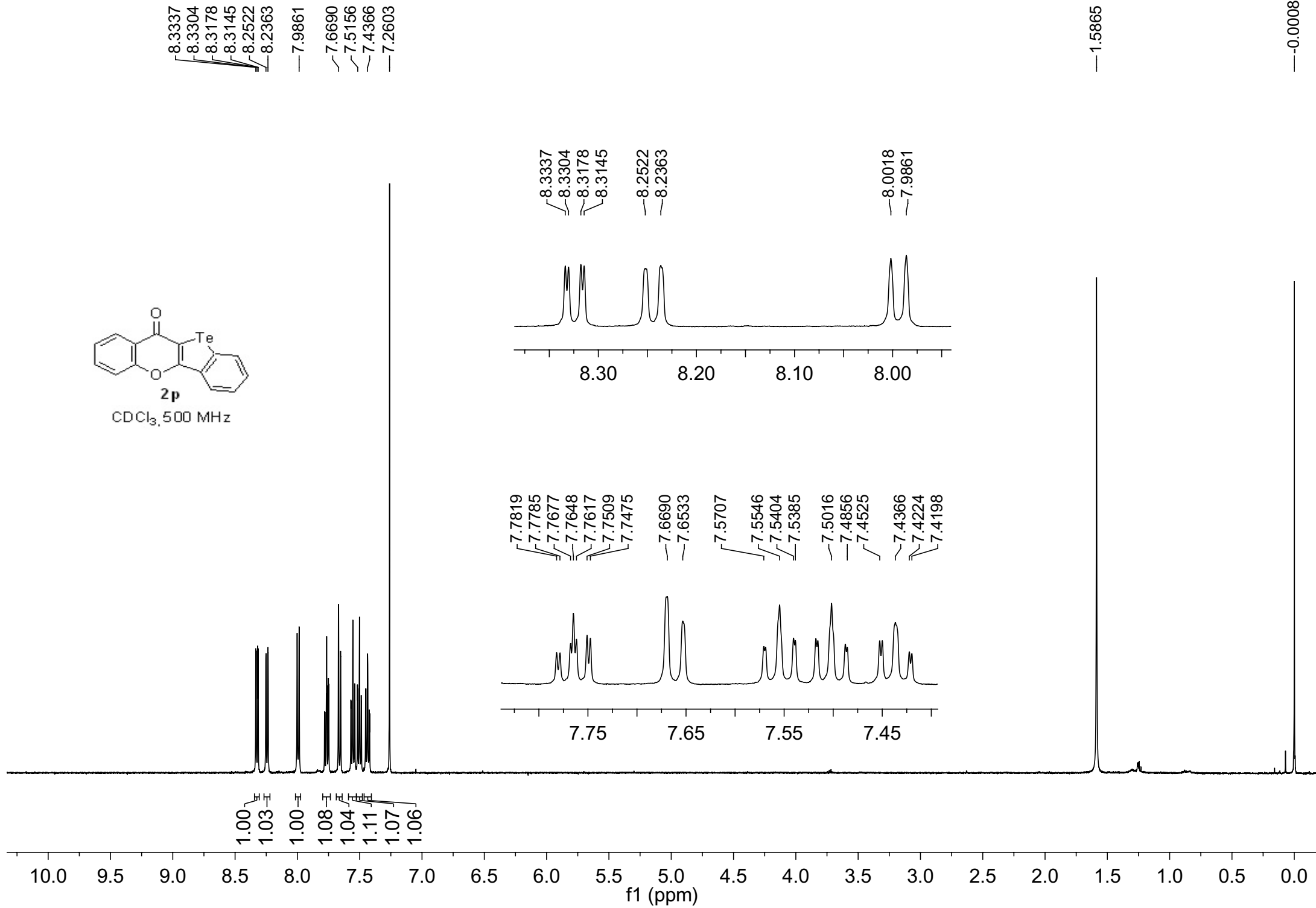


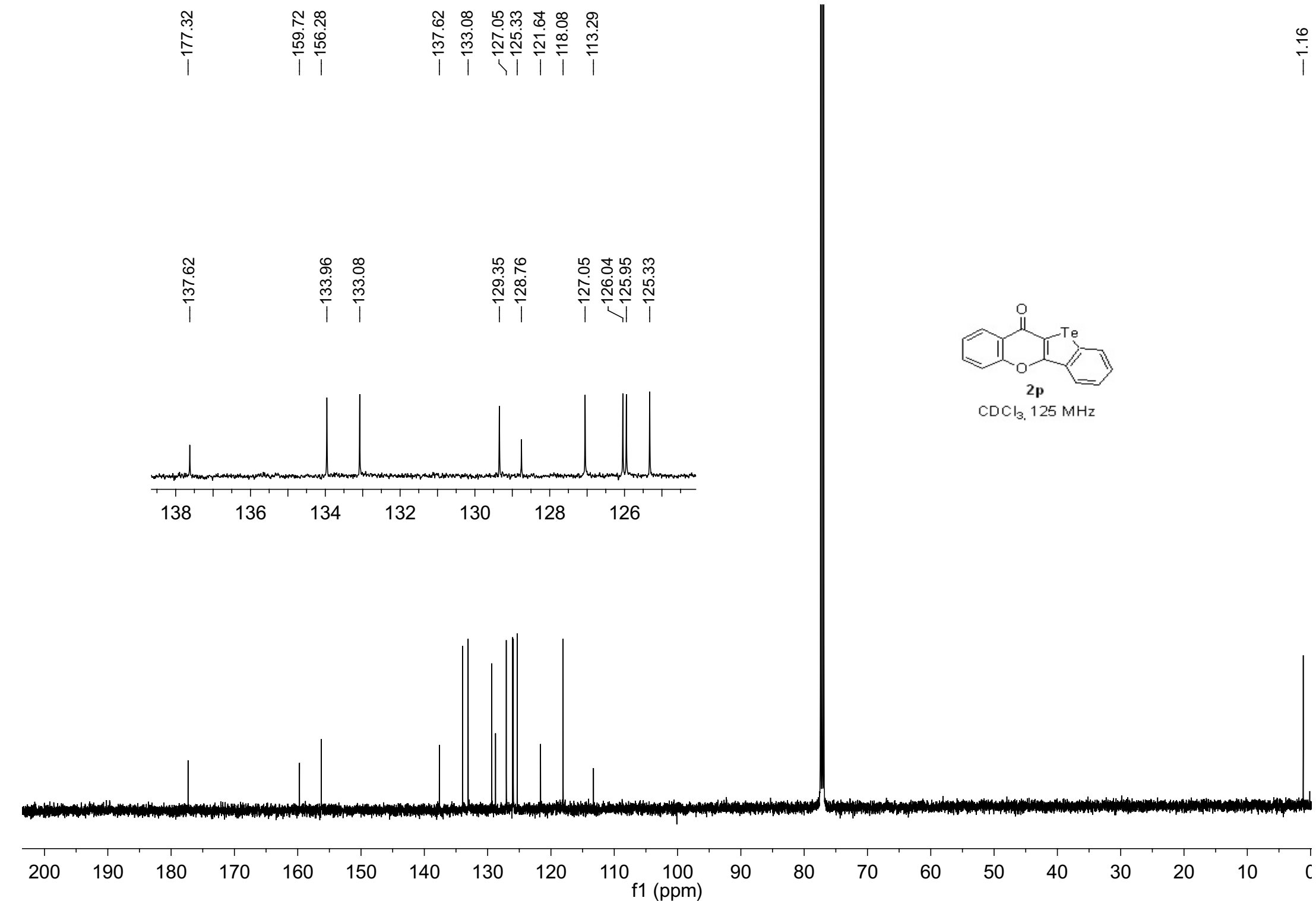


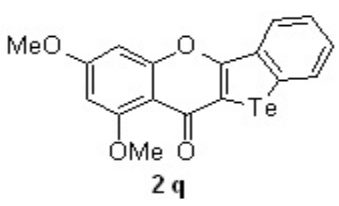
$\text{CDCl}_3, 125 \text{ MHz}$



$\text{CDCl}_3, 500 \text{ MHz}$

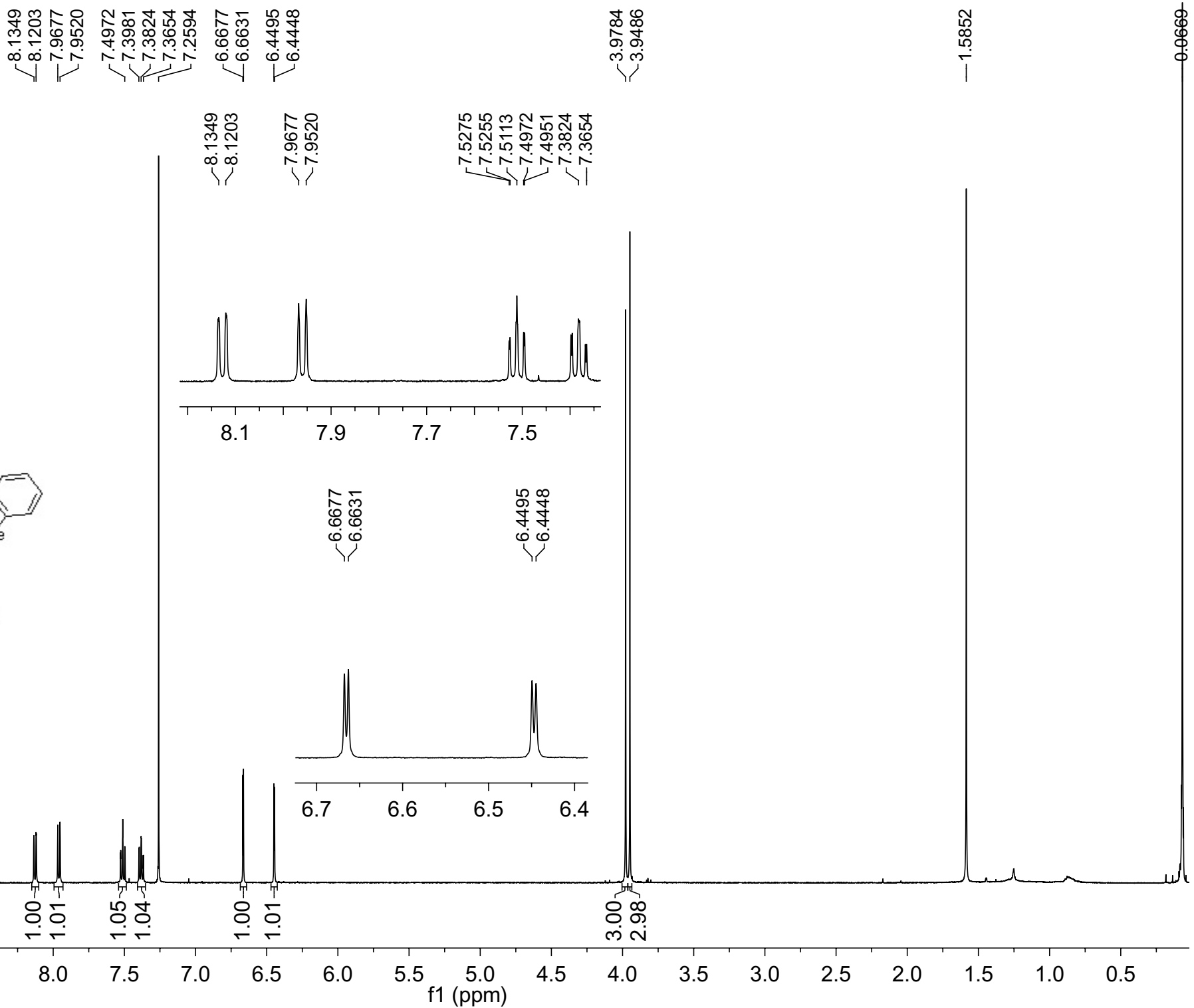


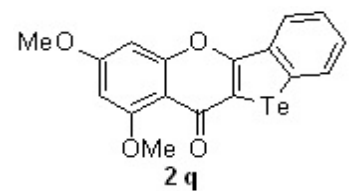




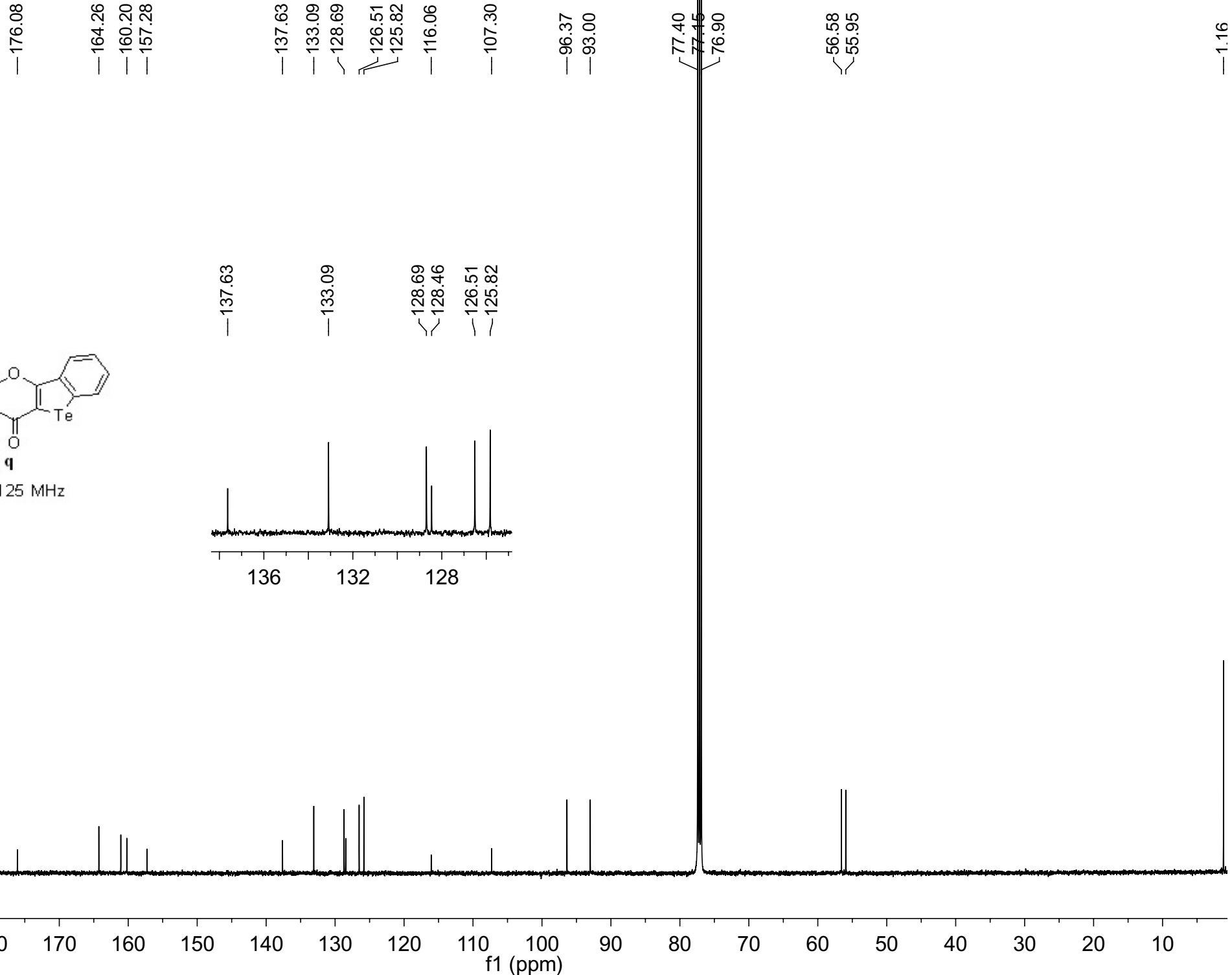
2q

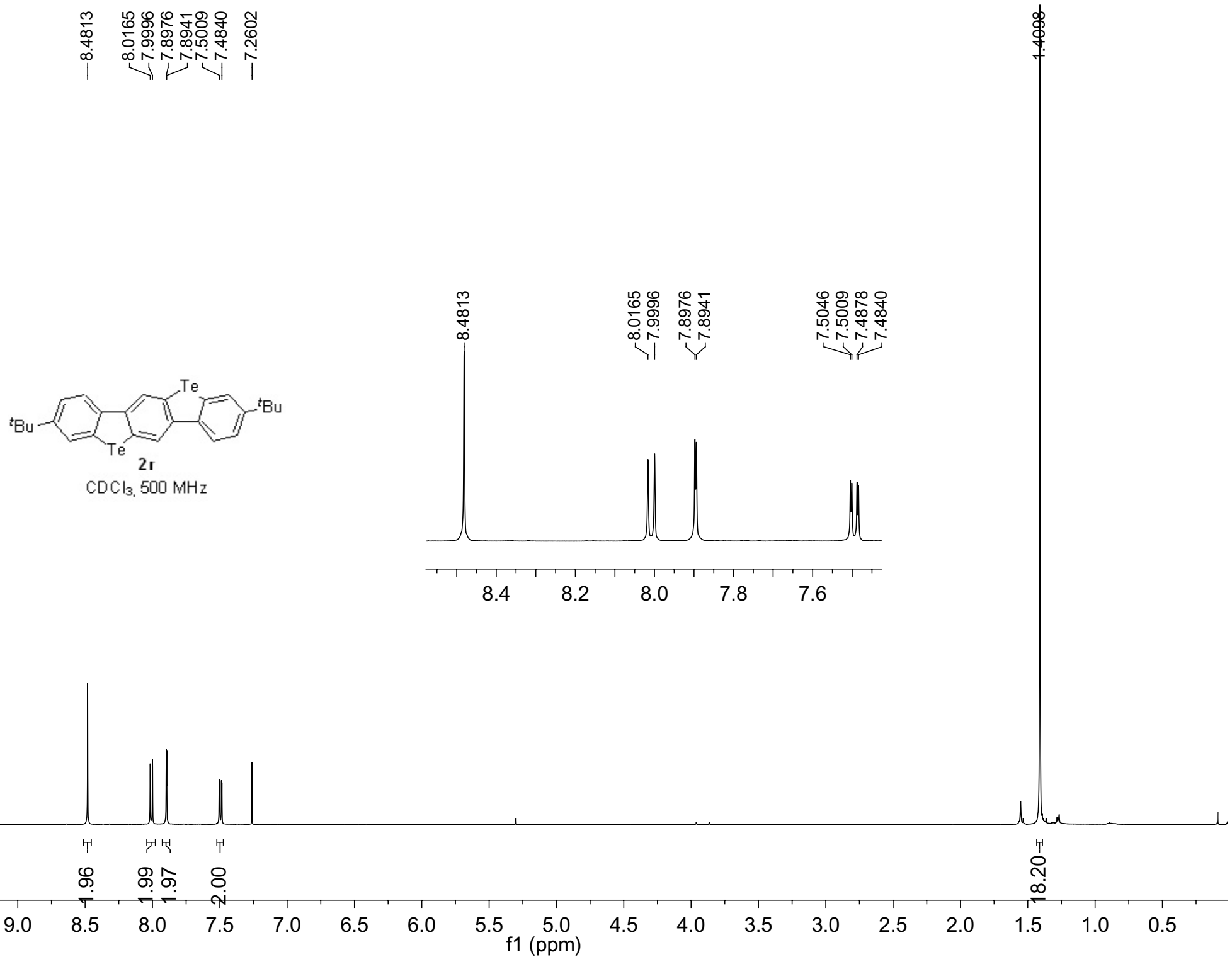
$\text{CDCl}_3, 500 \text{ MHz}$

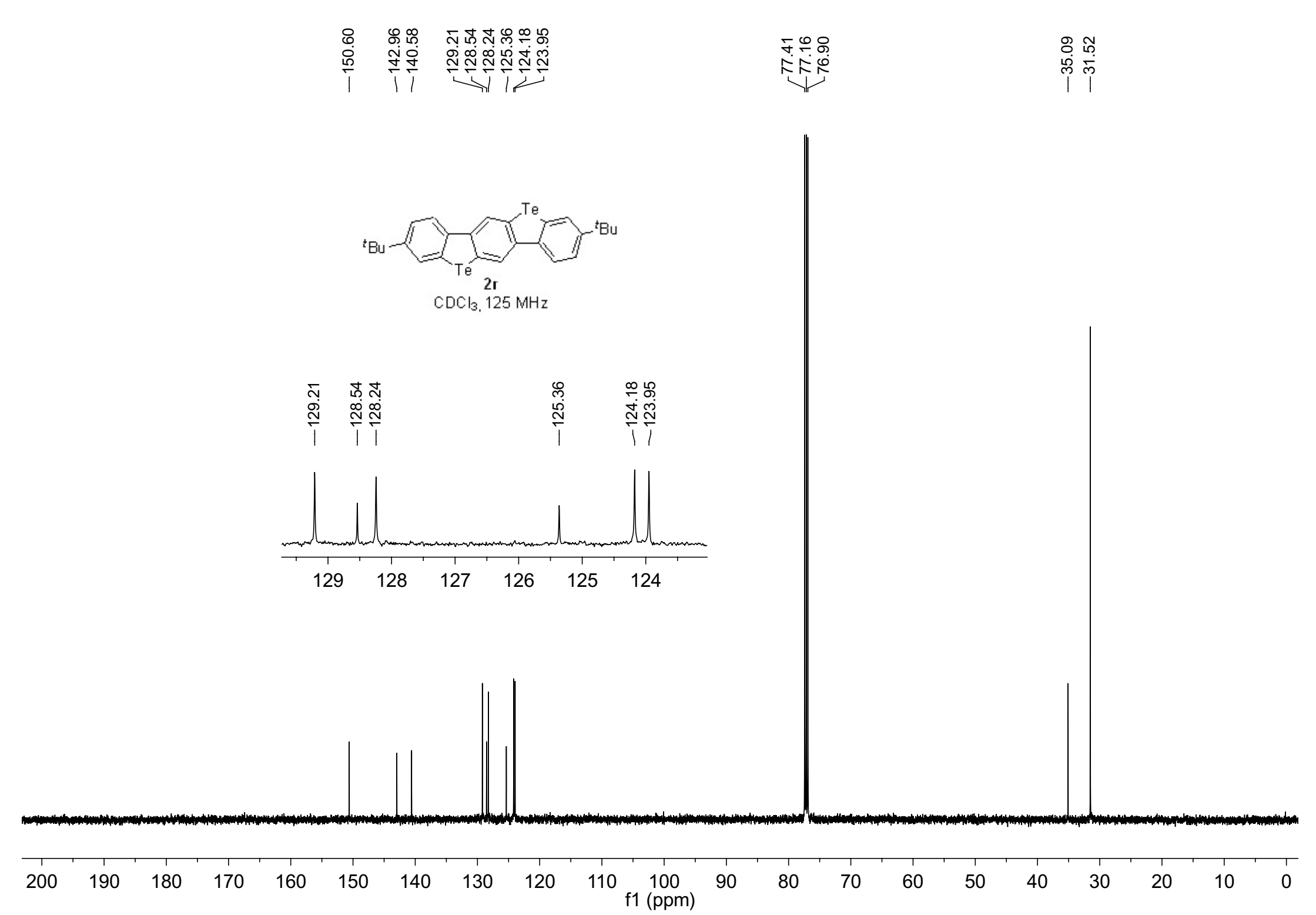




CDCl₃, 125 MHz



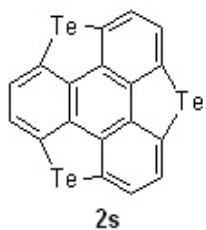




-8.3077

-3.3482

-2.5040

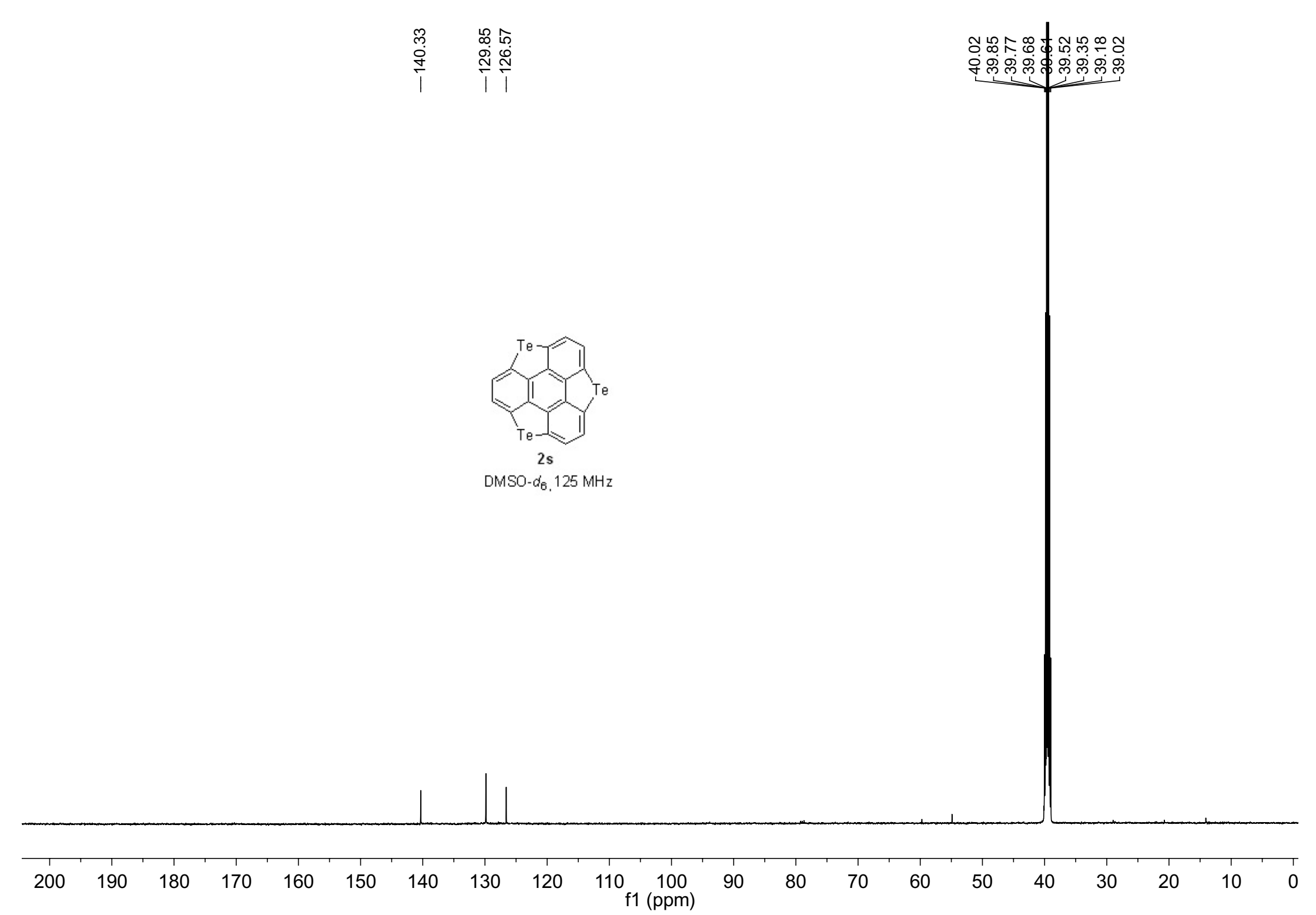


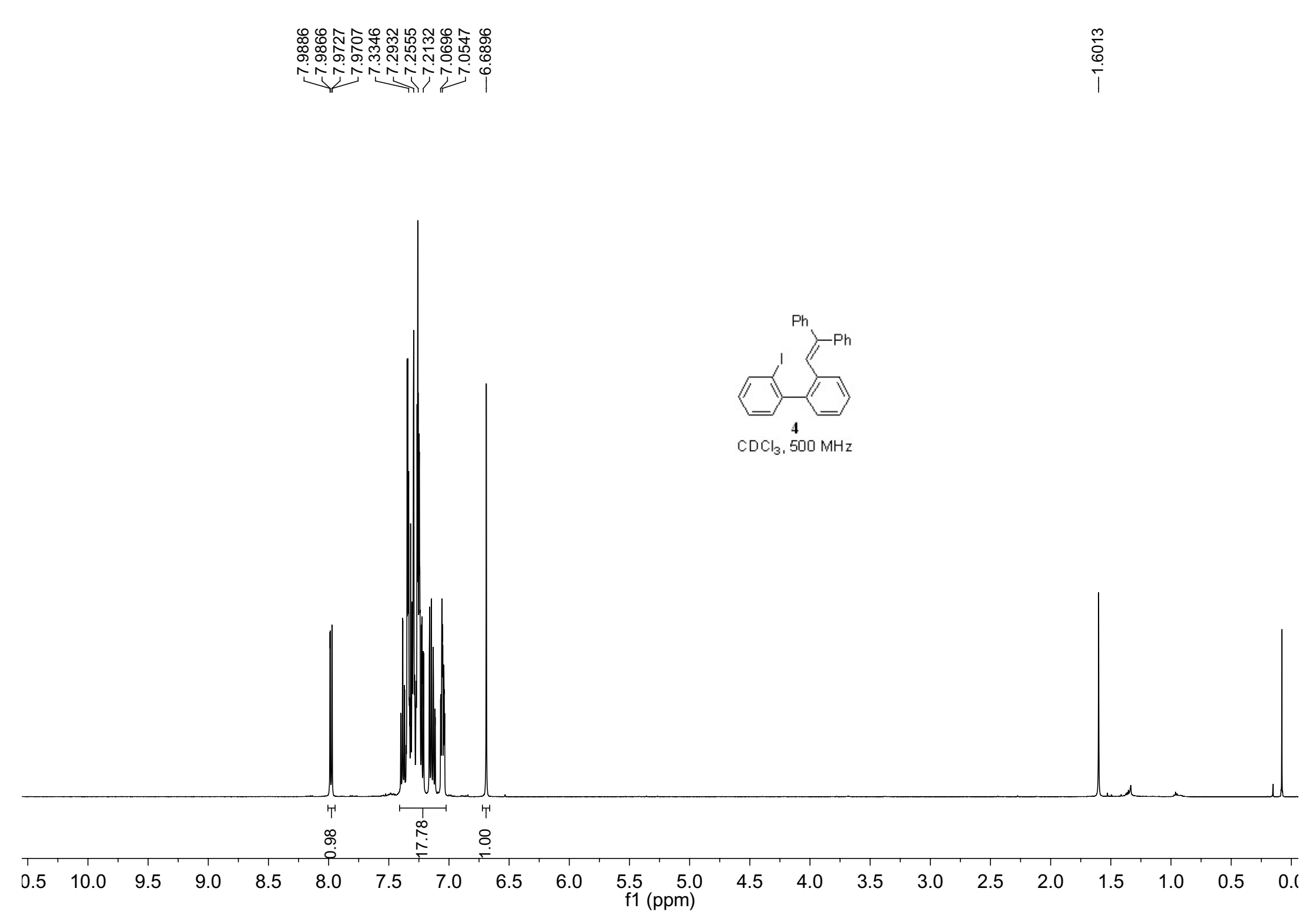
DMSO-*d*₆, 500 MHz

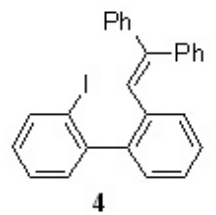
6.00

10.0 9.5 9.0 8.5 8.0 7.5 7.0 6.5 6.0 5.5 5.0 4.5 4.0 3.5 3.0 2.5 2.0 1.5 1.0 0.5 0.0

f1 (ppm)







4

CDCl₃, 125 MHz

